Antiepileptic drug transport at the blood-brain barrier, the role of SLC transporters

Thesis submitted in accordance with the requirements of the University of Liverpool for the degree of Doctor of Philosophy

By
Hayley Louise Jones
October 2014

I declare that this thesis is a result of all my own work. The material contained within this thesis has not been submitted either wholly or in part, for any other degree.

Hayley Louise Jones

Acknowledgements

I would firstly like to express my sincere gratitude to my primary supervisor Dr. Graeme Sills for giving me the opportunity to study this PhD and for his constant tutoring and support throughout this process. Particularly towards the end when juggling writing and a full time job was a challenge to put it lightly! I would also like to thank my supervisors Professor Andrew Owen, for his guidance and ideas and Professor Munir Pirmohamed for giving me the opportunity to work with some great people at the Wolfson Centre. I would also like to recognise Dr. David Dickens for his experimental guidance and training in the initial few months which aided me to go on and work independently. I also would like to thank Catherine Birch, Dr. Neil Liptrott and Dr. Darren Moss for giving their time to show me unfamiliar techniques and equipment. Epilepsy UK also deserve acknowledgement for funding this PhD project.

I also owe a thank you to my fellow PhD students Steffen, Philippe, Rana, Andrew, Lewis and Sebastian who have listened to me blow off steam and made the stressful times that bit easier and Karen who has become a great friend. The Wolfson Centre has been a fantastic place to work and I would like to thank all of my colleagues there for making me feel incredibly welcome from the start.

Finally I would like to convey my appreciation of the support my family have provided. Rebecca and Chelsea for putting up with me monopolising the family computer for almost a year and making me laugh when things were particularly stressful. Karl for his support and understanding despite the lack of time spent together this past year and my devoted mum and dad who have encouraged me throughout my study and who without I wouldn't be where I am today.

Contents

Table of tables and figures

Abbreviations

4-MBA	4-(hydroxymercuri) benzoic acid
ABC	ATP binding cassette
ACE	Angiotensin converting enzyme
AED	Antiepileptic drug
ANOVA	Analysis of variance
AQP	Aquaporin
ATP	Adenosine triphosphate
BBB	Blood-brain barrier
BCRP	Breast cancer resistance protein
BSA	Bovine serum albumin
Caco-2	Human epithelial colorectal adenocarcinoma cell line
cAMP	Cyclic adenosine monophosphate
CAT	Cationic amino acid transporter
CBZ	Carbamazepine
cDNA	Complementary DNA
CFTR	Cystic fibrosis transmembrane conductance regulator
cGMP	Cyclic guanosine monophosphate
CHO	Chinese hamster ovary cell line
CNS	Central nervous system
C_t	Comparative threshold
CYP	Cytochrome P450 enzyme
CZP	Clonazepam
DDI	Drug-drug interaction
DIDS	Diisothiocyanatostilbene-2, 2′-disulfonic acid
DMEM	Dulbecco's modified eagle medium
DMSO	Dimethyl sulphoxide
DNA	Deoxyribonucleic acid
dNTP	Deoxynucleoside triphosphate
DPM	Disintegrations per minute
E3S	Estrone-3-sulfate
EBM-2	Endothelial growth medium 2
EDTA	Ethylenediaminetetetraacetic acid

ESM	Ethosuximide
FBS	Foetal bovine serum
GABA	ɣ-aminobutyric acid
GAPDH	Glyceraldehyde 3-phosphate dehydrogenase
GBP	Gabapentin
GHB	γ-hydroxybutyrate
GLUT	High affinity glucose transporter
GUSB	Beta-glucuronidase
HBSS	Hanks balanced salt solution
hCMEC/D3	Human cerebral microvascular endothelial cells
HEK	Human embryonic kidney cells
HEPES	4-(2-Hydroxyethyl)piperazine-1-ethanesulfonic acid
HPRT1	Hypoxanthine phosphoribosyltransferase
JAM	Junctional adhesion molecule
LA	L-lactic acid
LAT	L-type amino acid transporter
LB	Luria-Bertani broth
LC-MS/MS	Liquid chromatography tandem mass spectrometry
LEV	Levetiracetam
Log D	Distribution coefficient
Log P	Partition coefficient
LTG	Lamotrigine
LXR	Liver X receptor
MATE	Multidrug and toxin extrusion pump
MCD	Malformation of cortical development
MCT	Monocarboxylate transporter
MDCK	Madin-Darby canine kidney epithelial cell line
MDR	Multidrug resistance protein
mRNA	Messenger RNA
MRP	Multidrug resistance associated protein
MTT	3-(4, 5-Dimethylthiazol-2-yl)-2, 5-diphenyltetrazolium bromide
MVP	Major vault protein
NPPB	5-nitro-2-(3-phenylpropylamino) benzoic acid
NSAID	Non-steroidal anti-inflammatory drug

OAT	Organic anion transporter
OATP	Organic anion transporting polypeptide
OCT	Organic cation transporter
OCTN	Organic cation/carnitine transporter
OPTI-MEM	Reduced serum Eagle's minimum essential medium
PAH	p-Aminohippuric acid
PB	Phenobarbital
PcDNA	Plasmid cytomegalovirus promoter DNA
pCMBS	*p*-Chloromercuribenzene sulfonate
PCR	Polymerase chain reaction
PEPT	Peptide transporter
PG	Prostaglandin
P-gp	P-glycoprotein
PHT	Phenytoin
pKa	Acid dissociation constant
PRM	Primidone
QC	Quality control
qRT-PCR	Quantitative real time PCR
RNA	Ribonucleic acid
RT-PCR	Real time PCR
SA	Salicylic acid
SD	Standard deviation of the mean
SEM	Standard error of the mean
SITS	4-acetamido-4′-isothiocyanato-2,2′-stilbenedisulfonic acid SLC
SLC	Solute carrier
SMAT	Sodium dependent multivitamin transporter
SOC	Super optimal broth with catabolite repression
SUR	Sulfonylurea receptors
SV2A	Synaptic vesicle protein 2A
T2	3, 5-Diiodo-L-thyronine
rT3	Reverse triiodothyronine
T3	Triidothyronine
T4	Thyroxine
TAP	Transporter associated with antigen processing

TBE	Tris-borate EDTA
TBS	Tris-buffered saline
TBS/T	Tris buffered saline plus Tween
TLE	Temporal lobe epilepsy
TPM	Topiramate
UGT	Uridine 5'-diphospho-glucuronosyltransferase
URAT1	Urate anion exchanger 1
UTR	Untranslated region
UV	Ultraviolet
VDAC	Voltage dependant anion channel
VGB	Vigabatrin
VPA	Valproic acid

Publications

Published abstracts

Jones HL, Dickens D, Owen A, Pirmohamed M, Sills GJ. Investigation of antiepileptic drug transport by solute carriers OATP1A2 and MCT1. Epilepsia 2012; 53 (suppl 5): 101.

Jones HL, Owen A, Pirmohamed M, Sills GJ. Antiepileptic drug transport at the blood-brain barrier by monocarboxylic acid transporters. Epilepsy Curr 2012; 13 (supplement 1): 2.234.

Jones HL, Owen A, Pirmohamed M, Sills GJ. Antiepileptic drug transport at the blood-brain barrier by monocarboxylate transporters. British Neurosci Assoc Abstr 2013: 22; 574.

Manuscripts in preparation

Jones HL, Dickens D, Owen A, Pirmohamed M, Sills GJ. Investigation of antiepileptic drug transport by the solute carrier transporters OATP1A2 and MCT1 in *Xenopus laevis* oocytes. Eur J Pharmacol. *In preparation*.

Jones HL, Owen A, Pirmohamed M, Weksler B, Romero IA, Couraud P-O, Sills GJ. Monocarboxylic acid transporters do not influence antiepileptic drug disposition. Pharmacol Res. *In preparation*.

Jones HL, Owen A, Pirmohamed M, Sills GJ. Generation of novel organic anion transporter over-expressing cell-lines and profiling of antiepileptic drug transport. Mol Pharmacol. *In preparation*.

Abstract

The transporter hypothesis has been postulated to explain pharmacoresistance in epilepsy. Despite over a decade of research surrounding the drug transporter hypothesis, the role that solute carrier (SLC) transporters might play in this theory remains largely unaddressed. Hence, the major focus of this thesis was to investigate and identify SLC transporter systems of interest that are expressed at the blood-brain barrier (BBB) and to determine which, if any, of commonly prescribed antiepileptic drugs (AEDs) are substrates for such transporter systems.

Characterisation of AED transport was undertaken using widely reported model systems such as *Xenopus laevis* oocytes and the human cerebral microvascular endothelial cell line (hCMEC/D3), together with novel stably-transfected MDCK II cell lines. Organic anion transporter 1A2 (OATP1A2), the monocarboxylate transporter (MCT) family and the organic anion transporter (OAT) family were specifically selected for investigation. Valproic acid and gabapentin showed the greatest evidence for SLC-mediated transport by OAT1/OAT3 and MCT1 respectively, while other compounds were largely unremarkable in this respect. Valproic acid transport increased OAT1 overexpressing cells compared to control but decreased in OAT3 overexpressing cells. Gabapentin uptake increased in MCT1 transfected *Xenopus laevis* oocytes and was shown to decrease in hCMEC/D3 cells in the presence of a panel of MCT inhibitors.

The induction/suppression of expression of SLC transporters by AEDs was explored in the hCMEC/D3 cell line, in an attempt to understand how AEDs might influence the functionality of endogenous transport pathways. A number of AEDs were observed to induce/suppress expression of transporter genes involved in transport and detoxification

A further study explored the fundamental physiochemical properties of AEDs, which is relevant to their penetration into the brain. A number of AEDs, including lamotrigine, gabapentin and topiramate, observe adequate uptake in the hCMEC/D3 model of the BBB despite having physiochemical properties, such as a high polar surface area and negative log D value which may limit passive entry into the brain. This would suggest that a carrier mediated system may be involved in the uptake of these drugs into the brain.

The work described in this thesis has shown that a number of AEDs may be subject to carrier mediated uptake into the brain. Individual differences in transporter expression at the BBB may be responsible for variability in brain concentrations of AEDs. However, at present, this does not provide us with an adequate explanation for why some people with epilepsy experience pharmacoresistant seizures.

Chapter 1

General Introduction

1.1. Epilepsy epidemiology

Epilepsy is the most common brain disorder in the world; currently the World Health Organisation estimates epilepsy to affect 50 million people worldwide with people in developing countries accounting for 80% of this figure (WHO, 2012). In the UK, 412,000 people are registered as having epilepsy, a prevalence of 6.2 per 1000 individuals (Booth *et al.*, 2010). Epilepsy refers not to a distinct disorder but to a collection of syndromes characterised by a predisposition to unprovoked seizures (Dreifuss *et al.*, 1981) - 'transient occurrences of signs and/or symptoms due to abnormal excessive or synchronous neuronal activity in the brain' (Fisher *et al.*, 2005). Epilepsy syndromes fall into two broad categories: generalised or partial epilepsies, which can be classified based on clinical seizure type, electroencephalography (EEG) findings and the presence/absence of neurological or developmental abnormalities (Dreifuss *et al.*, 1981; Cundy *et al.*, 2004). Classification can also be made based on the epilepsy aetiology, recently three distinct causative factors for developing epilepsy have been advised: 'genetic', where the epilepsy is the direct result of a genetic defect, 'structural/metabolic', where another distinct metabolic/ structural disease has been demonstrated to substantially increase the risk of developing epilepsy, and 'unknown,' where the underlying cause of the epilepsy is currently unknown (Enerson *et al.*, 2003).

Although thought to have affected people since humans' early evolution, the first descriptive reports of epilepsy date to ancient Mesopotamia around 2000 B.C. (Anonymous, 2003). In 400 B.C. the ancient Greek physician Hippocrates was the first to characterise epilepsy as a disease that needed treatment with diet and drugs not as a divine 'possession' or 'choosing,' contrary to popular belief (Temkin, 1945). In the late 17th century scientific understanding of epilepsy began to advance, culminating in the 19th century with John Hughlings Jackson's first attempts to characterise the pathophysiology of epilepsy, the first use of therapeutics in the treatment of epilepsy, and the birth of modern neurology (Wang *et al.*, 2006; Morris *et al.*, 2008).

1.2. Treatment of epilepsy

The first reasonable therapeutic treatment of epilepsy began in the mid-1800s when Sir Charles Locock reported that he had been able to cure 'hysterical epilepsy' in women with potassium bromide (Markovich, 2008). Thereafter, potassium bromide was used regularly for catamenial as well as other types of epilepsy and by the early 1900s was the mainstay of epilepsy treatment. The discovery of potassium bromide brought about new understanding that epilepsy could be well controlled with drugs. In 1912, Alfred Hauptmann serendipitously observed that the then marketed hypnotic, phenobarbital (PB) possessed antiepileptic properties (Hauptmann, 1912). The use of PB as an anticonvulsant was not rapidly taken up internationally and was only first used in the UK and United States in the early 1920s, but by the 1940s PB had become the mainstay of treatment throughout the world and today is still the most commonly prescribed antiepileptic drug (AED) in the developing world (Kwan *et al.*, 2004; Shorvon, 2009a).

The next milestone in the treatment of epilepsy was the development of sodium diphenylhydantoinate (phenytoin (PHT)) by Merritt and Putnam in 1937 (Merritt *et al.*, 1938a; Merritt *et al.*, 1938b). Their aim was to develop a less sedative anticonvulsant than PB and by testing non-sedative phenyl compounds using a cat model of electrically induced seizures discovered PHT. PHT was sufficiently non-toxic for routine administration and could elicit greater protection from electrically induced seizures than bromide or PB without causing sedation. The cat electroshock model was the first attempt of screening AEDs in a model of epilepsy and the first to accurately predict efficacy in humans, transforming the future development of antiepileptic agents (Pedley, 2009). The next significant development was that of carbamazepine (CBZ) in the 1960s. First developed as a drug for the treatment of depression and later licenced as an anticonvulsant, CBZ was the first AED to be licenced on a strong evidence base from both animal and clinical trial data. The advent of CBZ represented a shift in how AEDs were developed, moving away from academia with the rise and domination of the pharmaceutical industry. CBZ continues to be the most prescribed AED in Europe (Schindler *et al.*, 1954; Blom, 1962).

Around the same time period the serendipitous discovery of sodium valproate (VPA) was published by a group at the small pharmaceutical company, La Laboratoire (Meunier *et al.*, 1963). The group were testing a range of compounds for a

tranquillising action in a rat model using VPA as the chosen solvent. Surprisingly all compounds tested were observed to elicit antiepileptic effects and VPA was subjected to testing as an AED alone. VPA showed considerable efficacy in both animal models and human clinical trials and was ultimately licenced in 1967. Together with CBZ, VPA continues to be one of the two most commonly prescribed AEDs in the developed world (Meunier *et al.*, 1963; Shorvon, 2009b).

By the 1970s, the modern era of AED discovery had begun. Mainly owing to the establishment of the Anticonvulsant Drug Development program in the United States, huge efforts were put into high throughput target orientated design of compounds, largely based around the discovery of ɣ-aminobutyric acid (GABA) as the major inhibitory neurotransmitter in the central nervous system (CNS). An extensive list of AEDs was successfully developed as a result of the Anticonvulsant Drug Development program, which undoubtedly improved epilepsy treatment. Of note is the development of lamotrigine (LTG), gabapentin (GBP), topiramate (TPM) and levetiracetam (LEV), which along with CBZ and VPA comprise the most commonly prescribed AEDs at present (Lamb *et al.*, 1985; UK Gabapentin Study Group, 1990; Shorvon, 2009b; Brodie, 2010). Today, antiepileptic agents form the mainstay of epilepsy therapy; however in certain individuals neurosurgery to resect epileptic foci can be advantageous. In addition, the ketogenic diet can be a powerful tool in some individuals, for example those who are known to have a mutation in the high affinity glucose transporter 1 (GLUT1) (Leen *et al.*, 2010).

1.3 Pharmacology of commonly prescribed AEDs

1.3.1 Phenytoin

Although PHT is one of the drugs of choice for the treatment of epilepsy in the developing world and is still commonly used in the United States, its use in Europe has declined due to an extensive adverse effects profile and non-linear pharmacokinetics (Elger *et al.*, 2008). The antiepileptic activity of PHT is thought to occur through binding to voltage-gated sodium channels and prolonging their inactivation (*figure 1.1*). At higher concentrations PHT is also suggested to inhibit axonal and nerve terminal calcium channels (Macdonald, 1999). Oral absorption rates of PHT differ according to the formulation used, with capsule formulations possessing approximately 90% bioavailability (Neurvonen, 1979). In plasma, PHT is 90% protein bound and less than

5% is excreted in the urine unchanged. Consequently, the majority of PHT is metabolised, largely in the liver by cytochrome P450 2C9 (CYP2C9) oxidation (90%) but also by CYP2C19 oxidation (10%). CYP2C9 dependent metabolism of PHT is saturable, which largely explains its non-linear pharmacokinetics. PHT is an enzyme inducer and is known to induce metabolising enzymes including its own major metabolising enzyme CYP2C9 and CYP3A4, which mediates the metabolism of many drugs (Brodie *et al.*, 1996a). As a result of its variable absorption and the strong association between serum level and seizure control, therapeutic drug monitoring of PHT is advised (Kutt *et al.*, 1964; Eadie, 2009).

1.3.2 Carbamazepine

CBZ is used clinically as a first line or adjunctive therapy for partial and generalised tonic-clonic seizures, exerting its effects through the inhibition of voltage gated sodium channels (*figure 1.1*) similarly to PHT (Kuo, 1998). CBZ is orally administrated and titrated over a period of a few weeks until a maintenance dose of around 600mg/day is reached, although this varies according to inter-individual variation in kinetics and whether other CYP450 inhibitors/inducers are prescribed (Brodie *et al.*, 1996a). Absorption of orally administered CBZ is relatively slow and variable, reflected in a half life of around 15-35 hours depending on the degree of auto-induction and a bioavailability of 75-85%. CBZ is moderately protein bound (75-80%) and undergoes extensive, mainly CYP3A4 mediated oxidative metabolism in the liver to an epoxide metabolite (carbamazepine 10-11, epoxide). As a result, only negligible amounts of CBZ are excreted unchanged in the urine (Morselli, 1995; Sillanpää *et al.*, 2009). The main issues of CBZ use surround its ability to induce the metabolism of co-administered drugs, resulting in a large number of drug-drug interactions and adverse hypersensitivity reactions associated with CBZ in predisposed individuals (Tomson *et al.*, 1989; Brodie, 1992).

1.3.3 Sodium valproate

VPA is a broad spectrum AED with activity against different seizures types including almost all primary generalised seizures and remains a first line treatment in idiopathic generalised epilepsies (Anonymous, 1988). Its mechanism of action is controversial and likely multi-faceted, however it is agreed that VPA acts upon voltage-gated sodium channels and increases GABA concentrations in the brain (*figure 1.1*), albeit through

mechanisms that are not fully understood (Löscher, 2002). VPA is usually prescribed at a starting dose of 500mg once or twice daily and increased according to individual response (Brodie *et al.*, 1996a). VPA is rapidly absorbed within 0.5-8 hours depending on how it is formulated; is not subject to extensive first pass metabolism and consequently has almost complete bioavailability. VPA is substantially (up to 90%) protein bound, which at therapeutic concentrations can become saturated and is eliminated almost entirely by hepatic metabolism (Franke *et al.*, 1995). Biotransformation is mediated by several pathways including uridine 5'-diphospho-glucuronosyltransferase (UGT) mediated glucuronidation (UGT1A3, UGT2B7) and CYP450 (CYP2C9, CYP2C19, CYP2B6) mediated oxidation (Anari *et al.*, 2000). VPA clearance can be affected by enzyme inducers such as PHT and CBZ due to its extensive CYP450 mediated metabolism. It is also a potent metabolic inhibitor itself and so readily inhibits the metabolism of many drugs, including the glucuronidation of LTG, markedly reducing LTG elimination (Kanner *et al.*, 2000; Patsalos, 2005). Although VPA is possibly the most efficacious of all AEDs, its use is restricted by its teratogenic effects with increased rates of neural tube defects reported in the offspring of women receiving VPA treatment during pregnancy (Samrén *et al.*, 1997).

1.3.4 Lamotrigine

LTG is a 2nd generation AED used clinically as monotherapy or as adjunctive therapy in the treatment of partial seizures and in some generalized epilepsy syndromes (Brodie *et al.*, 1996b). LTG exerts its antiepileptic action by the blockade of voltage activated sodium and possibly calcium channels (Leach *et al.*, 1986; *figure 1.1*). LTG is more than 95% bioavailable following oral administration and is rapidly absorbed into the blood in 1-3 hours. LTG is moderately (55%) bound to plasma proteins and undergoes extensive metabolism in the liver via N-glucuronidation, predominantly by UGT1A4. Around 80-90% of a LTG dose is excreted as the glucuronide metabolite via the urine (Cohen *et al.*, 1987; Matsuo *et al.*, 2009).

1.3.5 Gabapentin

GBP is currently licensed as a second line drug for the treatment of partial seizures in both adults and children, usually as an add-on therapy (UK Gabapentin Study Group, 1990; Anhut *et al.*, 1994). Structurally GBP is very similar to GABA suggesting an agonistic mechanism of action to increase GABA transmission; however its

antiepileptic effect is largely mediated by the blockade of voltage gated calcium channels (*figure 1.1*), although this is not thoroughly understood (Sills, 2006). GBP is rapidly absorbed and reaches peak plasma concentrations 2-3 hours after administration. However, in contrast with other AEDs, GBP has a bioavailability of less than 65% which is further reduced with increased dose, suggesting a saturable absorption process from the gut (Cundy *et al.,* 2004). In the plasma, GBP is found in its free drug form, shows no protein binding and is not subject to metabolism in the liver; GBP is excreted entirely unchanged in the urine with an elimination half-life of 5-9 hours (Brodie *et al.*, 1996b; Somerville *et al.*, 2009).

1.3.6 Topiramate

The antiepileptic action of TPM is multi-faceted, involving several pathways including the inhibition of kainate evoked currents, enhancement of GABA signalling, blockade of voltage gated sodium and calcium channels (*figure 1.1*) and inhibition of carbonic anhydrase, although the latter is now thought to occur independently of TPM's antiepileptic action (Brodie *et al.*, 1996b). Partly due to its multiple pharmacological actions and as a result of its relative success in the treatment of various seizure types, TPM is classified as a broad spectrum AED and is approved for use in the treatment of Lennox-Gastaut syndrome in addition to various generalised and partial seizures (Bourgeois, 2000). As with many AEDs, TPM is almost 100% bioavailable and is absorbed rapidly reaching peak plasma levels within 2-4 hours. TPM is mainly excreted unchanged in the urine (60-70%), however a small percentage is subject to oxidative metabolism by microsomal cytochrome P450 (CYP450) enzymes. CYP450 metabolism of TPM can be induced to the extent that it accounts for up to 40% of elimination when TPM is co-administered with enzyme inducing drugs such as PHT and CBZ (Cross *et al.*, 2009).

1.3.7 Levetiracetam

LEV is a pyrrolidone compound related to the cognitive enhancer piracetam (Genton *et al.*, 2000) and is unusual in the respect that it was developed using non-classical animal models of seizures. As a result, LEV has no activity in classical seizure models (Rogawski *et al.*, 1990), though it has a broad and efficacious mechanism of action unlike any other AED. Although LEV weakly reduces voltage activated calcium currents and potentiates GABA signalling, its major antiepileptic effects arise from a

unique mechanism involving inhibition of neurotransmitter release from nerve terminals via binding to the synaptic vesicle protein SVA2 (*figure 1.1*), which is involved in neurotransmitter exocytosis (Patsalos, 2005). LEV is a first line therapy in the treatment of partial seizures, however as a result of its unique mechanism of action, LEV is becoming known as a broad spectrum AED (Stephen *et al.*, 2011). LEV is rapidly absorbed and almost 100% orally bioavailable, reaching peak plasma concentrations in 0.5-2 hours. LEV plasma protein binding is minimal (less than 10%) and most is excreted unchanged in the urine (66%). The remainder is subject to metabolism, mostly by hydrolysis to a carboxylic acid metabolite (24%) but also by oxidation (Splinter, 2005; French *et al.*, 2009).

1.4 AED resistance and the transporter hypothesis

Although AED therapy successfully controls seizures in the majority of people with epilepsy, up to 30% of people with epilepsy are not adequately controlled with AEDs and are classified as pharmacoresistant, i.e. they experience seizures which are resistant to AED action. Drug resistant epilepsy is defined as: 'failure of adequate trials of two tolerated and appropriately chosen and used AED schedules (whether as monotherapies or in combination) to achieve sustained seizure freedom' (Kwan *et al.*, 2010). The majority of observed drug resistance occurs relatively soon after diagnosis in early treatment and any further attempt to control seizures with drug treatment is usually futile. This suggests the mechanism by which individuals become resistant is *de novo*, does not develop over time, and is not associated with prolonged therapy (Kwan *et al.*, 2000). Although the causative biological mechanism of drug resistance in epilepsy is likely to be multifactorial, a number of hypotheses have been postulated over the last decade aiming to elucidate plausible causes of resistance.

1.4.1 The target hypothesis

The target hypothesis proposes a pharmacodynamic explanation for drug resistant epilepsy - that functional alterations in the cellular targets of AEDs lead to a reduced sensitivity to treatment. The main evidence directly supporting this hypothesis is that alterations in common AED targets such as changes in expression of the subunits which comprise voltage-gated sodium/calcium channels and $GABA_A$ receptors are observed in both animal models and human temporal lobe epilepsy (TLE) (Remy *et al.*, 2003). However, association between observed changes in AED targets and sensitivity to

AEDs has thus far not been observed *in vivo*. The main argument against this hypothesis is that a complete understanding of the molecular action of most AEDs is lacking but is likely to result from concerted efficacy at multiple targets. Given that people with drug resistant epilepsy are, by definition, resistant to multiple AEDs, the target hypothesis would only be plausible if the sensitivity of all of those targets to modulation by AEDs was impaired equally (Margineanu *et al.*, 2009).

1.4.2 The transporter hypothesis

The arguments against the target hypothesis point towards a pharmacokinetic explanation of resistance which takes into account the heterogeneous nature of drug resistant epilepsy. The transporter hypothesis postulates that over-expression of drug efflux transporters on cerebral microvascular endothelial cells which contribute to the integrity of the blood-brain barrier may reduce AED accumulation in the brain, preventing therapeutically active concentrations of AEDs from reaching their targets in the brain. The evidence supporting this hypothesis focuses on one drug efflux transporter in particular: P-glycoprotein (P-gp). P-gp has been shown to be overexpressed in cerebral microvascular endothelial cells from epileptic brain tissue resected from people with pharmacoresistant epilepsy and in rodent seizure models, particularly in those animals with drug resistant seizures (Tishler *et al.*; Sisodiya *et al.*, 2002; Volk *et al.*, 2005). Several AEDs, including PHT, CBZ, LTG and GBP, have also been suggested to be substrates for multidrug transporters, further supporting the transporter hypothesis (Sills *et al.*, 2002; Löscher *et al.*, 2005b; Luna-Toetos *et al.*, 2008). However, not all AEDs are substrates for multidrug transporters and of the AEDs implicated as substrates for P-gp none have consistently been shown to be transported to a significant extent. Moreover, conflicting evidence exists which suggests P-gp mediates very weak transport of AEDs at best (Owen *et al.*, 2001; Sills *et al.*, 2002; Dickens *et al.*, 2013).

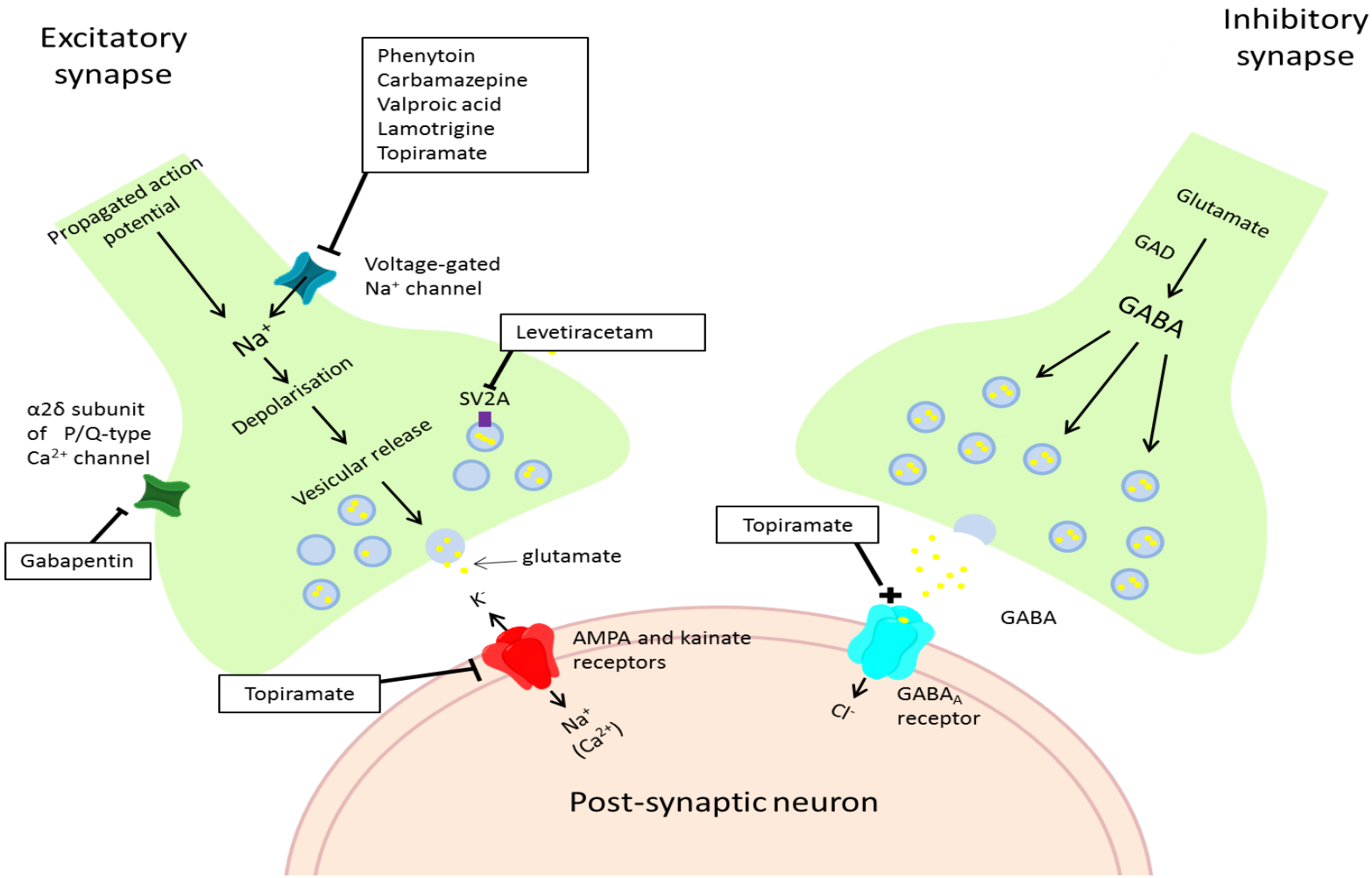

Figure 1.1: Common molecular targets of AEDs used in this project. Adapted from (Bialer *et al.*, 2010).

1.4.3 Alternative hypotheses

The target and transporter hypotheses of drug resistant epilepsy are both the longest standing and most researched hypotheses attempting to explain drug resistant epilepsy. However, more recently several alternative hypotheses have been postulated. One hypothesis that has recently been postulated is that seizures are a manifestation of impaired mitochondrial energy production in the epileptogenic zone. There is a significant correlation between lower bienergetic state in the epileptogenic i.e. impaired mitochondrial function and thus energy production and higher extracellular glutamate. High extracellular glutamate is linked with increased hyperexcitability hence there is a close relationship between metabolic dysfunction and hyperexcitability (Waldbaum *et al.*, 2010; Yuen *et al.*, 2011). One line of evidence supporting this hypothesis is that in many individuals with drug resistant epilepsy, the ketogenic diet is effective in reducing seizures (Masino *et al.*, 2012). Experimentally, the positive effects of the ketogenic diet have been associated with up-regulation of mitochondrial genes and increased mitochondrial biogenesis (DeVivo *et al*., 1978). Therefore increased cerebral mitochondrial function and thus energy may result in increased neuronal stability and seizure control. However, the proponents of this hypothesis acknowledge that it is the interplay of mitochondrial energy production along with the ictogenic potential of the epileptic focus and efficacy of AEDs that determine the likelihood of a seizure occurring (Yuen *et al.*, 2011).

Another hypothesis recently postulated is the epigenetic hypothesis which proposes that drug resistance may result from epilepsy associated epigenetic alterations (Kobow *et al.*, 2013). This is based on the observation that the expression of many of the genes involved in processes such as inflammation, synaptic plasticity and synaptic transmission, which share common regulatory mechanisms such as histone tail modifications and DNA methylation are altered long term following seizures. However, the mechanisms of epigenetic alterations are still poorly understood (Kobow *et al.*, 2013). One final hypothesis that is beginning to receive attention is the intrinsic severity hypothesis (Rogawski, 2013). Rather than trying to explain resistance by dependent cellular mechanisms, the intrinsic severity hypothesis simply suggests that pharmacoresistance is an inherent property of the epilepsy and results from factors relating to the underlying aetiology of the disease – the more severe the epilepsy, the

more likely it is to be resistant (Rogawski, 2013). It should be borne in mind that these hypotheses, whether target, transporter or more recent alternatives, are not mutually exclusive. They are all potentially involved in the phenomenon of drug resistant epilepsy and two or more may be at play at any given time in any given patient who does not respond to AED therapy.

1.5 The blood-brain barrier

For any neurotherapeutic agent to reach its molecular target in the brain and exert its pharmacological effects, it must first penetrate a specialised, protective barrier which lines almost all cerebral microvessels, otherwise known as the blood-brain barrier (BBB; *figure 1.2*). The blood-brain barrier compromises a monolayer of endothelial cells, specialised in their barrier function due to the presence of elaborate junctional complexes (*zonulae occludentes*) that eliminate gaps between neighbouring cells and prevent toxins and blood-borne substances from penetrating the brain via paracellular diffusion (Abbott *et al.*, 1996; Abbott *et al.*, 2010). These junctional complexes between endothelial cells include tight junctions and adherens junctions. Adherens junctions consist of cadherin proteins spanning the intercellular cleft and are linked to the cell cytoplasm by scaffolding proteins such as catenin. These scaffolding proteins link to the actin cytoskeleton of neighbouring cells and tether endothelial cells together to give structural support (Abbott *et al.*, 2010). Adherens junctions are critical for the formation of tight junctions, tight junctions consist of occludins and claudins which also span the intercellular cleft and along with junctional adhesion molecules (JAMs) connect adjacent endothelial cells. JAMs also link to a number of cytoplasmic scaffolding and regulatory proteins, such as zonula occludens and cingulin, which link the junctional complex to the actin cytoskeleton and initiate signalling between neighbouring cells (Abbott *et al.*, 2010).

However, the BBB is not simply a protective barrier. It also serves as a dynamic interface interacting with CNS cells such as pericytes, astrocytes and microglia to form the neurovascular unit (Cardoso *et al.*, 2010). Within the neurovascular unit, the BBB is crucial for homeostasis of the CNS and contributes to the control of molecular traffic to preserve neuronal connectivity, the maintenance of ion concentrations for optimal signalling, and immune surveillance to minimise inflammation and cell damage (Redzic, 2011; Benarroch, 2012).

Transporter	Alias	Cellular location (if known)
ABCB1	MDR1/P-glycoprotein	Apical
ABCG2	Breast cancer resistance protein (BCRP)	Apical
ABCC1	Multidrug resistance protein 1 (MRP1)	Apical and basolateral
ABCC2	Multidrug resistance protein 2 (MRP2)	
ABCC3	Multidrug resistance protein 3 (MRP3)	
ABCC4	Multidrug resistance protein 4 (MRP4)	Apical
ABCC5	Multidrug resistance protein 5 (MRP5)	Apical
ABCC6	Multidrug resistance protein 6 (MRP6)	
SLCO1A2	Organic anion transporting polypeptide 1A2 (OATP1A2)	Apical
SLCO1A4	Organic anion transporting polypeptide 1A4 (OATP1A4)	Basolateral
SLCO1C1	Organic anion transporting polypeptide 1C1 (OATP1C1)	
SLCO2B1	Organic anion transporting polypeptide 2B1 (OATP2B1)	Apical
SLC22A1	Organic cation transporter 1 (OCT1)	Apical
SLC22A2	Organic cation transporter 2 (OCT2)	Apical
SLC22A3	Organic cation transporter 3 (OCT3)	
SLC22A5	Organic carnitine transporter 2 (OCTN2)	Apical
SLC22A6	Organic anion transporter 1 (OAT1)	
SLC22A7	Organic anion transporter 2 (OAT2)	Apical
SLC22A8	Organic anion transporter 3 (OAT3)	
SLC47A1	Multidrug and toxin extrusion pump 1 (MATE1)	
SLC16A1	Monocarboxylic acid transporter 1 (MCT1)	Apical and basolateral
SLC16A7	Monocarboxylic acid transporter 2 (MCT2)	Basolateral
SLC16A3	Monocarboxylic acid transporter 4 (MCT4)	
SLC16A2	Monocarboxylic acid transporter 8 (MCT8)	Apical and basolateral
SLC28A1	Nucleoside transporter CNT1	Basolateral
SLC28A2	Concentrative nucleoside transporter 2 (CNT2)	
SLC28A3	Concentrative nucleoside transporter 3 (CNT3)	
SLC29A1	Equilibrative nucleoside transporter 1 (ENT1)	Apical
SLC29A2	Equilibrative nucleoside transporter 2 (ENT2)	
SLC29A4	Equilibrative Nucleoside Transporter 4 (PMAT/ENT4)	Basolateral
SLC2A13	Facilitated glucose transporter 13 (GLUT13)	
SLC5A1	Sodium/glucose co-transporter 1 (SGLT1)	Basolateral
SLC5A3	Sodium myoinositol co-transporter (SMIT)	Apical
SlC7A1	Cationic L-amino acid transporter 1 (CAT1)	Apical
SlC7A3	Cationic L-amino acid transporter 2 (CAT2)	
SLC7A5	L type acid transporter 1 (LAT1)	Apical and basolateral
SLC7A6	Y+L type amino acid transporter 2 (LAT2)	Apical and basolateral
SLC38A2	System N amino acid transporter 2 (SNAT2)	Basolateral
SLC38A3	System N amino acid transporter 3 (SNAT3)	Basolateral
SLC28A5	System N amino acid transporter 5 (SNAT5)	
SLC1A3	Excitatory amino acid transporter 1 (EAAT1)	Basolateral
SLC1A2	Excitatory amino acid transporter 2 (EAAT2)	
SLC1A1	Excitatory amino acid transporter 3 (EAAT3)	
SLC1A4	Glutamate/neutral amino acid transporter 4 (ASCT1)	Basolateral
SLC1A5	Neutral amino acid transporter 5 (ASCT2)	
	High affinity aspartate/glutamate transporter 6 (EEAT4)	Apical
SLC6A9	Glycine/neurotransmitter transporter 9 (GLYT1)	Apical
SLC6A6	Neurotransmitter transporter 6 (TAUT)	Apical and basolateral
SLC44A1	Choline transporter 1 (CTL1)	Apical

Table 1.1: Transporters which have been shown to be functional at the blood-brain barrier, adapted from (Abbott *et al*., 2010; Stieger *et al*., 2015). In addition a number of transporters not included have been shown to be expressed at gene and/or protein level in isolated brain microvessels (Shawahna *et al*., 2011; Geier *et al*., 2013).

One characteristic of the BBB that aids in its homeostasis role is the expression of transporter proteins. These proteins function to actively transport nutrients into the CNS and to restrict toxins from entering (Urquhart *et al.*, 2009). The distribution of transporter proteins at the BBB is polarized and expression is usually either apical or basolateral, depending on the particular function of the transporter protein (table 1.1). Efflux transporters are largely expressed on the basolateral surface of the BBB due to their role in pumping toxins out of the brain into the blood, thus preventing chemical insult (Abbott, 2013). Influx transporters mainly function to supply the brain with nutrients and macromolecules which otherwise could not penetrate the BBB (Pardridge, 1986) and thus are largely expressed at the apical surface (Abbott, 2013). In addition to their homeostasis role, transporter proteins expressed at the BBB are known to transport a variety of chemically diverse drugs and have been shown to impact on CNS accumulation of substrate drugs (König *et al.*, 2013).

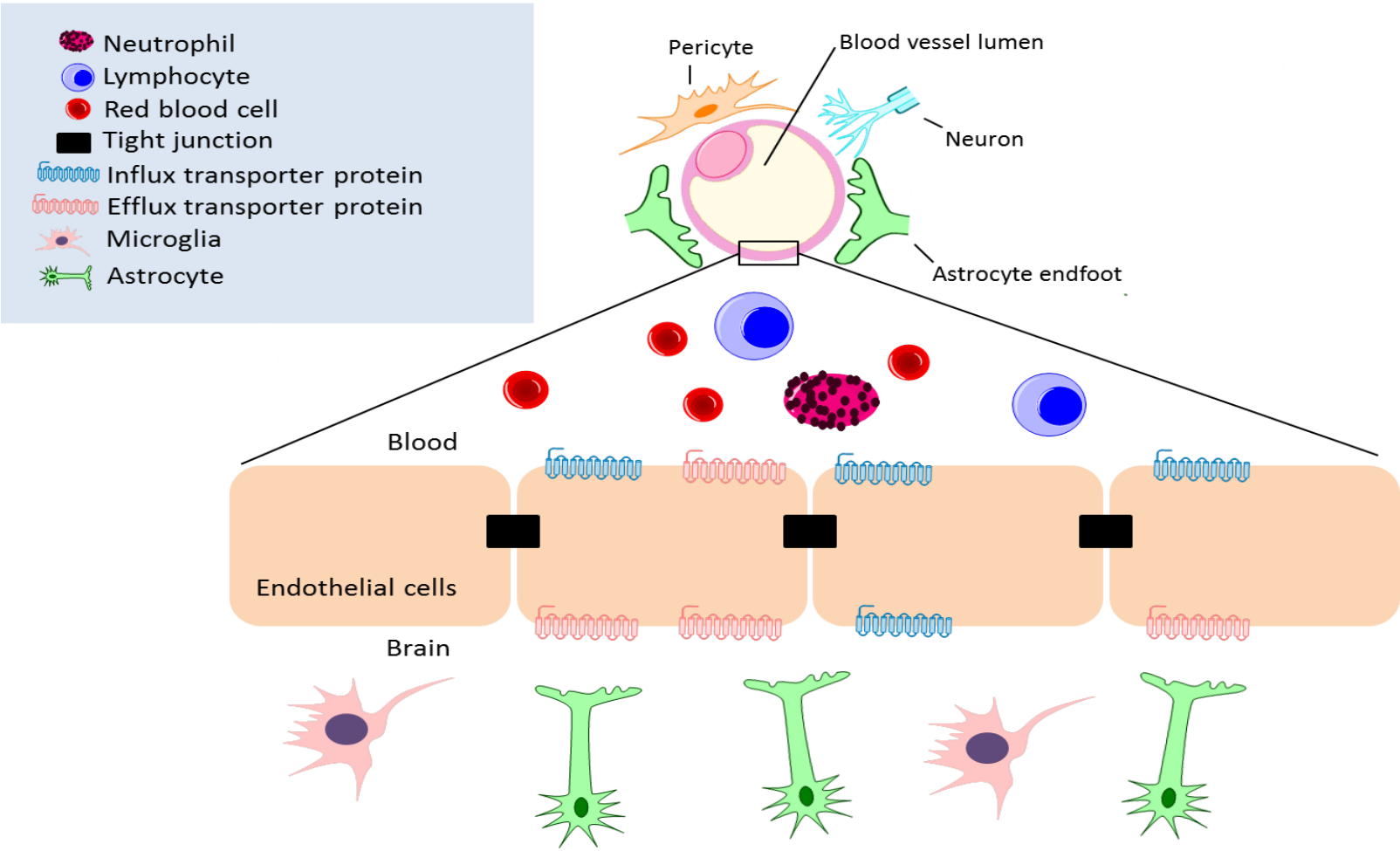

Figure 1.2: The blood brain barrier, adapted from (Abbott *et al.*, 2010).

1.6 The ABC superfamily of transporters

The ATP-binding cassette (ABC) superfamily of transporter proteins includes 49 membrane bound proteins divided into seven families, designated ABC A to G *(table 1.2).* ABC transporters share a common mechanism, utilising energy by hydrolysing ATP to translocate a broad range of molecules including vitamins, ions, peptides and xenobiotics across the plasma membrane and are specifically identified by the presence of a highly conserved ATP-binding cassette of 200-250 amino acids (Dallas *et al.*, 2006). Generally, the structure of ABC transporters consists of two linked functional units, each containing an ATP binding cassette and a 12-transmembrane domain complex (Stanley *et al.*, 2009).

1.6.1 The ABCB subfamily

The ABCB subfamily contains the most comprehensively researched ABC transporter protein, multidrug resistance protein 1 (MDR1), more commonly known as P-gp. Although P-gp is commonly reported as the gene product of the *ABCB1* gene, it is also encoded by the *ABCB4* gene (van der Bliek *et al.*, 1988). P-gp is ubiquitously expressed at the apical membrane of epithelial and endothelial cells, including those at the BBB. The highest expression of P-gp is found in tissues with an excretory function, such as the liver, kidneys and gastrointestinal tract (Klaassen *et al.*, 2010). P-gp was the first drug transporter to be discovered after it was shown to be over- expressed in CHO cells resistant to colchicine and various cytotoxic chemotherapy drugs (Juliano *et al.*, 1976). Since its discovery as a drug transporter, P-gp has been shown to efflux a range of chemically diverse amphipathic drugs. As a result, it impacts on the bioavailability and accumulation of substrate drugs at target organs and therefore has been associated with drug resistance (de Lange, 2004).

The transport of AEDs by P-gp has been extensively investigated however such investigation has reported conflicting findings with *in vitro* studies returning largely negative data while *in vivo* investigations have returned largely positive or inconclusive data. In rodent models of epilepsy P-gp has been shown to contribute to pharmacoresistance. Increased cerebral endothelial cell expression of P-gp is observed at the seizure focus of pharmacoresistant rats compared to pharmacosensitive rats and increased P-gp expression is associated with decreased brain concentrations of AEDs that are P-gp substrates (Potschka *et al.*, 2001; Potschka *et al.*, 2002; Sills *et al.*, 2002;

Volk *et al.*, 2005; van Vliet *et al.*, 2007). Furthermore, seizures transiently increase P-gp expression at the BBB (Bankstahl *et al.*, 2008) and inhibition of P-gp has been shown to enhance efficacy of AEDs (Brandt *et al.*, 2006). Conversely investigation into AED transport by P-gp using *in vitro* models including models of the BBB and cell lines overexpressing P-gp has produced almost exclusively negative results (Crowe *et al.*, 2006; Dickens *et al.*, 2013). In human epilepsy tissue, P-gp expression is increased at the BBB in people with pharmacoresistant epilepsy, both in epileptogenic tissues removed in resection surgery (Tishler *et al.*, 1995; Sisodiya *et al.*, 2002; Aronica *et al.*, 2003) and post mortem (Liu *et al.*, 2012). Recently new technology utilising *in-vivo* PET imaging with the P-gp substrate (R)-[^{11}C] verapamil has provided direct *in vivo* evidence that there is over-activity of P-gp at the epileptic focus of patients with pharmacoresistant TLE, as compared with seizure free patients with TLE. Furthermore such over-activity is associated with increased seizure frequency (Feldmann *et al.*, 2013). Other efflux transporters have received some attention but similarly have returned ambiguous findings (Potschka *et al.*, 2001; Cerveny *et al.*, 2006).

ABC family	Subfamily members	Protein product
ABCA	*ABCA1*	
	ABCA2	
	ABCA3	
	ABCA4	
	ABCA5	
	ABCA6	
	ABCA7	
	ABCA8	
	ABCA9	
	ABCA10	
	ABCA11	
	ABCA12	
	ABCA13	
ABCB	*ABCB1*	Multidrug resistance protein 1(MDR1)
	ABCB2	Transporter associated with antigen processing 1 (TAP1)
	ABCB3	Transporter associated with antigen processing 2 (TAP2)
	ABCB4	Multidrug resistance protein 3 (MDR3)
	ABCB5	
	ABCB6	
	ABCB7	
	ABCB8	
	ABCB9	
	ABCB10	
	ABCB11	
ABCC	*ABCC1*	Multidrug resistance associated protein 1 (MRP1)
	ABCC2	Multidrug resistance associated protein 2 (MRP2)
	ABCC3	Multidrug resistance associated protein 3 (MRP3)
	ABCC4	Multidrug resistance associated protein 4 (MRP4)
	ABCC5	Multidrug resistance associated protein 5 (MRP5)
	ABCC6	Multidrug resistance associated protein 6 (MRP6)
	ABCC7	Cystic fibrosis transmembrane conductance regulator (CFTR)
	ABCC8	Sulfonylurea receptor 1 (SUR)
	ABCC9	Sulfonylurea receptor 2 (SUR2)
	ABCC10	Multidrug resistance associated protein 7 (MRP7)
	ABCC11	Multidrug resistance associated protein 8 (MRP8)
	ABCC12	
ABCD	*ABCD1*	
	ABCD2	
	ABCD3	
	ABCD4	
ABCE	*ABCE1*	
ABCF	*ABCF1*	
	ABCF2	
	ABCF3	
ABCG	*ABCG1*	
	ABCG2	Breast cancer resistance protein (BCRP)
	ABCG4	
	ABCG5	
	ABCG8	

Table 1.2: Currently identified ATP-binding cassette (ABC) transporter genes, according to the HUGO gene nomenclature committee http://www.genenames.org/.

1.6.2 The ABCC subfamily

The ABCC sub-family encodes the multidrug resistance associated proteins (MRPs). The MRPs function endogenously to transport organic anions and are described as multidrug resistance transporters due to their associated resistance to many chemotherapy agents. The human ABCC family has 12 members, including the cystic fibrosis transmembrane conductance regulator (CFTR) encoded by *ABCC7*, the sulfonylurea receptors (SURs) encoded by *ABCC8* and *ABCC9*, and ten transporter proteins known as the MRPs, six of which have been fully characterised and shown to transport drugs (Toyoda *et al.*, 2008). MRPs are known to mediate the active efflux of many anionic drugs such as methotrexate, although MRP1, MRP2 and MRP3 have also been shown to transport neutral organic compounds (Löscher *et al.*, 2005a). Homology between MRP isoforms varies, with MRP1, MRP2, MRP3 and MRP6 sharing around 50% homology and accordingly possessing very similar substrate specificities. In contrast, MRP4 and MRP5 share less than 40% amino acid sequence homology with other isoforms due to their smaller size and lack of one transmembrane and N-terminal domain (Borst *et al.*, 2000). As with all major efflux transporters, expression of MRPs is largely limited to blood-tissue barriers and organs with excretory functions such as the liver and kidneys. However, MRP3 and MRP4 are also expressed in tissues such as the pancreas, bladder, reproductive organs and gut, while MRP1 and MRP5 are ubiquitously expressed (Szakács *et al.*, 2008).

1.6.3 The ABCG subfamily

The most widely known product of the ABCG gene family is breast cancer resistance protein (BCRP), which is encoded by the *ABCG2* gene. In addition to P-gp and the MRP series of ABC transporters, BCRP has been widely implicated in multiple drug resistance. BCRP is a 70kDa protein which, like P-gp and MRP1, was discovered in cell lines resistant to chemotherapy drugs (Qian *et al.*, 2013). At present, BCRP is known to actively extrude a wide variety of therapeutics including antivirals, chemotherapeutic drugs and antibacterials (Estudante *et al.*, 2013). However, its role in the transport of AEDs is unclear with previous research finding no evidence of BCRP-mediated extrusion of the AEDs, including Primidone (PRM), PB, PHT, CBZ, LTG, clonazepam (CZP), ethosuximide (ESM) and VPA, in a stably transfected MDCK cell line (Cerveny *et al.*, 2006).

1.7 The solute carrier superfamily

The solute carrier (SLC) superfamily of transporters move molecules at around 10^2 – 10^4 s^{-1} and include symporters, antiporters and passive transporters. The human SLC superfamily consists of 55 gene families *(table 1.3)* which comprise at least 362 putatively functional genes whose protein products are predominantly transmembrane transporters (He *et al.*, 2009). Each protein within a single SLC family is thought to share around 20-25% amino acid sequence identity. Several significant families exist, including the organic cation transporters (OCTs), organic cation/carnitine transporters (OCTNs), organic anion transporters (OATs), organic anion transporting polypeptides (OATPs) and nutrient transporters including monocarboxylate transporters (MCTs), high affinity glucose transporters (GLUTs) and a variety of amino acid transporters. In addition multiple less well-characterised transporters such as peptide transporters, nucleoside transporters, neurotransmitter transporters and bicarbonate transporters are known (Klaassen *et al.*, 2010).

1.7.1 Organic anion transporting polypeptides

OATPs are members of the *SLCO* gene family of SLC transporters, of which there are 11 known transporter proteins. Members of the same family of OATP transporter have around 40% amino acid sequence identity, with a total of six families described e.g. OATP1, OATP2, OATP3, OATP4, OATP5 and OATP6 (table 1.4). Members of the same sub-family, e.g. OAPT1A, OATP1B, share 60% amino acid homology (Hagenbuch *et al.*, 2004). Structurally, OATPs consist of 12 transmembrane domains, with a large extracellular domain containing conserved cysteine residues between transmembrane segments 9 and 10 and N-glycosylation sites in extracellular loops two and five (Hagenbuch *et al.*, 2004). OATP orthologues vary in length from 643 amino acids (OATP2A1) to 848 amino acids (OATP5A1) and mediate the sodium-independent transport of various amphipathic organic compounds, particularly those with high molecular weight and high albumin binding (Kullak-Ublick *et al.*, 2001; Tirona *et al.*, 2001; Mikkaichi *et al.*, 2004; Huber *et al.*, 2007; Hagenbuch *et al.*, 2008). These include bile salts, steroid conjugates, drugs and other xenobiotics that are transported on an anion exchange based mechanism, coupling the cellular uptake of organic compounds with the efflux of anions such as bicarbonate (Hagenbuch *et al.*, 2003). Although a collection of OATP transporters are involved solely in hepatic clearance, most OATPs are ubiquitous and found in various tissues such as the BBB, choroid plexus, lung, heart, kidney, intestine, testis and placenta (Kalliokoski *et al.*, 2009) *(table 1.4)*.

Gene Family	Endogenous transport function
SLC1	Glutamate and amino acid transporters
SLC2	Facilitated glucose/fructose transporters
SLC3	Heavy chain amino acid transporters
SLC4	Sodium bicarbonate/ anion exchangers
SLC5	Sodium coupled sugar/vitamin/ monocarboxylate transporters
SLC6	Neurotransmitter/ neutral amino acid transporters
SLC7	Amino acid transporters
SLC8	Sodium/calcium transporters
SLC9	Proton linked cation antiporters
SLC10	Sodium-bile co-transporters
SLC11	Divalent metal ion transporters
SLC12	Sodium/chloride/sulphate/ transporters
SLC13	Sodium dependent dicarboxylate/citrate transporters
SLC14	Urea transporters
SLC15	Oligopeptide transporters
SLC16	Monocarboxylate transporters
SLC17	Vesicular glutamate/nucleotide transporters
SLC18	Vesicular acetylcholine/ monoamine transporters
SLC19	Folate/thiamine transporters
SLC20	Phosphate transporters
SLC22	Organic cation/anion transporters
SLC23	Ascorbic acid transporters
SLC24	Sodium/potassium/calcium exchangers
SLC25	Mitochondrial carriers
SLC26	Anion exchangers
SLC27	Fatty acid transporters
SLC28	Concentrative nucleoside transporters
SLC29	Equililbrative nucleoside transporters
SLC30	Zinc transporters
SLC31	Copper transporters
SLC32	Vesicular GABA transporters
SLC33	Acetyl-CoA transporters
SLC34	Sodium/phosphate transporters
SLC36	Nucleotide/sugar transporters
SLC37	Proton linked amino acid symporters
SLC38	Unknown
SLC39	Zinc transporters
SLC40	Iron regulated transporters
SLC41	Magnesium transporters
SLC43	L-amino acid transporters
SLC44	Choline transporters
SLC45	Unknown
SLC46	Folate transporters
SLC47	Multidrug and toxin extrusion pumps
SLC48	Heme transporters
SLC50	Sugar efflux transporters
SLC52	Riboflavin transporters
SLCO	Organic anion transporters

Table 1.3: A comprehensive list of known SLC families approved by the HUGO gene nomenclature committee: http://www.genenames.org/.

	Expression	Endogenous substrates	Substrate drugs	Inhibitors
OATP1A	Ubiquitous	Estrone-3-sulphate/ bile salts/steroid conjugates prostaglandin E2/	Beta-blockers/ celiprolol/fexofenadine/ levofloxacin/ methotrexate/ quinidine/ protease inhibitors/ erythromycin/ imatinib	Naringin/ narringenin/ ritonavir/ lopinavir/ saquinavir/ rifampicin
OATP1B	Hepatocytes	Estrone-3-sulphate/ thyroxine (T4)/ triidothyronine (T3)	Benzyl penicillin/statins/fluorescein/methotrexate/ olmesartan/saquinavir	Ritonavir/ cyclosporine/ rifampicin/ lopinavir
OATP1C	BBB/choroid plexus/ ciliary body epithelium	thyroxine (T4)/ triidothyronine (T3)	Bromosulfophthalein	Phenytoin/ fenamic acid/ diclofenac
OATP2A	Ubiquitous	Prostaglandin $E_1/E_2/H_2$ other eicosanoids	Unknown	Unknown
OATP2B	Liver/placenta/ heart/ciliary body	Estrone-3-sulphate/ prostaglandin E_2/ thyroxine(T4)	Statins/ benzyl penicillin/ bosentan/fenofenadine/ talinolol	Rifampicin/ cyclosporine
OATP3A	Ubiquitous	Prostaglandin E_1/ prostaglandin E_2/thyroxine OATP3A1_v1 only: estrone-3-sulphate OATP3A1_v2 arachidonic acid	Vasopressin OATP3A1_V1 only: benzyl penicillin deltorphin	Unknown
OATP4A	Ubiquitous	Triiodothyronine T3/ prostaglandin E_2/ estrone-3-sulfate	Benzyl penicillin	*p*-aminohippuric acid
OATP4C	Kidney	Thyroxine (T4)/ triiodothyronine (T3)/ estrone-3-sulphate/ cAMP	Digoxin/methotrexate/ ouabain/ sitagliptin/	Unknown
OATP5A	Uncharacterised	Unknown	Unknown	Unknown
OATP6A	Testis, spleen, brain, foetal brain, placenta	Unknown	Unknown	Unknown

Table 1.4: Classification of OATP family members on the basis of tissue distribution and substrate and inhibitor specificity. Substrates and inhibitors included are for illustrative purposes only and do not reflect the full repertoire of known OATP substrates/inhibitors (Fujiwara *et al.*, 2001; Hagenbuch *et al.*, 2004; Lee *et al.*, 2004; Kusuhara *et al.*, 2005; Kalliokoski *et al.*, 2009; Westholm *et al.*, 2009; Giacomini *et al.*, 2010; Roth *et al.*, 2012).

1.7.2 Organic anion transporters

The OATs are a group of proteins belonging to a distinct and significant family of SLC transporters encoded by the *SLC22A* genes. OATs are membrane proteins, 542-553 amino acids in length and are predicted to have 12 transmembrane domains arranged in two sets of six helices with two large loop structures expected between transmembrane domains 1 and 2 and 6 and 7 (Cha *et al.*, 2000; Klaassen *et al.*, 2010; Riedmaier *et al.*, 2012). OATs function via a sodium-independent dicarboxylic acid exchange, whereby organic anions are pumped into the cell in exchange for dicarboxylate ions against a chemical and electrical gradient, thereby forcing anions into an already negative intracellular environment (Sekine *et al.*, 2000; VanWert *et al.*, 2010). The substrate specificity of OATs is incredibly diverse and includes important pharmacological agents, steroid hormones and their metabolites, biogenic amine metabolites, environmental contaminants, and toxins (VanWert *et al.*, 2010). Currently, 12 OAT isoforms have been identified of which 7 have human variants and 4 of which have been extensively investigated as drug transporters (Giacomini *et al.*, 2010). Each of these is described briefly below.

OAT1, encoded by the *SLC22A6* gene, is predominantly expressed in the kidney proximal tubule and to a lesser extent in the placenta and brain (Giacomini *et al.*, 2010; VanWert *et al.*, 2010). OAT1 is known to mediate the high affinity transport of prostaglandins E2 and F2α, in addition to several acidic neurotransmitter metabolites and the second messenger cyclic guanosine monophosphate (cGMP) (Burckhardt *et al.*, 2011). Functional studies using expression systems such as *Xenopus laevis* oocytes, Chinese hamster ovary (CHO) cells, *Drosophila melanogaster*, and human embryonic kidney (HEK) cells have all been successful in characterising drug substrates and inhibitors of OAT1 (VanWert *et al.*, 2010), as outlined in table 1.5.

Drug	Substrate	Inhibitor
Angiotensin II receptor blockers		
Candesartan		+
Losartan		+
Olmesartan	+	+
Pratosartan		+
Telmisartan		+
Valsartan		+
Diuretics		
Bumetanide	+	+/-
Chlorothiazide		+
Cyclothiazide		+
Ethacrynate		+
Furosemide	+	+
Hydrochlorothiazide		+/-
Methazolamide		+
Torasemide		+
Trichlormethiaz		+
Statins/fibrates		
Atorvastatin		-
Bezafibrate		+
Fluvastatin		+
Pravastatin	-	+/-
Rosuvastatin	-	-
Simvastatin		+
Antivirals		
Acyclovir	+	+
Adefovir	+	+
Cidofovir	+	+
Ganciclovir	+	+
Tenofovir	+	
Zalcitabine	+	+
Zidovudine	+	+
Antidiabetics		
Metformin	-	
Sitagliptin	-	-
H2 antagonists/PPI's		
Cimetidine	+	+
Famotidine	-	-
Omeprazole		+
Ranitidine	+	
Other		
Valproate		+
Allopurinol		+
Benzbromarone		+
Probenecid		+
Fenofenadine	-	
ACE Inhibitors		
Captopril	+	+
Quinaprilat	+	
Antineoplastics		
Azathioprine		-
Imatinib	-	
6-Mercaptopurine		
Methotrexate	+/-	-

Drug	Substrate	Inhibitor
Antibiotics		
Benzyl penicillin	+/-	+/-
Cefaclor		+
Cefadroxil		+
Cefamandol		+
Cefazolin	-	+
Cefdinir	+	+
Cefoperazone		+
Cefoselis	-	+
Cefotaxime		+
Cefotiam	-	+
Ceftibuten	+	+
Ceftizoxime	+	+
Ceftriaxone		+
Cephalexin		
Cephaloridine	+	+
Cephalothin		
Cephradine		+
Cinoxacin		+
Ciprofloxacin	-	-
Doxycyclin		+
Erythromycin		
Gentamycin		
Grepofloxacin		-
Levofloxacin	-	-
Minocyclin		+
Nalidixate		+
Oxytetracycline		+
Tetracycline	+	+
NSAIDs		
Acetaminophen		+
Acetylsalicylate	-	+
Antipyrine		+
Diclofenac		+
Diflusinal		+
Etodolac		+
Flufenamate		+
Flurbiprofen		+
Ibuprofen	+/-	+
Indomethacin	+	+
Ketoprofen	+/-	+
Loxoprofen		+
Mefenamate		+
Naproxen		+
Phenacetin		+
Phenylbutazone		+
Piroxicam		+
Salicylic acid	+	+
Sulindac		+
Tolmetin		+
Immunosuppressant's		+
Cyclosporin A		-
Mycophenolate	-	+
Tacrolimus		-

Table 1.5: Substrates and inhibitors of the organic anion transporter 1 (OAT; adapted from (Burckhardt *et al.*, 2011)). + transported/inhibits, - not transported/inhibited, +/- transport/inhibition disputed.

OAT2, encoded by the *SLC22A7* gene, is the only OAT transporter which has ubiquitous expression and is highly abundant in most tissues (Cropp *et al.*, 2008). Like OAT1, OAT2 also mediates the transport of endogenous prostaglandins, transporting prostaglandin E2 at a higher affinity than OAT1 (Sekine *et al.*, 2000). In addition, OAT2 is thought to transport endogenous nucleobases, nucleosides, and nucleotides, particularly guanine analogues and cyclic nucleotides, most prominently cGMP (Cropp *et al.*, 2008). The drug substrate profile of OAT2 is somewhat similar in chemical diversity to OAT1, however at present the number of known substrates is significantly less (Cropp *et al.*, 2008; VanWert *et al.*, 2010; Burckhardt *et al.*, 2011).

OAT3, encoded by the *SLC22A8* gene, possesses a very similar substrate-inhibitor profile to OAT1 (Giacomini *et al.*, 2010; VanWert *et al.*, 2010) but has much lower affinity for substrate drugs (Anzai *et al.*, 2006). However, OAT3 mediates the transport of endogenous prostaglandins at the highest affinity of all OAT transporters and additionally transports cGMP, cAMP, cortisol and bile salts (Burckhardt *et al.*, 2011). OAT3 is expressed in the proximal tubule of the kidney and is thought to be expressed in the brain both at the choroid plexus and BBB (Rizwan *et al.*, 2007; Giacomini *et al.*, 2010).

OAT4 is the only OAT isoform specific to humans and has been reported to be expressed in the kidneys, adrenal gland and placenta only (Rizwan *et al.*, 2007). Endogenous transport functions include the high affinity transport of estrone and its derivatives, prostaglandins E2 and F2α and urate. OAT4 exhibits a similar but less extensive drug substrate profile to other OATs discussed (Anzai *et al.*, 2006; VanWert *et al.*, 2010; Burckhardt *et al.*, 2011).

1.7.3 Organic cation transporters

Like OATs, OCTs belong to the *SLC22A* gene family. OCTs are responsible for the transport of both endogenous and exogenous cations, which are positively charged at physiological pH. Due to the heterogeneous nature of substrates transported by OCTs, they are classified as polyspecific and have been shown to transport cations electrogenically using a Na^+ independent mechanism (Ciarimboli, 2008). Three human isoforms of OCT exist, OCT1, OCT2 and OCT3, ranging from 550 to 560 amino acids in length. These proteins share similar membrane topology, consisting of 12

transmembrane domains, intracellular C- and N-termini, a large glycosylated extracellular loop between transmembrane domains 1 and 2 and a large intracellular loop with phosphorylation sites between transmembrane domains 6 and 7 (Choi *et al.*, 2008). Despite structural similarities and overlapping substrate specificities, tissue expression of the different OCT isoforms is relatively distinct (Ciarimboli, 2008).

OCT1, encoded by the *SLC22A1* gene, is a protein of 553 amino acids in length that is largely expressed in hepatocytes and intestinal enterocytes but has also been detected in placenta, on the apical membrane of ciliated epithelial cells in the lung, and most recently on the apical membrane of brain microvascular endothelial cells (Ciarimboli, 2008; Giacomini *et al.*, 2010). OCT1 has been shown to transport substrates such as tetraethylammonium, N-methylpyridinium, oxaliplatin and metformin, and is inhibited by compounds such as quinine, quinidine and verapamil (Giacomini *et al.*, 2010). Most significantly with regard to epilepsy, OCT1 has recently been shown to mediate the high affinity transport of LTG in an *in vitro* BBB model and in a stably transfected OCT1 cell line (Dickens *et al.*, 2012).

OCT2, encoded by the *SLC22A2* gene, is two amino acids longer than OCT1, has broader tissue expression than its orthologue and has been shown to be expressed in proximal tubule cells of the kidney and has also been detected in the spleen, placenta, small intestine and brain (Ciarimboli, 2008; Giacomini *et al.*, 2010). Substrates of OCT2 include dopamine, N-methylpyridinium, tetraethylammonium, metformin, pindolol, procainamide, ranitidine, amantadine, amiloride, oxaliplatin, varenicline, cisplatin and lamivudine. Transport of these substrates by OCT2 can be inhibited by cimetidine, quinidine, testosterone and pilsicainide (Giacomini *et al.*, 2010).

OCT3, encoded by the *SLC22A3* gene, is a 556 amino acid protein that has a wide tissue distribution, including the brain, placenta, heart, skeletal muscle, blood vessels and liver (Choi *et al.*, 2008). Although OCT3 is the most widespread OCT protein, it has been shown to transport a smaller number of substrates than OCT1 and OCT2. These include atropine, dopamine, epinephrine and tetraethylammonium (Klaassen *et al.*, 2010). OCT3 mediated transport of these substances is inhibited by several steroids, and most potently by β-estradiol (Wu *et al.*, 1998).

OCTN1 and OCTN2, encoded by the genes *SLC22A4* and *SLC22A5* respectively, comprise a subfamily of organic carnitine/cation transporters with approximately 30% homology to classical OCT proteins. The OCTNs are so called because of their predominant endogenous function, which is to transport carnitine for use in fatty acid oxidation (Koepsell *et al.*, 2007). OCTN1 and OCTN2 are 551 and 557 amino acids in length respectively and, like many other members of the SLC superfamily, are predicted to have 12 transmembrane domains. OCTN1 and OCTN2 are ubiquitously expressed, with strongest expression in the kidney (Dresser *et al.*, 2000). OCTNs have a similar but less extensive substrate specificity to OCT1 and OCT2, but exhibit a much lower affinity for these substrates (Koepsell *et al.*, 2007).

In addition to the OCTs discussed above, there are two additional cation-specific transporters within the SLC transporter superfamily known as the multidrug and toxic compound extrusion (MATE) proteins. These proteins, MATE1 and MATE2, are encoded by the *SLC47A1* and *SLC47A2* genes respectively. The resulting proteins, which are 570 and 602 amino acids in length respectively, share around 50% sequence homology and consist of 13 transmembrane helices (Zhang *et al.*; Komatsu *et al.*, 2011). MATE transporters are unusual in comparison to other SLC family members by the fact that they function physiologically as efflux rather than influx transporters. However, depending on cellular pH, MATEs can also function as influx transporters, with a more acidic pH increasing MATE mediated extrusion of substrate drugs and a more alkaline pH promoting MATE mediated uptake (Müller *et al.*, 2013). As their name suggests MATE transporters are involved in the elimination of toxins and xenobiotics from the body, thus they are primarily found in the excretory organs: liver and kidney where they work in concert with OCTs to provide an elimination pathway for organic cations (Ciarimboli, 2008). Nevertheless, expression has also been observed in the CNS (Koepsell *et al.*, 2007). MATEs are known to mediate the transport of over 40 clinically relevant cationic drugs such as metformin, cisplatin and captopril in a cation-proton antiport system, with the extrusion of cations enhanced by an opposing (influx) gradient of protons (Staud *et al.*, 2013).

1.7.4 Monocarboxylic acid transporters

The MCT family currently contains 14 identified member genes, 7 of which encode functional transporters and 7 of which encode orphan proteins with no known transport role (table 1.6). All MCTs are predicted to have 12 conserved transmembrane domains, with intracellular C- and N-termini, and a large cytosolic loop between transmembrane segments 6 and 7 (Halestrap *et al.*, 2004; Halestrap, 2013). MCT1 to MCT4, which are encoded by *SLC16A1, SLC16A7, SLC16A8* and *SLC16A4* respectively, have been well characterised experimentally and shown to transport important monocarboxylic fuels such as lactate, pyruvate and ketone bodies in a proton linked mechanism (Halestrap *et al.*, 1990). More recently, MCT8 *(*encoded by *SLC16A2)* and MCT10 *(*encoded by *SLC16A10)* have been shown to mediate the high affinity transport of thyroid hormones and aromatic amino acids, respectively. Interestingly transport by these isoforms is thought to be facilitative rather than proton or sodium linked as with other family members (Friesema *et al.*, 2003; Heuer *et al.*, 2009).

1.7.5 Other SLC families of significance

The GLUT family is a group of 13 SLC transporter proteins that are responsible for the facilitated transport of hexoses into mammalian cells down an electrochemical gradient (Joost *et al.*, 2001). All members of the GLUT family share a common 12 transmembrane helical structure, with both carboxyl and amino terminals located at the cytosolic face and a unique N-linked oligosaccharide side-chain present in either the first or forth extracellular loop (Joost *et al.*, 2001). Of particular interest is GLUT1, which is encoded by the *SLC2A1* gene. GLUT1 is found in almost every tissue in the body reflecting its role as the predominant facilitator of glucose transport into cells. Cell and tissue specific expression of GLUT1 is thus related to the rate of cellular glucose metabolism. For example, high expression is observed at the BBB due to the brain using glucose as its predominant energy source (Uldry *et al.*, 2004). A genetic deficiency in cerebral GLUT1-mediated can result in an infantile epileptic encephalopathy, amongst other CNS complications. A less severe GLUT-1 deficient phenotype has been associated with sporadic epilepsies (Byrne *et al.*, 2011; Mullen *et al.*, 2011).

Alias	Gene name	Tissue distribution (high-low)	Endogenous substrates	Substrate drugs	Inhibitory drugs
MCT1	*SLC16A1*	Ubiquitous (except pancreatic β cells)	Lactate Pyruvate Ketone bodies	Salicylic acid XP13512	Salicylic acid XP13512
MCT2	*SLC16A7*	Testis, spleen, heart, kidney, pancreas, skeletal muscle, brain, leucocytes	Pyruvate Lactate Ketone bodies		GHB
MCT3	*SLC16A8*	Retina, choroid plexus	Lactate		
MCT4	*SLC16A3*	Skeletal muscle, chondrocytes, leucocytes, testis, lung, ovary, placenta, heart, brain	Lactate Ketone bodies		Fluvastatin Atorvastatin Lovastatin Simvastatin
MCT5	*SLC16A4*	Brain, muscle, liver, kidney, lung, ovary, placenta, heart	N/A (Orphan transporter)	N/A	N/A
MCT6	*SLC16A5*	Kidney, muscle, brain, heart, pancreas, prostate, lung, placenta	Unknown	Bumetanide Probenecid Nateglinide	Furosemide Azosemide
MCT7	*SLC16A6*	Brain, pancreas, muscle, prostate	N/A (Orphan transporter)	N/A	N/A
MCT8	*SLC16A2*	Most tissues: liver, heart, brain, intestine, ovary, placenta, lung, kidney, skeletal muscle	T2, T3/ rT3 T4		Imatinib Bosatinib Dasatinib Sunitinb
MCT9	*SLC16A9*	Endometrium, testis, ovary, breast, brain, kidney, spleen, retina	N/A (Orphan transporter)	N/A	N/A
MCT10 (TAT1)	*SLC16A10*	Kidney, intestine, muscle, placenta, heart	Phenylalanine L-tyrosine L-tryptophan T3/T4	L-DOPA	
MCT11	*SLC16A11*	Skin, lung, ovary, breast, lung, pancreas, retina, choroid plexus	N/A (Orphan transporter)	N/A	N/A
MCT12	*SLC16A12*	Kidney, retina, lung, testis	N/A (Orphan transporter)	N/A	N/A
MCT13	*SLC16A13*	Breast, bone marrow	N/A (Orphan transporter)	N/A	N/A
MCT14	*SLC16A14*	Brain, heart, muscle, ovary, prostate, breast, lung, pancreas, liver, spleen, thymus	N/A (Orphan transporter)	N/A	N/A

Table 1.6: The monocarboxylic acid transporter (MCT) family, adapted from (Morris *et al.*, 2008; Halestrap, 2013). L-DOPA (Levodopa), T2 (3, 5-Diiodo-L-thyronine), rT3 (reverse triiodothyronine), T3 (triidothyronine), T4 (thyroxine), TAT-1 (T-type amino acid transporter 1).

Members of the SLC7 family are expressed in most tissues of the body. They can be grouped into two main categories, each of which transports specific amino acids; the cationic amino acid transporters (CATs) and the L-type amino acid transporters (LATs) (Fotiadisa *et al.*, 2013). CATs are N-glycosylated 14 transmembrane domain proteins and form the major route of entry for all cationic amino acids into cells via a sodium-dependant facilitative mechanism. Conversely, LAT proteins consist of 12 transmembrane domains and mediate the high affinity transport of large neutral amino acids via an exchange mechanism (Verrey *et al.*, 2003).

1.8 Aims

The aims of the experiments described in this thesis were to investigate SLC transporters known to be expressed at the BBB and to determine which (if any) mediated the active transport of AEDs at therapeutic concentrations. Throughout these experiments, seven commonly prescribed AEDs, namely PHT, CBZ, VPA, LTG, GBP, TPM and LEV, were consistently studied.

Characterisation of AED transport was undertaken using widely reported model systems such as *Xenopus laevis* oocytes and the human cerebral microvascular endothelial cell line hCMEC/D3, together with novel stably transfected MDCK II cell lines. OATP1A2, the MCT family and the OAT family were specifically selected for investigation due to current knowledge of their substrate specificity, their abundant expression at the BBB, the availability of pharmacological inhibitors, and also because they had not previously been investigated for their potential to transport AEDs.

In addition to investigation of AED transport by MCTs, OATs and OATP1A2, the induction/inhibition of expression of SLC transporters by AEDs was explored in the hCMEC/D3 cell line, in an attempt to understand how AEDs might influence the functionality of endogenous transport pathways. A further study explored the fundamental physiochemical properties of AEDs, which is relevant to their penetration into the brain.

Chapter 2

Transport of antiepileptic drugs by OATP1A2 and MCT1 in a *X. laevis* transport model

2.1 Introduction

The transporter hypothesis aims to explain resistance to AEDs as a result of changes in expression of transporters at the BBB, which may reduce AED accumulation in the brain. The majority of research surrounding this hypothesis has focused on the role of efflux transporters, in particular P-gp, whilst the role of influx transporters of the SLC family has been largely overlooked. Transporters of the SLC family are critical for uptake and homeostasis of many essential nutrients (Pardridge *et al.*, 1977; Pardridge, 1986). In addition it is becoming increasing clear that a number of drugs are subject to transport by the SLC family and that SLC transporters may influence the pharmacokinetics of substrate drugs (König *et al.*, 2013).

The organic anion transporting polypeptides (OATPs) are a well characterised family of SLC transporters encoded by the *SLCO* gene family and have been shown to mediate the sodium-independent transport of a range of chemically diverse drugs (Tamai *et al.*, 2000; Zhang *et al.*, 2002). OATP1B1 and OATP1B3 are the best studied members of the OATP family due to their expression at the sinusoidal membrane of hepatocytes (Hagenbuch *et al*., 2003; Hagenbuch *et al*., 2004). Here they mediate the rate limiting step in the hepatic clearance of many substrate drugs such as statins by transporting them across the sinusoidal membrane into hepatocytes where they are metabolically cleared by the CYP450 system (Hirano *et al*., 2004; Hirano *et al*., 2006).

One isoform of this family, OATP1A2 is a 670 amino acid glycoprotein which shares 66-77% homology with its rodent orthologs (Hagenbuch *et al.*, 2003). OATP1A2 is predominantly expressed at the BBB and although the precise location of its membrane expression is debated, the majority of evidence suggests that OATP1A2 is expressed on the apical membrane of brain endothelial cells (Urquhart *et al.*, 2009). OATP1A2 would thus likely act to pump drugs into brain endothelial cells that comprise the blood-brain barrier from the blood, therefore a reduction in the expression of OATP1A2 might reasonably explain the lack of accumulation of substrate drugs in the brain.

OATP1A2 has been shown to transporter a number of therapeutic agents including imatinib (Eechoute *et al.*, 2011a; Eechoute *et al.*, 2011b), methotrexate (Badagnani *et al.*, 2006), levofloxacin (Maeda *et al.*, 2007) and antiretroviral protease inhibitors (Hartkoorn *et al.*, 2010).

Monocarboxylic acid transporters (MCTs), encoded by the *SLC16* gene family function endogenously to transport fuels and so are predominantly expressed in tissues with high energy demands (Halestrap, 2013). One MCT isoform, MCT1 is known to be expressed at the basolateral and apical membranes of cerebral microvascular endothelial cells (Pierre *et al.*, 2005). The MCT transporter system is critical for brain uptake of fuels such as lactate, pyruvate and in times of calorific restriction ketones and utilises a proton dependent transport mechanism (Pardridge *et al*., 1986).

MCT1 was the first MCT isoform to be cloned from Chinese hamster ovary (CHO) cells in 1994 (Garcia *et al.*, 1994). MCT1 is a 494 amino acid protein, (Enerson *et al.*, 2003) and is ubiquitously expressed (Halestrap *et al.*, 1999). MCT1 transports lactate and pyruvate with high affinity and K_m values of 3-5mM and 0.7mM respectively have been reported depending on the expression system employed (Halestrap *et al.*, 2004).

Both membrane expression and activity of MCT1 has been shown to be dependent on its association with an essential accessory protein basigin (Wilson *et al.*, 2005). Although MCT1 preferentially associates with basigin, it can also associate with another accessory protein embigin in the absence of its primary partner (Poole *et al.*, 1997; Kirk *et al.*, 2000). Basigin and embigin are glycoproteins containing a single transmembrane span which acts as a chaperone, translocating MCT1 to the plasma membrane where the transporter and its accessory protein remain tightly bound. Furthermore dissociation from the accessory protein renders the transporter defunct (Manoharan *et al.*, 2006).

MCT1 has been implicated in the transport of a number of drugs including the drug of abuse γ-hydroxybutyrate (GHB) and the gabapentin pro-drug XP13512 (Cundy *et al.*, 2004; Wang *et al.*, 2006; Morris *et al.*, 2008). More interestingly, MCT1 has been implicated in the transport of VPA (Utoguchi *et al.*, 2000; Fischer *et al.*, 2008) and recently a deficiency of MCT1 on cerebrovascular endothelial cells has been shown in both animal models of temporal lobe epilepsy (TLE) and human tissue resected in the surgical treatment of TLE (Lauritzen *et al.*, 2011; Lauritzen *et al.*, 2012).

Many *in vitro* models have been used previously to investigate functional transport of drugs including surrogate transport cell lines such as Caco-2 cells, overexpressing cell

lines (where the transporter of interest is cloned and transfected into cell lines such as MDCK or HEK293), and *Xenopus laevis* oocytes.

The *X. laevis* oocyte method of transporter expression is a proven, robust tool in the identification of drug transport. cDNAs cloned from cells or other sources can, after *in vitro* transcription to cRNAs, be injected into individual *X. laevis* oocytes and transporter function determined after just 3 days using a radiotracer uptake assay. The main advantages of the *X. laevis* system over somatic cell expression systems are that genetic information can be transferred easily and rapidly, transfection rates are high and the oocytes express very few endogenous transporter proteins to interfere with results (Xia *et al.*, 2007; Markovich, 2008).

The aim of the study described in this chapter was to firstly develop *X. laevis* expression models for both OATP1A2 and MCT1 and to characterise their functional transport using well described control substrates, estrone-3-sulfate and L-lactic acid respectively. These models could then be used in radiotracer uptake assays to determine if OATP1A2 and MCT1 actively transport commonly prescribed antiepileptic drugs at therapeutically relevant concentrations.

2.2 Materials and methods

2.2.1 Materials

Animals: Adult female *X.laevis* were purchased from Xenopus Express (France). *Chemicals:* [^{3}H]-estrone-3-sulfate (specific activity 54.3 Ci/mmol), [^{14}C]-L-lactic acid (specific activity 130.8mCi/mmol), [^{14}C]-phenytoin (specific activity 53.1mCi/mmol) were purchased from Perkin Elmer (Massachusetts, USA). [^{3}H]-lamotrigine (specific activity 5Ci/mmol), [^{3}H]-levetiracetam (specific activity 5Ci/mmol), [^{3}H]-topiramate (specific activity 8Ci/mmol), [^{14}C]-valproic acid (specific activity 8Ci/mmol) were purchased from American Radiolabeled Chemicals Inc. (St. Louis, USA). [^{14}C]-carbamazepine (specific activity 49mCi/mmol) was kindly gifted by Professor Kevin Park (University of Liverpool). *SLC16A1* cDNA I.M.A.G.E. clone was purchased from Source Bioscience Life Sciences (Nottingham, UK), who also carried out sequencing of positive pBluescriptII-KSM-MCT1 clones. *Cla*I, *Spe*I, *Sac*I restriction enzymes, restriction digest buffers 1, 3 and 4, bovine serum albumin (BSA), T4 ligase, Antarctic phosphatase and 5-alpha chemically competent *E.coli* were purchased from New England Biolabs (Hitchen, UK). T3 mMessage mMachine Transcription kit was purchased from Ambion Ltd (Warrington, UK). Fast Start High Fidelity PCR system reagents were purchased from Roche Diagnostics (Burgess Hill, UK). Unless otherwise stated, all other materials were purchased from Sigma-Aldrich (Poole, UK).

2.2.2 Extraction of human *SLC16A1* I.M.A.G.E. cDNA clone plasmid DNA from *E.coli* glycerol stocks

A 50ml culture of LB (Luria-Bertani) broth supplemented with 50µg/ml ampicillin was firstly inoculated with the *SLC16A1* cDNA I.M.A.G.E. clone agar stock and the culture grown overnight at 37^{0}C with vigorous shaking (300rpm; ThermoScientific Thermo Max Q 4450). The following day, overnight cultures were streaked onto LB agar plates (autoclaved, 1M agar supplemented with 50µg/ml ampicillin) at various serial dilutions (neat, 1 in 10, 1 in 100, 1 in 1000) and grown overnight at 37^{0}C. Distinct, single colonies were selected the following day and grown firstly for 8 hours in a small (9ml) LB broth culture (supplemented with appropriate antibiotic) at 37^{0}C with vigorous shaking and secondly overnight in a 50ml culture at the same conditions. The following day plasmid DNA was extracted using the GenElute plasmid maxiprep extraction kit according to manufacturer's protocol as follows.

Overnight cultures were centrifuged at 3,000 *x g* for 15 minutes and the supernatant discarded. The pellet was then resuspended in a total of 12ml resuspension fluid by pipetting up and down. Suspended cells were lysed with 12ml lysis buffer, inverted 6-8 times to mix and left for 3-5 minutes. Lysis was then neutralised with 12ml neutralisation buffer, inverted 4-6 times, and 9ml of binding fluid added. The mixture was then inverted 1-2 times, poured into a filter syringe and incubated for 5 minutes at room temperature to form a white aggregate. Binding columns were prepared by adding 12ml of column preparation to a GenElute column inserted in a 50ml Falcon tube and centrifuging at 3000 *x g* for 2 minutes. Half of the lysed material was then filtered into the prepared column and centrifuged at 3000 *x g* for 2 minutes. The eluant was discarded, the remainder of the lysed material filtered into the column and the column centrifuged at 3000 *x g* for 2 minutes. The column containing the bound plasmid DNA was then washed in 12ml of wash solution 1 and centrifuged at 3000 *x g* for 2 minutes. The eluant was discarded and the column washed in 12ml of wash solution 2 and centrifuged at 3000 *x g* for 5 minutes. The column was then transferred to a new 50ml Falcon tube and 1.2ml of elution solution added, incubated for a few minutes and centrifuged at 3000 *x g* for 5 minutes to elute the bound plasmid DNA. Plasmid DNA was then quantified using the Nanodrop spectrophotometer (see section 2.2.3 for protocol) and stored at 4^0C for immediate use or -20^0C for long term storage.

2.2.3 Using the NanoDrop spectrophotometer

DNA/RNA was quantified using the NanoDrop 8000 spectrophotometer (Thermo Scientific). Briefly, the NanoDrop software was opened and the nucleic acid module selected. The nucleic acid type (DNA/cDNA/RNA) for quantification was then selected and the spectrophotometer initialised by adding 1.5µl of milliQ water to each optical surface, lowering the arm and selecting initialise. A blank measurement was then made by adding 1.5µl of the buffer in which samples are dissolved (for quantification of plasmid DNA this was elution solution provided in the GenElute plasmid maxiprep extraction kit) and selecting 'blank'. Samples (1.5µl) were then measured by loading onto the machine and selecting 'measure'. The concentration of the sample in ng/µl is then displayed on the screen. The NanoDrop additionally provides purity readings of the samples (260/280 ratio). The 260/280 ratio of a sample is the ratio of absorbance at 260 and 280 nm. DNA with a 260/280 absorption ratio of ~ 1.8 is accepted as adequate purity, while RNA with a 260/280 absorption ratio of ~ 2.0 is accepted as adequate

purity. If the ratio is substantially lower it may indicate phenol or protein contamination.

2.2.4 Linearisation of *SLC16A1* cDNA clone plasmid DNA

Extracted *SLC16A1* cDNA clone plasmid DNA was linearised in a 2 hour restriction digest reaction in a thermal cycler (Applied Biosystems Verti 96 well thermal cycler) at 37^0C with the *Sac*I restriction endonuclease. *Sac*I produces a single cut in the supercoiled DNA after the *SLC16A1* coding region. A 50µl reaction was prepared containing 2µg of plasmid DNA, 5µl of NewEngland Biolabs (NEB) buffer 1 (1 x final concentration), 0.5µl (1µg/ml final concentration) BSA and 0.5µl (10 units) of *Sac*I made up to 50µl with water. Digested DNA was then visualised along with supercoiled DNA by agarose gel electrophoresis. A 1% agarose gel containing 1µg/ml ethidium bromide in 1 x Tris-borate EDTA (TBE) was cast and allowed to set before transfer to an electrophoresis tank containing 1 x TBE. Both linear and supercoiled plasmid DNA was then prepared (5µl) with 2µl of 6x loading buffer and loaded onto the gel along with 5µl of a 10kb DNA ladder (NEB ladder: 2µl diluted with 2µl loading buffer and 4µl water) as a reference. Gel electrophoresis was then allowed to run for 30 minutes at 100V before visualisation under UV light. Successful linearisation produced a DNA band which migrates slower than the supercoiled form (*figure 2.1*).

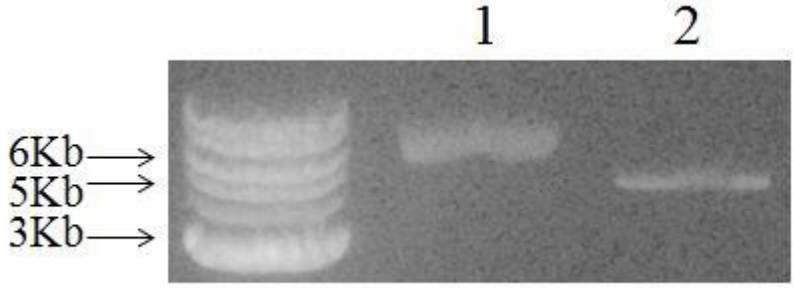

Figure 2.1: Visualisation of linear **(1)** and supercoiled **(2)** *SLC16A1* cDNA I.M.A.G.E. clone DNA on a 1% agarose gel using NEB 10kb ladder.

2.2.5 Amplification of *SLC16A1* template DNA

The *SLC16A1* coding sequence was amplified from linear plasmid DNA using Fast Start High Fidelity PCR system reagents (Roche Diagnostics, Burgess Hill, UK). This hot start PCR kit utilises an enzyme blend containing hot start Taq polymerase with a proofreading enzyme to achieve high accuracy amplification of template DNA. A single round of PCR was applied to amplify the full coding sequence of *SLC16A1*. Two primers (Sigma-Aldrich) were used to amplify the coding sequence of human *SLC16A1* from the I.M.A.G.E. clone plasmid DNA; a sense primer *5'* CTTATCGATGCCACCATGCCACCAGCAG *3'* containing a *Cla*I restriction site and corresponding to the *5'* end of *SLC16A1* and an antisense primer *5'* AAGACTAGTTCAGACTGGACTTTCCTCC *3'* containing a *Spe*I restriction site and corresponding to the *3'* end of *SLC16A1*. Each PCR reaction contained the following: 5µl of 10X reaction buffer with 18mM $MgCl_2$, 1µl of PCR grade nucleotide mix (200nM final concentration of each dNTP), 0.5µl FastStart High Fidelity Enzyme Blend (mix of Taq polymerase (5U/µl) plus proof-reading enzyme), 27.5µl PCR grade water, 5µl of both sense and anti-sense primers (400nM final concentration), 5µl template DNA (30ng/µl) and 1µl DMSO. Negative control reactions were also carried out in the absence of DNA to check for PCR reagent contamination. Reactions were prepared in 100µl low density plastic PCR tubes and thermal cycling performed on a 96 well block thermal cycler (Applied Biosystems Verti) using the following thermal profile: Initial denaturation (94^0C for 15 minutes), 45 cycles of denaturation (94^0C for 10 seconds), annealing (70^0C for 30 seconds) and elongation (72^0C for 2 minutes), before a final elongation (72^0C for 7 minutes). Amplification products were then visualised using agarose gel electrophoresis as described in section 2.2.4 to determine if the *SLC16A1* coding region (1.6Kb) had been successfully amplified *(figure 2.2)*.

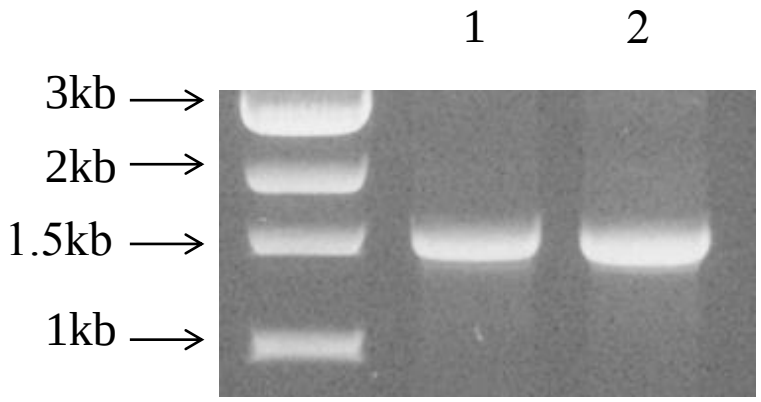

Figure 2.2 Visualisation of amplified *SLC16A1* template DNA (1) and (2) on a 1% agarose gel using NEB 10kb ladder.

2.2.6 Restriction digest of *SLC16A1* template/pBluescriptII-KSM plasmid

Successfully amplified *SLC16A1* template DNA was purified using the GenElute PCR clean-up kit according to the manufacturer's protocol as follows. Miniprep binding columns were firstly prepared by adding 0.5ml of column preparation to a binding column inserted into a 1.5ml collection tube and centrifuging at 12,000 *x g* for 1 minute in a table top centrifuge. Purified DNA was then mixed with binding solution in a 5:1 ratio (binding solution: DNA) to form complexes and transferred 500µl at a time to the binding column. Columns were then centrifuged at 12,000 *x g* for 1 minute, the eluant discarded and centrifugation repeated with any remaining DNA-binding solution. The column was then washed with 0.5ml of wash solution containing ethanol, centrifuged at 12,000 *x g* for 1 minute and the eluant discarded. The column (without any wash solution) was then centrifuged again at 12,000 *x g* for 2 minutes to remove any residual wash solution and any eluant discarded. The binding column was then transferred to a clean collecting tube and 25µl of elution solution added, allowed to incubate at room temperature for 1 minute and centrifuged at 12,000 *x g* for 1 minute to collect the now purified DNA. Concentration and purity was then quantified using the Nanodrop spectrophotometer (see section 2.2.3 for protocol) and DNA kept at 4^0C.

The *SLC16A1* template DNA and linear pBluescriptII-KSM DNA (linearised using *Sac*I restriction digest as described in section 2.2.4) were then correspondingly digested in consecutive single restriction digest reactions with *Cla*I and *Spe*I restriction endoucleases respectively to produce complementary restriction sites for subsequent ligation. Restriction reaction conditions were as follows; *SLC16A1* template DNA and pBluescriptII-KSM were digested firstly with *Cla*I at 37^0C for 2 hours 15 minutes with reactions assembled as follows: 2µg pBluescriptII-KSM/*SLC16A1* template DNA, 5µl NEB buffer 3 (1 x final concentration), 1µl (10 units) of *Cla*I, 0.5µl BSA (1µg/ml final concentration), and water up to 50µl. The *Cla*I digested DNA was then purified using the GenElute PCR clean-up kit as described previously and sequentially digested with *Spe*I at 37^0C for 2 hours and 30 minutes with reactions assembled as follows: 2µg pBluescriptII-KSM/*SLC16A1* template DNA, 5µl of NEB buffer 4 (1 x final concentration), 1µl (10 units) of *Spe*I, 0.5µl BSA (1µg/ml final concentration) and water up to 50µl. The double digested pBluescriptII-KSM and *SLC16A1* template DNA was then purified using the using the GenElute PCR clean-up kit according to the manufacturer's protocol as described previously and visualised by ethidium bromide

stained agarose gel electrophoresis as described in section 2.2.4 to confirm successful digestion *(figure 2.3).*

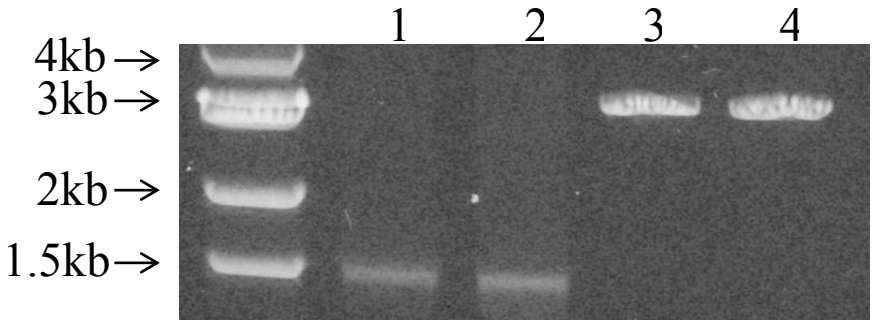

Figure 2.3: Visualisation of *ClaI* and *SpeI* sequentially digested *SLC16A1* template DNA (1) and (2) and pBluescriptII-KSM plasmid (3) and (4) on an agarose gel (1%) using NEB 10kb ladder.

Purified double digested DNA was subsequently isolated from a crystal violet agarose gel and extracted using the GenElute gel extraction kit as follows. A 1% agarose gel containing 1mg/ml crystal violet was cast and transferred to an electrophoresis tank containing 1 X TBE (plus 1mg/ml crystal violet). 5µl of digested pBluescriptII-KSM DNA and *SLC16A1* template DNA was mixed with 2µl crystal violet loading buffer (30% glycerol, 20mM EDTA and 100µl/ml crystal violet), loaded onto the gel and allowed to run at 100V until bands had fully migrated. The corresponding pBluescriptII-KSM DNA and *SLC16A1* template DNA bands were then excised from the gel using a sterile scalpel and weighed. The gel bands were then dissolved in solubilisation solution in a 1:3 ratio of weight (mg) to volume (µl) and incubated at 50-60^{0}C for 10 minutes until completely solubilised. Binding columns were prepared by inserting GenElute G columns containing 500µl of column preparation into 1.5ml collecting tubes, centrifuging for 1 minute at 12,000 *x g* and discarding the eluant. Isopropanol was then added to the solubilised gel solutions in a 1:1 weight to volume ratio and the solution loaded into the prepared binding columns. Columns were centrifuged for 1 minute at 12,000 *x g* to bind DNA contained in the gel slice and the eluant discarded. The columns were washed with 700µl of wash solution, centrifuged at 12,000 *x g* for 1 minute and the eluant discarded. The binding columns were then transferred to clean collecting tubes; 50µl of elution solution (at 65^{0}C) was added and incubated at room temperature for 1 minute. DNA was recovered by centrifugation at 12,000 *x g* for 1 minute and quantified using the Nanodrop spectrophotometer as described in section 2.2.3. DNA was stored at -20^{0}C until downstream ligation.

2.2.7 Ligation of *SLC16A1* template DNA into pBluescriptII-KSM

To enable ligation with the *SLC16A1* template DNA, pure pBluescriptII-KSM DNA was dephosphorylated in a 1 hour reaction at 37^0C, reaction reagents were as follows: 1µl (5 units) antarctic phosphatase, 5µl antarctic phosphatase buffer (1 x final concentration), 1µg pBluescriptII-KSM DNA, and water up to a total volume of 50µl. The reaction was then terminated by heat inactivation at 65^0C for 10 minutes. Subsequent ligation was achieved using T4 DNA ligase in an overnight reaction at 4^0C. A total of 150µg of DNA was required for a 20µl ligation reaction in a 3:1 ratio of insert (*SLC16A1* template DNA) to vector (pBluescriptII-KSM) set up as follows: 6µl of *SLC16A1* template DNA (112.5µg), 2µl of phosphatase treated vector (37.5µg), 2µl (1x final concentration) T4 DNA ligase buffer (with 1mM ATP), 1µl (400 units) T4 DNA ligase and 9µl of water. The following day ligated pBluescriptII-KSM-*SLC16A1* and a negative control (pBluescriptII-KSM vector only) were transformed into NEB 5-alpha chemically competent *E.coli* using the NEB high efficiency transformation protocol.

Briefly, 5-alpha competent *E.coli* were allowed to thaw on ice for 10 minutes before adding 3µl of pBluescriptII-KSM-*SLC16A1* plasmid DNA/vector only negative control. The tubes were then carefully flicked 4-5 times to mix and incubated on ice for 30 minutes. The *E.coli* mix was heat shocked for exactly 30 seconds at 42^0C and placed on ice for 5 minutes. A 950µl aliquot of super optimal broth with catabolite repression (SOC) medium was added and *E.coli* cultured for 60 minutes at 37^0C with vigorous shaking (250rpm). The transformed *E.coli* was then mixed by flicking and inverting and several 10-fold serial dilutions were prepared in SOC medium. A 100µl volume of each dilution was spread using a bacterial loop to warmed agar selection plates (containing 100µg/ml ampicillin) and incubated overnight at 37^0C.

The following day, vector-only negative control culture plates were observed for any bacterial growth and clear, single *E.coli* clones transformed with the pBluescriptII-KSM-*SLC16A1* plasmid were selected and analysed for *SLC16A1* expression using PCR *(figure 2.4)* according to the conditions described in section 2.2.5. Any *SLC16A1* positive colonies were grown overnight in LB broth (plus 100µg/ml ampicillin) at 37^0C with vigorous shaking (250rpm). The following day, plasmid DNA was extracted from overnight cultures using the GenElute maxi-prep kit as described in section 2.2.2.

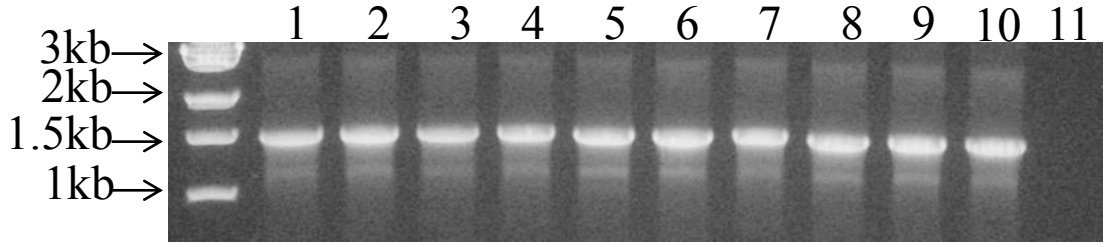

Figure 2.4: Agarose gel visualisation of positive pBluescriptII-KSM-*SLC16A1* clones (1-10) and the vector-only transformation negative control (11) using NEB 10kb ladder after analysis by PCR.

Five clones shown to express the ligated plasmid and therefore *SLC16A1* template were sent to Source Bioscience Lifesciences (Cambridge, UK) for single tube sequencing. Linear plasmid DNA at a concentration of 100ng/µl was supplied and the plasmid DNA sequenced from the T3 promoter and T7 reverse sites within the pBluescriptII-KSM vector sequence; this enabled the full insertion site of the vector to be sequenced. Sequence results were then analysed to ensure the inserted *SLC16A1* template was identical to the published protein coding sequence. A single clone was then selected for subsequent transfection.

2.2.8 Sub-cloning of *SLCO1A2* into pBluescriptII-KSM

Sequence verified pBluescriptII-KSM-*SLCO1A2* plasmid transcript was available in the department and was kindly gifted for use in the project by Professor Andrew Owen. The *SLCO1A2* gene insert was cloned from cDNA obtained from A549 and Huh-7D12 cells, and sub-cloned into the pBluescriptII-KSM plasmid using the same techniques as described in sections 2.2.4 – 2.2.7.

2.2.9 In-vitro transcription

Confirmed full length pBluescriptII-KSM-*SLCO1A2* and pBluescriptII-KSM-*SLC16A1* clones were firstly linearised using the *Sac*I restriction endonuclease *(figure 2.5)* and visualised by agrose gel electrophoresis (according to conditions outlined in section *2.2.4*). Complementary RNA (cRNA) was then prepared by *in vitro* transcription using the T3mMessage mMachine kit as per the manufacturer's protocol. Briefly, reagents were vortexed until thawed (RNA polymerase kept on ice) and kept at room temperature (NTP/CAP (a neutralised buffer containing 15mM ATP, 15mM CTP, 15mM UTP, 3mM GTP and 12mM cap analog) kept on ice). A 20µl reaction was prepared with the following reagents made up to 20µl with nuclease free water: 10µl NTP/CAP, 1µg of linear pBluescriptII-KSM-*SLCO1A2*/ pBluescriptII-KSM-*SLC16A1*

template DNA, 2µl of reaction buffer (1x final concentration), 2µl of enzyme mix (RNase inhibitor plus RNA polymerase; concentration not specified). The reaction mix was then incubated in a thermal cycler for 2 hours at 37^0C and immediately transferred to ice. A 30µl volume of nuclease free water and 30µl of 7.5M lithium chloride (LiCl) precipitation solution (with 50mM EDTA) was added to terminate the polymerase reaction and the reaction mixed thoroughly and incubated at -20^0C for 2 hours. The LiCl precipitate was then centrifuged at 16,000 *x g* for 15 minutes at 4^0C to pellet the RNA, the supernatant was carefully discarded and the pellet washed in 1ml of 70% ethanol. The pellet was centrifuged again at 16,000 *x g* for 15 minutes at 4^0C, the ethanol carefully discarded, and the pellet allowed to air dry for 5 minutes before re-suspension in 15µl of nuclease free water. The cRNA concentration and was determined using the Nanodrop spectrophotometer (as described in section 2.2.3) and cRNA diluted to 1µg/ul. Aliquots (5µl) were prepared and stored at -80^0C for future transfection.

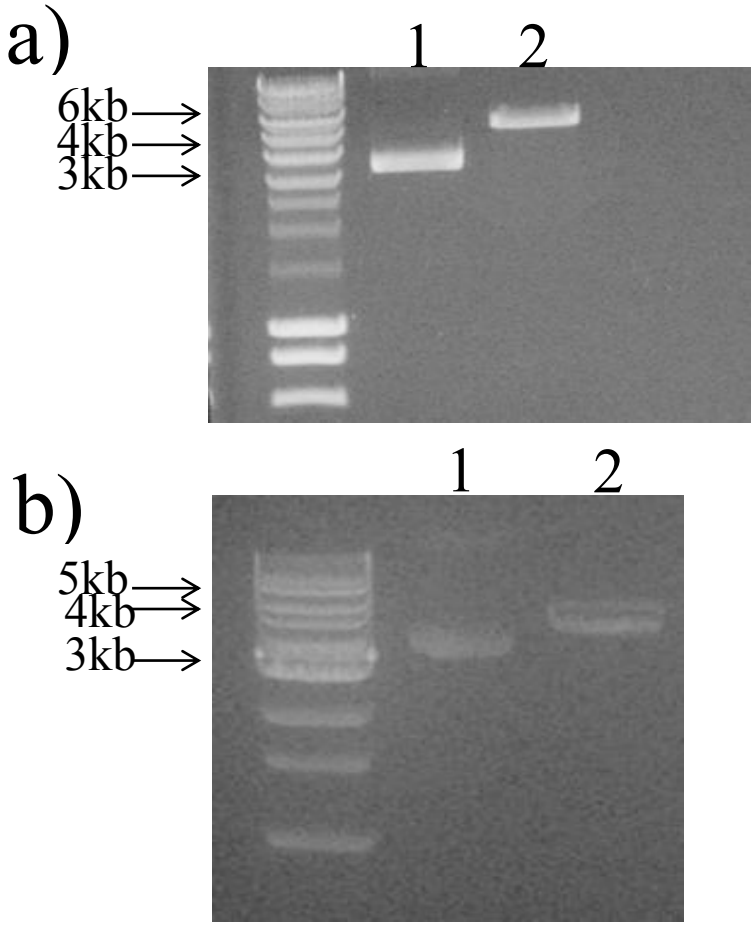

Figure 2.5: Visualisation of supercoiled **(1)** and linear **(2)** pBluescript-KSM-*SLCO1A2* **(a)** and pBluescriptII-KSM-*SLC16A1* **(b)** DNA on a 1% agarose gel using NEB 10kb ladder.

2.2.10 *X. laevis* husbandry

Adult female *X. laevis* were kept in fresh water filtered tanks; water temperature was maintained at ~17^{0}C with heater systems. Tanks included light and dark areas and were cleaned fortnightly. Animals were fed specialised *X. laevis* pellets twice per week and handled in a net. Animals were sacrificed by submerging the animal in MS222 anaesthetic solution (5g/L) for 45 minutes.

2.2.11 *X. laevis* oocyte extraction and microinjection

Oocytes were extracted from the frog abdomen by dissection, with ovary lobes isolated using forceps and collagenase treated in calcium negative Barth's solution (88mM NaCl, 1mM KCl, 15mM HEPES, 1% penicillin streptomycin) containing 1mg/ml collagenase for ~1 hour (shaking). Oocytes were then washed three times with calcium containing Barth's solution (88mM NaCl 1mM KCl, 15mM HEPES, 0.3mM $CaCNO_3.6H_2O$, 41mM CaCl2_6H2O, 0.82mM MgSO4_7H2O, 1% penicillin streptomycin), and stored overnight at 18^{0}C. Healthy, mature oocytes with distinct hemispheres were selected for microinjection the following day. Needles were firstly prepared from thin wall glass capillaries (1mm diameter, 102mm length) using the PUL-1 machine (World Precision Instruments), loaded onto the micro-manipulator and trimmed using forceps. OATP1A2/ MCT1 cRNA (1ug/ul) or water (50nl) was then loaded into the needle by vacuum pump (DA7C, Charles Austen Pumps) where it was held by compressed air using the picopump PV830 (World Precision Instruments). The drop size was then calibrated to 4µm in diameter and injected into the yolk side of the oocyte. Around 200 oocytes were injected per condition (water injected control and *SLC01A2/SLC16A1* transfected) and maintained in modified Barth's solution (calcium positive) at 18^{0}C for three days.

2.2.12 Cellular uptake assay in *X. laevis* expression system

Uptake experiments employed a radiolabelled concentration of 0.3µCi/ml supplemented with non-radiolabelled drug to give final concentrations of 2µM estrone-3-sulfate (E3S; OATP1A2 positive control substrate) and 5µM of L-lactic acid (LA; MCT1 positive control substrate) prepared in transport medium (HBSS supplemented with 25mM HEPES and 0.1% bovine serum albumen (BSA), at pH7.4). A radiolabel concentration of 0.3µCi/ml afforded sufficient disintegrations per minute to give accurate readings of radioactive content without saturating the scintillation counter.

On the day of the assay, control (water injected) and *SLCO1A2/SLC16A1* transfected oocytes were selected, washed three times in transport buffer and eight oocytes (in 250µl of transport buffer) added to a single well per condition (water injected or *SLCO1A2/SLC16A1* transfected) for each drug. Transport medium (250µl) containing the radiolabelled drug (dosing solution) with either vehicle (0.1% DMSO), or inhibitor (100µM naringenin for OATP1A2, 100µM salicylic acid for MCT1) was added to control or *SLCO1A2/SLC16A1* transfected oocytes and incubated at room temperature for 90 minutes (OATP1A2) or 60 minutes (MCT1). In the meantime, samples (20µl) of transport buffer alone (blanks) and samples (20µl) of dosing solution (standards) were taken and added to scintillation vials for later determination of background radiation and radioactive content of a known concentration of each drug solution, respectfully. After incubation, oocytes were washed three times in ice cold HBSS, transferred to scintillation vials and solubilised with 500µl of 10% sodium dodecyl sulphate (SDS). The solubilised solution was mixed with 4ml scintillation fluid (Goldstar Multipurpose liquid scintillation cocktail (Meridian, UK) and vials mixed by inverting several times before radioactive content was determined using a scintillation counter (1500 Tri Carb LS Counter; Packard). Results in dpm were corrected for background counts, quantified in relation to standards of known concentration and expressed in pmol/oocyte.

The above method was repeated with AEDs at final concentrations of 25µM PHT, 20µM CBZ, 300µM VPA, 10µM LTG, 10µM TPM, 10µM GBP and 6µM LEV.

2.2.13 Statistical analysis

All data are presented as mean ± standard error of the mean (SEM) from three (MCT1 data) or four (OATP1A2 data) independent experiments where n=8 for each group, with the exception of data described in sections 2.*3.1* and *2.3.4* which are presented as mean ± standard deviation from one experiment where n=8. In order to correct for differential uptake between drugs and to account for inter-batch variation in oocytes, data were expressed as percentage of the mean control value for each experimental day, where control equals 100% uptake. For data derived from uptake comparisons of control vs *SLCO1A2/SLC16A1* transfected oocytes with or without inhibitor, normal distribution was assessed using the Shapiro-Wilk test and statistical differences determined using analysis of variance (ANOVA), with Tukey's post hoc test to correct for multiple comparisons. A p value of <0.05 was taken to indicate significance.

2.3 Results

2.3.1 Kinetics of estrone-3-sulfate transport in *SLCO1A2* transfected *X. laevis* oocytes

A time course study of the known OATP1A2 substrate estrone-3-sulfate in control (water-injected) oocytes compared to *SLCO1A2*-transfected oocytes was undertaken to determine the optimum time point for further investigation with AEDs *(figure 2.6).* Optimum transport of 2µM estrone-3-sulfate was observed between 90 and 120 minutes before reaching a plateau and then falling away by 180 minutes. The 90 minute time point at the peak of the linear phase for estrone-3-sulfate transport was chosen for subsequent experiments with AEDs in *SLCO1A2*-transfected oocytes.

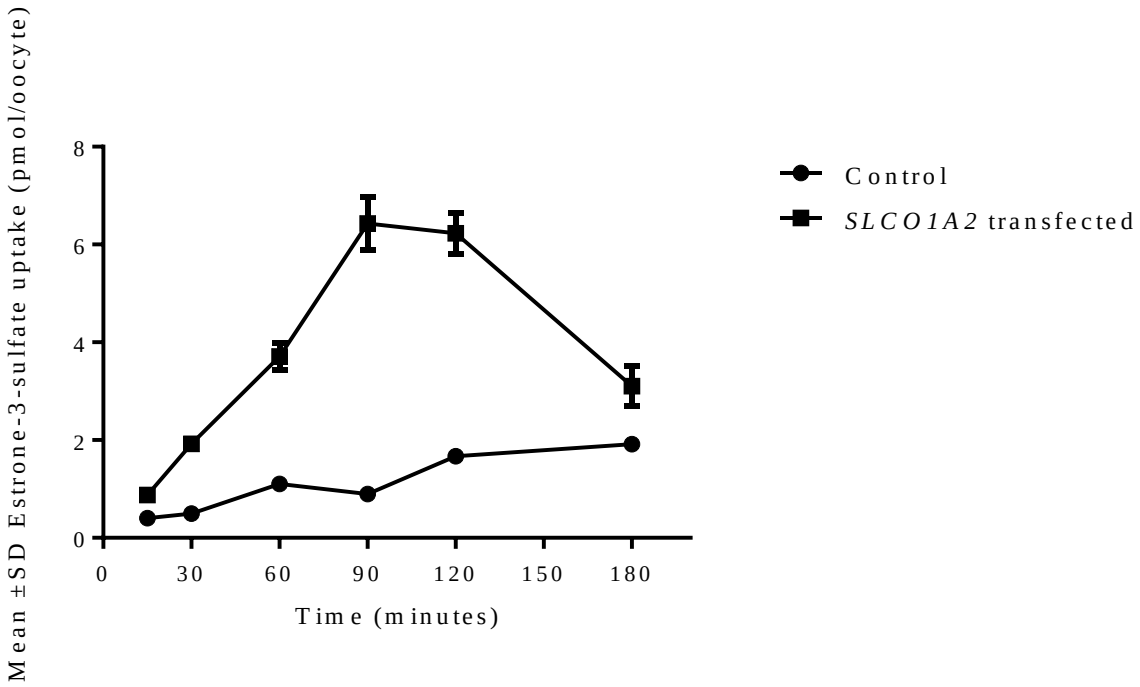

Figure 2.6: A comparison of estrone-3-sulfate uptake over time in control (solid circles) and *SLCO1A2*-transfected (solid squares) oocytes. Results are expressed as mean (± standard deviation) uptake in pmols per oocyte following exposure to 2µM estrone-3-sulfate over a 3 hour period. Each data point represents the mean of eight observations (n=8), obtained from a single experiment.

2.3.2 Estrone-3-sulfate uptake in *X. laevis* oocytes transfected with *SLCO1A2*

To confirm *SLCO1A2* transfection of *X. laevis* oocytes was successful and to validate the experimental model, uptake of 2µM estrone-3-sulfate was investigated in control (water-injected) oocytes compared to *SLCO1A2*-transfected oocytes with and without co-incubation with the OATP1A2 inhibitor naringenin (100µM; *figure 2.7)*. Mean uptake of estrone-3-sulfate was 1326 ± 171% of the control value (100 ±21%) in *SLCO1A2*-transfected oocytes ($p \leq 0.001$). Co-incubation with the OATP1A2 inhibitor naringenin reduced uptake in *SLCO1A2*-transfected oocytes to 378 ± 44% of the control value ($p \leq 0.01$). This finding suggests that *SLCO1A2* transfection was successful and confirmed the validity of the experimental model.

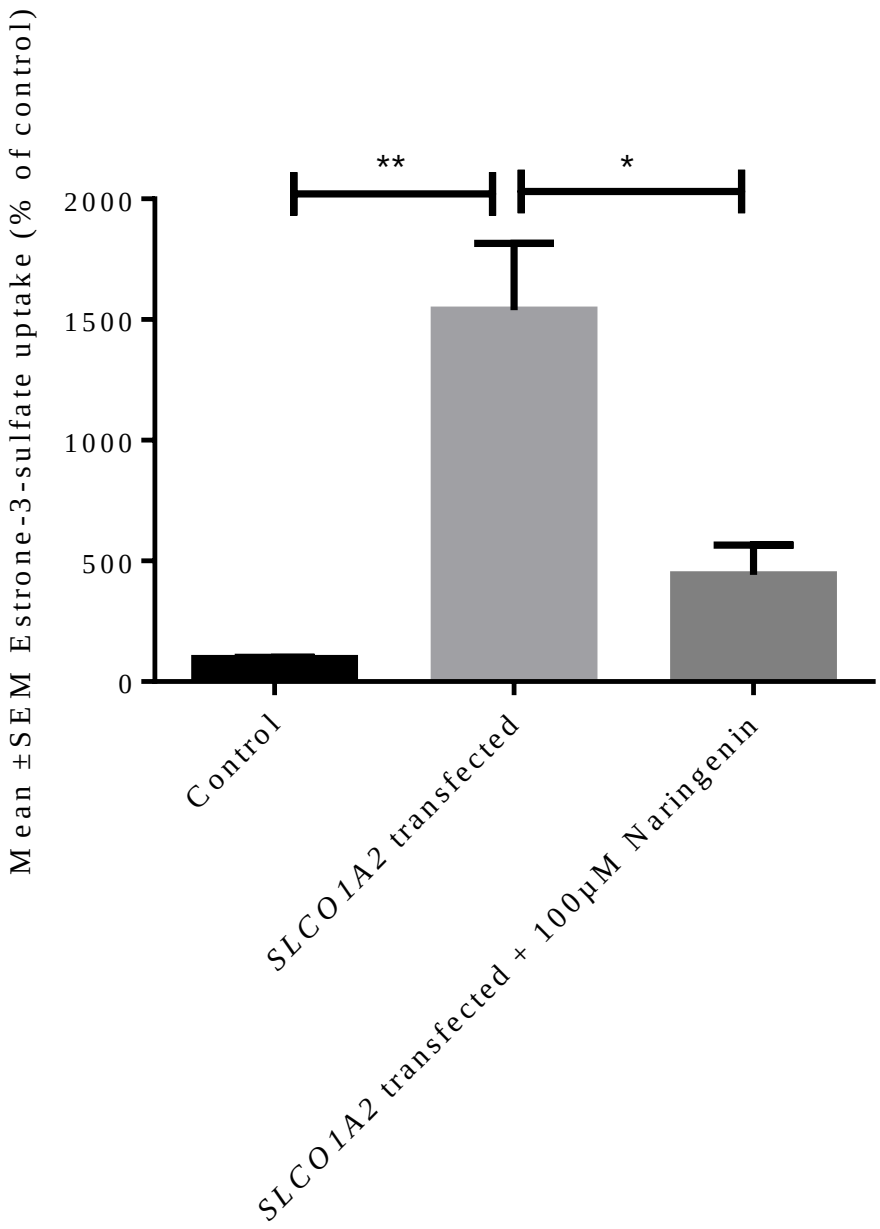

Figure 2.7: Estrone-3-sulfate (E3S) uptake into *SLCO1A2*-transfected *X. laevis* oocytes compared to control water injected oocytes with and without the OATP1A2 inhibitor naringenin. Cultures were exposed to 2µM radiolabelled E3S with or without naringenin at 100µM for 90 minutes at room temperature. Results are expressed as the mean ± standard error of the mean (SEM) percentage of the mean control value of E3S uptake (in pmols/oocyte) on each experimental day. The experiment was performed on four separate occasions with percentage of control data calculated on each occasion and with n=8 oocytes in each group each time. Statistical significance (* $p \leq 0.01$, **p<0.001) was determined by one-way analysis of variance with Tukey's correction for multiple testing.

2.3.3 Uptake of AEDs in *SLCO1A2* transfected *X. laevis* oocytes

Seven commonly prescribed AEDs were investigated to determine whether they were subject to OATP1A2-mediated transport at therapeutically relevant concentrations. These were phenytoin (25µM), carbamazepine (20µM), valproate (300µM), lamotrigine (10µM), gabapentin (10µM), topiramate (10µM) and levetiracetam (6µM). Each drug was incubated with both control and *SLCO1A2*-transfected oocytes, with or without the OATP1A2 inhibitor naringenin (100µM). No significant difference in uptake was seen for any of the seven AEDs in *SLCO1A2*-transfected oocytes compared to controls, with only minor changes in relative AED transport observed *(table 2.1)*. GBP uptake increased to 304 ± 47% of the control value in the presence of 100µM naringenin (*p≤0.001)*. No such effect was observed for any of the other AEDs tested *(table 2.1).*

Antiepileptic drug	Concentration (µM)	Control	*SLCO1A2* transfected	*SLCO1A2* transfected plus inhibitor
		Mean ± SEM uptake (% of control)		
Estrone-3-sulfate	2	100 ± 21	1326 ± 171**	378 ± 44*
Phenytoin	25	100 ± 2.3	98.1 ± 8.2	105 ± 8.8
Carbamazepine	20	100 ± 3.5	91.3 ± 2.8	98.0 ± 3.2
Sodium valproate	300	100 ± 9.0	111 ± 7.3	101 ± 6.1
Lamotrigine	10	100 ± 6.1	128 ± 7.7	138 ± 8.8
Gabapentin	10	100 ± 19	104 ± 17	304 ± 47**
Topiramate	10	100 ± 4.5	111 ± 6.5	127 ± 8.8
Levetiracetam	6	100 ± 7.3	94.5 ± 7.0	124 ± 12

Table 2.1: Comparison of antiepileptic drug uptake in control and *SLCO1A2*-transfected *X. laevis* oocytes and effects of the OATP1A2 inhibitor naringenin (100µM). Estrone-3-sulfate (2µM) was employed as a positive control compound. Results are expressed as mean ± standard error on the mean (SEM) percentage of mean control uptake following exposure to antiepileptic drugs for 90 minutes. The experiment was performed on four separate occasions with percentage of control data calculated on each occasion and with n=8 oocytes in each group each time. Statistical significance (*p<0.01, **p<0.001) was determined by one-way analysis of variance with Tukey's correction for multiple testing.

2.3.4 Kinetics of L-lactic acid transport in *SLC16A1* transfected *X.laevis* oocytes

A time course study of the known MCT1 substrate L-lactic acid in control (water-injected) oocytes compared to *SLC16A1*-transfected oocytes was undertaken to determine the optimum time point for further investigation with AEDs *(figure 2.8).* Optimum transport of 5µM L-lactic acid was observed between 60 and 90 minutes, with uptake falling away thereafter. The 60 minute time point at the peak of the linear phase for lactic acid transport was chosen for subsequent experiments with AEDs in *SLC16A1*-transfected oocytes.

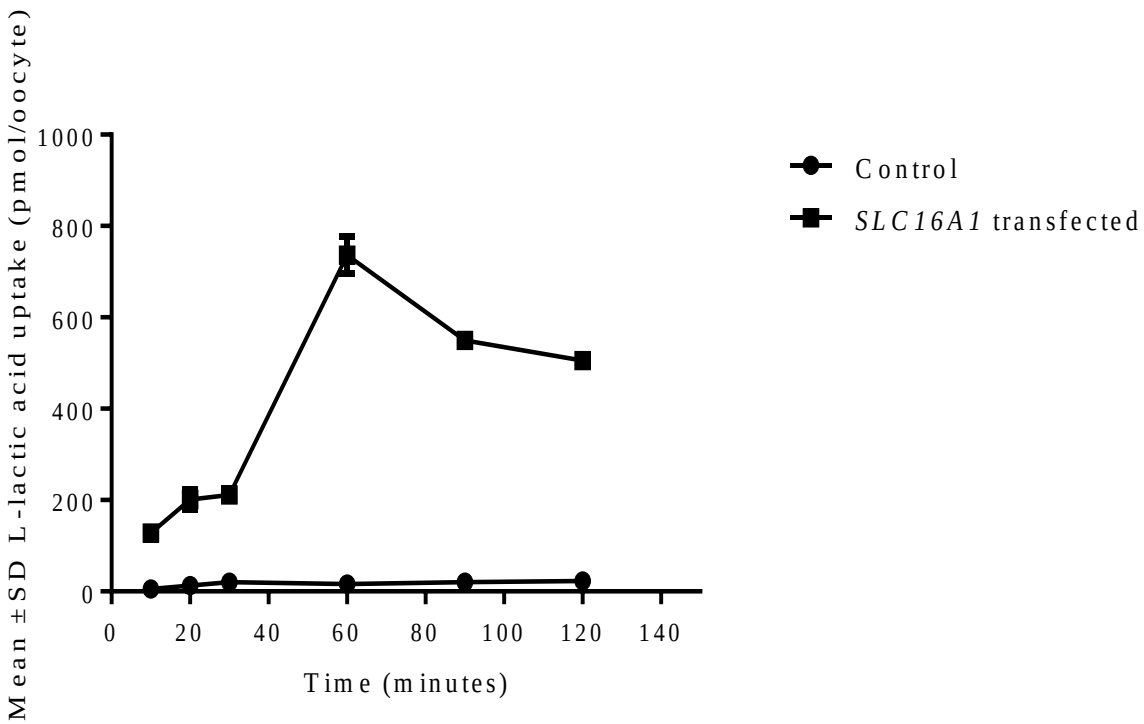

Figure 2.8: A comparison of L-lactic acid uptake over time in control (solid circles) and *SLC16A1*-transfected (solid squares) *X. laevis* oocytes. Results are expressed as mean (± standard deviation) uptake in pmols per oocyte following exposure to 5µM L-lactic acid over a 2 hour period. Each data point represents the mean of eight observations (n=8), obtained from a single experiment.

2.3.5 L-lactic acid uptake in *X. laevis* oocytes transfected with *SLC16A1*

To confirm successful *SLC16A1* transfection of *X. laevis* oocytes and to validate the experimental model, uptake of L-lactic acid (LA; 5µM) was investigated in control (water injected) oocytes compared to MCT1 transfected oocytes with and without co-incubation with the MCT1 inhibitor salicylic acid (100µM; *figure 2.9)*. Mean uptake of LA was 2607 ±240% of the control value (100 ±5.9%) in *SLC16A1*-transfected oocytes (*p≤0.001*). Co-incubation with the MCT1 inhibitor salicylic acid reduced uptake in *SLC16A1*-transfected oocytes to 1134 ± 110% of the control value *(p≤0.01*). This finding suggests that *SLC16A1* transfection was successful and confirmed the validity of the experimental model.

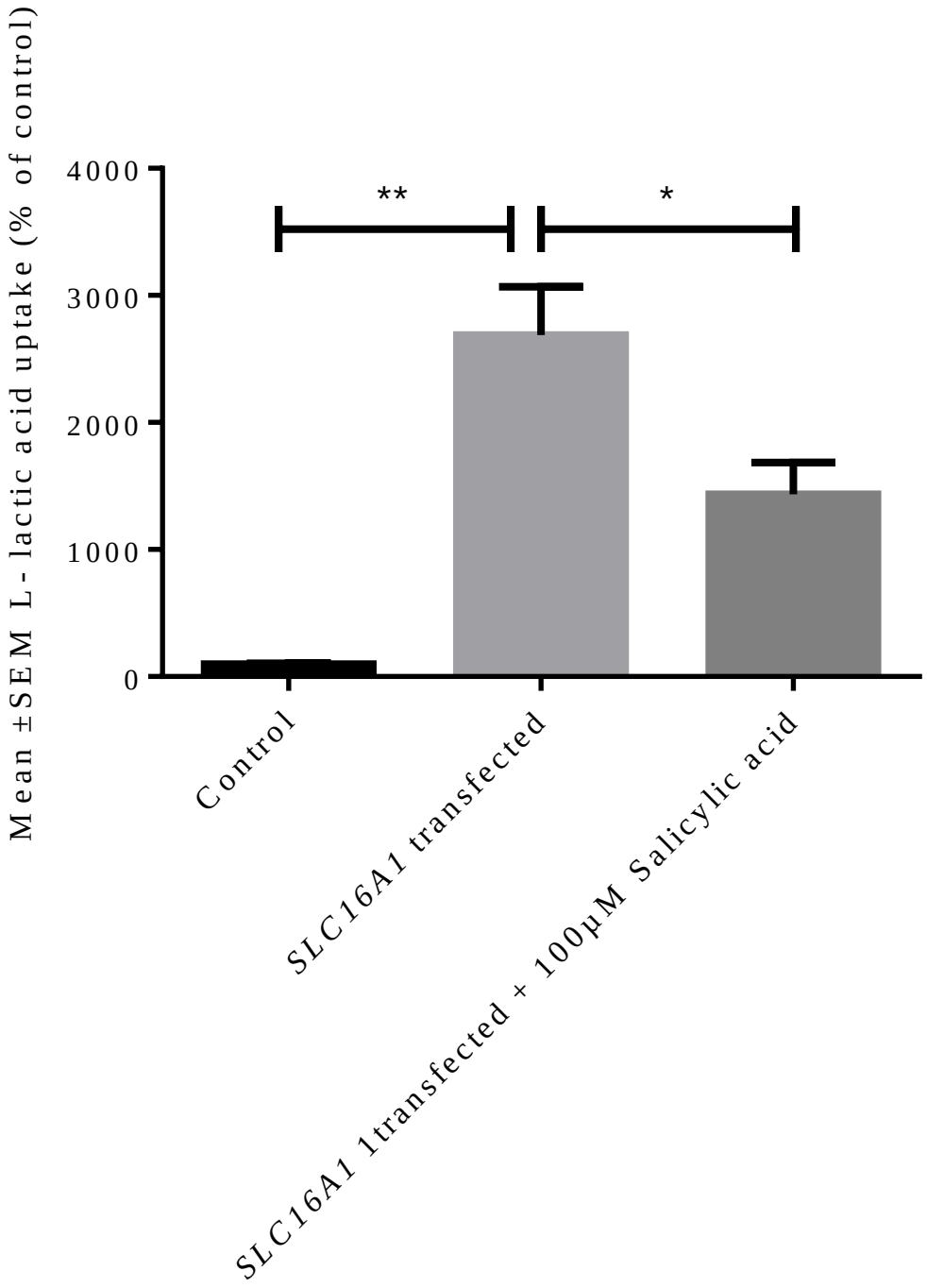

Figure 2.9: L-lactic acid (LA) uptake into *SLC16A1*-transfected *X. laevis* oocytes compared to control water injected oocytes with and without the MCT1 inhibitor salicylic acid. Cultures were exposed to 5µM radiolabelled LA with or without salicylic acid at 100µM for 60 minutes at room temperature. Results are expressed as the mean ± standard error of the mean (SEM) percentage of the mean control value of LA uptake (in pmols/oocyte) on each experimental day. The experiment was performed on four separate occasions with percentage of control data calculated on each occasion and with n=8 oocytes in each group each time. Statistical significance (* $p \leq 0.01$, **p<0.001) was determined by one-way analysis of variance with Tukey's correction for multiple testing.

2.3.6 Uptake of AEDs in *SLC16A1* transfected *X. laevis* oocytes

To determine which, if any of the seven commonly prescribed AEDs namely: phenytoin (25µM), carbamazepine (20µM), valproate (300µM), lamotrigine (10µM), gabapentin (10µM), topiramate (10µM) and levetiracetam (6µM) are transported by MCT1; each drug was incubated with control and *SLC16A1*-transfected oocytes with/without the MCT1 inhibitor salicylic acid (100µM). Gabapentin uptake was increased to 164% ±15% in *SLC16A1*-transfected oocytes compared to control (100 ±10%; $p \leq 0.05$), however this could not be inhibited significantly by salicylic acid (123% ±12%). No significant difference in uptake was seen for the other AEDs tested *(table 2.2)*.

Antiepileptic drug	Concentration (µM)	Control	*SLC16A1* transfected	*SLC16A1* transfected plus inhibitor
		Mean ± SEM uptake (% of control)		
L-lactic acid	5	100 ±5.9	2607 ±240**	1134 ±110*
Phenytoin	25	100 ±3.9	108 ±2.6	109 ±3.6
Carbamazepine	20	100 ±1.8	110 ±4.1	113 ±2.6
Sodium valproate	300	100 ±5.7	94.0 ±3.8	86.3±3.0
Lamotrigine	10	100 ±4.1	77.6 ±5.7	78.0 ±4.0
Gabapentin	10	100 ±10	164±15*	123 ±12
Topiramate	10	100±3.2	110 ±3.0	122 ±4.5
Levetiracetam	6	100 ±6.0	115 ±5.9	114 ±4.8

Table 2.2: Comparison of antiepileptic drug uptake in control and *SLC16A1*-transfected *X. laevis* oocytes and effects of the MCT1 inhibitor salicylic acid (100µM). L-lactic acid (5µM) was employed as a positive control compound. Results are expressed as mean ± standard error on the mean (SEM) percentage of mean control uptake following exposure to antiepileptic drugs for 60 minutes. The experiment was performed on three separate occasions with percentage of control data calculated on each occasion and with n=8 oocytes in each group each time. Statistical significance (*p<0.01, **p<0.001) was determined by one-way analysis of variance with Tukey's correction for multiple testing.

2.4 Discussion

Despite their common use, the mechanisms by which AEDs penetrate into the brain remain largely unknown. A lot of attention has centred on the role of efflux transporters in the brain disposition of AEDs in particular P-gp; however the role of the SLC transporter family has been largely overlooked.

Due to its predominant expression at the BBB, OATP1A2 was selected as a potential candidate for the transport of AEDs. Although the precise location of its membrane expression is debated, the majority of evidence suggests that OATP1A2 is expressed on the apical membrane of brain endothelial cells (Urquhart *et al.*, 2009). OATP1A2 would thus likely act to pump drugs into brain endothelial cells that comprise the BBB from the blood, therefore a reduction in the expression of OATP1A2 might reasonably explain the lack of accumulation of substrate drugs in the brain.

OATP1A2 is known to be involved in the transport of various drugs including the folate antimetabolite methotrexate and the quinolone antibacterial agent levofloxacin (Badagnani *et al.*, 2006; Maeda *et al.*, 2007). The *X. laevis* model was used to demonstrate transport in both cases. Interestingly, many of the side effects associated with levofloxacin are central nervous system related including seizures, toxic psychoses, increased intracranial pressure and central nervous system stimulation (Maeda *et al.*, 2007; Urquhart *et al.*, 2009). Brain accumulation of levofloxacin as a result of OATP1A2-mediated transport may be at least partly accountable for its adverse central nervous system effects; this would also lend weight to the relative importance of OATP1A2-mediated transport at the BBB. More recently it was shown again using *X. laevis* oocytes transfected with *SLCO1A2* that OATP1A2 also transports the HIV protease inhibitors saquinavir and lopinavir (Hartkoorn *et al.*, 2010).

Such studies suggest that OATP1A2 transports diverse substrates from different chemical and pharmacological groups and can partly explain why certain drugs attain greater than expected central nervous system concentrations. Therefore, OATP1A2 has the potential to transport antiepileptic drugs, a chemically diverse group of drugs, at the BBB.

Following the MCT family of transporters were chosen as a rational target to investigate possible AED transport as several members of the family are thought to be expressed at

the BBB (Geier *et al*., 2013; Shawahna *et al*., 2011; Uchida *et al*., 2011). Furthermore there is mounting research suggesting VPA entry into the brain may be MCT mediated. Firstly in a human intestinal epithelial (Caco-2) and rat brain endothelial (RBE4) cell line various monocarboxylic acids such as benzoate, salicylate, acetate, propionate, butyrate, hexanoate, diclofenac and ibuprofen were shown to be strong inhibitors of valproate uptake and that uptake was a proton dependent rather than sodium dependent process. From this the authors concluded that due to lack of expression of any other MCT protein at the rat brain endothelium, MCT1 is the predominant VPA uptake system at the rat BBB (Fischer *et al.*, 2008). However this could not be said for VPA transport at the intestinal epithelium, where a specific proton dependent, DIDS – insensitive mechanism not identical with MCT1 was identified as the probable mechanism of VPA transport (Fischer *et al.*, 2008). In concurrence with these findings, apical to basolateral transport of VPA was shown to be inhibited by monocarboxylic acids but not dicarboxylic acids or anion exchange inhibitors in a human trophoblast cell line (BeWo). Furthermore, on analysis of Lineweaver-Burk plots of VPA uptake into BeWo cells, benzoic acid, a marker for MCT1, was found to compete with VPA for transport, thus suggesting an MCT sensitive system for VPA transport, presumed to be MCT1 mediated (Utoguchi *et al.*, 2000).

Corresponding to data suggesting a MCT mediated mechanism is likely to be responsible for VPA transport, MCT1 was shown to be severely deficient on the endothelium of microvessels at the epileptogenic focus from tissue surgically resected in the treatment of individuals with drug resistant TLE. A similar deficiency was also observed on the endothelium of microvessels in three novel rat models of TLE (Lauritzen *et al.*, 2011; Lauritzen *et al.*, 2012). These studies provide evidence to suggest that VPA penetration into the brain is mediated by an MCT transporter, presumably MCT1 and furthermore that a deficiency of MCT expressed in brain microvessels may explain why lower than expected concentrations of VPA are observed in the brain.

In this chapter, the possibility that OATP1A2 and/or MCT1 transport commonly prescribed antiepileptic drugs, including PHT, CBZ, VPA, LTG, GBP, TPM and LEV was evaluated using a *X. laevis* oocyte model. Positive control substrates estrone-3-sulfate and L-lactic acid were shown to be transported by OATP1A2 and MCT1, respectively. A significant increase in uptake in *SLCO1A2* and *SLC16A1*-transfected

oocytes compared to controls was observed and was substantially inhibited by the OATP1A2 and MCT1 inhibitors naringenin and salicylic acid respectively, confirming the validity of the model and the reliability of the data.

Subsequent data generated using this model clearly showed that none of the seven antiepileptic drugs investigated in this study was a substrate for OATP1A2-mediated transport. No significant increase in antiepileptic drug uptake was observed in *SLCO1A2*-transfected oocytes compared to control oocytes that had been injected with water alone. Furthermore no decrease in transport was observed in the presence of the OATP1A2 inhibitor naringenin. Thus it would appear that OATP1A2 is not responsible for the transport of any of the antiepileptic drugs tested.

However, OAPT1A2 demonstrates strong pH dependence, showing increased transport at lower pH. Imatinib is a substrate of OATP1A2 where pH dependent transport has been well characterised (Eechoute *et al.*, 2011a). Although antiepileptic drug transport at low pH is not applicable to penetration at the BBB, where it is expected to be close to the physiological value of 7.4, it may potentially be important in intestinal absorption of AEDs, which up to now has gone largely uncharacterised.

Although no increase in the transport of AEDs tested were observed in *SLCO1A2*-transfected oocytes compared to control, GBP transport was seen to significantly increase in *SLCO1A2*-transfected oocytes in the presence of the OATP1A2 inhibitor naringenin. Flavonoid compounds such as naringenin have been demonstrated to effect the activity of mammalian enzyme systems including protein kinases, ATPase phospholipase and cyclooxygenases. It is not known if these effects extend to non-mammalian enzyme systems, however the increase in GBP observed in the presence of naringenin could possibly be accounted for by such metabolic changes in *X. laevis* oocytes (Middleton *et al*., 2000). It would however be expected that these effects would be observed in the presence of naringenin irrespective of the expression of human *SLCO1A2* and the AED being tested. As the effect is only observed with GBP it is unlikely this effect is due to interference with enzyme systems in *X. laevis* oocytes but perhaps a result of a chemical interaction between naringenin and GBP, seemingly aiding GBP uptake. Alternatively the increase in GBP uptake observed in the presence of naringenin in the *SLCO1A2*-transfected oocytes may due to upregulation of an

endogenous transport system caused either by narringenin effects on cellular metabolic pathways or by the transfection process, in which GBP is able to exploit.

A significant increase in gabapentin uptake was observed in *SLC16A1*-transfected oocytes compared to water injected controls, suggesting MCT1 mediated transport of gabapentin. The inclusion of the MCT1 inhibitor salicylic acid reduced the elevation in gabapentin transport observed, however failed to reach statistical significance. It therefore remains unclear whether MCT1 transports gabapentin or not. The lack of inhibition by salicylic acid may be due to a lack of specificity at the concentration tested. It is also possible that gabapentin transport by MCT1 is mediated through an alternative binding site to that which accommodates lactic acid. If so, the simple competitive inhibition observed would appear to be without effect.

No significant difference in PHT, CBZ, VPA, LTG, TPM and LEV uptake was observed in *SLC16A1*-transfected oocytes compared to water injected controls. Although strongly suggested in two functional studies using rat brain endothelial cells and trophoblasts, human MCT1 does not appear to transport VPA in a *X. laevis* oocyte model. These conflicting findings could suggest that the inhibition of VPA uptake by monocarboxylic acids, shown by other groups previously (Utoguchi *et al.*, 2000; Fischer *et al.*, 2008), may be due to competition at another monocarboxylic acid transporter other than MCT1. In total, there are ten known MCTs, of which 6 are functionally characterised and 3 have been shown to be expressed at least at mRNA level in a human BBB model. MCT1, MCT4 and MCT8 (Price *et al.*, 1998; Pellerin *et al.*, 2005). It is therefore possible that another MCT isoform is responsible for the transport of VPA observed in previous investigation (Utoguchi *et al.*, 2000; Fischer *et al.*, 2008). This will be investigated further in chapter 3.

The *X. laevis* transport model was chosen to investigate the ability of OAPT1A2 and MCT1 to transport AEDs. The model was selected based on its proven use in transport studies and its non-mammalian origin. A non-mammalian model is useful over physiologically relevant human cell lines, as endogenous expression of other transporters, efflux transporters in particular, may impact on the results. Furthermore as *X. laevis* oocytes have to grow in unfavourable conditions in their natural environment, they are resilient and intrinsically possess substrates needed for growth and translation of proteins. As the oocytes do not rely on uptake of exogenous nutrients from the

environment they also express very low numbers of endogenous membrane transporters (Wagner *et al*., 2000). *X. laevis* oocytes have also been shown to inherently express the accessory protein basigin (Kirk *et al*., 2000), essential for the function of MCT1, therefore *X. laevis* oocytes are suitable as a vehicle for successful MCT1 expression.

The main limitations of this study were predominantly associated with the labour intensive and time consuming nature of the *X.laevis* oocyte model, meaning that high throughput screening of multiple compounds at different concentrations with and without a number of inhibitors at a range of concentrations is almost impossible to achieve. Another limitation of the model is that as a frog is poikilothermic therefore experiments with oocytes had to be performed at room temperature rather than the preferred mammalian physiological temperature. Active transport is a temperature sensitive process, therefore transporter kinetics determined for OATP1A2 and MCT1 in oocytes may not represent that observed at mammalian physiological temperatures. In addition although the levels of endogenous transporters and ion channels expressed in *X. laevis* oocytes are low, exogenously expressed proteins have been described to interfere with endogenous proteins. For example when LAT-1 is transfected into X.laevis oocytes along with 4F2hc, a glycoprotein essential for heterodimer formation and therefore LAT-1 function, the activity of several endogenous amino acid transporters was induced (Wagner *et al*., 2000). It is therefore possible that the transfection process and presence of high levels of exogenous protein may have induced the expression of endogenous transporter systems.

In conclusion OATP1A2 and MCT1 do not appear to transport the AEDs PHT, CBZ, VPA, LTG, TPM and LEV. Thus, it is reasonable to assume that these transporters do not influence the brain penetration of most AEDs and do not contribute to pharmacoresistance in general. Although it should not be discounted completely, attempts to test additional AEDs are probably not worthwhile as any remaining agents not investigated in this study are not commonly used in the clinic. There is, however, some evidence from this study of MCT1-mediated transport of GBP. This merits further investigation to determine whether this is a potentially relevant mechanism in the brain penetration of GBP and perhaps even in the systemic disposition of the drug.

Chapter 3

AED transport in hCMEC/D3 cells and the effects of MCT inhibitors

3.1 Introduction

In the previous chapter, the ability of two distinct isoforms of SLC transporter, OATP1A2 and MCT1, to transport AEDs was investigated in a *X.laevis* transport model. In addition to MCT1, 13 human MCT transporters have been identified and their tissue distributions at cDNA level defined (Price *et al.*, 1998). Of these, 5 have been functionally characterised and are discussed in detail below (Halestrap *et al.*, 1999).

MCT4 has striking similarities to MCT1 in terms of structure and substrate/inhibitor specificity however differs in respect to its substrate affinity and hypothesised endogenous role (Morris *et al.*, 2008). In contrast to the ubiquitous tissue distribution of MCT1, MCT4 is predominantly expressed in tissues with a high glycolytic requirement such as white muscle and white blood cells, reflecting its suggested role in the efflux of lactate (Wilson *et al.*, 1998). Similarly to MCT1, MCT4 is known to transport the endogenous fuels lactate and pyruvate, however their affinity for MCT4 is markedly lower with Km values of 28mM and 150mM observed respectively (Dimmer *et al.*, 2000). MCT1 and MCT4 are also both sensitive to inhibition by organomercurial compounds such as *p*-chloromercuribenzene sulfonate (pCMBS). Inhibition by such compounds has been shown to be through the disruption of the essential accessory protein basigin which is required for membrane expression and catalytic activity of both MCT1 and MCT4 (Wilson *et al.*, 2005). Basigin is a glycoprotein containing a single transmembrane span which acts as a chaperone, translocating MCT1/MCT4 to the plasma membrane where the transporter and basigin remain tightly bound. Dissociation of MCT1/MCT4 from basigin renders the transporter defunct (Manoharan *et al.*, 2006). In addition to inhibition by organomercurials, MCT4 has been shown to be inhibited by HMG-CoA reductase inhibitors (i.e. statin drugs) which possess monocarboxylate structures. In a stably co-transfected MCT4/CD147 pig kidney epithelial cell line, lipophilic statins such as fluvastatin, atorvastatin, lovastatin acid, simvastatin acid and cerivastatin were shown to significantly inhibit L-lactic acid transport, with IC_{50} values between 32µM and 96µM (Kobayashi *et al.*, 2006). Therapeutic agents known to inhibit MCT1 are described in the previous chapter.

MCT2 shares around 60% sequence identity with MCT1 and is expressed in most of the same tissues. Vital for membrane expression of MCT2 is its interaction with an accessory protein, embigin. Embigin is a glycoprotein, homologous to the MCT1/MCT4 accessory protein basigin which similarly acts as a chaperone,

translocating MCT2 to the plasma membrane where the two proteins remain tightly associated (Wilson *et al.*, 2005). Although MCT1 and MCT4 preferentially associate with basigin and MCT2 with embigin, all three transporters can interact with either accessory protein in the absence of its primary partner (Poole *et al.*, 1997; Kirk *et al.*, 2000; Wilson *et al.*, 2002). Due to its preferential association with embigin in mammalian cells, MCT2, unlike MCT1/MCT4, is insensitive to organomercurial inhibition (Wilson *et al.*, 2005). The ability to specifically inhibit MCT1 has recently been pursued by AstraZeneca who have developed a new class of specific and high affinity MCT1 inhibitors such as AR-C155858 as part of their immunosuppressive drug discovery programme (Murray *et al.*, 2005; Guile *et al.*, 2006). AR-C155858 exhibits maximal inhibition of L-lactic acid transport by MCT1 at concentrations as low as 2nM, independent of its associated accessory protein. Interestingly, MCT4 is insensitive to AR-C155858 inhibition, an observation attributed to differences in the structure of transmembrane domains 7-10 in MCT1 and MCT4. Unlike with MCT1, AR-C155858 inhibition of MCT2 was found to be dependent on its interaction with either basigin or embigin. When associated with embigin, the binding affinity of AR-C155858 to MCT2 is greatly reduced (Ovens *et al.*, 2010a; Ovens *et al.*, 2010b).

MCT1 to MCT4 represent the lactate transporting members of the MCT family and share many structural and functional similarities. A number of molecules have been shown to inhibit these transporters and can be divided into 3 chemical categories. The most potent MCT inhibitors are diverse amphiphilic compounds such as bioflavonoids and anion transport inhibitors which exhibit Ki concentrations of 1-10μM. MCT transport is also potently inhibited by bulky or aromatic monocarboxylates such as phenylpyruvate and derivatives of α-cyancinnamate which exhibit Ki values of 50-500μM. MCT2 is more sensitive to inhibition by derivatives of α-cyancinnamate than MCT1 whereas little inhibition of MCT4 is observed. Finally, some stilbene-2, 2'disulphonates such as 4, 4′-diisothiocyanatostilbene-2, 2′-disulfonic acid (DIDS) are known to inhibit MCT transport; MCT2 is more sensitive to stilbene-2, 2'disulphonate inhibition than MCT1 and only very little inhibition of MCT4 is observed. MCT transport is also irreversibly inhibited by a range of thiol reagents, MCT1 and, to a lesser extent, MCT4 are sensitive to organomercurial inhibition, whereas MCT2 is insensitive as described previously (Halestrap *et al.*, 2004; Halestrap, 2013). Detailed inhibitor specificity for MCT3 is lacking and although very similar to MCT1, MCT2 and MCT4 in terms of structure and substrate specificity, MCT3 has a very restricted

tissue distribution and is confined to the basal membrane of the retinal pigment epithelium and choroid plexus epithelia (Morris *et al.*, 2008).

MCT8 and MCT10 share around 30% sequence identity with MCT1 to MCT4 and the tissue distribution of both proteins is generally widespread. In the brain, MCT8 expression was originally thought to be restricted to neurons, however a recent study reported additional expression in human cerebral microvessels (Roberts *et al.*, 2008). Unlike MCT1 to MCT4, MCT8 and MCT10 do not transport fuels such as lactate and pyruvate and instead function via a proton- independent, Na^+-dependent mechanism to transport thyroid hormones and aromatic amines respectively (Morris *et al.*, 2008). Data summarising the sensitivity of MCT8 and MCT10 to generic MCT inhibitors is not available, however MCT8 has been suggested to be inhibited by tyrosine kinase inhibitors in a non-competitive manner. In MCT8 transfected canine kidney epithelial cells, sunitinib, imatinib, bosutinib and dasatinib were all shown to inhibit MCT8-mediated transport of both iodothyronine (T3) and thyroxine (T4) with IC_{50} values between 13µM and 38µM (Braun *et al.*, 2011).

The need for an *in vitro* BBB model that mimics the *in vivo* properties of the human BBB and that can be cultured easily and used in high throughput screening is essential for CNS compound development in industry and academic CNS research (Eigenmann *et al.*, 2013). The immortalised human cerebral microvascular endothelial cell line (hCMEC/D3) represents such a model. hCMEC/D3 cells were derived from human temporal lobe microvessels, isolated during resective surgery for the treatment of epilepsy. The cells were sequentially immortalised by lentiviral vector transduction and the resulting clones characterised in terms of their biological properties (Weksler *et al.*, 2013). hCMEC/D3 cells were found to phenotypically mimic the *in vivo* human BBB, constitutively expressing endothelial cell markers, tight junction proteins and transporter proteins at the appropriate subcellular location (Tai *et al.*, 2009; Eigenmann *et al.*, 2013; Weksler *et al.*, 2013). In addition to the initial characterisation of hCMEC/D3 cells, a recent array study described the expression of a variety of SLC transporters at mRNA level. Relatively high expression of *SLC16A1* (MCT1) and *SLC16A3* (MCT4) was observed, while little to no expression of *SLC16A2* (MCT8) was described. Expression of other MCT transporters was not investigated in this analysis (Carl *et al.*, 2010).

The hCMEC/D3 cell line has been successfully used in a number of drug transport studies aiming to characterise BBB uptake of drugs of interest. A recent study used hCMEC/D3 cells to elucidate the reason for strikingly different rates of brain uptake between two very structurally similar anti-influenza drugs: adamantine and rimantadine. Uptake of the two drugs was inhibited by various cationic transporter inhibitors and was dependent on pH, membrane depolarisation and Na^+/Cl^- ions, indicating the involvement of a neutral and cationic amino acid transporter in the uptake of these drugs (Kooijmans *et al.*, 2012). The hCMEC/D3 cell line was also recently utilised with a panel of organic cation transporter inhibitors in a similar study to demonstrate the involvement of OCT1 in the uptake of LTG (Dickens *et al.*, 2012).

The studies described in this this chapter utilised the hCMEC/D3 cell line and a panel of MCT inhibitors (table 3.1) in an effort to identify whether any commonly used AEDs, including PHT, CBZ, VPA, LTG, GBP, TPM and LEV, are subject to MCT mediated transport and if so, to elucidate which particular MCT transporter may be responsible.

3.2 Materials and methods

3.2.1 Experimental plan

To fully characterise MCT mediated transport of seven commonly prescribed AEDs (as listed above), a panel of MCT transport inhibitors were selected. Incubation concentrations of inhibitors were chosen based on previous findings from available literature, with the exception of simvastatin acid which concentration was reduced from 100µM to 10µM after significant cell death was observed at the higher concentration in initial experiments. A number of non-specific MCT transport inhibitors along with compounds thought to selectively inhibit specific MCT transporters were included and are listed in table 3.1. These inhibitors were co-incubated with AEDs in the hCMEC/D3 BBB model.

Inhibitor	Concentration (µM)	Chemical class	Known MCT selectivity
Phenyl-pyruvate	100	Aromatic monocarboxylate	None
Ethyl-cyancinnomate	100	α-cyancinnamate derivative	Higher affinity for MCT2
Methyl-cyancinnomate	100	α-cyancinnamate derivative	Higher affinity for MCT2
Phloretin	1000	Bioflavanoid	None
Quercetin	1000	Bioflavanoid	None
Niflumic acid	100	Anion transport inhibitor	None
NPPB	100	Anion transport inhibitor	None
DIDS	1000	Stilbene-2,2'disulphonate	Higher affinity for MCT2
SITS	1000	Stilbene-2,2'disulphonate	Higher affinity for MCT2
4-MBA	100	Organomercurial	MCT1 and MCT4
Simvastatin acid	10	Statin	Unknown
Imatinib	100	Tyrosine kinase inhibitor	MCT8
L-lactic acid	1000	Monocarboxylate	Higher affinity for MCT2
Salicylic acid	1000	Monocarboxylate	None

Table 3.1: Summary of monocarboxylic acid transporter (MCT) inhibitors used in this chapter. NPPB (5-nitro-2-(3-phenylpropylamino) benzoic acid), DIDS (4, 4′-diisothiocyanatostilbene-2, 2′-disulfonic acid), SITS (4-acetamido-4′-isothiocyanato-2, 2′-stilbenedisulfonic acid), 4-MBA (4-(hydroxymercuri) benzoic acid).

3.2.2 Materials

[^{14}C]-L-lactic acid (specific activity, 130.8mCi/mmol) was purchased from Perkin Elmer (Massachusetts, USA). [^{3}H]-lamotrigine (specific activity, 5Ci/mmol), [^{3}H]-levetiracetam (specific activity, 5Ci/mmol), [^{3}H]-topiramate (specific activity, 8Ci/mmol) and [^{3}H]-gabapentin (specific activity, 110Ci/mmol) were purchased from American Radiolabeled Chemicals Inc (St. Louis, USA). [^{3}H]-phenytoin (specific activity 1.1Ci/mmol), [^{3}H]-carbamazepine (specific activity 10Ci/mmol) and [^{3}H]-valproic acid (specific activity 55Ci/mmol) were purchased from Moravek (Brea, California, USA). Rat tail collagen type I and chemically defined lipid concentrate were purchased from Invitrogen (Paisley, UK). Cell culture plasticware was purchased from Nunc Fisher Scientific (Loughborough, UK). EBM-2 medium was purchased from Lonza (Slough, UK). All other drugs and chemicals were purchased from Sigma-Aldrich (Poole, Dorset, UK), unless otherwise stated. The hCMEC/D3 cell line was provided courtesy of Dr Ignacio Romero (Department of Life Sciences, The Open University, Milton Keynes, UK) and Professor Pierre Couraud (Institut Cochin, Université Paris Descartes, Paris, France).

3.2.3 Human cerebral microvascular endothelial cell (hCMEC/D3) culture

hCMEC/D3 cells were cultured in collagen type I (100ug/ml) coated T175 flasks, maintained in EBM-2 medium supplemented with 5% foetal calf serum (FCS), 1% penicillin-streptomycin, 0.5% chemically defined lipid concentrate, 10mM HEPES, 1.4µM hydrocortisone, 5µg/ml ascorbic acid and 1ng/ml basic fibroblast growth factor (figure 3.1) and housed in an incubator at 37^{0}C, 5% CO_2 (Thermo Scientific Function Line). Cells were passaged every 2-3 days and seeded onto collagen type I coated six-well plates at a concentration of 3x10^{6}cells/well as required. The passage/seeding procedure was as follows; media was removed from flasks using a serological pipette and flasks washed twice in 10ml of warm Hanks balanced salt solution (HBSS). Cells were then cleaved from the flask surface with 10ml of 0.25% trypsin-EDTA and left to incubate at 37^{0}C for 5 minutes. Thereafter, 20ml of EBM-2 media was added to neutralise the trypsin, and the cell suspension transferred to a 50ml Falcon tube and centrifuged at 250 x *g* for 5 minutes to pellet the cells (Thermo Scientific Heraus Megafuge IIR). Cells were resuspended in 10ml of complete media and a cell count made (see section 3.2.4). The cell suspension was diluted with complete media to 1.5x10^{6}cells/ml and 2ml of the suspension added to each well, cells were then incubated

at 37^0C for 2 days. The remainder of the suspension was returned to T175 flasks at a 1:5 dilution to grow on.

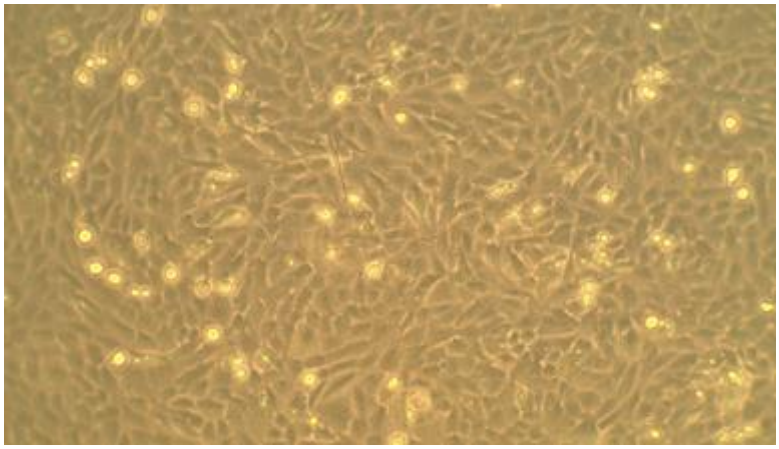

Figure 3.1: A light microscopy image of a confluent hCMEC/D3 monolayer.

3.2.4 Cell Counting

Before seeding the hCMEC/D3 cells, a cell count was made using the Countess automated cell counter (Invitrogen, Paisley, UK). A 10µl volume of the resuspended cell pellet was added to a 1.5ml Eppendorf tube and mixed with 10µl of 0.4% trypan blue. The mixture was then pipetted under the cover slip of a Countess cell counting chamber slide and inserted into the instrument.

3.2.5 Cellular uptake of AEDs and effects of a panel of MCT inhibitors

Uptake experiments employed a radiolabelled concentration of 0.3µCi/ml supplemented with non-radiolabelled drug to give final concentrations of 25µM PHT, 20µM CBZ, 300µM VPA, 10µM LTG, 10µM TPM, 10µM GBP and 6µM LEV, all prepared in transport medium (HBSS supplemented with 25mM HEPES and 0.1% bovine serum albumen (BSA), at pH7.4). A radiolabel concentration of 0.3µCi/ml afforded sufficient disintegrations per minute to give accurate readings of radioactive content without saturating the scintillation counter. Final concentrations of monocarboxylate transporter (MCT) inhibitors employed are listed in table 3.1.

On the day of the assay, media was aspirated from the cells and cells allowed to equilibrate in transport medium at 37^0C for 30 minutes. A dosing solution was made for each AED using transport medium containing the respective radiolabelled/non-radiolabelled drug (to a final concentration as stated previously) with either inhibitor or vehicle (DMSO; for control purposes). This solution was added to the cells, which were

then incubated at 37^0C for 60 minutes. In the meantime, samples (20µl) of transport buffer alone (blanks) and samples (20µl) of dosing solution (standards) were taken and added to scintillation vials for later determination of background radiation and radioactive content of a known concentration of each drug solution, respectfully. After incubation, cells were washed three-times in ice cold HBSS to terminate uptake and solubilised for 30 minutes at 37^0C with 400µl of 10% sodium dodecyl sulphate. The resulting solution was then transferred to individual scintillation vials and 4ml of scintillation fluid (Goldstar Multipurpose Scintillation Cocktail (Meridian, UK) added to all vials. Vials were mixed by inverting several times before radioactive content was determined using a scintillation counter (1500 Tri Carb LS Counter; Packard). Results in dpm were corrected for background counts, quantified in relation to standards of known concentration and expressed (in pmol/100,000 cells) in relation to the number of cells per well.

3.2.6 Statistical testing

All data is presented as the mean (± standard error of the mean) percentage of mean control transport (AED without inhibitor) for each AED on each experimental day. Individual experiments were performed in triplicate and repeated on at least three occasions ($n \geq 9$). Data was assessed for normality using the Shapiro-Wilk test and found to be normally distributed. An analysis of variance (ANOVA) was performed on the data with Tukey's post hoc test for multiple comparisons. A value of $p \leq 0.05$ was taken to indicate statistical significance.

3.3 Results

3.3.1 PHT uptake and effects of a panel of MCT inhibitors

A significant decrease in PHT uptake was observed in the presence of the bioflavonoids phloretin and quercetin, reducing PHT uptake to 14 ± 0.9% and 53 ± 2.4% of the control value (100 ± 2.0%), respectively ($p \leq 0.001$). A significant decrease in PHT uptake was also observed in the presence of simvastatin, reducing uptake to 52 ± 6.4% of control (100 ± 1.1%; $p \leq 0.001$). Conversely, a significant increase in PHT uptake was seen in the presence of lactic acid (126 ± 9.9%) in comparison to control (100 ± 2.0%; $p \leq 0.05$). Minor changes in PHT uptake were observed in the presence of ethyl-cyancinnomate (116 ± 7.1%), methyl-cyancinnomate (117 ± 8.7%), DIDS (118 ± 7.2%) and SITS (82 ± 6.3%) compared to control; however none was statistically significant (*figure 3.2; table 3.2*).

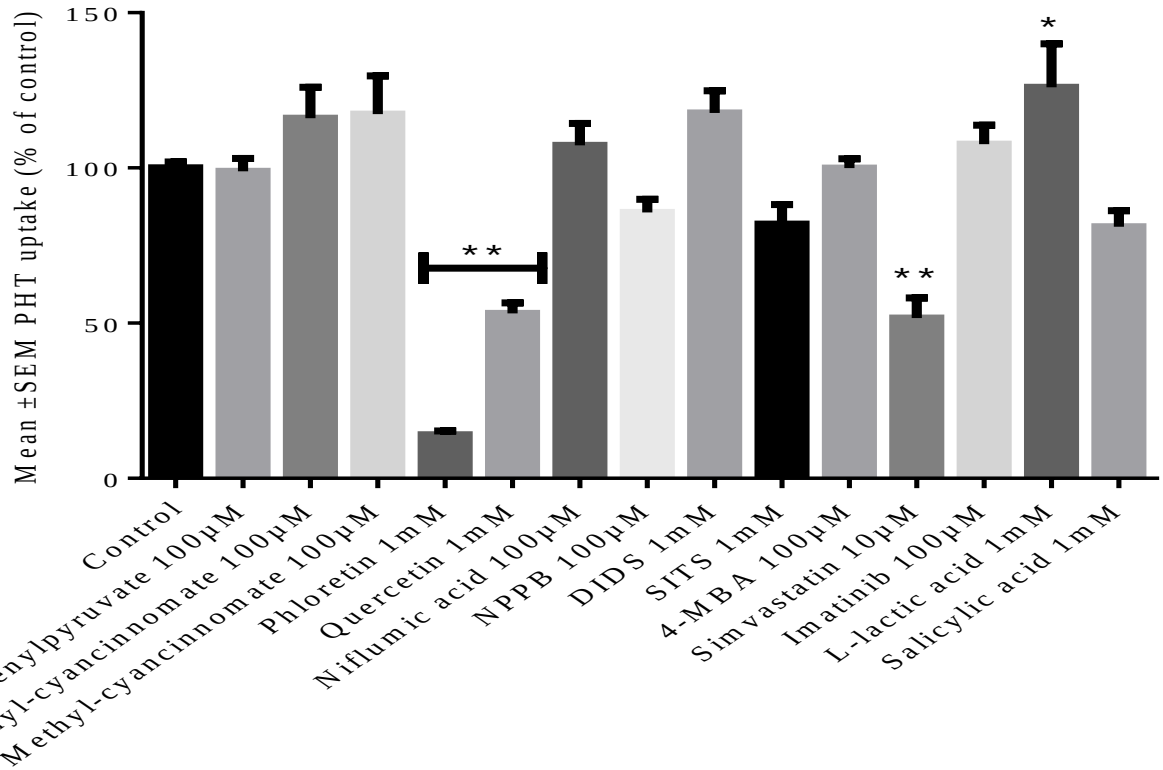

Figure 3.2: Effects of a panel of MCT inhibitors on the uptake of phenytoin (PHT) into hCMEC/D3 cells. Cultures were exposed to 25µM radiolabelled PHT with or without inhibitors at the concentrations shown for one hour at 37^0C. Results are expressed as the mean ± standard error of the mean (SEM) percentage of the mean control value of PHT uptake (in pmols/100,000 cells) on each experimental day. Experiments were performed in triplicate on three separate occasions (n=9). Statistical significance (**p<0.001, *p<0.05) was determined by one-way analysis of variance with Tukey's correction for multiple testing. (NPPB, 5-nitro-2-(3-phenylpropylamino) benzoic acid); DIDS, 4,4′-diisothiocyanatostilbene-2,2′-disulfonic acid; SITS, 4-acetamido-4′-isothiocyanato-2,2′-stilbenedisulfonic acid; 4-MBA, 4-(hydroxymercuri)benzoic acid.

3.3.2 CBZ uptake and effects of a panel of MCT inhibitors

The bioflavanoid quercetin significantly increased CBZ uptake to 408 ± 60% of the control value (100 ± 3.0%; $p \leq 0.001$); none of the remaining MCT inhibitors demonstrated any significant effect on CBZ uptake (*figure 3.3; table 3.2*).

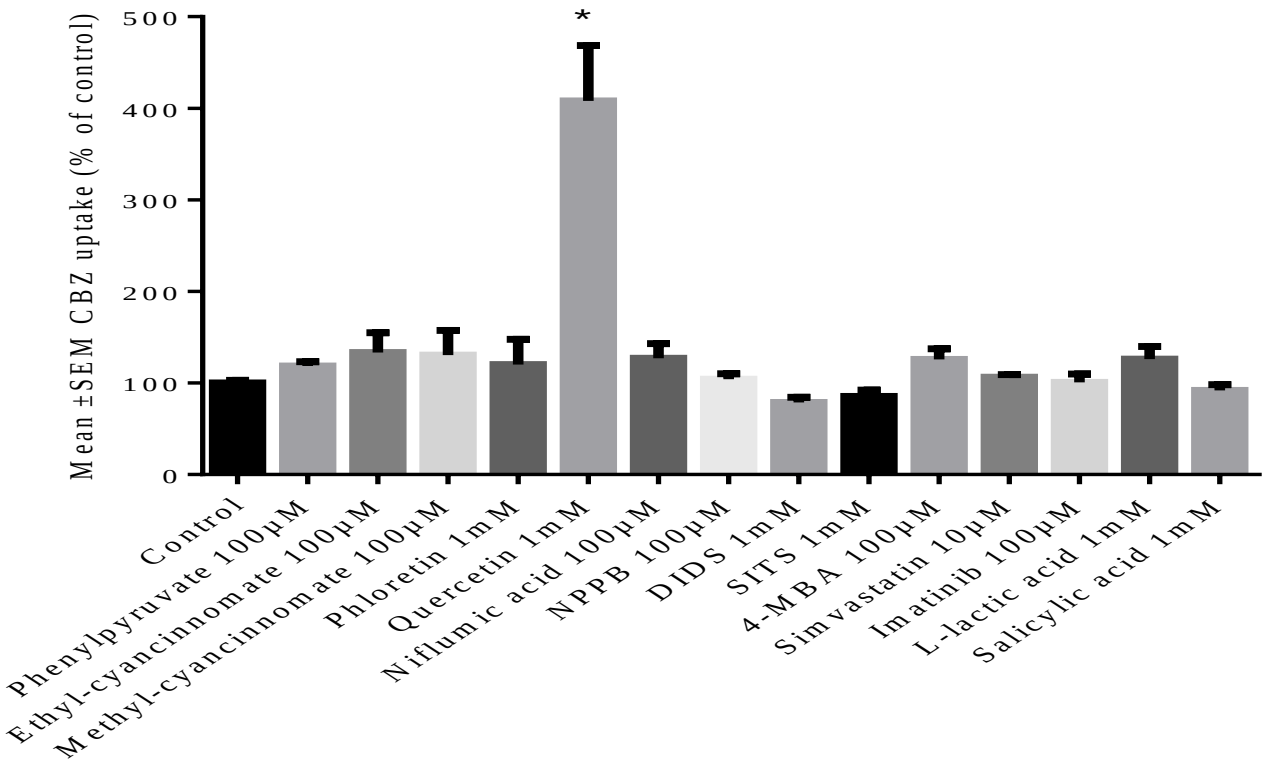

Figure 3.3: Effects of a panel of MCT inhibitors on the uptake of carbamazepine (CBZ) into hCMEC/D3 cells. Cultures were exposed to 20µM radiolabelled CBZ with or without inhibitors at the concentrations shown for one hour at 37^0C. Results are expressed as the mean ± standard error of the mean (SEM) percentage of the mean control value of CBZ uptake (in pmols/100,000 cells) on each experimental day. Experiments were performed in triplicate on three separate occasions (n=9). Statistical significance (*$p<0.001$) was determined by one-way analysis of variance with Tukey's correction for multiple testing. (NPPB, 5-nitro-2-(3-phenylpropylamino) benzoic acid); DIDS, 4,4′-diisothiocyanatostilbene-2,2′-disulfonic acid; SITS, 4-acetamido-4′-isothiocyanato-2,2′-stilbenedisulfonic acid; 4-MBA, 4-(hydroxymercuri)benzoic acid).

3.3.3 VPA uptake and effects of a panel of MCT inhibitors

An increase in VPA uptake to 168 ± 10% of the control value (100 ± 8.0%) was observed in the presence of the bioflavanoid compound quercetin ($p \leq 0.001$). VPA uptake also increased to 138 ± 6.5% of the control in the presence of 4-MBA, but this effect failed to reach statistical significance. None of the remaining MCT inhibitors demonstrated any significant effect on VPA uptake (*figure 3.4; table 3.2*).

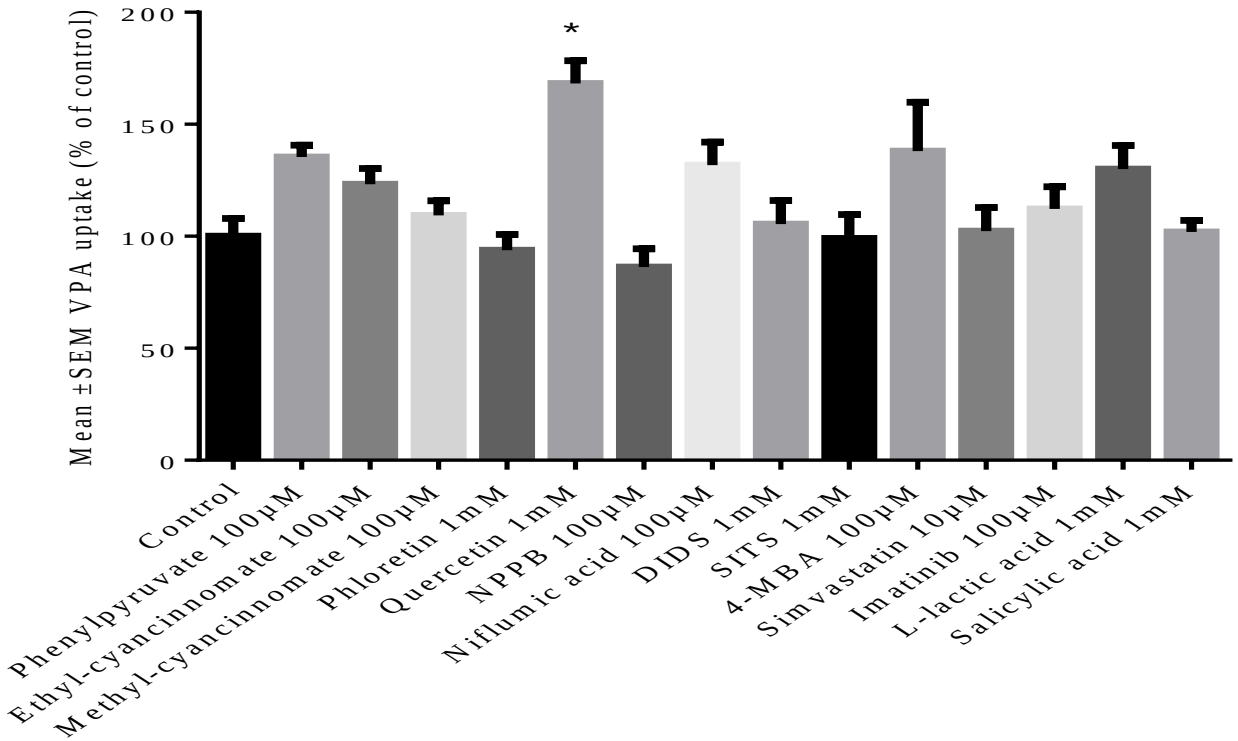

Figure 3.4: Effects of a panel of MCT inhibitors on the uptake of valproic acid (VPA) into hCMEC/D3 cells. Cultures were exposed to 300µM radiolabelled VPA with or without inhibitors at the concentrations shown for one hour at 37^0C. Results are expressed as the mean ± standard error of the mean (SEM) percentage of the mean control value of VPA uptake (in pmols/100,000 cells) on each experimental day. Experiments were performed in triplicate on three separate occasions (n=9). Statistical significance (*$p<0.001$) was determined by one-way analysis of variance with Tukey's correction for multiple testing. (NPPB, 5-nitro-2-(3-phenylpropylamino) benzoic acid); DIDS, 4,4′-diisothiocyanatostilbene-2,2′-disulfonic acid; SITS, 4-acetamido-4′-isothiocyanato-2,2′-stilbenedisulfonic acid; 4-MBA, 4-(hydroxymercuri)benzoic acid).

3.3.4 LTG uptake and effects of a panel of MCT inhibitors

The bioflavanoid compound quercetin and the anion transport inhibitors niflumic acid and NPPB increased LTG uptake to 180 ± 8.4% ($p \leq 0.001$), 132 ± 7.1% ($p \leq 0.01$) and 147 ± 11% ($p \leq 0.01$) of the control value (100 ± 3.2%), respectively. A decrease in LTG uptake was observed in the presence of phloretin and imatinib, reducing LTG uptake to 26 ± 2.0% and 33 ± 2.5% of control (both $p \leq 0.001$), respectively. Minor changes in LTG transport were observed in the presence of DIDS (120 ± 24%) and SITS (77 ± 3.0%), but these did not reach statistical significance (*figure 3.5; table 3.2*).

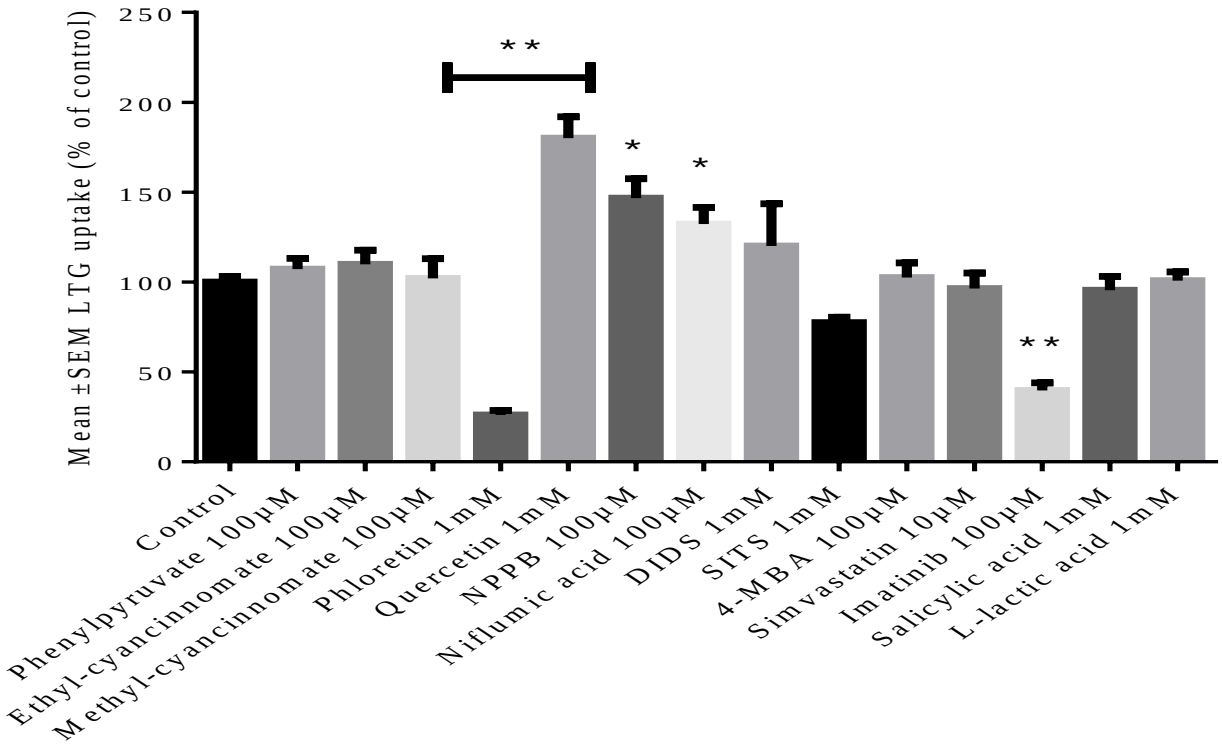

Figure 3.5: Effects of a panel of MCT inhibitors on the uptake of lamotrigine (LTG) into hCMEC/D3 cells. Cultures were exposed to 10µM radiolabelled LTG with or without inhibitors at the concentrations shown for one hour at 37^0C. Results are expressed as the mean ± standard error of the mean (SEM) percentage of the mean control value of LTG uptake (in pmols/100,000 cells) on each experimental day. Experiments were performed in triplicate on three separate occasions (n=9). Statistical significance (**$p<0.001$, *$p<0.05$) was determined by one-way analysis of variance with Tukey's correction for multiple testing. (NPPB, 5-nitro-2-(3-phenylpropylamino) benzoic acid); DIDS, 4,4′-diisothiocyanatostilbene-2,2′-disulfonic acid; SITS, 4-acetamido-4′-isothiocyanato-2,2′-stilbenedisulfonic acid; 4-MBA, 4-(hydroxymercuri)benzoic acid).

3.3.5 GBP uptake and effects of a panel of MCT inhibitors

Increases in GBP uptake were observed in the presence of quercetin, NPPB, DIDS, SITS, simvastatin and salicylic acid, with GBP uptake increasing to 242 ± 20% ($p \leq 0.001$), 261 ± 22% ($p \leq 0.001$), 159 ± 16% ($p \leq 0.001$), 131 ± 5.1% ($p \leq 0.01$), 129 ± 3.3% ($p \leq 0.05$) and 128 ± 2.6% ($p \leq 0.05$) of the control value (100 ± 3.7%), respectively. In contrast, a decrease in GBP uptake compared to control was observed in the presence of phloretin (5.3 ± 1.0%, $p<0.001$) and 4-MBA (3.0 ± 0.2%, $p<0.001$) (*figure 3.6; table 3.2*).

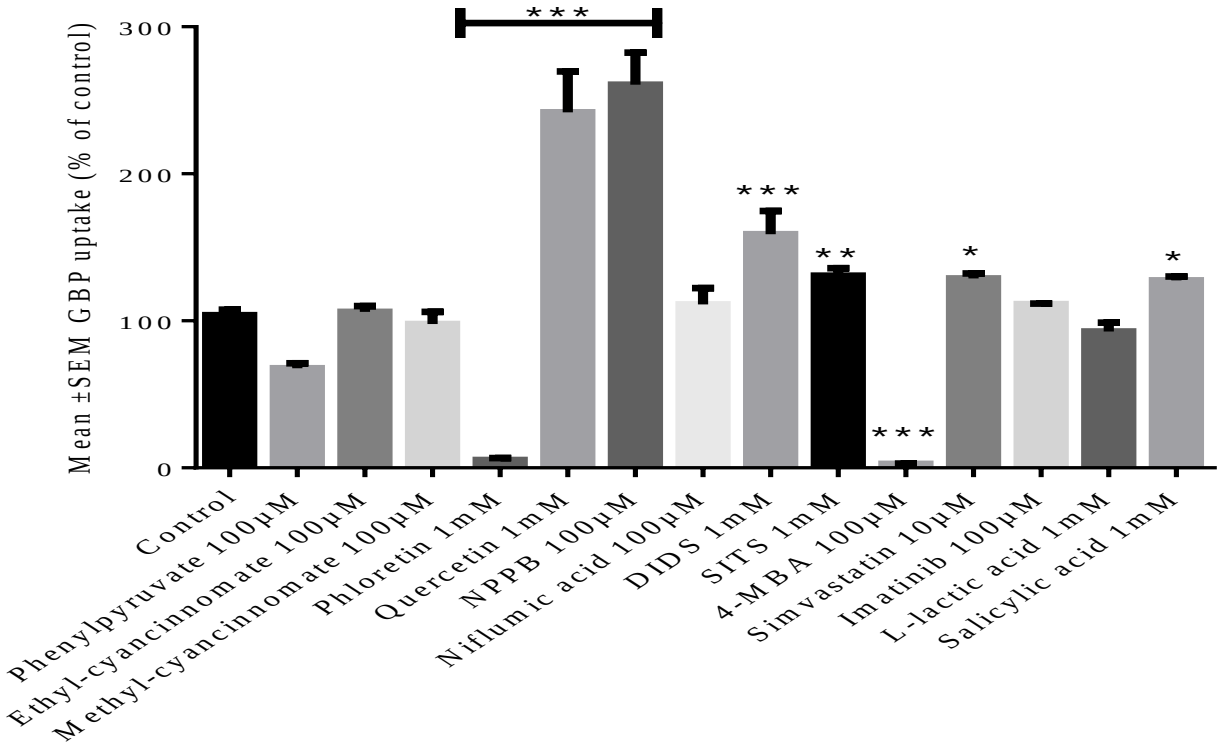

Figure 3.6: Effects of a panel of MCT inhibitors on the uptake of gabapentin (GBP) into hCMEC/D3 cells. Cultures were exposed to 10µM radiolabelled GBP with or without inhibitors at the concentrations shown for one hour at 37^0C. Results are expressed as the mean ± standard error of the mean (SEM) percentage of the mean control value of GBP uptake (in pmols/100,000 cells) on each experimental day. Experiments were performed in triplicate on three separate occasions (n=9). Statistical significance (***p<0.001, **p<0.01, *P<0.05) was determined by one-way analysis of variance with Tukey's correction for multiple testing. (NPPB, 5-nitro-2-(3-phenylpropylamino) benzoic acid); DIDS, 4,4′-diisothiocyanatostilbene-2,2′-disulfonic acid; SITS, 4-acetamido-4′-isothiocyanato-2,2′-stilbenedisulfonic acid; 4-MBA, 4-(hydroxymercuri)benzoic acid).

3.3.6 TPM uptake and effects of a panel of MCT inhibitors

The presence of phloretin and SITS decreased TPM uptake to 49 ± 3.9% ($p \leq 0.001$) and 75 ± 3.4% ($p \leq 0.001$) of the control value (100 ± 2.3%), respectively. Conversely, ethyl-cyancinnamate, quercetin and niflumic acid increased TPM uptake to 115 ± 2.5% ($p \leq 0.05$), 168 ± 2.1% ($p \leq 0.001$) and 117 ± 1.6% ($p \leq 0.01$) of control, respectively *(figure 3.7; table 3.2).*

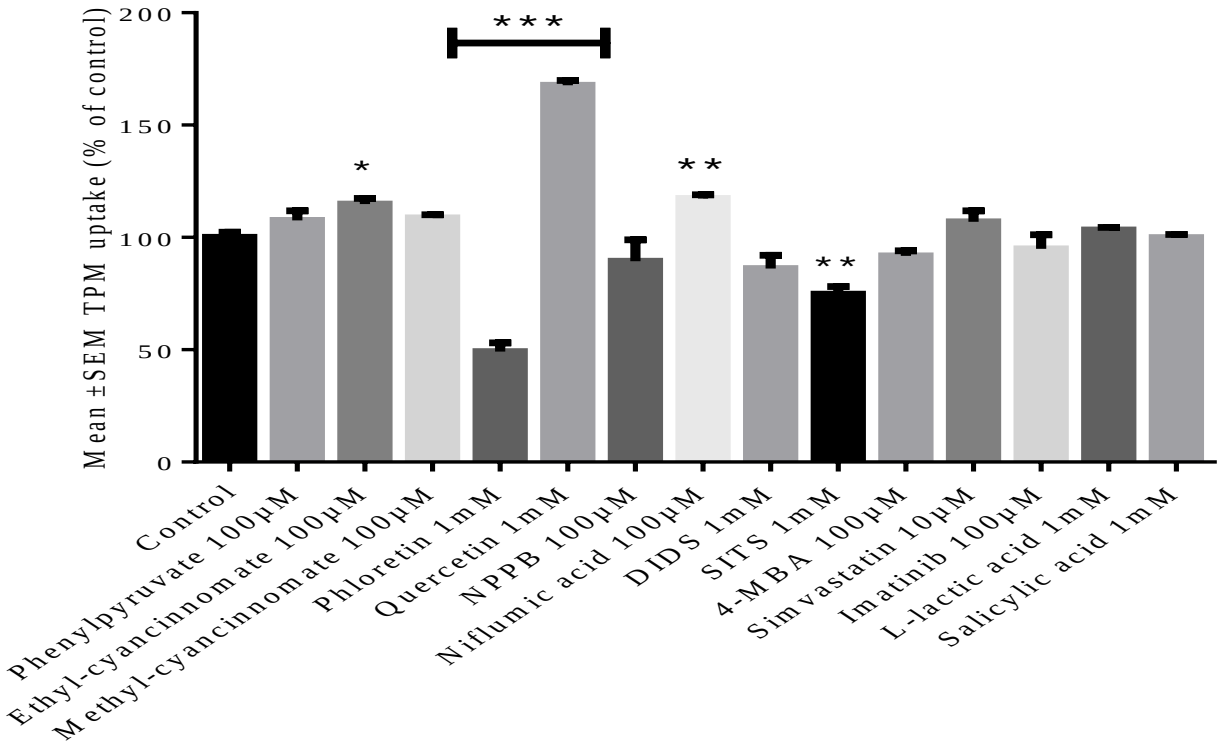

Figure 3.7: Effects of a panel of MCT inhibitors on the uptake of topiramate (TPM) into hCMEC/D3 cells. Cultures were exposed to 10µM radiolabelled TPM with or without inhibitors at the concentrations shown for one hour at 37^0C. Results are expressed as the mean ± standard error of the mean (SEM) percentage of the mean control value of TPM uptake (in pmols/100,000 cells) on each experimental day. Experiments were performed in triplicate on three separate occasions (n=9). Statistical significance (***$p<0.001$, **$p<0.01$, *$p<0.05$) was determined by one-way analysis of variance with Tukey's correction for multiple testing. (NPPB, 5-nitro-2-(3-phenylpropylamino) benzoic acid); DIDS, 4,4′-diisothiocyanatostilbene-2,2′-disulfonic acid; SITS, 4-acetamido-4′-isothiocyanato-2,2′-stilbenedisulfonic acid; 4-MBA, 4-(hydroxymercuri)benzoic acid).

3.3.7 LEV uptake and effects of a panel of MCT transporter inhibitors

A decrease in LEV uptake was observed in the presence of the bioflavanoid phloretin, reducing LEV uptake to 20 ± 9.1% ($p \leq 0.001$) of the control value (100 ± 3.2%). No changes in uptake were observed in the presence of any other MCT inhibitor *(figure 3.8; table 3.2).*

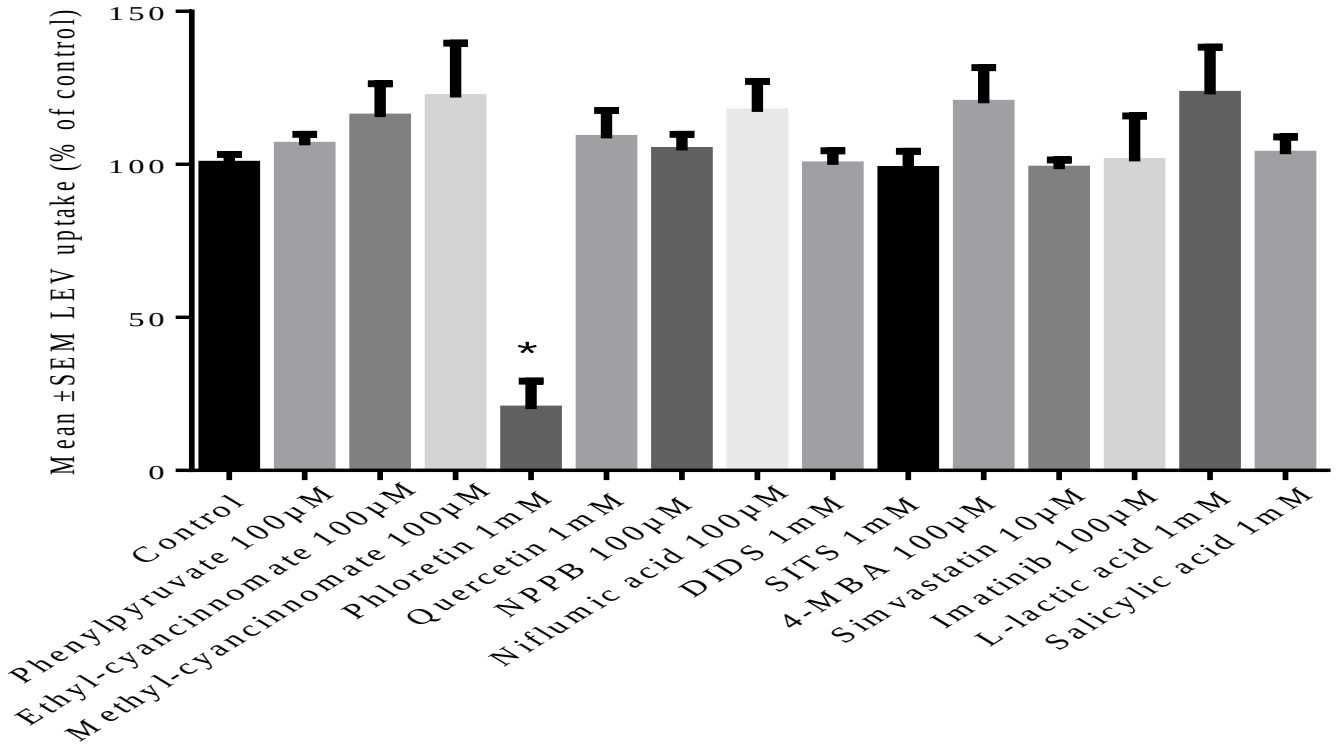

Figure 3.8: Effects of a panel of MCT inhibitors on the uptake of levetiracetam (LEV) into hCMEC/D3 cells. Cultures were exposed to 6µM radiolabelled LEV with or without inhibitors at the concentrations shown for one hour at 37^0C. Results are expressed as the mean ± standard error of the mean (SEM) percentage of the mean control value of LEV uptake (in pmols/100,000 cells) on each experimental day. Experiments were performed in triplicate on three separate occasions (n=9). Statistical significance (*$p<0.001$) was determined by one-way analysis of variance with Tukey's correction for multiple testing. (NPPB, 5-nitro-2-(3-phenylpropylamino) benzoic acid); DIDS, 4,4′-diisothiocyanatostilbene-2,2′-disulfonic acid; SITS, 4-acetamido-4′-isothiocyanato-2,2′-stilbenedisulfonic acid; 4-MBA, 4-(hydroxymercuri)benzoic acid).

	Mean ± SEM uptake (% of control)						
	Phenytoin	Carbamazepine	Sodium valproate	Lamotrigine	Gabapentin	Topiramate	Levetiracetam
Control	100 ±1.9	100 ±3.0	100 ±8.0	100 ±3.2	104 ±3.7	100 ±2.3	100 ±3.2
Phenylpyruvate 100µM	98.9 ±4.2	118 ±4.8	135 ±5.2	107 ±5.9	67.7 ±3.5	108 ±4.4	106 ±3.6
Ethyl-cyancinnomate 100µM	116 ±10	133 ±22	123 ±7.0	110 ±7.8	106 ±3.9	115 ±2.4*	115 ±11
Methyl-cyancinnomate 100µM	117 ±12	130 ±27	109 ±6.4	102 ±11	97.9 ±8.1	109 ±1.4	122 ±18
Phloretin 1000µM	14.0 ±1.3***	120 ±27	93.8 ±7.0	26.0 ±2.5***	5.31 ±1.4***	49.2 ±3.9***	20.1 ±9.1***
Quercetin 1000µM	53.2 ±3.4***	408 ±60***	168 ±10***	180 ±12***	242 ±20***	168 ±2.1***	109 ±9.1
Niflumic acid 100µM	107 ±7.1	127 ±16	86.2 ±8.2	147 ±11*	261 ±22	89.4 ±9.6**	105 ±5.3
NPPB 100µM	85.7 ±4.2	104 ±6.1	132 ±10	132 ±9.2*	111 ±11***	117 ±1.6	117 ±9.9
DIDS 1000µM	118 ±7.2	78.7 ±5.9	105 ±11	120 ±24	159 ±16***	86.2 ±5.9	100 ±4.6
SITS 1000µM	81.9 ±6.3	85.4 ±6.9	99.1 ±11	77.4 ±3.0	131 ±5.1**	74.8 ±3.3**	98.4 ±5.9
4-MBA 100µM	100 ±3.0	126 ±11	138 ±22	102 ±8.2	2.75 ±0.23***	91.7 ±2.3	120 ±12
Simvastatin 10µM	51.6 ±6.4***	106 ±2.8	102 ±10	96.5 ±8.5	129 ±3.3*	107 ±4.9	98.4 ±3.0
Imatinib 100µM	108 ±6.1	101 ±8.9	112 ±9.9	39.8 ±4.2***	111 ±0.46	94.9 ±6.3	101 ±15
L-lactic acid 1000µM	126 ±14*	126 ±14	130 ±10	95.5 ±7.5	92.8 ±6.0	103 ±1.1	123 ±15
Salicylic acid 1000µM	81.1 ±5.2	91.8 ±6.5	102 ±5.1	101 ±4.9	128 ±2.6*	100 ±1.4	103 ±5.6

Table 3.2: Effects of a panel of MCT inhibitors on the uptake of a panel of antiepileptic drugs into hCMEC/D3 cells. Cultures were exposed to 25µM radiolabelled phenytoin, 20µM radiolabelled carbamazepine, 300µM radiolabelled sodium valproate, 10µM radiolabelled lamotrigine, 10µM radiolabelled gabapentin, 10µM radiolabelled topiramate and 6µM radiolabelled levetiracetam with or without inhibitors at the concentrations shown for one hour at 37^0C. Results are expressed as the mean ± standard error of the mean (SEM) percentage of the mean control value of uptake (in pmols/100,000 cells) on each experimental day. Experiments were performed in triplicate on three separate occasions (n=9). Statistical significance (***p<0.001, **p<0.01, *p<0.05) was determined by one-way analysis of variance with Tukey's correction for multiple testing. (NPPB, 5-nitro-2-(3-phenylpropylamino) benzoic acid); DIDS, 4,4′-diisothiocyanatostilbene-2,2′-disulfonic acid; SITS, 4-acetamido-4′-isothiocyanato-2,2′-stilbenedisulfonic acid; 4-MBA, 4-(hydroxymercuri)benzoic acid).

3.4 Discussion

Members of the MCT family are known to be expressed at the BBB where they function to supply the brain with nutrients and to transport thyroid hormones (Pierre *et al.*, 2005; Roberts *et al.*, 2008). In addition, a number of drugs have been suggested to be substrates and/or inhibitors of MCT-mediated transport (Neuhoff *et al.*, 2005; Kobayashi *et al.*, 2006; Wang *et al.*, 2006; Braun *et al.*, 2011) including the AED VPA (Utoguchi *et al.*, 2000; Fischer *et al.*, 2008) and the GBP prodrug, gabapentin enacarbil (Cundy *et al.*, 2004; Lal *et al.*, 2010).

In this chapter the transport of commonly prescribed AEDs was investigated in the hCMEC/D3 cell line, with the aim of characterising any MCT-mediated transport by the inclusion of various chemical inhibitors of MCTs. The hCMEC/D3 cells were chosen as the investigative *in vitro* model of the BBB as they are phenotypically very similar to brain endothelial cells *in vivo* (Weksler *et al., 2013*). In addition, hCMEC/D3 cells have been reported to express several MCT transporters (Carl *et al.*, 2010). To summarise the findings, the inclusion of various chemical MCT inhibitors had a significant impact on the transport of PHT, LTG, GBP and TPM and minor influences on the transport of CBZ, VPA and LEV.

PHT uptake was seen to both increase and decrease with the inclusion of MCT inhibitors. The bioflavonoids phloretin and quercetin and the HMG-CoA inhibitor simvastatin significantly decreased PHT uptake, whereas lactic acid significantly increased PHT uptake (*figure 3.1*; table 3.2). HMG-CoA inhibitors have been demonstrated to inhibit MCT4 transport (Kobayashi *et al.*, 2006) suggesting the decrease in PHT uptake in the presence simvastatin acid is due to inhibition of MCT4 mediated transport. However it is not known whether inhibition is specific to MCT4 or if activity extends to multiple MCT transporters. Given the overlapping substrate specificity of MCT1 - 4 it is conceivable that simvastatin acid inhibits all four proteins albeit with varying potency. Furthermore both phloretin and quercetin are non-specific MCT transport inhibitors therefore it cannot be confirmed which MCT transporter, if any, is responsible for the decreases in PHT uptake observed. Alternatively, it is plausible that the inhibition of PHT uptake observed in the presence of these inhibitors is not MCT-mediated. In addition to MCT4, HMG-CoA inhibitors such as simvastatin have been demonstrated to be both substrates and inhibitors of the organic anion

transporting polypeptides OATP1B1, OATP1B3 and OATP2B1 (Hirano *et al*., 2004; Chen *et al*., 2005; Kopplow *et al*., 2005; Hirano *et al*., 2006; Ho *et al*., 2006), the latter of which has been demonstrated to be expressed in hCMEC/D3 cells (Carl *et al*., 2010). Furthermore OATP2B1-mediated transport of estrone-3-sulphate in X.*laevis* oocytes has also been shown to be subject to inhibition by phloretin and quercetin (Shirasaka *et al.*, 2012). In addition inhibition of GLUT1-mediated transport of glucose in erythrocytes (Martin *et al.*, 2003) and GLUT2/GLUT8-mediated transport of dihydroascorbic acid in *SLC2A2/SLC2A8* transfected X.*laevis* oocytes (Corpe *et al.*, 2013) has also been demonstrated to be potently inhibited by both flavonoids. Due to the demonstrated activity of simvastatin, phloretin and quercetin at other transporters, the changes in PHT uptake observed in hCMEC/D3 cells cannot be confidently attributed to inhibition of MCT-mediated transport and further work is necessary to identify the transporter implicit in the uptake of PHT into hMEC/D3 cells.

The modest increase in PHT uptake observed in the presence of L-lactic acid could be explained by potential efflux of PHT by an MCT. In white skeletal muscle fibres MCT4 has been demonstrated to be expressed in a muscle to blood orientation on the muscle fibre membrane, where it functions to efflux lactic acid into the blood (Manning Fox *et al*., 2000; Halestrap *et al*., 2004). Expression of MCT4 in hCMEC/D3 cells has only been shown at mRNA level (Carl *et al*., 2010), therefore the membrane location of the protein product it is not known. However if orientated in the brain to blood orientation at the apical membrane of cerebral endothelial cells, it may function to efflux lactic acid and other substrates. If so, the increase in PHT uptake in the presence of lactic acid observed may be due to competition for MCT4, therefore less PHT is effluxed from the cell.

LTG uptake was dramatically reduced in the presence of imatinib and phloretin (*figure 3.5*; table 3.2). Imatinib has recently been shown to inhibit MCT8-mediated transport in an MDCK cell line stably expressing MCT8 (Braun *et al.*, 2011). However, as with phloretin which has been shown to inhibit a number of SLC transporters as discussed previously, imatinib has also been implicated in the inhibition of other SLC transporters in addition to MCT8. Recently, imatinib has been shown to be transported by both cationic and anionic transporters. Imatinib was demonstrated to be subject to OATP1A2-mediated transport in a HEK293 cell line stably expressing OATP1A2 (Hu *et al.*, 2008). In addition, LTG and imatinib have been shown to be substrates for

organic cation transporter 1 (OCT1) in a KCL22 cell line stably expressing OCT1 and a human T-lymphoblastoid (CCRF-CEM) cell line, respectively (Thomas *et al.*, 2004; Dickens *et al.*, 2012). The inhibition of LTG uptake observed in the presence of imatinib could therefore be a result of competitive inhibition for OATP1A2 or OCT1 transport. However, in chapter 2 LTG was not observed to be transported by OATP1A2 and furthermore OATP1A2 was shown not to be expressed in hCMEC/D3 cells, therefore LTG transport in hCMEC/D3 cells is unlikely to be mediated by OATP1A2. Interestingly, Braun *et al*, 2011 showed that inhibition of MCT8 by imatinib was non-competitive whereas OCT1/OATP1A2 mediated inhibition has been demonstrated to be competitive.

Conversely, an increase in LTG uptake was observed in the presence of the bioflavonoid quercetin and the anion transport inhibitors NPPB and niflumic acid, suggesting active efflux of LTG. Although this cannot be attributed to MCT transporters due to the overlapping specificity of these chemical inhibitors with anion transporters (Halestrap *et al*., 2004). Given the ability to effect LTG transport with chemical inhibition in this study and that LTG has previously been shown to be transported by OCT1 (Dickens *et al*., 2012), it is likely that LTG transport in and out of the brain occurs as a result of active transport. This is potentially mediated by several transporters from various families including MCT transporters, however this hypothesis is speculative and cannot be proven without significant further investigation.

TPM transport was also subject to inhibition, with increases in uptake observed in the presence of ethyl-cyancinnomate, quercetin and nuflumic acid and decreases seen with phloretin and SITS (*figure 3.7*; table 3.2). All of the inhibitors observed to influence TPM uptake into hCMEC/D3 cells are non-specific MCT inhibitors. Although these observations may potentially be attributed to MCT transporter, identification of the isoform/s involved cannot be achieved without further investigation. Furthermore a number of the MCT inhibitors shown to significantly effect TPM uptake, namely nuflumic acid, phloretin, quercetin and SITS are also known to inhibit anionic transport (Forman *et al*., 1982; Halestrap *et al.*, 2004). Given that TPM is known to form an anion at physiological pH (Maryanoff *et al.*, 1987), the changes in TPM transport observed in this study might equally be due to inhibition of an anion transporter expressed in hCMEC/D3 cells.

In addition, the bioflavonoids quercetin and phloretin have been shown to inhibit P-gp (Conseil *et al*., 1998; Zhang *et al*., 2003) and TPM has been demonstrated to be subject to active efflux by P-gp (Sills *et al*., 2002). P-gp is known to be expressed at the apical membrane of the BBB *in vivo* where it actively effluxes substrate drugs from the brain (Klassen *et al*., 2010). Furthermore P-gp has been shown to be relatively highly expressed in hCMEC/D3 cells (Carl *et al*., 2010). Therefore the increases in TPM uptake observed in the presence of chemical inhibitors may be a result of inhibition of P-gp mediated efflux of TPM out of hCMEC/D3 cells, therefore more TPM is accumulating inside the cell.

More than half of the inhibitors included in this investigation inhibited GBP transport into hCMEC/D3 cells (*figure 3.6*; table 3.2). Phloretin and 4-MBA both dramatically reduced GBP uptake; 4-MBA is known to exert its inhibitory effects by interacting with the MCT1/MCT4 accessory protein basigin (Wilson *et al.*, 2005). Moreover, MCT2 is insensitive to 4-MBA inhibition (as described previously) suggesting that GBP uptake in hCMEC/D3 cells is MCT1 or possibly MCT4 mediated, compounding the observation in chapter 2 of this thesis that GBP may be transported by MCT1. Interestingly, the presence of quercetin, NPPB, DIDS, SITS, simvastatin and salicylic acid significantly increased GBP uptake, suggesting efflux of GBP. MCT1expression is known to be polarised in brain endothelial cells and there is support that MCT1 mediates bidirectional transport of substrates and so may play a role in both influx and efflux of substrate drugs (Gerhart *et al.*, 1997; Hertz *et al.*, 2004). Given that MCT4 has been demonstrated to be expressed apically in other organ tissues where it functions to efflux lactic acid (Manning Fox *et al*., 2000), it is possible the changes in GBP transport in the presence of the chemical inhibitors tested are attributed to inhibition of MCT mediated efflux and influx in hCMEC/D3 cells. The influence MCT transport inhibitors were observed to have on the transport of GBP in hCMEC/D3 cells provides the strongest justification of all the AEDs tested for an MCT mediated transport mechanism. Although overlapping substrate specificity of many of the inhibitors observed to influence GBP transport means involvement of other transporters in the transport of GBP in hCMEC/D3 cells cannot be completely discounted. These observations along with observations from chapter 2 of this thesis suggest that MCT transporters, most likely MCT1 could be involved (at least partly) in the transport of GBP at the BBB.

In the previous chapter, MCT1 was demonstrated not to transport VPA in a X.*laevis* model, an observation that disagreed with previous research reports in which several groups had suggested an MCT1 involvement in the cellular uptake of VPA (Utoguchi *et al.*, 2000; Fischer *et al.*, 2008). Data from hCMEC/D3 cells, however, is in agreement with findings in chapter 2 of this thesis; none of the MCT inhibitors (with the exception of a modest enhancing effect of phloretin) had any significant effect on VPA transport (*figure 3.4*; table 3.2). This observation was unexpected and suggests that contrary to previous research and to the monocarboxylic acid structure of VPA, VPA is not transported by MCTs. There are various explanations for the discrepancy between these and previous findings, one possibility is that another transporter expressed in the cell lines used previously not belonging to the MCT family was responsible for the observed VPA transport. For example, a recent study used a *Dictyostelium* model to explore cell signalling pathways regulated by VPA and reported transport of VPA by a bicarbonate transporter (Terbach *et al.*, 2011). There is sufficient sequence homology between *Dictyostelium* and human forms of this transporter to suggest that VPA might also be transported by the human form (encoded by *SLC4A11*) (Terbach *et al.*, 2011). The disparity observed in MCT-mediated VPA uptake could also be explained by pH dependence. The MCT-mediated transport of VPA demonstrated by Utoguchi *et al*, 2000 was much more pronounced at pH 6 than pH 7.4. This might suggest that at low pH when VPA is not in its anionic form it is transported by an MCT transporter, whereas at higher pH VPA uptake is not mediated by MCTs (Utoguchi *et al.*, 2000). Although transport at pH 6 is not of interest when investigating VPA permeation into the brain, it may be of importance in VPA absorption from the gut.

No significant changes in CBZ and LEV uptake were observed in the presence of MCT inhibitors, except with quercetin and phloretin, respectively (*figures 3.3 and 3.8*; table 3.2). Interestingly, phloretin and quercetin showed at least modest influences on the transport of all AEDs included in this investigation (*figures 3.2 to 3.8*; table 3.2). Phloretin and quercetin are notoriously promiscuous transport inhibitors and are known to interact with many transporter families including influx and efflux transporters (Forman *et al*., 1982; Conseil *et al*., 1998; Leslie *et al*., 2001; Zhang et al., 2003; Halestrap *et al.*, 2004; Zhang et al., 2004). This might suggest that all of the AEDs tested are subject to active transport in hCMEC/D3 cells. However flavonoid compounds such as phloretin and quercetin have been demonstrated to effect the

activity of mammalian enzyme systems including protein kinases, ATPase phospholipase and cyclooxygenases (Middleton *et al.*, 2000). It is therefore plausible that changes in AED transport observed in hCMEC/D3 cells may be a result of cellular metabolic changes rather than direct transporter protein inhibition.

The hCMEC/D3 cell line has been proven to share phenotypic characteristics of the human BBB *in vivo* and provides a useful model with which to investigate drug transport at the BBB (Poller; *et al.*, 2008). Although the chemical inhibition technique employed in this investigation is a powerful screening tool in identifying whether a drug is subject to active transport at the BBB, its sensitivity in terms of identifying drug interactions with specific transporters responsible is limited by the lack of availability of potent and selective inhibitors. This proved a major limitation of this study and may explain the largely ambiguous data generated in which clear conclusions cannot be drawn. Several potent MCT1-selective inhibitors have recently been developed by AstraZeneca (Murray *et al.*, 2005; Guile *et al.*, 2006; Ekberg *et al.*, 2007) and would be valuable in further studies aimed at determining whether the chemical inhibition of PHT, LTG, GBP and TPM uptake was mediated via MCT1. However, when approached, AstraZeneca was not in a position to allow the use of these inhibitors in this project.

The experiments described in this chapter suggest that multiple AEDs may be subject to MCT-mediated transport at the BBB but that this cannot be reliably concluded or the individual transporter(s) identified because of the limitations of the available inhibitors in terms of selectivity and overlapping specificities. Of all AEDs tested, GBP appeared to be most susceptible to MCT-mediated transport, most probably by MCT1 but possibly by MCT4.

This study has highlighted the limitations of the use of chemical inhibitors to identify specific transporter proteins responsible for the uptake of AEDs into hCMEC/D3 cells. An alternative experimental approach is the use of small interfering RNA (siRNA) to target specific transporters. Using this approach the expression of functional MCT transporter proteins and combinations of MCT transporter proteins can be significantly reduced by interference and ultimate breakdown of target gene mRNA, therefore preventing protein translation. Uptake of AEDs in siRNA treated and non-treated hCMEC/D3 cells can then be compared and any differences analysed. The use of such

techniques could be utilised to follow up the observations made in this study and identify which, if any MCT transporter is involved in the transport of PHT, LTG, TPM and GBP in hCMEC/D3 cells.

Chapter 4

Antiepileptic drug transport by OAT transporters

4.1 Introduction

Organic anion transporters (OATs) are a subset of major facilitator transporters and belong to the SLC transporter superfamily. OATs have become a major area of transporter research due to their role in the elimination of a number of therapeutically relevant drugs (Riedmaier *et al.*, 2012). OATs transport chemically diverse, mainly hydrophilic anions up to 400-500Da in size but are also known to transport amphiphilic anions, uncharged molecules and even cationic molecules. Transport of such molecules, although energy dependent, does not directly utilize ATP hydrolysis (Rizwan *et al.*, 2007). OATs instead function via a specialised secondary active transport mechanism, often termed 'tertiary' active transport (VanWert *et al.*, 2010). This involves the exchange of intracellular anions such as α-ketoglutarate (the intracellular dicarboxylate preferred by OAT1 and OAT3) for extracellular anions. The intracellular anion concentration is kept above that of the extracellular environment by sodium coupled anion transporters, which are co-expressed with OAT transporters to fulfil this function (Rizwan *et al.*, 2007; Burckhardt, 2012). OAT transporters are found in the brain and most organs with excretory or barrier functions, including liver and placenta, however by far the highest and most diverse expression of OAT transporters is in the kidney. Here OAT transporters, including OAT1, OAT2 and OAT3, expressed on the interstitial (basolateral) membrane of proximal tubule cells are believed to represent the rate limiting step in the *in vivo* renal clearance of anionic drugs, metabolites and toxins due to their role in the uptake of such molecules from the blood into proximal tubule cells (Sekine *et al.*, 2000; Gallegos *et al.*, 2012). OATs expressed at the luminal membrane of the proximal tubule, including OAT4, OAT10 and the urate anion exchanger 1 (URAT1), are also believed to play a pivotal role in the secretion of anionic drugs from proximal tubule cells into the filtrate to be excreted in the urine (Burckhardt, 2012; Volk, 2014).

In 1998, OAT1 was first cloned in humans from kidney mRNA (Reid *et al.*, 1998) and has since been detected at lower levels in the brain, placenta and skeletal muscle (Anzai *et al.*, 2006). The prototypic control substrate of OAT1 is p-aminohippuric acid (PAH), an amide derivative of glycine first used in the functional characterisation of human OAT1 in *X.laevis* oocytes (Race *et al.*, 1999). PAH is transported by OAT1 with high affinity and K_m values of 3.1μM-112.7μM have been reported depending on the expression system employed (Riedmaier *et al.*, 2012). PAH is almost completely cleared from the blood by OAT transporters expressed at the proximal tubule cells in a

single pass through the kidney. As a result PAH is used clinically to estimate renal plasma flow (Sekine *et al.*, 2000). Rapid transport of PAH into the brain suggests that OAT1 is also likely to be expressed at the BBB (Kusuhara *et al.*, 1999), and there is evidence that OAT1 is expressed in both rat and human brain (Sekine *et al.*, 1997; Cihlar *et al.*, 1999; Eraly *et al.*, 2003; Bleasby *et al.*, 2006).

Human OAT3 was first cloned from human kidney and fully characterised in 1999 in *X.laevis* oocytes (Race *et al.*, 1999). Of the OAT transporters, OAT3 is thought to have the highest expression in human brain and has been shown to be expressed at the basolateral membrane of rat brain endothelial cells (Ohtsuki *et al.*, 2002; Kikuchi *et al.*, 2003; Mori *et al.*, 2003). Interestingly the OAT3 gene, *SLC22A8,* is found paired with the OAT1 gene *SLC22A6* on chromosome 11q12.3. Such pairing is thought to reflect a potential partnership in both tissue distribution and transport function (Eraly *et al.*, 2003). In contrast to OAT1, PAH is not widely employed as a prototypic test substrate for OAT3, due to its much lower affinity for OAT3 (K_m ~87µM) (Cha *et al.*, 2001). Instead estrone-3-sulphate (E3S) is commonly used, which has a high affinity for OAT3, with K_m values between 2.2µM and 21.2µM reported (Burckhardt, 2012). The ability of OAT3 to transport E3S at high affinity also distinguishes OAT3 mediated transport from OAT1, which mediates only very low affinity transport of E3S, if any (Burckhardt *et al.*, 2011).

OAT2 was first identified in rat liver in 1994 (Simonson *et al.*, 1994) and in 2001 the human homologue was cloned from human liver and functionally characterised (Sun *et al.*, 2001). OAT2 has received less interest than OAT1 and OAT3 as its expression in the kidneys is much lower than its homologues. As a consequence, its contribution to the renal clearance of anionic therapeutic agents is thought to be minimal. Although it is predominantly expressed in the liver and to a lesser extent in the kidneys, OAT2 has also been detected in pancreas, small intestine, testis, lung, brain, spinal cord and heart (in order of descending expression) (Cropp *et al.*, 2008). In contrast to OAT1 and OAT3, which preferentially exchange intracellular α-ketoglutarate (a 5-carbon dicarboxylate) for extracellular anions, OAT2 was found to favour intracellular succinate or fumarate, suggesting that OAT2 preferentially exchanges 4-carbon dicarboxylates (Kobayashi *et al.*, 2005; Burckhardt *et al.*, 2011). The prototypic test substrate used in the study of OAT2 transport is also more ambiguous than OAT1 and OAT3. Both PAH and E3S have been employed previously, in addition to salicylate

and prostaglandin $F_{2\alpha}$ (Enomoto *et al.*, 2002; Kobayashi *et al.*, 2005; Burckhardt *et al.*, 2011).

A number of routinely prescribed therapeutic agents have been shown to be substrates and/or inhibitors of both OAT1 and OAT3 and in some cases OAT2 also. These include antihypertensives, antibiotics, antiviral agents, non-steroidal anti-inflammatory drugs (NSAIDS) and HMG CoA reductase inhibitors (Burckhardt, 2012). As a result of their overlapping substrate specificity, many studies have investigated both OAT1 and OAT3 in the transport of anionic drugs. For example, in HEK293 cells stably expressing OAT1 and OAT3, the angiotensin II receptor blocker olmersartan was shown to be transported by both OAT1 and OAT3 with respective K_m values of 0.07µM and 0.12µM (Yamada *et al.*, 2007). Furthermore, in Flp293 cells stably transfected with OAT1 and OAT3, candesartan, valsartan, olmesartan, losartan, pratosartan and telmisartan all inhibited OAT1 transport and, with greater potency, OAT3 transport of uric acid (IC_{50} values obtained ranged from 0.28µM to 17µM for OAT1 and 0.027µM to 1.6µM for OAT3). Telmisartan was found to be the exception in this class of drugs, which elicited greater inhibition of OAT1 (IC_{50} 0.46µM) than OAT3 (IC_{50} 1.6µM) (Sato *et al.*, 2008).

For some years, the AED VPA has also been suggested to be transported by an anion transporter. Despite VPA being more than 99% ionised at physiological pH and reasonably hydrophilic, it is known to readily penetrate the BBB (Loscher *et al.*, 1984). It was therefore hypothesised that VPA must enter the brain via a facilitated process. Adkinson and colleagues investigated this in an *in situ* rat brain perfusion model and found that not only was VPA uptake into the brain a saturable process but uptake could be inhibited in the presence of anion transport substrates/inhibitors, such as octanoate, PAH and probenecid (Adkinson *et al.*, 1996). The same investigators had previously investigated VPA transport in isolated rat brain endothelial cells and observed similar results, although interestingly PAH did not significantly inhibit VPA uptake (Naora *et al.*, 1995).

OAT1 and OAT3 have been shown to be critical in the renal clearance of a number of therapeutic agents due to their role in anion uptake from the blood into the kidney proximal tubule cells. This presents potential for drug-drug interactions (DDIs) to occur between drugs which are heavily dependent on OAT1 and OAT3 uptake for efficient

renal clearance. For example the loop diuretic furosemide was shown to inhibit uptake of the thiazide diuretic chlorothiazide in CHO and HEK293 cells stably transfected with OAT1 or OAT3 respectively (Juhász *et al.*, 2013). Furthermore the renal clearance of furosemide has been observed to be dependent on OAT1 and OAT3 transport *in vivo*. In a clinical study investigating the effects of co-administration of the uricosuric drug (and prototypic OAT inhibitor) probenecid with furosemide, renal clearance of furosemide decreased by 75% when co-administered with probenecid (Chennavasin *et al.*, 1979). Similarly the NSAIDs indomethacin and ketoprofen have been shown to significantly impair renal clearance of the immunosuppressant methotrexate, which is up to 90% cleared by the kidneys (Maiche, 1986; Thyss *et al.*, 1986; Elmorsi *et al.*, 2013). Such DDIs can cause nephrotoxic precipitation of methotrexate and its metabolites in the tubular lumen, which can ultimately lead to severe and potentially fatal renal impairment (Widemann *et al.*, 2006; Hagos *et al.*, 2010).

Although the hCMEC/D3 cell line represents a physiologically relevant model of the BBB, it has been shown to lack the expression of OATs, even though these are thought to be expressed at the BBB *in vivo (*Abbott *et al.*, 2010*;* Carl *et al.*, 2010*;* Weksler *et al.*, 2013*)*. Various epithelial cells stably expressing transporter proteins of interest have been used extensively to investigate transport of therapeutic agents. The main advantage of using such a model is that the transporter of interest can be selectively expressed at high levels, diminishing the contribution of endogenous transporters to the net transport of the investigated compound. On the other hand it is unknown what effect the transfection process has on cellular morphology and behaviour. A variety of cell lines have been used to stably transfect OAT transporter proteins including HEK293, MDCK and CHO cells (Aslamkhan *et al.*, 2003; Chu *et al.*, 2007; Hagos *et al.*, 2007; Shin *et al.*, 2010; Xue *et al.*, 2011). HEK293 cells are widely used as they are easy to culture and transfect, achieving high transfection rates and protein expression. MDCK II cells are an alternative cell line of choice, again due to their ease of culture and their ability to form polarised monolayers, reflecting the protein and lipid composition of epithelia *in vivo* (Ander *et al.*, 1984).

The work described in this chapter aimed to initially generate and characterise three novel MDCK II cell lines stably transfected with *SLC22A6*, *SLC22A7* and *SLC22A8*, over-expressing OAT1, OAT2 and OAT3 respectively. The novel cell lines were characterised on the basis of gene expression, protein expression and functional

transport of a test substrate. PAH was employed as the test substrate for *SLC22A6*_MDCK II cell analysis and E3S employed as the test substrate for both *SLC22A7*_MDCK II and *SLC22A8*_MDCK II cell analysis. PAH/E3S transport in *SLC22A6, SLC22A7* and *SLC22A8* transfected MDCK II cells was also assessed in the presence of the prototypic OAT transport inhibitor probenecid and compared to transport in control 'mock transfected' cells stably transfected with vector only (pcDNA_MDCK II cells). The fully characterised cell lines were then used to investigate potential OAT1, OAT2 and OAT3 mediated transport of commonly prescribed AEDs, including PHT, CBZ, VPA, LTG, GBP, TPM and LEV. AED transport in *SLC22A6, SLC22A7* and *SLC22A8* transfected MDCK II cells with and without probenecid (200µM) was compared to that of control pcDNA_MDCK II cells.

4.2 Materials and Methods

4.2.1 Materials

SLC22A6, *SLC22A7* and *SLC22A8* I.M.A.G.E. consortium cDNA clones were purchased from Source Bioscience Lifesciences (Nottingham, UK) who also carried out sequencing of *SLC22A6*_pcDNA3.1/V5-His TOPO and *SLC22A8*_pcDNA3.1/ V5-His TOPO clones. *Eco*RV, *Ale*I and *Xba*I restriction enzymes and buffers were purchased from New England Biolabs (Hitchin, UK). pcDNA3.1/V5-His TOPO expression kit, One Shot TOP10 chemically competent E.coli, Lipofectamine transfection reagent, FBS, OPTI –MEM/DMEM media, Taqman gene expression assays (canine β-actin/ human *SLC22A6*/canine *SLC22A6*/human *SLC22A7*/human *SLC22A8*), gene expression mastermix and all NuPAGE western blotting reagents and pre cut nitrocellulose membrane/filter paper sandwiches were purchased from Life Technologies (Paisley, UK). Prism protein ladder (10-175kDa), mouse monoclonal anti-*SLC22A6* antibody, mouse monoclonal anti-GAPDH [6C5] antibody, rabbit polyclonal anti-*SLC22A8* antibody and goat polyclonal secondary antibody to mouse IgG (HRP conjugated) were purchased from Abcam (Cambridge, UK). Goat secondary antibody to rabbit IgG (HRP conjugated) was purchased from Santa Cruz Biotechnology (Dallas, Texas, USA). [^{3}H]-estrone-3-sulfate (specific activity, 54.3 Ci/mmol) and [^{3}H]-p-aminohippuric acid (specific activity, 130.8mCi/mmol) were purchased from Perkin Elmer (Massachusetts, USA). [^{3}H]-lamotrigine (specific activity, 5Ci/mmol), [^{3}H]-levetiracetam (specific activity, 5Ci/mmol), [^{3}H]-topiramate (specific activity, 8Ci/mmol) and [^{3}H]-gabapentin (specific activity, 110Ci/mmol) were purchased from American Radiolabeled Chemicals Inc (St. Louis, USA). [^{3}H]-phenytoin (specific activity 1.1Ci/mmol), [^{3}H]-carbamazepine (specific activity 10Ci/mmol) and [^{3}H]-valproic acid (specific activity 55Ci/mmol) were purchased from Moravek (Brea, CA, USA). Fast Start High Fidelity PCR system reagents were purchased from Roche Diagnostics (Burgess Hill, UK). All other materials unless otherwise stated were purchased from Sigma-Aldrich (Poole, UK).

4.2.2 Extraction of human *SLC22A6, SLC22A7* and *SLC22A8* I.M.A.G.E. cDNA clone plasmid DNA from *E.coli* glycerol stocks

Purchased agar stocks of *SLC22A6, SLC22A7* and *SLC22A8* cDNA clones were firstly prepared in a 50ml culture of LB broth supplemented with either 50µg/ml ampicillin (*SLC22A6* cDNA clone) or 20µg/ml chloramphenicol (*SLC22A7*/*SLC22A8* cDNA clones) depending on which antibiotic resistance gene each cDNA clone carried. The culture was then grown overnight at 37^0C with vigorous shaking (300rpm; ThermoScientific Thermo Max Q 4450). The following day, overnight cultures were streaked onto LB agar plates (autoclaved, 1M agar supplemented with appropriate antibiotic as described previously) at various serial dilutions (neat, 1 in 10, 1 in 100, 1 in 1000) and grown overnight at 37^0C. Distinct, single colonies were selected the following day and grown firstly for 8 hours in a small (9ml) LB broth culture (supplemented with appropriate antibiotic) at 37^0C with vigorous shaking and secondly overnight in a 50ml culture at the same conditions. The following day, plasmid DNA of each culture was extracted using the GenElute plasmid DNA midi prep kit (Sigma Aldrich). The GenElute plasmid DNA midi prep protocol is described in chapter 2 (section 2.2.2.), however the volumes of reagents differ slightly and were as follows: 4ml re-suspension solution, lysis buffer, neutralisation solution, 3ml binding solution, 4ml wash solution 1 and 2, 1ml elution solution. The extracted DNA was then quantified using the Nanodrop spectrophotometer (see section 2.2.3 for details).

4.2.3 Linearisation of *SLC22A6, SLC22A7* and *SLC22A8* cDNA clone plasmid DNA

Extracted plasmid DNA was linearised in a 2 hour restriction digest reaction in a thermal cycler (Applied Biosystems Verti 96 well thermal cycler) at 37^0C for use in downstream amplification. A 50µl reaction volume was prepared for each cDNA clone as follows. *SLC22A6*: 32.2µl (2µg) of *SLC22A6* cDNA clone DNA, 0.1µl (10 units) *Eco*RV, 5µl of NEB buffer 3 (1x final concentration), 0.5µl (1µg/ml final concentration) of BSA and 12.2µl water. *SLC22A7*: 8.64µl (2µg) of *SLC22A7* cDNA clone DNA, 0.1µl (10 units) *Xba*I, 5µl of NEB buffer 4 (1 x final concentration), 0.5µl (1µg/ml final concentration) of BSA, 35.76µl water. *SLC22A8*: 9.02µl (2µg) of *SLC22A8* cDNA clone DNA, 0.1µl (10 units) *Xba*I, 5µl of NEB buffer 4 (1x final concentration), 0.5µl (1µg/ml final concentration) BSA, 35.38µl water. The resulting DNA was then analysed by gel electrophoresis (see section 2.2.4 for protocol) to confirm DNA was successfully linearised (linearised DNA migrates less far than the

supercoiled form on an agarose gel). *SLC22A7* and *SLC22A8* cDNA clone plasmid DNA was successfully linearised by restriction with *Xba*I, however *Eco*RV failed to linearise the *SLC22A6* cDNA clone DNA (*figure 4.1*). Linearisation of the *SLC22A6* cDNA clone DNA was achieved following a second attempt with *Xba*I instead of *Eco*RV (32.2µl (2µg) of *SLC22A6* cDNA clone DNA, 0.1µl (10 units) *Xba*I restriction endonuclease, 5µl of NEB buffer 4 (1x final concentration), 0.5µl (1µg/ml final concentration) BSA, 12.2µl water; *figure 4.1*). Restriction digest reactions were then repeated in a total volume of 150µl (3 x 50µl reaction volumes) to achieve enough DNA for amplification and purified using the GenElute PCR clean up kit (Sigma Aldrich; see section 2.2.6 for details of manufacturer's protocol).

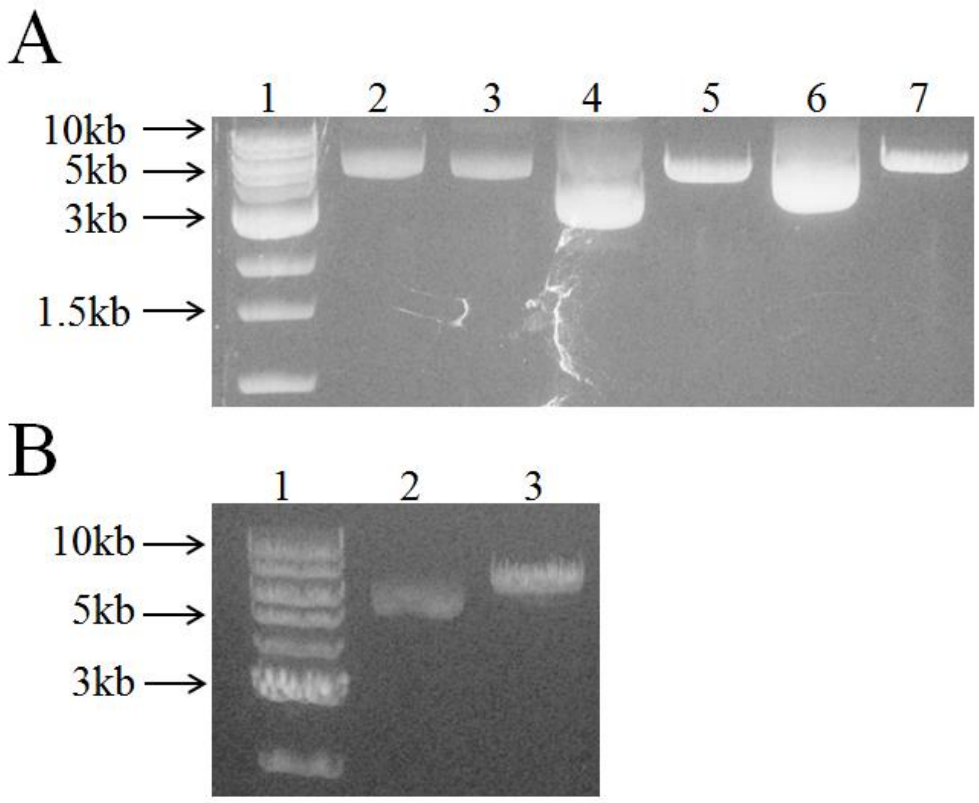

Figure 4.1: Visualisation of linearised *SLC22A6*, *SLC22A7* and *SLC22A8* cDNA clones pre and post restriction digest with *Xba*I and *Eco*RV on a 1% agarose gel using NEB 10kb DNA ladder as a reference **(A)**. From left to right: 1kb DNA ladder (1), supercoiled *SLC22A6* DNA (2), *SLC22A6* DNA post restriction digest (3), supercoiled *SLC22A7* DNA (4), *SLC22A7* DNA post restriction digest (5), supercoiled *SLC22A8* DNA (6), *SLC22A8* DNA post restriction digest (7). *SLC22A7* and *SLC22A8* were successfully linearised by restriction digest. Linearisation of the *SLC22A6* cDNA clone was unsuccessful and restriction digest subsequently repeated successfully with *Xba*I and visualised on a 1% agrose gel using NEB 10kb DNA ladder as reference **(B)**. From left to right: 1kb DNA ladder (1), supercoiled *SLC22A6* DNA (2), *SLC22A6* DNA post restriction digest (3).

4.2.4 Amplification of *SLC22A6, SLC22A7* and *SLC22A8* templates from plasmid DNA

Purified, linear *SLC22A6, SLC22A7* and *SLC22A8* cDNA clone plasmid DNA was amplified by PCR using Fast Start High Fidelity PCR system reagents (Roche Diagnostics, Burgess Hill, UK) as described in section 2.2.5 (see table 4.1 for primer sequences) using the following thermal profile: an initial denaturing step for two minutes at 95^0C, followed by 40 cycles of denaturation at 95^0C for 30 seconds, annealing at 67^0C (*SLC22A6*) or 69^0C (*SLC22A7*) or 72^0C (*SLC22A8*) for 30 seconds, and elongation at 72^0C for two minutes. This was followed by a terminal elongation step at 72^0C for seven minutes. The annealing temperature for each template was determined based on primer melting temperatures (Tm^o).

Template	Reverse (upstream) primer sequence (5'-3')	Forward (downstream) primer sequence (5'-3')
SLC22A6	CTTCTCACAGTCCTCAGAGTCC	CCCAATGGCCTTTAATGACCTC
SLC22A7	TTAGTTCTGGACCTGCTTCATGGG	GCCACCAGCATGGGCTTT
SLC22A8	CGTTGTCCTCAGCTGGAG	GCCACCGTGCCATGACCTTCT

Table 4.1 Full sequence of each primer pair used in *SLC22A6, SCL22A7* and *SLC22A8* template DNA amplification.

Templates were analysed by gel electrophoresis (*figure 4.2*) to ensure successful amplification of the correct size template (gel electrophoresis protocol is described in section 2.2.4). Template DNA was then purified using the GenElute PCR clean up kit (see section 2.2.6 for details of manufacturer's protocol). At this point due to the inability to amplify the *SLC22A7* template from its respective I.M.A.G.E cDNA clone, *SLC22A7* cloning was abandoned. Following further troubleshooting it was discovered that the *SLC22A7* I.M.A.G.E. cDNA clone contained a truncated *SLC22A7* sequence; no alternative full sequence cDNA clones with the correct *SLC22A7* template were available.

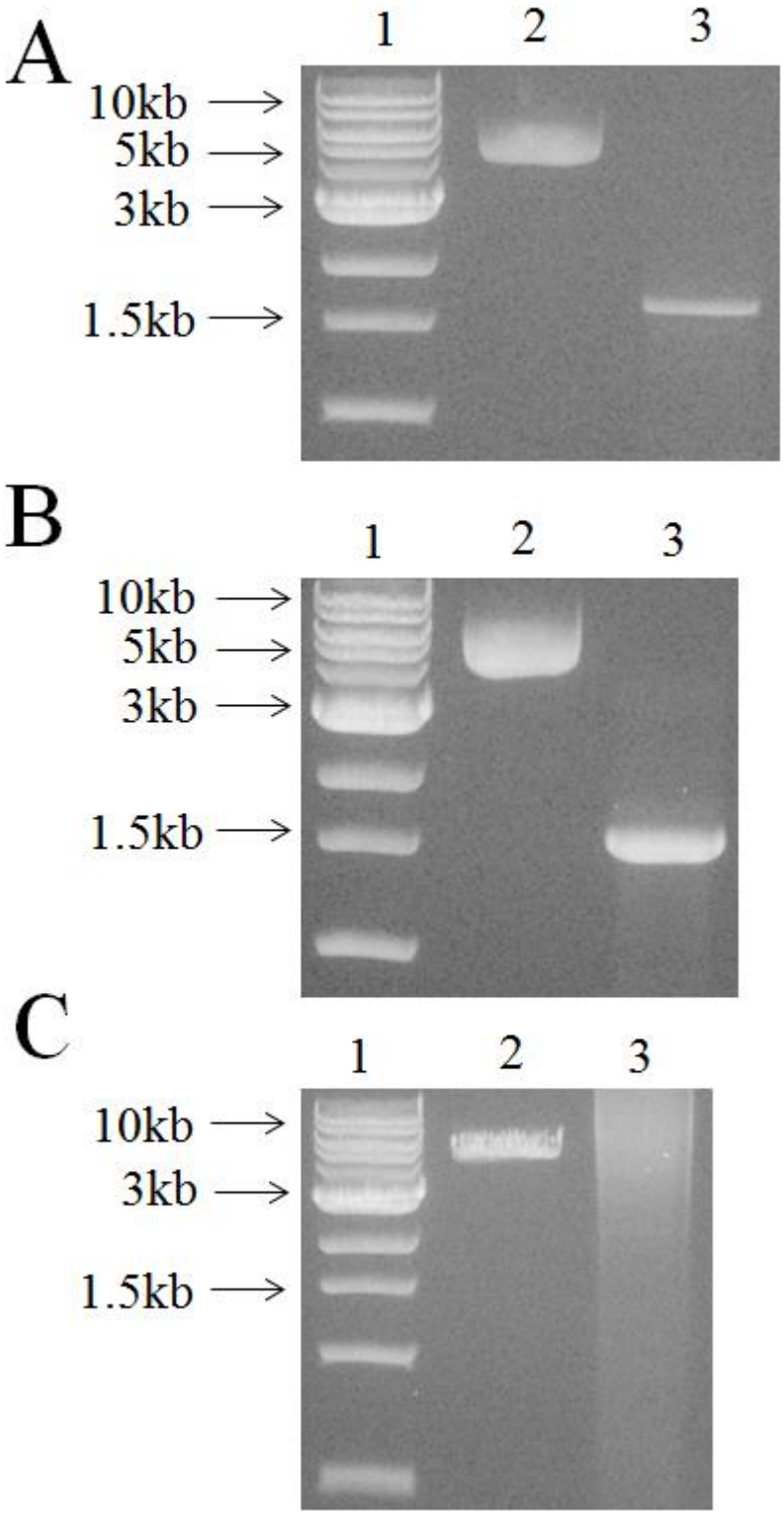

Figure 4.2: Amplified *SLC22A6* **(A)** and *SLC22A8* **(B)** and *SLC22A7* **(C)** templates visualised on a 1% agarose gel using NEB 10kb ladder as reference. From left to right: 1kb DNA ladder (1), cDNA clone (2), amplified template (3). *SLC22A6* and *SLC22A8* template DNA containing its respective protein coding sequence (1.6kb) was successfully amplified from its respective cDNA clone. The *SLC22A7* template could not be amplified from its respective cDNA clone.

4.2.5 Ligation of *SLC22A6* and *SLC22A8* templates into a mammalian expression vector

SLC22A6 and *SLC22A8* template DNA was ligated into a mammalian expression vector (pcDNA 3.1/V5-His-TOPO®) and transformed into chemically competent *E. coli* (One Shot® TOP10). The pcDNA 3.1/V5-His TOPO® TA Expression kit provides a high efficiency one step cloning strategy for direct insertion of Taq polymerase amplified PCR products into a plasmid vector. Topoisomerase I from *Vaccinia* cleaves the duplex plasmid DNA and binds to phosphate residues at the 5' and 3' ends of a cloning site within the plasmid, holding it in an 'open' conformation. The additional deoxyadenosine base added to the DNA templates by Taq amplification binds to the 3' deoxythymidine residue overhang of the plasmid, releasing the Topoisomerase and ligating the PCR template into the plasmid vector.

Firstly, agar plates (autoclaved, 1M agar supplemented with 50µg/ml ampicillin) were prepared and incubated at 37^0C for later transformation. The ligation reaction was prepared in a 1.5ml Eppendorf tube according to manufacturer's protocol and contained the following: 3µl fresh PCR product (*SLC22A6*/*SLC22A8* template), 1µl salt solution, 1µl sterile water, 1µl Topo vector. A control ligation reaction was also prepared for each ligation reaction containing: 1µl salt solution, 4µl sterile water, 1µl Topo vector. 3 ligation reactions were prepared in total (*SLC22A6*/*SLC22A8* ligation and a vector only reaction). The vector only reaction acts as a control to detect non-plasmid expressing bacterial growth; no growth should be observed in the control, only bacteria expressing the pcDNA 3.1/V5-His TOPO® TA plasmid (expressing ampicillin resistance gene) should grow. Each ligation reaction was mixed by flicking the Eppendorf tube 3-4 times and incubated at room temperature for 30 minutes. Thereafter, each ligation reaction was placed on ice and 2µl of each reaction added to thawed chemically competent *E.coli* bacteria that had previously been stored at -80^0C. The bacterial solutions were then incubated with the ligation reaction on ice for 15 minutes before being heat-shocked at 42^0C for 30 seconds. After heat-shock, the bacterial solution was immediately returned to ice for a further 5 minutes to complete transformation of the ligated plasmid into the *E.coli* host. A 250µL volume of SOC medium was then added to the *E.coli* and the bacteria allowed to multiply for 1 hour at 37^0C with vigorous shaking (200rpm; ThermoScientific Thermo Max Q 4450). A 200µl aliquot of the transformed bacterial cultures was then streaked onto agar plates

using a sterile loop at various serial dilutions (neat, 1 in 10, 1 in 100, and 1 in 1000) and allowed to incubate overnight at 37^0C.

4.2.6 Analysis of resultant bacterial colonies

After overnight incubation, distinct single colonies were selected for analysis by PCR to determine if the ligation had been successful. PCR was carried out at the conditions described in section 2.2.5. Each 20µl reaction contained the following: transformed bacterial clone DNA (achieved by inoculating the PCR tube with a pipette tip containing each bacterial colony), 2µl of 10x FastStart High Fidelity reaction buffer with 18mM $MgCl_2$, 0.4µl PCR grade nucleotide mix (200nM final concentration of each dNTP), 0.4µl DMSO, 13µL PCR grade water, 0.2µL FastStart High Fidelity Enzyme Blend (5U/µl), 2µl of both sense and anti-sense primers (400nM final concentration; see table 4.1 for primer sequences). Ten colonies were selected for each ligation reaction (*SLC22A6* and *SLC22A8*). Negative control reactions were also carried out in the absence of bacterial DNA to check for PCR reagent contamination. At the same time, aliquots of 3ml LB broth (supplemented with 50µg/ml ampicillin) were inoculated with each of the 10 colonies selected from each ligation reaction. Any colonies in which the *SLC22A6* or *SLC22A8* template could be amplified by PCR were subsequently grown for 8 hours in the culture to allow the transformed bacteria to reach exponential growth rate. The 8 hour cultures were then transferred to a larger culture (15ml LB broth supplemented with 50µg/ml ampicillin) and grown overnight at 37^0C with vigorous shaking (300rpm; ThermoScientific Thermo Max Q 4450).

The following day, *SLC22A6* and *SLC22A8* template positive bacterial colonies grown overnight were further analysed by restriction digest. The plasmid DNA of 8 colonies from which *SLC22A6* and *SLC22A8* had been successfully amplified (*figure 4.3*) was first extracted as described in section 4.2.2 before a 2 hour restriction digest reaction. The *Ale*I and *Eco*RV restriction endonucleases were used as both the *SLC22A6* and *SLC22A8* plasmid DNA contains one *Ale*I and one *Eco*RV restriction site in the insert and vector section of the sequence respectively. The 50µl reactions were set up in 200µl low density plastic PCR tubes and incubated at 37^0C in a 96 well block thermo cycler for 2 hours. Reaction mixtures contained the following components, made up to 50µl with water: 2µg plasmid DNA, 10 units (*Ale*I; 1µl, EcoRV; 0.1µL) of restriction endonuclease, 5µl (1 x final concentration) of appropriate buffer (NEB buffer 4 for *Ale*I reactions, NEB buffer 3 for *Eco*RV reactions), 0.5µl (1µg/ml final concentration) BSA

(*Eco*RV reactions only). Resulting DNA was visualised by gel electrophoresis (see section 2.2.4). Plasmid DNA containing the successfully ligated vector, positive for the *SLC22A6* or *SLC22A8* template, was linearised by digestion with both *Ale*I and *Eco*RV, with successfully linearised DNA traveling less far on an agarose gel than its respective supercoiled form (*figures 4.4-4.5*).

Three of the clones shown to express the ligated plasmid and therefore *SLC22A6* or *SLC22A8* template were sent to Source Bioscience Lifesciences (Cambridge, UK) for single tube sequencing. Linear plasmid DNA at a concentration of 100ng/µl was supplied and the plasmid DNA sequenced from the T7 promoter and BGH reverse priming sites within the pcdna3.1/V5-His TOPO vector sequence; this enabled the full insertion site of the vector to be sequenced. Sequence results were then analysed to ensure the inserted *SLC22A6* or *SLC22A8* template was identical to the published protein coding sequence for each gene. A single clone for *SLC22A6* and *SLC22A8* was then selected for subsequent transfection.

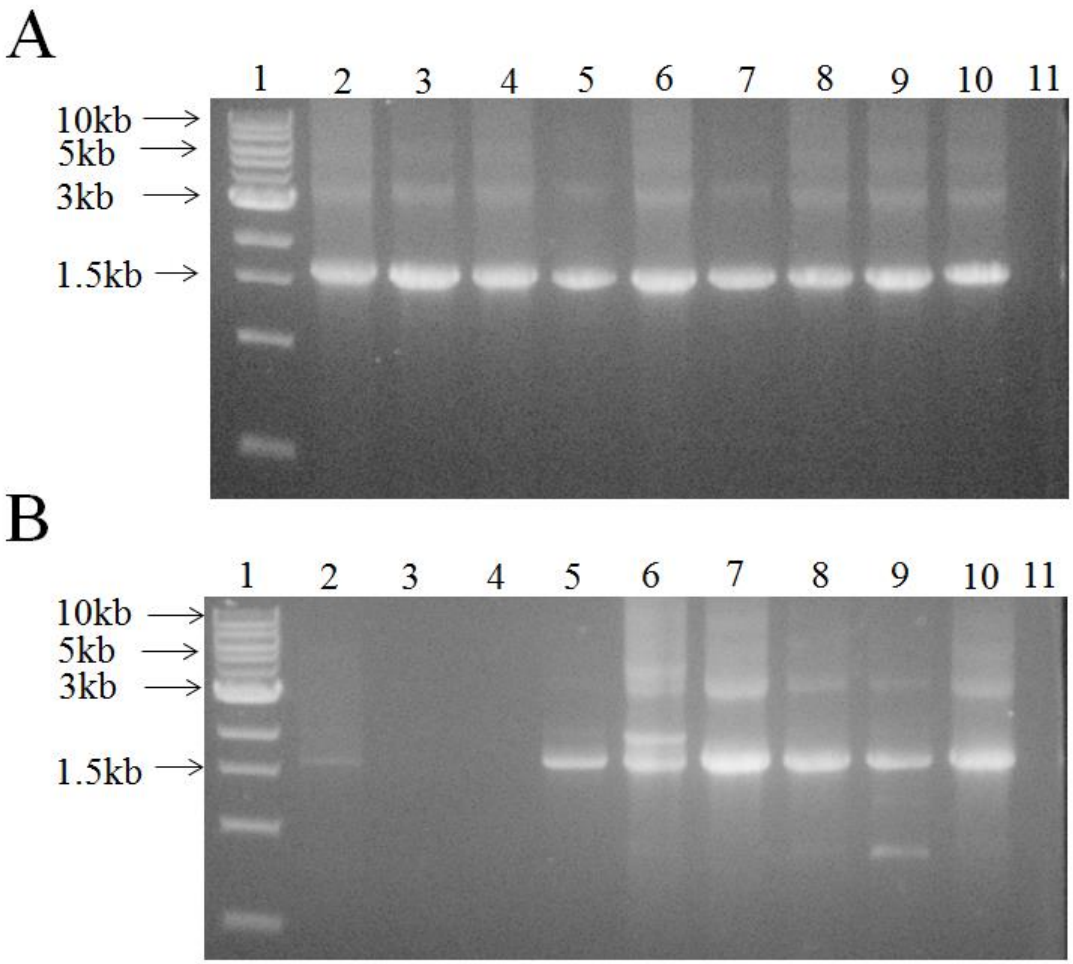

Figure 4.3: Visualisation of successfully amplified *SLC22A6* **(A)** and *SLC22A8* **(B)** template DNA from plasmid DNA of transformed *E.coli* cultures. Samples were run on a 1% agarose gel using NEB 10kb ladder as a reference. From left to right: 1kb DNA ladder (1), positive control (template amplified from cDNA clone; (2)), *SLC22A6* **(A)** or *SLC22A8* **(B)** template DNA amplified from plasmid DNA (3-10), negative control reaction containing no DNA (11). *SLC22A6* template DNA was successfully amplified from plasmid DNA in all 8 colonies of transformed *E.coli* (part A, lanes 3-10). *SLC22A8* template DNA was successfully amplified from plasmid DNA in 6 of the 8 colonies of transformed *E.coli* included (part B, lanes 5-10).

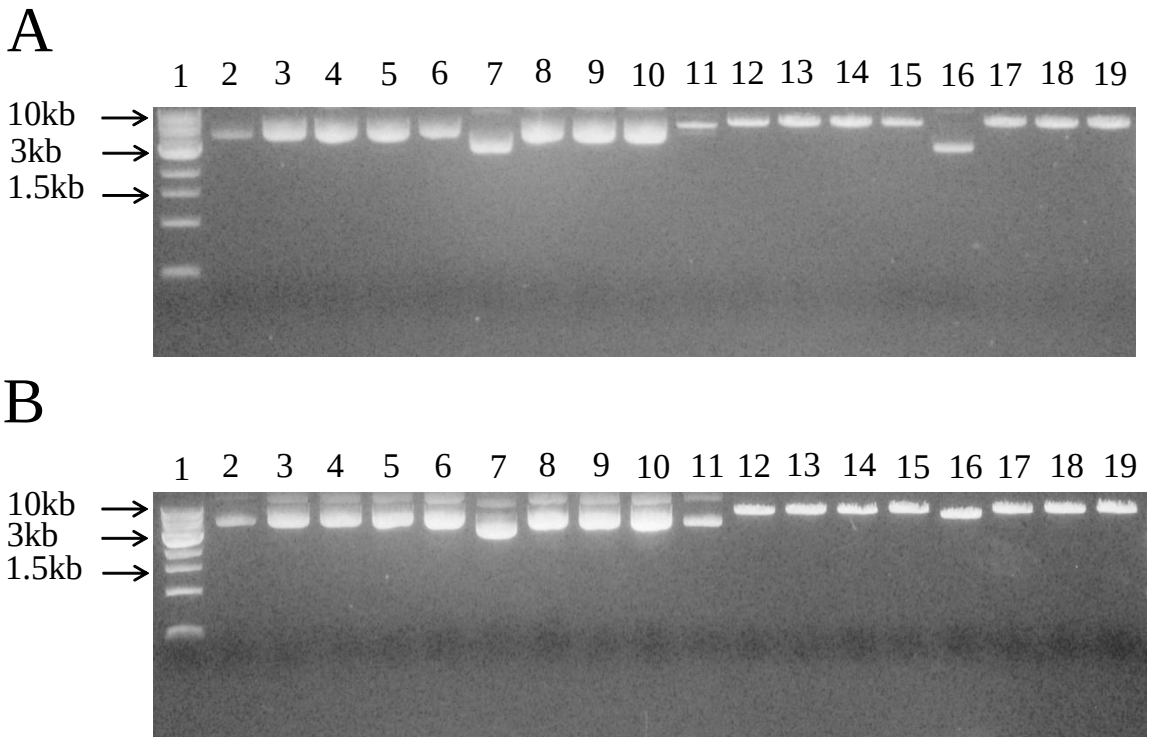

Figure 4.4: Restriction digest of *SLC22A6* positive plasmid DNA from transformed *E.coli* cultures with *Ale*I **(A)** and *Eco*RV **(B)**. Samples were run on a 1% agarose gel using NEB 10kb ladder as reference. From left to right: 1kb DNA ladder (1), supercoiled *SLC22A6* cDNA clone as a positive control (2), supercoiled *SLC22A6* positive plasmid DNA (lanes 3-10), digested *SLC22A6* CDNA clone (11), *Ale*I **(A)** or *Eco*RV **(B)** digested *SLC22A6* positive plasmid DNA (lanes 12-19). Restriction digests with *Ale*I **(A)** and *Eco*RV **(B)** successfully linearised plasmid DNA from 7 of the 8 transformed *E.coli* colonies included. Colony 5 (lane 16) produced an unexplained band ~3kb.

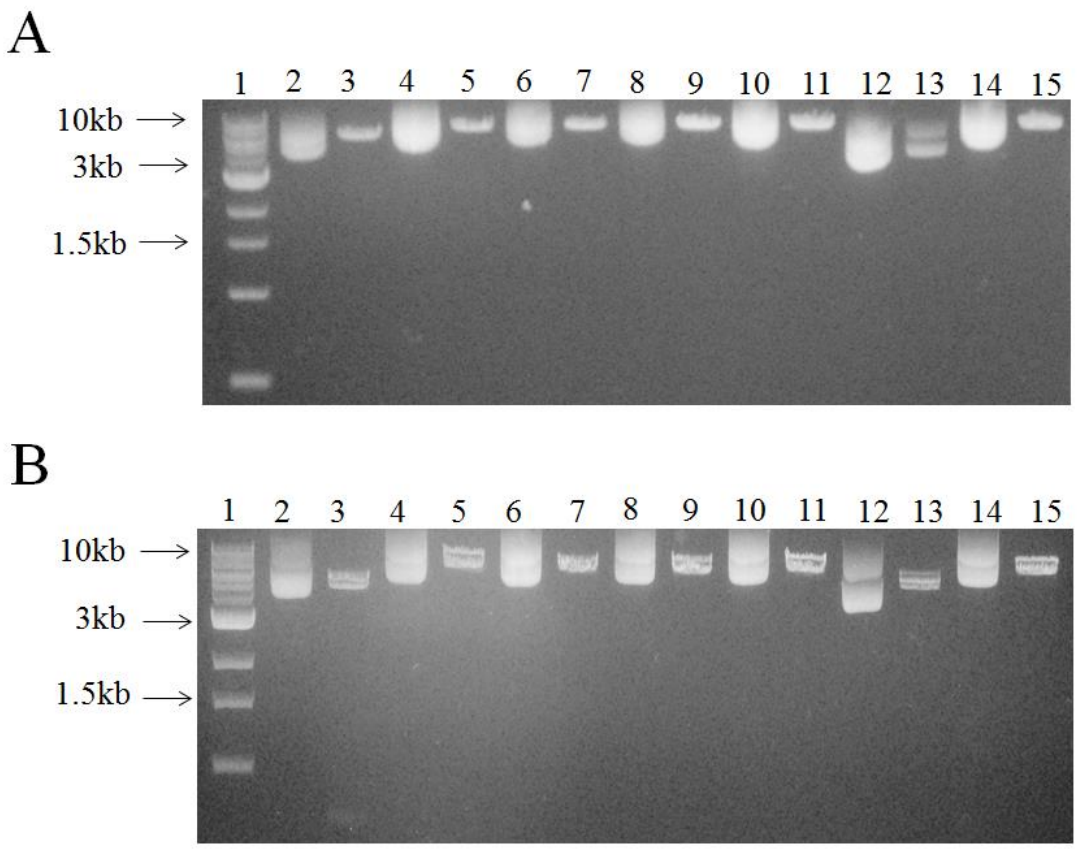

Figure 4.5: Restriction digest of *SLC22A8* positive plasmid DNA from transformed *E.coli* cultures with *Ale*I **(A)** and *Eco*RV **(B)**. Samples were run on a 1% agarose gel using NEB 10kb ladder as reference. From left to right: 1kb DNA ladder (1), supercoiled *SLC22A8* cDNA clone (2), digested *SLC22A8* cDNA clone as a positive control (3), supercoiled *SLC22A8* positive plasmid DNA (lanes 4,6,8,10,12,14), *Ale*I **(A)** or *Eco*RV **(B)** digested *SLC22A8* positive plasmid DNA (lanes 5,7,9,11,13,15). Restriction digests with *Ale*I **(A)** and *Eco*RV **(B)** successfully linearised plasmid DNA from 5 of the 6 transformed *E.coli* colonies included. Colony 5 (lanes 12-13) produced a double band when digested with *Ale*I **(A)** and *Eco*RV **(B)** suggesting incomplete ligation of the full *SLC22A8* template or insertion at the incorrect ligation site.

4.2.7 MDCK II cell culture

WT MDCK II cells and MDCK II cells stably transfected with *SLC22A6* and *SLC22A8* were maintained in complete media consisting of DMEM supplemented with 10% FBS and 1% penicillin streptomycin (for stably transfected cells complete media was also supplemented with 0.8µg/ml gentamycin) and kept in an incubator (Thermo Scientific Function Line) at 37^0C with 5% CO_2. All cell culture was performed in a class II microbiological safety cabinet. Cells were grown in three T175 flasks at any one time and passaged and seeded to further flasks and/or 12-well plates every 3-4 days, as follows. Briefly, media was removed from each flask using a 25ml serological pipette and each flask washed twice with warm HBSS. A 10ml volume of 0.25% trypsin-EDTA was then added to each flask and flasks were returned to the incubator for 10-15 minutes. Once all cells were detached from the flask, trypsin was neutralised with 20ml of complete media and flask contents transferred to a 50ml Falcon tube before centrifugation at 250 *x g* for 5 minutes (Thermo Scientific Heraeus Megafuge IIR). The supernatant was removed and the resulting pellet resuspended in 1ml of complete media. Pellet suspensions were combined (three in total) and made up to a total volume of 10ml. If seeding to flasks only 2ml of the resuspended cells were added to 3x T175 flasks to give a 1:5 dilution and allowed to grow on. When seeding to plates, a cell count was first made (as described in section 3.2.4) to give the number of cells per ml and the cell solution subsequently diluted with complete media to a density of $1.5x10^5$ cells per ml. A 1ml aliquot was then added to each well of a 12-well plate.

4.2.8 Generation of *SLC22A6*_MDCK II and *SLC22A8*_MDCK II cell lines

Fresh cultures of sequence verified *SLC22A6*, *SLC22A8* and pcDNA plasmid DNA were transfected into low passage number MDCK II cells using Lipofectamine transfection reagent according to manufacturer's protocol. Briefly, MDCK II cells were seeded into 24-well plates at a density of $6x10^4$ cells per well in DMEM media supplemented with 10% FBS only. Cells were transfected the following day or when cells were 60-80% confluent. Firstly, the transfection was optimised, with various concentration combinations of plasmid DNA and Lipofectamine reagent trialled (9 combinations in total; see *figure 4.6*).

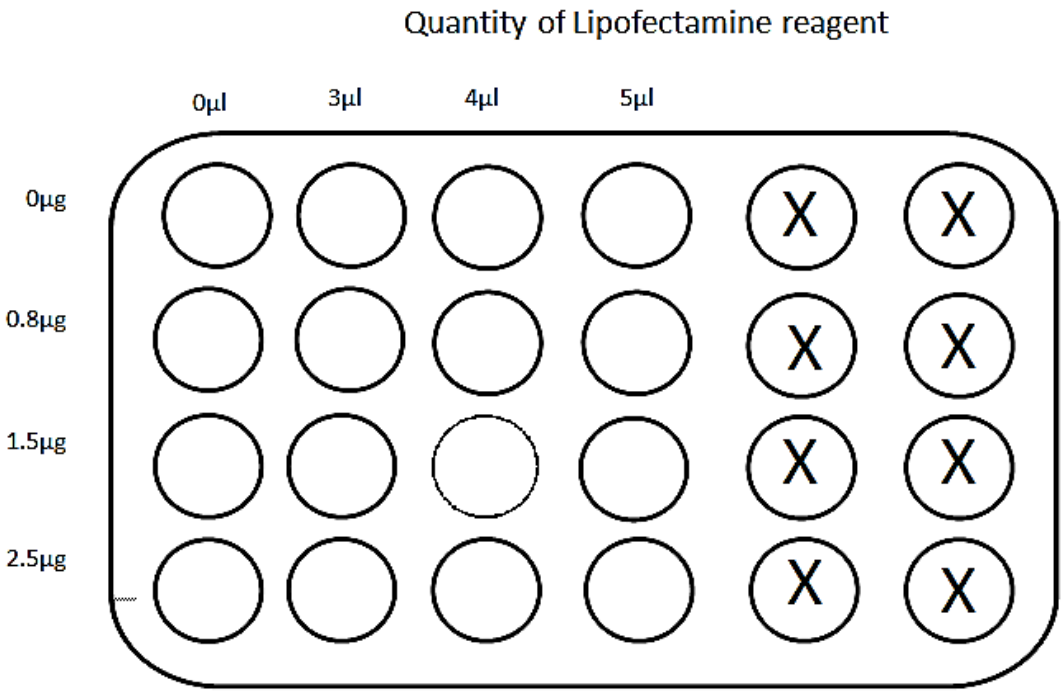

Figure 4.6: Plate layout used for optimisation of transfection conditions. Low passage MDCK II cells were seeded at a density of $6x10^4$ cells per ml into a 24 well plate and various combinations of plasmid DNA and Lipofectamine reagent trialled to determine the optimal conditions for high yield transfection. No lipofectamine and/or no plasmid DNA was added to 7 wells as negative controls.

The transfection process was carried out as follows; pcDNA plasmid DNA was diluted in 50µl of OPTI MEM (reduced serum Eagle's minimum essential medium) to give 0.8µg, 1.5µg and 2.5µg concentrations of DNA. 3µl, 4µl and 5µl volumes of Lipofectamine reagent were then diluted in 50µl of OPTI MEM and allowed to incubate at room temperature for 5 minutes. The OPTI MEM plasmid DNA solution was then added to the diluted Lipofectamine reagent (100µl total volume) and incubated at room temperature for 20 minutes to allow complexes to form. Thereafter, 100µl of the DNA-Lipofectamine complex solution was added to the appropriate well. A 100µl volume of OPTI MEM containing various concentrations (as stated previously) of plasmid DNA without Lipofectamine was also added to appropriate wells as negative controls (see figure 4.6 for plate layout). Cells were allowed to recover for 24 hours before the existing media was replaced with one supplemented with 0.8mg/ml gentamycin (G418) to select for successfully transfected cells containing the vector (the pcDNA 3.1/V5-His TOPO vector expresses gentamycin resistance gene). After 7 days selection, the well with the optimum growth was used for single cell clone selection. A total of 0.8µg of plasmid DNA and 3µl of Lipofectamine reagent was determined as the optimum

combination for transfection and was utilised for subsequent *SLC22A6* and *SLC22A8* transfection. To select single clones, the transfected cells were first passaged as follows. Briefly, media was aspirated from the well using a vacuum and cells were washed twice with 0.5ml warm HBSS, 0.5ml of 0.25% trypsin-EDTA was then added and the plate returned to the incubator for 10-15 minutes or until cells were fully detached. Trypsin was then neutralised in 2ml of complete media supplemented with 0.8mg/ml gentamycin (selection media). The resulting cell suspension was then centrifuged at 250 *x g* for 5 minutes to collect a cell pellet and resuspended in 1ml of selection media. A cell count was then made and cells seeded at various serial dilutions in 96-well plates to obtain single cell clones. Cells were fed every 3 days with fresh selection media and after two weeks of selection, 12 wells were selected based on growth rate and passaged into 24 well and ultimately 6 well plates. The 12 single cell clones were then crudely analysed for *SLC22A6* and *SLC22A8* expression by PCR (section 4.2.10) before quantitative RT-PCR analysis to determine which clones possessed the highest expression of *SLC22A6* or *SLC22A8* (section 4.2.13). To determine functional transport differences between the 12 clones, each clone was incubated with a well characterised positive hOAT1/hOAT3 substrate (section 4.2.18).

4.2.9 DNA extraction of MDCK II clones stably transfected with *SLC22A6* and *SLC22A8*

On the day of extraction the media was aspirated from each well of selected clones from section 4.2.8 and each washed twice with warm HBSS. A 1ml volume of 0.25% trypsin-EDTA was then added and plates were then returned to an incubator for around 5 minutes, or until cells were fully detached. A 2ml volume of complete media was added to neutralise the trypsin and the contents of each well transferred to a 1.5ml Eppendorf tube and centrifuged at 250 *x g* for 5 minutes to obtain a cell pellet. The supernatant was then discarded and cell pellets kept at room temperature for subsequent DNA extraction. DNA was then extracted using the GenElute mammalian DNA extraction kit reagents according to manufacturer's protocol (Sigma Aldrich). Briefly a heat block was first set to 70^0C and the supplied Proteinase K solution prepared in water to give a final concentration of 20mg/ml. Each cell pellet was firstly resuspended in 200µl of resuspension solution and a 20µl aliquot of RNase A solution was then added and each sample incubated at room temperature for 2 minutes to obtain RNA free-genomic DNA. Cells were then lysed by the addition of 20µl of 20mg/ml proteinase K solution and 200µl of lysis solution and vortexed briefly before incubation at 70^0C for 10 minutes. In the meantime, centrifuge columns for each sample were prepared in collecting tubes, labelled and 500µl of column preparation added to the column and centrifuged at 12,000 *x g* for 1 minute to maximise subsequent DNA binding. Once the sample incubation had elapsed, 200µl of 95% ethanol was added to each sample and mixed thoroughly to obtain a homogeneous solution by vortexing for 5-10 seconds. The sample lysate was then transferred to the binding column and centrifuged at 6,500 *x g* for 1 minute. Binding columns were then transferred to clean collecting tubes, the flow-through discarded and 500µl of wash solution added to the column. The columns were then centrifuged at 6,500 *x g* for 1 minute, the flow through discarded and the binding column transferred to a new collecting tube. The wash step was then repeated and columns centrifuged at 12,000 *x g* for 3 minutes to dry the column. The binding columns were then transferred to clean collecting tubes and 200µl of elution solution added and incubated for 5 minutes before a final centrifugation at 6,500 *x g* for 1 minute to elute the bound DNA. The concentration and purity of resulting DNA was then analysed on the Nanodrop spectrophotometer (see section 2.2.3 for protocol details) and the samples used for subsequent PCR analysis.

4.2.10 Amplification of *SLC22A6* and *SLC22A8* template DNA from MDCK II clones stably transfected with *SLC22A6* and *SLC22A8*

Genomic DNA extracted in section 4.2.9 was used in subsequent PCR, carried out as described in section 4.2.4. PCR products for each MDCK II clone stably transfected with *SLC22A6* and *SLC22A8* were then visualised by gel electrophoresis (see section 2.2.4 for protocol details), with MDCK II clones positive for the human *SLC22A6* gene displaying an amplified fragment at 1.6Kb (figure 4.8**(B)**; figure 4.9**(B)**.

4.2.11 RNA extraction of MDCK II clones stably transfected with *SLC22A6* and *SLC22A8*

The RNA of 12 MDCK II clones transfected with *SLC22A6* and *SLC22A8* along with three MDCK II clones that were 'mock' transfected with empty pcDNA3.1 vector alone was extracted using Trizol reagent according to manufacturer's protocol (Sigma Aldrich,UK), as follows. On the day of extraction, the media was aspirated from each well and 1ml of Trizol reagent added directly to the cells. Cells were lysed and homogenised in the well by pipetting up and down several times and each clone was subsequently removed to individual RNAse and DNAse free 1.5ml Eppendorf tubes. Homogenised samples were incubated at room temperature for 5 minutes to permit dissociation of the nucleoprotein complex. After 5 minutes had elapsed, 200µl of chloroform (Sigma Aldrich, UK) was added to each sample, the caps were secured and each tube was vigorously shaken by hand for 15 seconds. Samples were then incubated at room temperature for 2-3 minutes before centrifugation at 12,000 *x g* for 15 minutes at 4^0C to separate the sample into a lower phenol-chloroform phase, an interphase and a colourless upper aqueous phase. The aqueous upper phase of each sample (containing the RNA) was transferred to a clean RNAse and DNAse free Eppendorf and 500µl of 100% isopropanol added. Samples were then allowed to incubate for 10 minutes at room temperature before a second centrifugation step at 12,000 *x g* for 10 minutes at 4^0C. After centrifugation, a small, clear RNA pellet was visible. The supernatant was then removed from the tube to leave only the pellet and the pellet washed in 1ml of 75% ethanol. Samples were vortexed briefly before a final centrifugation step at 7500 *x g* for 5 minutes at 4^0C. The supernatant was then discarded, the resulting RNA pellet allowed to air dry at room temperature for 5-10 minutes (care was taken not to allow the pellet to dry out completely) and the pellet resuspended in 30µl of RNAse free water. The concentration and purity of each sample was then analysed on the Nanodrop

spectrophotometer (see section 2.2.3 for details) and the samples used for later reverse transcription.

4.2.12 Reverse transcription

Extracted RNA was reverse transcribed to cDNA for use in quantitative RT-PCR using High capacity cDNA reverse transcription reagents (Life Technologies) according to manufacturer's protocol, as follows. Reagents were thawed on ice and vortexed briefly before use. A 2 x reverse transcription mastermix was made up with the following constituents: 2µl of reverse transcription buffer (10 x initial concentration), 0.8µl of dNTPs mix (100mM), 2µl of reverse transcription random primers (10 x final concentration), 1µl of multiscribe reverse transcription enzyme (50U/µl) and 4.2µl of nuclease free water (quantities given are for one reaction (20µl total), quantities of each constituent were factored up according to the number of samples). The mastermix was inverted to mix and 10µl added to labelled PCR tubes and kept on ice. A 10µl aliquot (2µg) of RNA was then added to the relevant tube and flicked to mix. Tubes were centrifuged briefly and kept on ice. Each PCR tube was then transferred to the heat block of a 96 well thermal cycler and the following incubation steps followed: 10 minutes at 25^0C, 37^0C for 2 hours, 85^0C for 5 minutes before cooling and holding at 4^0C. Following reverse transcription, the cDNA concentration and purity was determined using the Nanodrop spectrophotometer (see section 2.2.3 for details).

4.2.13 Analysis of MDCK II clones stably transfected with *SLC22A6* and *SLC22A8* by quantitative RT-PCR

Quantitative real time PCR (qRT-PCR) was carried out using Taqman technology according to manufacturer's protocol. Each Taqman assay contains forward and reverse primers specific to the gene transcript (*SLC22A6*, canine *SLC22A6*, *SLC22A8*, canine β-actin) and a third oligonucleotide labelled with a fluorescent reporter molecule and quencher molecule covalently attached. This third oligonucleotide binds to the transcript between the binding sites of the two target-specific primers and when permanently separated from the quencher (i.e. during Taq amplification of the target sequence) the reporter generates a fluorescent signal which is directly proportional to template amplification. The endogenous control assay chosen (canine β-actin) contains a different reporter dye (VIC labelled) than the *SLC22A6* and *SLC22A8* assays (FAM labelled), therefore a duplex reaction could be achieved in which both the target transcript (*SLC22A6* or *SLC22A8*) and the endogenous control transcript could be

quantified in the same reaction. A reaction mix was made up in a 1.5ml DNAse and RNAse free Eppendorf containing 5µl of the target assay (*SLC22A6* or *SLC22A8*), 5µl of the endogenous control assay (canine β-actin), 50µl of Taqman mastermix (containing reaction buffer and Taq polymerase), 20µl of RNAse free water and 20µl of cDNA template (20ng/µl). This volume allowed 4 replicate reactions to be included. The reaction mix was flicked several times to mix and for each clone, 4 aliquots of 20µl were transferred to 4 separate wells of a 384 well plate. Once reactions for all samples had been loaded, the plate was sealed with an optical seal, centrifuged briefly (Thermo Scientific Heraeus Megafuge 16) and transferred to the heat block of a 7900HT Fast Start Real Time PCR System (Applied Biosystems). The following PCR conditions were used according to manufacturer's protocol: initial 2 minute step at 50^0C and 10 minute step at 95^0C, followed by 40 cycles of 95^0C for 15 seconds and 60^0C for 1 minute. SDS 2.3 software was used to quantify amplification plots and Rq manager was used to generate C_t values for each sample.

4.2.14 Quantitative RT-PCR data analysis

Relative *SLC22A6* and *SLC22A8* gene expression in stably transfected MDCK II cell clones was calculated using the comparative C_t method. Rq manager was used to generate C_t values (i.e. the PCR cycle at which the reporter signal crosses an arbitrary threshold) from amplification plots. The comparative C_t method uses the following equation to calculate the fold change expression ($2^{-\Delta\Delta C_t}$) of two samples where each sample is related to an internal control (canine β-actin).

$$2^{-\Delta\Delta CT} = [(C_t \text{ gene of interest} - C_t \text{ internal control}) \text{ sample A} - (C_t \text{ gene of interest} - C_t \text{ internal control}) \text{ sample B}]$$

Internal control (β actin) C_t values obtained in each duplex reaction were subtracted from target (*SLC22A6*/*SLC22A8*) C_t values for each sample (or clone). An average (ΔC_t) was then calculated from the 4 replicates included for each sample. Sample ΔC_t values were then compared to the ΔC_t value of a comparable sample, for the purposes of determining relative expression. For *SLC22A6*, the comparative sample employed was the canine homologue of *SLC22A6*. *SLC22A8* does not have a canine homologue; therefore the clone which generated the highest C_t value was used as a comparative sample in this case. The ΔC_t of the comparative sample was subtracted from the target

ΔC_t (comparative sample was subtracted from itself to give 0) to give the $\Delta\Delta C_t$ for each sample. The fold change in expression ($2^{-\Delta\Delta C_t}$) of each clone in relation to the comparative sample could then be calculated.

4.2.15 Generation of protein lysates and western blotting

Protein lysates from *SLC22A6*, *SLC22A8* and mock pcDNA3.1 transfected MDCK II cells were generated for use in western blot analysis. Briefly, frozen aliquots of $2x10^6$ cells were defrosted from -80^0C storage, transferred to a 1.5ml Eppendorf tube and centrifuged at 250 *x g* for 5 minutes to retrieve the cell pellet. The supernatant was removed and the cell pellet resuspended in 100µl of ice cold RIPA buffer (Thermo Scientific, Loughborough, UK), supplemented with 10µl/ml protease cocktail (Sigma Aldrich, UK). The samples were incubated on ice for 30 minutes and centrifuged (Thermo Scientific Heraeus Fresco 21) at 12,000 *x g* for 15 minutes at 4^0C. The lysate containing the cellular proteins was then transferred to a clean 1.5ml Eppendorf tube and then sonicated (VWR Ultrasonic cleaner) for 30 seconds followed by 20 seconds incubation on ice, three times. Protein concentration in each sample was then determined using the Bio-rad detergent compatible assay reagents (Bio-rad, Hemel Hempstead, UK) according to the manufacturer's instructions, as follows. First, standards of known concentrations (0.2, 0.4, 0.6, 0.8, 1.0, 1.5, 2.0, 2.5mg/ml) of BSA were prepared in RIPA buffer. Then, 5µl aliquots of standards and samples were transferred to a clean, clear, 96-well flat bottom Grenier plate in triplicate and 25µl of Reagent A (supplemented with 20µl/ml Reagent S) added. Thereafter, 200µl of Reagent B was added and the plate briefly shaken and incubated at room temperature. After 15 minutes, the absorbance of the standards and samples was read at 650nm on a DTX 880 Multimode detector (Beckman Coulter, UK). A standard curve was generated from the absorbance of known standard concentrations of protein (BSA) and each sample concentration determined from this.

4.2.16 Denaturing gel electrophoresis

Protein lysates prepared as described in section 4.2.15 were eluted by denaturing gel electrophoresis according to the NuPAGE manufacturer's protocol for use in subsequent western blotting. Samples were first prepared in 10µl aliquots containing 2.5µl NuPAGE loading buffer, 1µl NuPAGE reducing agent, *x*µl sample lysate (where x is the quantity required to give 20µg of protein), and *y*µl water (where y is the quantity required to make the reaction volume up to 10µl). Samples were briefly

vortexed, heated at 70^0C for 5 minutes in a heat block and incubated on ice until cool. Meanwhile, a 1.0mm 4-12% bis-tris pre cast NuPAGE gel was secured in an Xcell Sure lock electrophoresis chamber (Invitrogen, UK) and the outer and inner chambers filled with 1x running buffer (50ml 20x NuPAGE MOPS SDS running buffer in 950ml water) and 1x running buffer supplemented with NuPAGE antioxidant (500µl in 200ml 1x running buffer) respectively. The cooled samples and a reference protein ladder (10-175kDa Prism Protein Ladder) were then loaded onto the gel and the chamber topped up with 1 x running buffer to cover the loaded samples. Samples were then allowed to elute at an initial voltage of 70V for 10 minutes followed by 45 minutes at 170V.

4.2.17 Western blotting

Protein analysis by western blotting aimed to confirm OAT1 and OAT3 expression in MDCK II cells stably transfected with *SLC22A6* and *SLC22A8* respectively. OAT1 and OAT3 expression was also analysed in both mock transfected MDCK II cells and hCMEC/D3 cells. The expression of an endogenous control protein (GAPDH) was also analysed as an experimental control. First, the gel containing the eluted proteins as described in section 4.2.16 was transferred to a nitrocellulose membrane according to the NuPAGE manufacturer's protocol: 1x transfer buffer was prepared (50ml of 20x NuPAGE transfer buffer, 100ml methanol, and 850ml water), with blotting pads and a nitrocellulose sandwich soaked in the transfer buffer. The transfer chamber (Bio-Rad mini Trans-Blot cell) was then constructed and a gel sandwich prepared as follows: the gel cassette was broken open and the foot of the gel removed, a filter paper soaked in transfer buffer was then laid on a clean surface and the gel turned out onto the filter paper, the nitrocellulose membrane was then laid on top followed by a 2nd filter paper (all pre-cut to size). A 10ml serological pipette was then rolled over the gel sandwich to remove any bubbles and ensure a tight seal, before placing the sandwich between two blotting pads soaked in transfer buffer in a cassette and securing the cassette. The cassette was then transferred to the transfer chamber, ensuring the nitrocellulose membrane side of the sandwich was positioned away from the cathode core of the chamber. An ice pack was then inserted behind the transfer cassette adjacent to the cathode core, a magnetic flea placed in the chamber and the chamber filled with transfer buffer. The lid of the transfer chamber was then applied, the chamber positioned on a magnetic stirrer and connected to a power pac (Bio-Rad power-pac 300) at 110V for 1.25 hours.

Following transfer, the cassette containing the gel sandwich was opened and the membrane removed and washed in 0.2% ponceau red dye to visualise the protein bands that had been transferred. The membrane was then washed three times in 1x tris buffered saline plus tween (TBS/T), which constitiuted:100ml of 10 x TBS (80g NaCl, 2g KCl, 30.3g Trizma base, 800ml water adjusted to pH7.4 with pure HCl and made up to 1L with water), 1ml of tween and 899mlof water) to remove the dye. The membrane was blocked in 5% milk solution (5g skimmed milk powder in 100ml 1xTBS/T) for 2 hours at room temperature to minimise non-specific binding of the primary antibody before 10ml of the primary mouse monoclonal *SLC22A6* (2.5µg/ml in 5% milk solution) or rabbit polyclonal *SLC22A8* antibody (1µg/ml in 5% milk solution) was added to the membrane and incubated at room temperature for 1 hour with gentle rocking (Stuart Scientific gyro-rocker SSL3). The membrane was then washed three times for 5 minutes each in 1x TBS/T and incubated with 0.2µl/ml goat anti-mouse or goat anti-rabbit (0.2µl/ml) horseradish peroxidase (HRP) conjugated secondary antibody respectively, for 1 hour at room temperature. The membrane was again washed three times for 5 minutes each in 1 x TBS/T and then exposed to chemoluminescence substrate for detection of HRP conjugates.

Chemoluminescence substrate was prepared according to manufacturer's instructions (Sigma Aldrich, UK), 500µl of reagent A was added to 500µl reagent B and immediately added to the membrane. The membrane was placed on a sheet of acrylic and the chemoluminescence substrate added evenly across the membrane. The chemoluminescence was exposed to light for one minute, the excess blotted from the membrane with a tissue and a sheet of acrylic placed on top. Any bubbles were removed and the membrane secured in a photography cassette between the sheets of acrylic. An x-ray film (Carestream, Kodak, Biomax light film (Sigma Aldrich, UK)) was then exposed to the membrane for 5 minutes in a dark room. After exposure the x-ray film was placed in a tray containing developer (Carestream, Kodak, auto radiography GBX developer/replenisher (Signma Aldrich, UK)) and rocked back and forth until bands appeared. Once bands appeared the film was quickly removed to minimise background development, washed in water and allowed to incubate for a few minutes in fixative (Carestream, Kodak, auto radiography GBX fixer/replenisher (Signma Aldrich, UK)). The x-ray film was then washed again in water and allowed to dry overnight. Samples containing the target protein (OAT1 or OAT3) produced a band

in the corresponding lane at the correct protein size, with the intensity of the band representing the level of expression (figure 4.8(**C**); figure 4.9(**C**)).

After analysis of the target protein, the antibody was stripped from the membrane. This was achieved by incubating the membrane in stripping buffer (20ml 10% SDS, 12.5ml Tris HCl buffer at pH6.8, 66.8ml H_2O, and 700µl of β-mercaptoethanol) at 60^0C with moderate shaking for 30 minutes. The membrane was then blocked a second time with 5% milk solution for 1 hour at room temperature and incubated with the mouse monoclonal GAPDH primary antibody (0.2µl/ml in 5% milk solution) overnight at 4^0C with gentle rocking. The next day the membrane was washed three times for 5 minutes each in 1% TBS/T and incubated with goat anti-mouse HRP conjugated secondary antibody (0.2µl/ml in milk solution) for 1 hour. The membrane was then washed again in 1% TBS/T and the membrane exposed to chemoluminescence and an x-ray film developed as described previously. Following incubation with GAPDH antibody, bands are expected for all samples (figure 4.8(**C**); figure 4.9(**C**)).

4.2.18 Functional transport comparison of MDCK II cell clones stably transfected with *SLC22A6* and *SLC22A8*

Transport function of all 12 selected *SLC22A6* and *SLC22A8* clones was analysed utilising a well-characterised radiolabelled positive control substrate for each of *SLC22A6* and *SLC22A8*. [^{3}H]-PAH was used to explore *SLC22A6* mediated transport at an isotope concentration of 0.3µCi/ml and a final drug concentration on 2µM. [^{3}H]-E3S was used to explore *SLC22A8*-mediated transport also at an isotope concentration of 0.3µCi/ml and a final drug concentration of 8.8µM. Both radiolabelled drugs were prepared in transport medium (HBSS supplemented with 25mM HEPES and 0.1% BSA, at pH7.4). An isotope concentration of 0.3µCi/ml afforded sufficient disintegrations per minute to give accurate readings of radioactive content without saturating the scintillation counter.

MDCK II cell clones stably transfected with *SLC22A6* and *SLC22A8* were seeded into 12-well plates at a density of $1.5x10^6$ cells per ml. On the day of the assay (three days thereafter), media was aspirated from the cells and cells allowed to equilibrate in transport medium at 37^0C for 30 minutes. A dosing solution of PAH/E3S was prepared using transport medium containing the respective radiolabelled/non-radiolabelled drug (to the final concentrations reported above). The dosing solution was added to the cells,

which were then incubated at 37^0C for 60 minutes. In the meantime, 20µl samples of transport buffer alone (blanks) and dosing solution (standards) were taken and added to scintillation vials for later determination of background radiation and radioactive content of a known concentration of each drug solution, respectively. After incubation, cells were washed three-times in ice cold HBSS to terminate uptake and solubilised for 30 minutes at 37^0C with 400µl of 10% SDS. The resulting solution was then transferred to individual scintillation vials and 4ml scintillation fluid (Goldstar Multipurpose Scintillation Cocktail, Meridian, UK) added to all vials. Vials were mixed by inverting several times before radioactive content was determined using a scintillation counter (1500 Tri Carb LS Counter; Packard). Results in dpm were corrected for background counts, quantified in relation to standards of known concentration and expressed (in pmol/100,000 cells) in relation to the number of cells per well.

4.2.19 Kinetic analysis of *SLC22A6*_MDCK II and *SLC22A8*_MDCK II cells with a positive control substrate

For this and all subsequent uptake assays, the *SLC22A6* and *SLC22A8* transfected MDCK II cell clones which observed the greatest uptake of probe substrate and the most robust mRNA and protein expression were used. *SLC22A6*_MDCK II and *SLC22A8*_MDCK II cells were again incubated with radiolabelled PAH and E3S at final concentrations of 2µM and 8.8µM, respectively (isotope concentration = 0.3µCi/ml in both cases). Uptake assays were carried out as described in section 4.2.18 but with cells incubated with positive control drug for a range of times (5, 10, 20, 40, 60 and 120 minutes) to determine a time point to be used in subsequent experiments.

4.2.20 IC_{50} determination

IC_{50} values to determine the potency of OAT inhibitors on the uptake of OAT1 or OAT3 substrates were generated using the uptake assay method described in section 4.2.18. A dosing solution was made for each substrate drug (PAH and E3S) using transport medium containing the respective radiolabelled/non-radiolabelled drug (to the final concentration reported previously) with various concentrations of inhibitor (0-300µM).

4.2.21 Uptake of AEDs

Uptake experiments with AEDs (all at an isotope concentration of 0.3µCi/ml) were performed at final concentrations of 25µM PHT, 20µM CBZ, 300µM VPA, 10µM LTG, 10µM TPM, 10µM GBP and 6µM LEV, all prepared in transport medium. Uptake assays were carried out as described in section 4.2.18. Dosing solutions consisted of transport medium containing the respective radiolabelled AED (to the final concentrations shown above) with either inhibitor or vehicle (0.1% DMSO).

4.2.22 Statistical analysis

All data is presented as the mean (± standard error of the mean) percentage of mean control transport (pcDNA_MDCK II cells) for each AED on each experimental day. Individual experiments were performed in triplicate and repeated on at least three occasions ($n \geq 9$). Data was assessed for normality using the Shapiro-Wilk test and found to be normally distributed in all cases. An analysis of variance (ANOVA) was performed on the data with Tukey's post hoc test for multiple comparisons. A value of $p \leq 0.05$ was taken to indicate statistical significance.

4.3 Results

4.3.1 Abundance of OAT mRNA in brain endothelial cells

mRNA abundance (ΔCt; mean ± SEM; log_{10} scale) of human *SLC22A6* (OAT1), *SLC22A7* (OAT2) and *SLC22A8* (OAT3), relative to the endogenous control (human GAPDH), was analysed in hCMEC/D3 cells using quantitative RT-PCR. OAT1 abundance was detected at a very low level ($4.4x10^{-5}$), relative to GAPDH abundance (1.00). OAT2 and OAT3 were undetectable (*figure 4.7*).

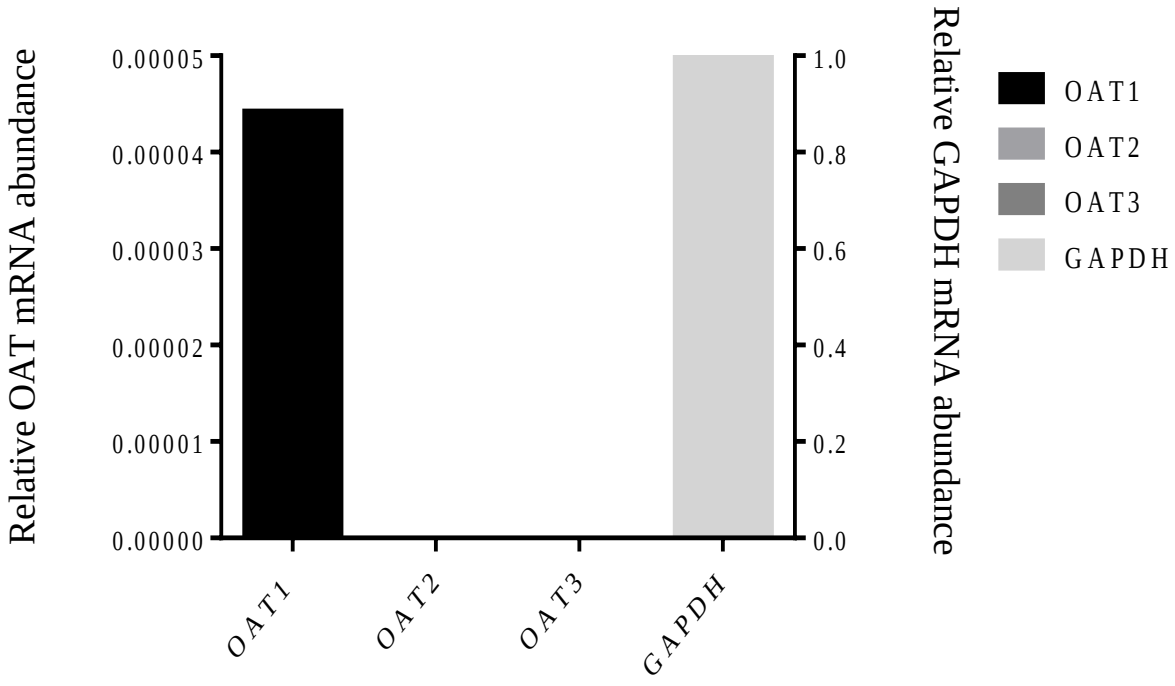

Figure 4.7: mRNA abundance (ΔCt; mean ± SEM; log_{10} scale) of human *SLC22A6* (OAT1), *SLC22A7* (OAT2) and *SLC22A8* (OAT3) in a human cerebral microvascular endothelial cell line (hCMEC/D3). Results are expressed as mean abundance relative to that of GAPDH, which was used as an endogenous control gene. OAT2 and OAT3 were undetectable in these cells.

4.3.2 *SLC22A6*_MDCK II clone analysis

To be confident that the newly-generated, stably transfected cells were expressing functional OAT1 protein, *SLC22A6* expression was first analysed at DNA and mRNA level. PCR analysis confirmed that all of the 11 clones analysed contained the *SLC22A6* gene sequence (*figure 4.8**(B)***). *SLC22A6* gene expression was subsequently quantified using qRT-PCR, confirming *SLC22A6* expression in all 11 clones selected. Of these, clone 10 had the highest relative expression, with a 7173 fold higher relative expression than that of the canine *SLC22A6* gene in mock pcDNA control MDCK cells (*figure 4.8**(A)***). OAT1 expression in clone 4 (moderate *SLC22A6* mRNA expression) and clone 10 (high *SLC22A6* mRNA expression) was also analysed at protein level and confirmed in both clones (*figure 4.8**(C)**)*. The functional capacity of OAT1 to transport the positive control substrate (PAH) in the 11 clones selected was also assessed. Clone 10 showed the greatest uptake of PAH (18948 ± 797%) after 5 minutes incubation compared to uptake in control pcDNA_MDCK II cells (100 ± 4.3%; *figure 4.8**(D))***and was subsequently selected for transfection.

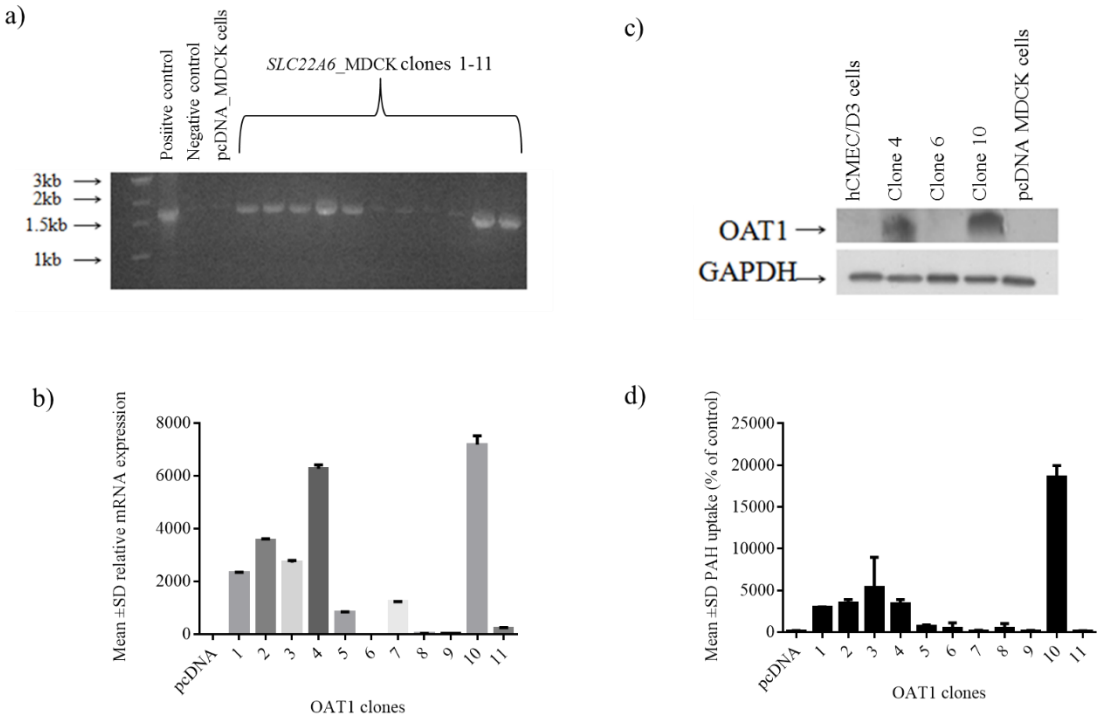

Figure 4.8: Analysis of *SLC22A6*_MDCK II clones. **a)** Agarose gel (1%) visualisation of *SLC22A6* DNA in a positive control **(1),** negative control **(2),** control pcDNA MDCK II cells **(3)** and 11 OAT1 single cell clones **(lanes 4-14)**. All clones were positive for *SLC22A6* template DNA following amplification of MDCK II_*SLC22A6* clones by PCR. **b)** qRT-PCR analysis of 11 single cell clones, of which clone 10 showed the highest mRNA expression. Total RNA was extracted from *SLC22A6*_MDCK II clones and reverse-transcribed into cDNA. The cDNA used was then used to quantify relative expression for each gene and the mean Ct values obtained from test gene amplification plots were normalised to the mean Ct of the housekeeping gene canine *β actin*. Data are presented as the relative test gene expression (ΔΔCt), according to the comparative Ct method. **c)** Analysis of OAT1 protein expression by western blotting. Sample lysates from left to right: hCMEC/D3 **(1)**, clone 4 **(2)**, clone 6 **(3)**, clone 10 **(4)** and control pcDNA **(5)**. **d)** Functional uptake of [3H]-p-aminohippuric acid (PAH; OAT1 substrate) in 11 MDCK II_*SLC22A6* clones compared to control (MDCK II_pcDNA). Cultures were exposed to 2µM radiolabelled PAH for 5 minutes at 37^0C. Results are expressed as the mean ± the standard error of the mean (SEM) percentage of the mean control value of PAH uptake (in pmols/100,000 cells) for one experiment where n=3.

4.3.3 *SLC22A8*_MDCK II clone analysis

SLC22A8 clones were first analysed at the DNA and mRNA level. PCR analysis confirmed that all of the 12 clones analysed contained the *SLC22A8* DNA sequence (*figure 4.9**(B)***). *SLC22A8* gene expression was subsequently quantified using qRT-PCR, confirming *SLC22A8* expression in all 12 clones selected. Of these, clone 2 had the highest relative expression, with a 258 fold higher relative expression than that of the lowest expressing clone (clone 5): given the arbitrary value 1; *figure 4.9**(A)***). A canine homologue of *SLC22A8* does not exist; therefore expression in mock pcDNA control MDCK cells was not determined. OAT3 protein expression in clone 7 and 8 (moderate *SLC22A8* mRNA expression) and clone 2 and 12 (high *SLC22A8* mRNA expression) was also analysed by western blotting and confirmed in all four clones (*figure 4.9**(C)**)*. The functional capacity of OAT3 to transport the control substrate E3S (8.8µM) in the 12 clones selected was also assessed. Clone 2 showed the greatest uptake of E3S (239 ± 18.3%) after 5 minutes incubation compared to uptake in control pcDNA_MDCK II cells (100 ± 9.27; *figure 4.9**(D)**)* and was subsequently selected for transfection.

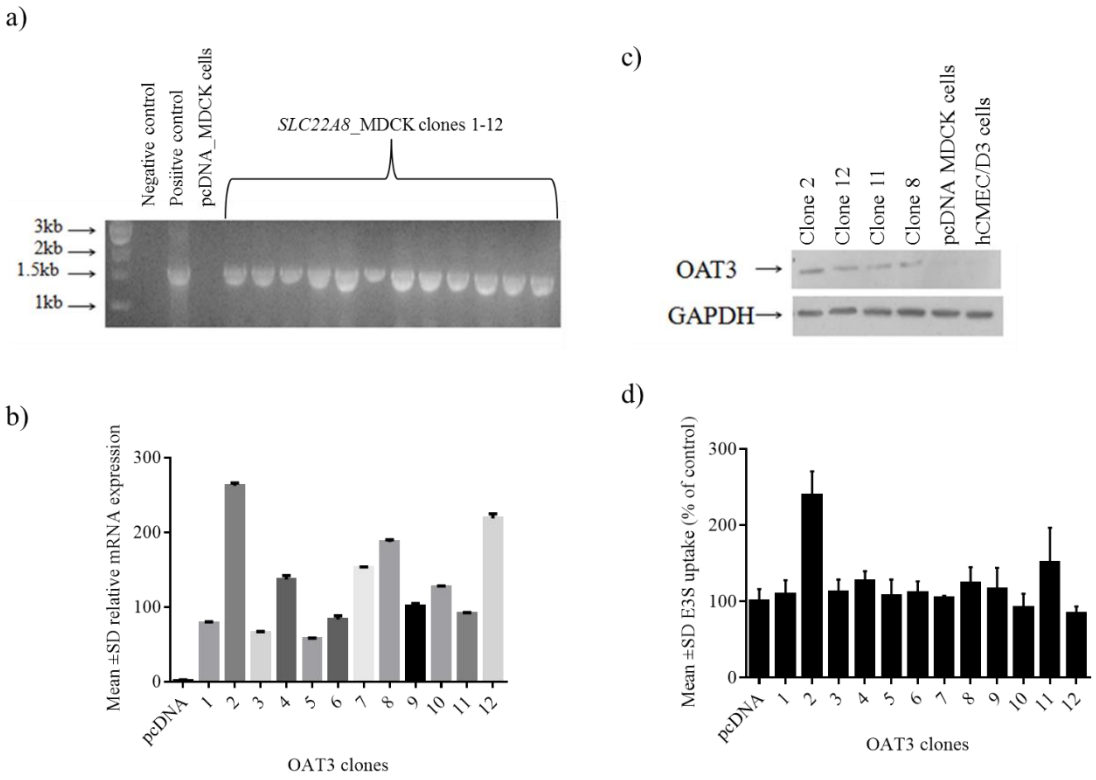

Figure 4.9: Analysis of *SLC22A8*_MDCK II clones. **a)** Agarose gel (1%) visualisation of *SLC22A8* DNA in a negative control **(1),** positive control **(2),** control (pcDNA) MDCK II cells **(3)** and 12 *SLC22A8* single cell clones **(lanes 4-15)**. All clones were positive for *SLC22A8* template DNA following amplification by PCR of MDCK II_*SLC22A8* clones. **b)** qRT-PCR analysis of 12 single cell clones, of which clone 2 showed the highest mRNA expression. Total RNA was extracted from *SLC22A8*_MDCK II clones and reverse-transcribed into cDNA and the cDNA used to quantify relative expression for each gene. Mean Ct values obtained from test gene amplification plots were normalised to the mean Ct of the clone with lowest expression (clone 5) and are presented as the relative test gene expression (ΔΔCt), according to the comparative Ct method. **c)** Analysis of OAT3 protein expression by western blotting. Sample lysates from left to right: clone 2 cell lysate **(1)**, clone 12 cell lysate **(2)**, clone 11 cell lysate **(3)**, clone 8 cell lysate **(4)** control pcDNA_MDCK II cell lysates **(5)** and hCMEC/D3 cell lysates **(6)**. **d)** Functional uptake of [^{3}H]-Estrone-3-sulfate (E3S; OAT3 substrate) in 12 MDCK II_*SLC22A8* clones compared to control (MDCK II_pcDNA). Cultures were exposed to 8.8µM radiolabelled E3S for 5 minutes at 37^{0}C. Results are expressed as the mean ± the standard error of the mean (SEM) percentage of the mean control value of E3S uptake (in pmols/100,000 cells) for one experiment where n=3.

4.3.4 Kinetics of the OAT1 substrate p-aminohippuric acid in a *SLC22A6* stably-transfected MDCK II cell line

A time course study of the OAT1 substrate PAH in *SLC22A6*_MDCK II cells compared to control (pcDNA transfected) MDCK II cells was undertaken to determine the optimum time point for further investigation with AEDs *(figure 4.10).* Optimum transport of 2µM PAH was observed between 40 and 60 minutes (104±16 pmol/1x10^6 cells) before uptake saturated. The 40 minute time point in the linear phase of PAH transport was therefore chosen for subsequent experiments with AEDs. PAH was subsequently incubated for 40 minutes with and without the OAT1 inhibitor probenecid. Uptake of PAH in *SLC22A6*_MDCK II cells was 3943±311% *(*$p \leq 0.001$*)* of the corresponding control value (100±5.1%) in pcDNA transfected cells. In the presence of 200µM probenecid, the increase in PAH transport in *SLC22A6*_MDCK cells relative to transport in control cells was attenuated to 247±14% of control ($p \leq 0.001$; *figure 4.11*). PAH uptake in *SLC22A6*_MDCK II cells was also investigated in the presence of various concentrations (0.1, 1.0, 3.0, 10, 30, 100 and 300µM) of probenecid to generate a concentration-response curve. Uptake of PAH at each concentration of probenecid in control (pcDNA-transfected) cells was deducted from uptake in *SLC22A6*_MDCK II cells and an IC_{50} value of 3.4µM determined (*figure 4.12*)

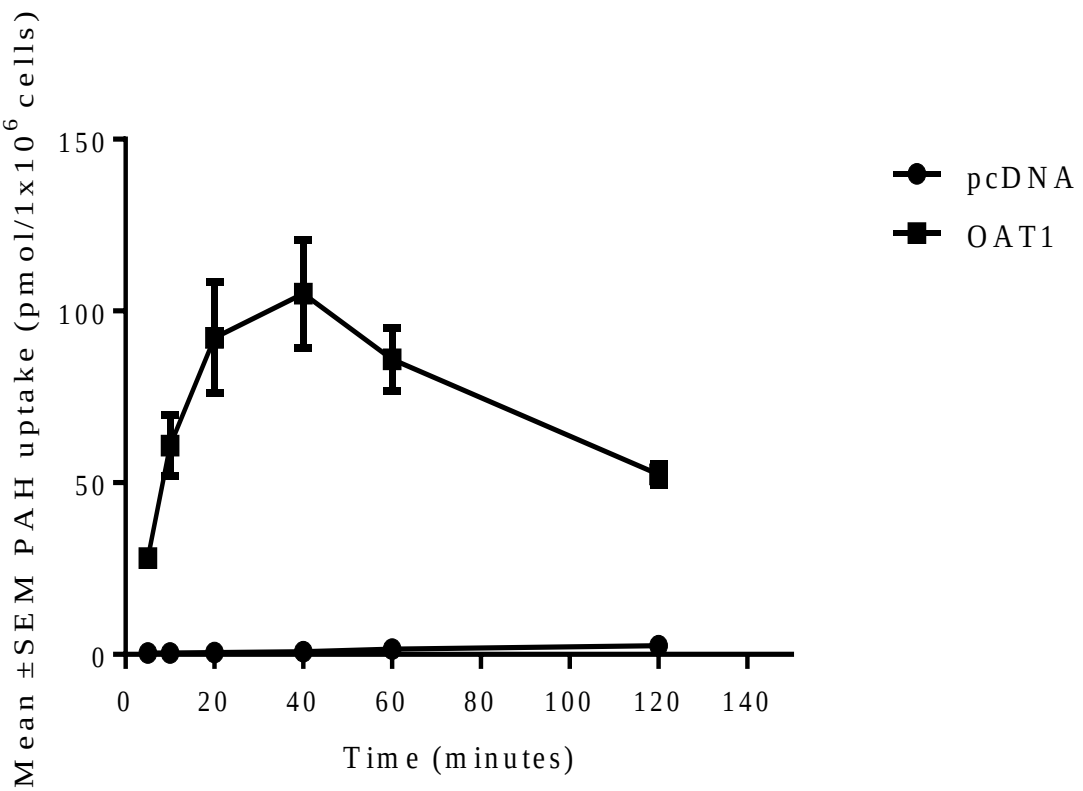

Figure 4.10: p-aminohippuric acid (PAH) uptake in *SLC22A6*_MDCK II cells (OAT1) compared to control pcDNA-transfected MDCK II cells over time. Cultures were exposed to 2μM radiolabelled PAH for 5, 10, 20, 40, 60 and 120 minutes at 37^0C. Results are expressed as mean PAH uptake ± standard error of the mean (SEM) (in pmols/100,000 cells) on each experimental day. Experiments were performed in triplicate on three separate occasions (n=9).

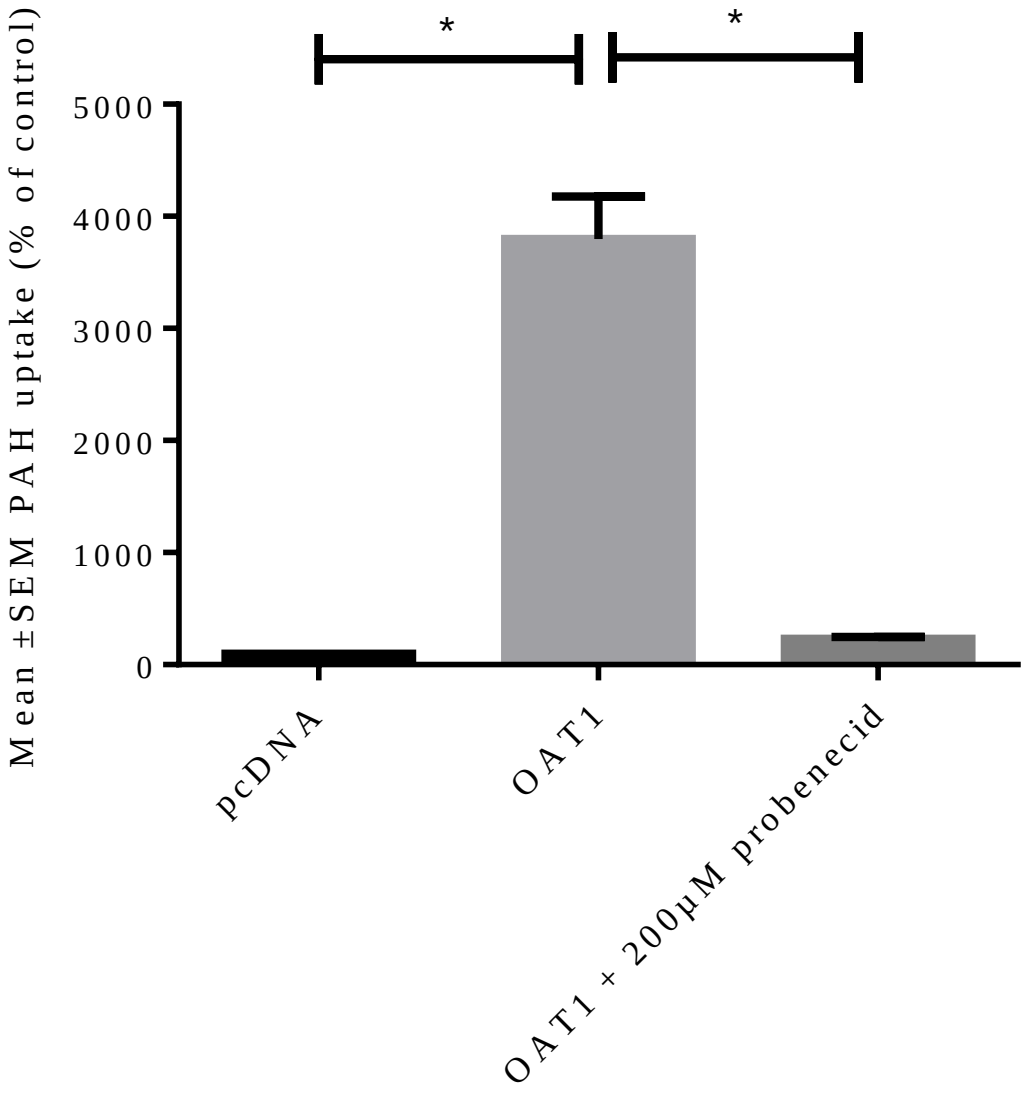

Figure 4.11: p-aminohippuric acid (PAH) uptake into *SLC22A6*_MDCK II cells (OAT1) compared to control pcDNA-transfected MDCK II cells with and without the OAT1 inhibitor probenecid. Cultures were exposed to 2µM radiolabelled PAH with or without probenecid at 200µM for 40 minutes at 37^0C. Results are expressed as the mean ± standard error of the mean (SEM) percentage of the mean control value of PAH uptake (in pmols/100,000 cells) on each experimental day. Experiments were performed in triplicate on three separate occasions (n=9). Statistical significance (*$p<0.001$) was determined by one-way analysis of variance with Tukey's correction for multiple testing.

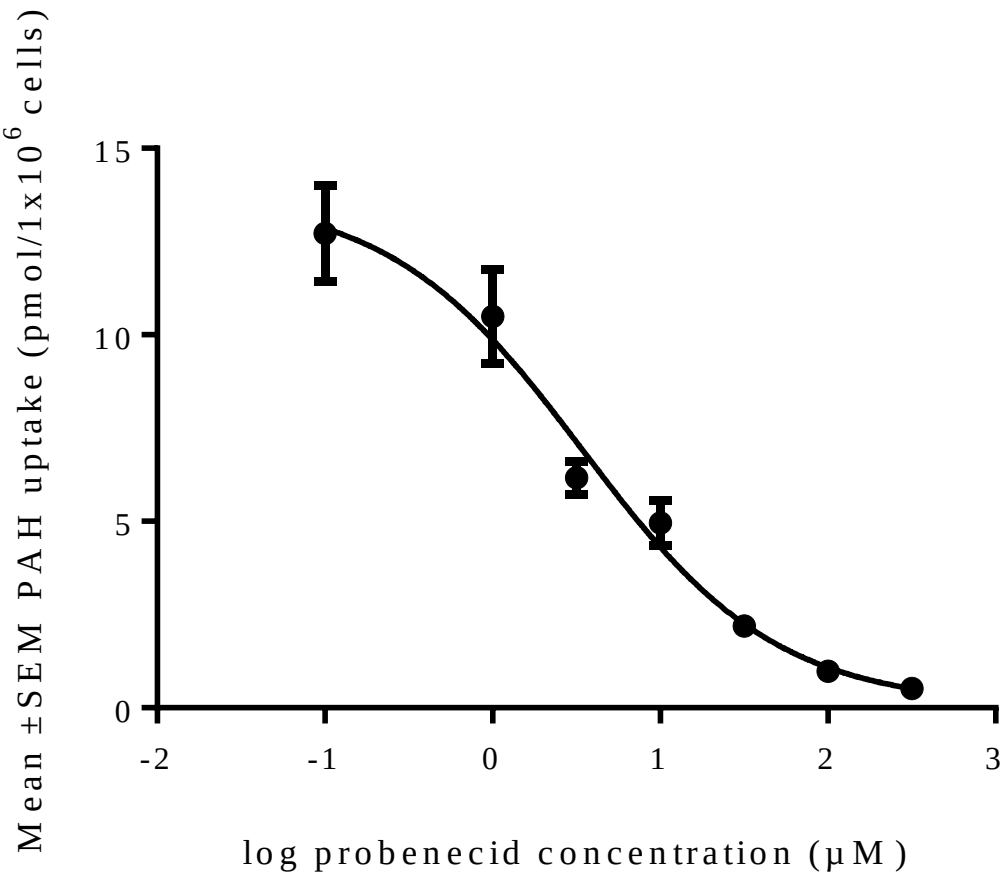

Figure 4.12: p-aminohippuric acid (PAH) uptake into *SLC22A6*_MDCK II cells in the presence of various concentrations of probenecid to determine inhibitory potency. Cultures were exposed to 2µM radiolabelled PAH with and without probenecid for 40 minutes at 37^0C to generate a concentration response. The concentration response included the following concentrations of probenecid: 0µM vehicle only (0.1% DMSO), 1µM, 3µM, 10µM, 30µM, 100µM and 300µM. Response in mock transfected cells at the corresponding concentrations was subtracted from that in *SLC22A6*_MDCK II cells to account for passive transport and to allow determination of inhibitory effects on OAT1 mediated transport only. Results are expressed as the mean ± standard error of the mean (SEM) PAH uptake in pmol/1,000,000 cells on each experimental day. Experiments were performed in triplicate on three occasions (n=9).

4.3.5 Kinetics of the OAT3 substrates estrone-3-sulphate and p-aminohippuric acid in a stably transfected *SLC22A8*_MDCK II cell line

A time course study employing the OAT3 substrate E3S in *SLC22A6*_MDCK cells was undertaken to determine the optimum time point for further investigation with AEDs *(figure 4.13).* Optimum transport of 8.8µM E3S (69.1±12 pmol/1x10^6 cells) was observed following 40 minutes incubation, with uptake saturating thereafter. The 40 minute time point was therefore chosen for subsequent experiments with AEDs in *SLC22A8*_MDCK II cells. Transport of E3S was then investigated with and without the OAT3 inhibitor probenecid. Uptake of E3S in *SLC22A8*_MDCK II cells was 256±24% *(*$p \leq 0.001$*)* of the corresponding control value (100±5.95%) in pcDNA transfected cells. In the presence of 200µM probenecid, the increase in E3S transport in *SLC22A8*_MDCK cells relative to transport in control cells was attenuated to 156±22.5% of control ($p \leq 0.001$; *figure 4.14*). *SLC22A8* transport of PAH in *SLC22A8*_MDCK II cells was also investigated with and without the OAT3 inhibitor probenecid. Uptake of PAH was 303±49% *(*$p \leq 0.001$*)* of the corresponding control value (100±5%) in pcDNA transfected cells. In the presence of 200µM probenecid, the increase in PAH transport relative to transport in control cells was attenuated to 200±17% of control ($p \leq 0.001$; *figure 4.15*). *SLC22A8* PAH uptake in *SLC22A8*_MDCK II cells was also investigated in the presence of various concentrations of probenecid (0.1, 1.0, 3.0, 10, 30, 100 and 300µM) to obtain a concentration response curve. Uptake of PAH at each concentration of probenecid in control (pcDNA-transfected) cells was deducted from uptake in *SLC22A8*_MDCK II cells and an IC_{50} value of 8.7µM determined (*figure 4.16*).

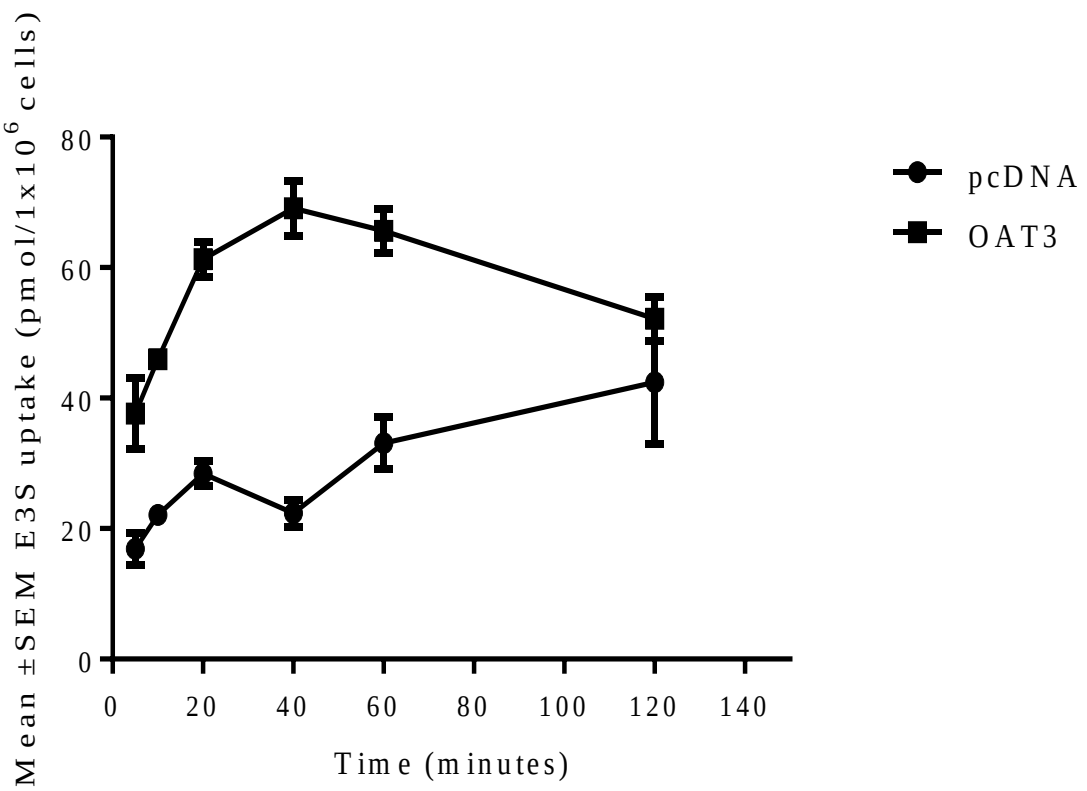

Figure 4.13: Estrone-3-sulfate (E3S) uptake in *SLC22A8*_MDCK II cells (OAT3) compared to control pcDNA-transfected MDCK II cells over time. Cultures were exposed to 8.8µM radiolabelled E3S for 5, 10, 20, 40, 60 and 120 minutes at 37^0C. Results are expressed as mean ± standard error of the mean (SEM) E3S uptake (in pmols/100,000 cells) on each experimental day. Experiments were performed in triplicate on three separate occasions (n=9).

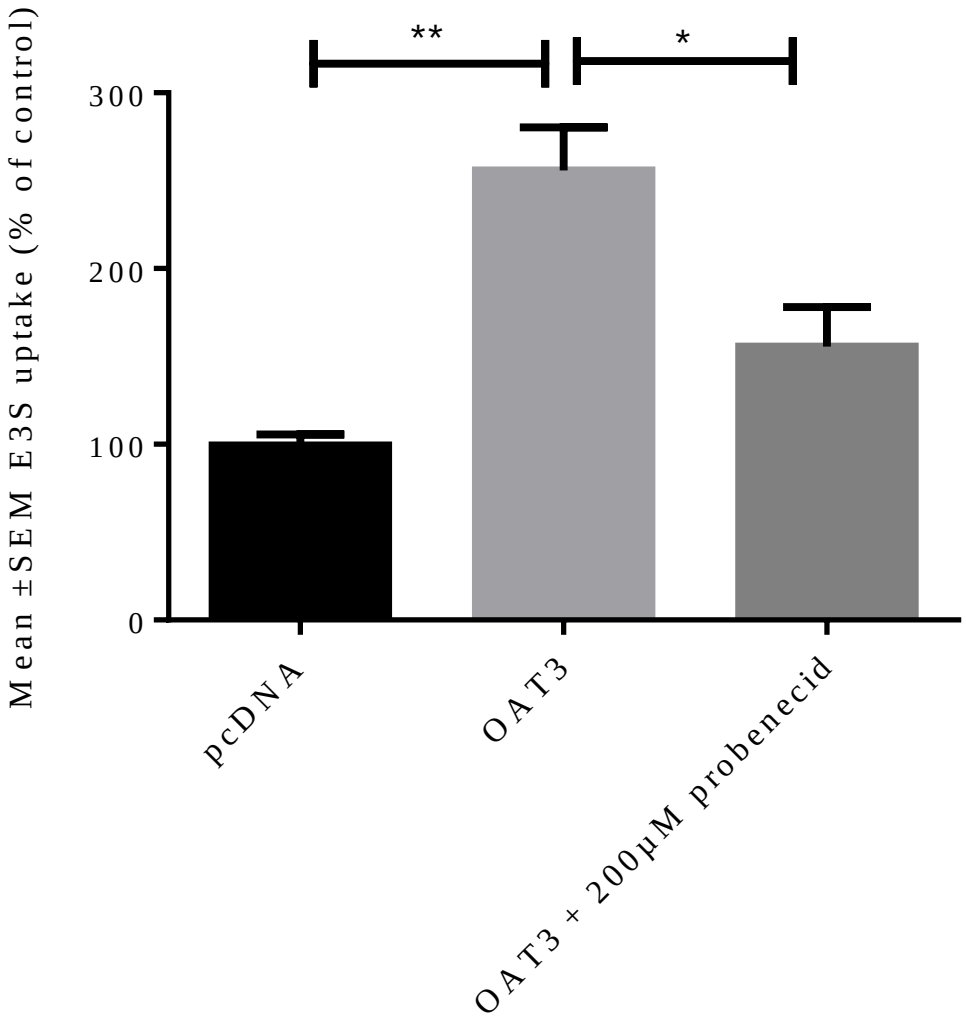

Figure 4.14: Estrone-3-sulfate (E3S) uptake into *SLC22A8*_MDCK II cells (OAT3) compared to control pcDNA-transfected MDCK II cells with and without the OAT3 inhibitor probenecid. Cultures were exposed to 8.8µM radiolabelled E3S with or without probenecid at 200µM for 40 minutes at 37^0C. Results are expressed as the mean ± standard error of the mean (SEM) percentage of the mean control E3S uptake (in pmols/100,000 cells) on each experimental day. Experiments were performed in triplicate on three separate occasions (n=9). Statistical significance (*$p<0.01$, **$p<0.001$) was determined by one-way analysis of variance with Tukey's correction for multiple testing.

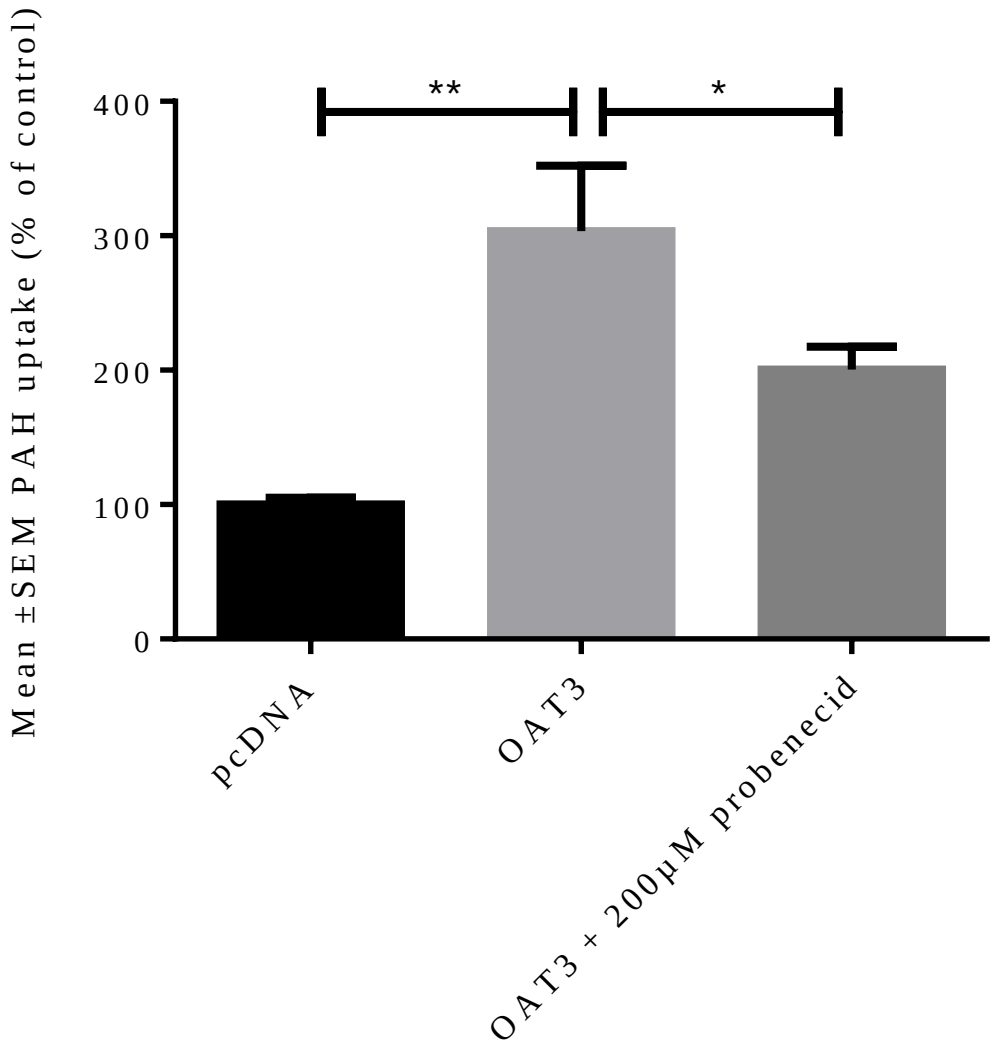

Figure 4.15: p-aminohippuric acid (PAH) uptake into *SLC22A8*_MDCK II (OAT3) cells compared to control pcDNA-transfected MDCK II cells with and without the OAT3 inhibitor probenecid. Cultures were exposed to 2µM radiolabelled PAH with or without probenecid at 200µM for 40 minutes at 37^0C. Results are expressed as the mean ± standard error of the mean (SEM) percentage of the mean control value of PAH uptake (in pmols/1,000,000 cells) on each experimental day. Experiments were performed in triplicate on three separate occasions (n=9). Statistical significance (*$p<0.05$, **$p<0.001$) was determined by one-way analysis of variance with Tukey's correction for multiple testing.

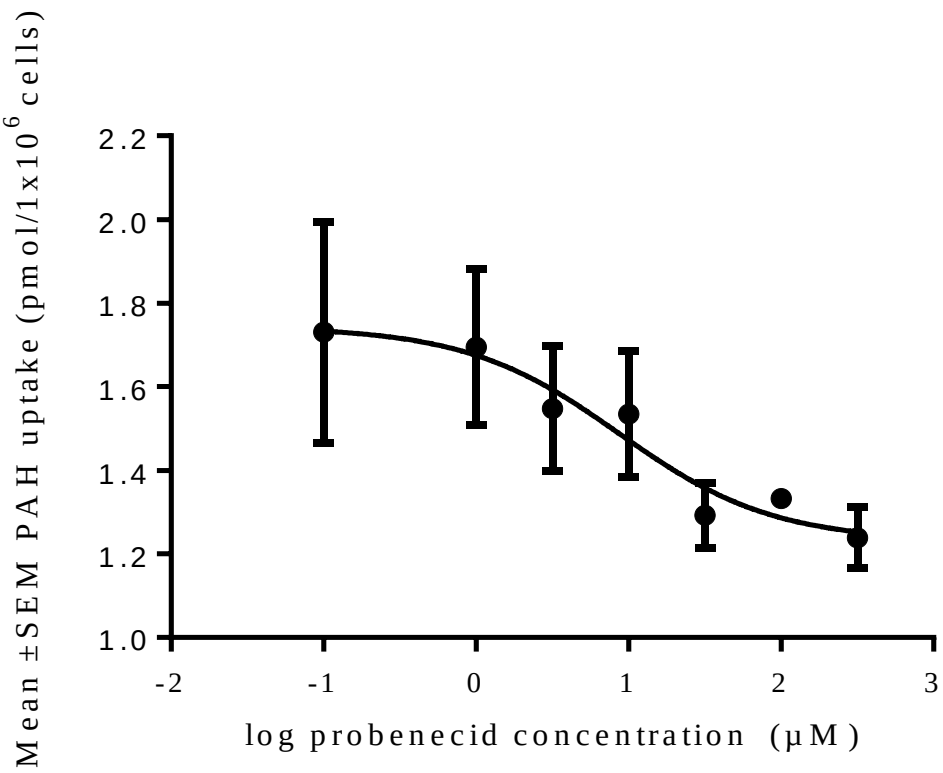

Figure 4.16: p-aminohippuric acid (PAH) uptake into *SLC22A8*_MDCK II cells in the presence of various concentrations of probenecid to determine inhibitory potency. Cultures were exposed to 2µM radiolabelled PAH with and without probeneid for 40 minutes at 37^0C to generate a concentration response. The concentration response included the following concentrations of probenecid: 0µM vehicle only (0.1% DMSO), 1µM, 3µM, 10µM, 30µM, 100µM and 300µM. Response in mock transfected cells at the corresponding concentrations was subtracted from that in *SLC22A8*_MDCK II cells to account for passive transport and to allow determination of inhibitory effects on OAT3 mediated transport only. Results are expressed as the mean ± standard error of the mean (SEM) PAH uptake in pmol/1,000,000 cells on each experimental day. Experiments were performed in triplicate on three occasions (n=9).

4.3.6 Antiepileptic drug transport in a stably transfected *SLC22A6* MDCK II cell line

AEDs were incubated with control (mock pcDNA transfected) and *SLC22A6*-transfected MDCK II cells with and without the OAT1 inhibitor probenecid (200µM) for 40 minutes at 37^0C. VPA uptake was 139±15% ($p \leq 0.01$) in *SLC22A6*_MDCK II cells compared to control (100±3.1%), but was not significantly inhibited in the presence of probenecid (124±6.3%*; figure 4.17*; table 4.2). Likewise, LTG uptake was 147±4.4% ($p \leq 0.01$) in *SLC22A6*_MDCK II cells compared to the control (100±0.93%) and although a decrease was observed in the presence of probenecid (131±4.3%), this did not reach statistical significance (*figure 4.17*; table 4.2). To elucidate if LTG transport observed may be due to a compensatory increase in endogenous canine cation transporters, LTG uptake in the presence of the cation transport inhibitor verapamil was investigated. Interestingly, when co-incubated with the organic cation transporter (OCT) inhibitor verapamil (100µM), the uptake of LTG in both control (24.3±1.5%; $p \leq 0.001$) and *SLC22A6*_MDCK II cells (22.4±1.4%; $p \leq 0.001$) was dramatically reduced *(figure 4.19*) in comparison to that of LTG alone in control cells. LTG was also seen to act as an inhibitor of the uptake of the prototypic OAT1 substrate PAH in *SLC22A6*_MDCK II cells, with an IC_{50} value of 32.9µM obtained (*figure 4.20*). No significant differences in uptake were observed for the other AEDs tested *(figures 4.17 and 4.18).*

Antiepileptic drug	Mean ± SEM uptake (% of control)		
	control pcDNA	OAT1	OAT1 + 200µM probenecid
Phenytoin	100 ±2.7	69.8 ±1.9	70.3 ±2.3
Carbamazepine	100 ±1.3	143 ±7.7	125 ±7.7
Sodium valproate	101 ±6.2	155 ±0.84*	158 ±4.4
Lamotrigine	100 ±0.93	138 ±5.0**	123 ±4.9
Gabapentin	100 ±1.7	133 ±22	138 ±18
Topiramate	100 ±1.7	91.0 ±3.5	81.2 ±2.9
Levetiracetam	100 ±4.6	108 ±8.9	102 ±5.7

Table 4.2: Antiepileptic drug uptake into *SLC22A6*_MDCK II cells (OAT1) compared to control pcDNA-transfected MDCK II cells with and without the OAT1 inhibitor probenecid. Cultures were exposed to 25µM radiolabelled phenytoin, 20µM radiolabelled carbamazepine, 300µM radiolabelled sodium valproate, 10µM lamotrigine, 10µM radiolabelled gabapentin, 10µM topiramate or 6µM levetiracetam with or without probenecid at 200µM for 40 minutes at 37^0C. Results are expressed as the mean ± standard error of the mean (SEM) percentage of the mean control value of uptake (in pmols/100,000 cells) on each experimental day. Experiments were performed in triplicate on three separate occasions (n=9). Statistical significance (*$p<0.01$, **$p<0.001$,) was determined by one-way analysis of variance with Tukey's correction for multiple testing.

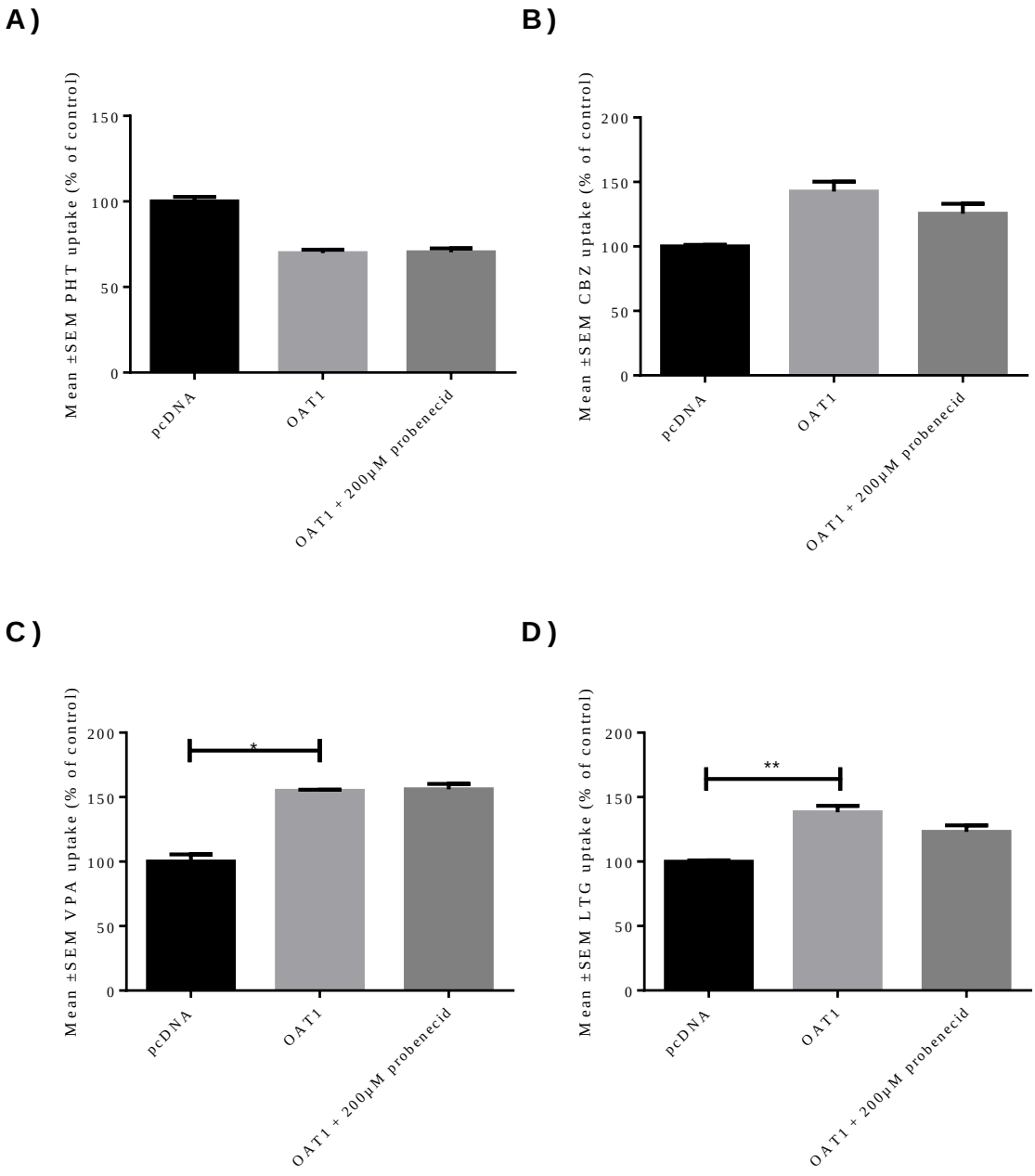

Figure 4.17 Phenytoin (PHT) **(A)**, carbamazepine (CBZ) **(B)**, valproic acid (VPA) **(C)** and lamotrigine (LTG) uptake **(D)** into *SLC22A6*_MDCK II cells compared to control pcDNA-transfected MDCK II cells with and without the OAT1 inhibitor probenecid. Cultures were exposed to 25µM radiolabelled PHT, 20µM radiolabelled CBZ, 300µM radiolabelled VPA or 10µM radiolabelled LTG respectively with or without probenecid at 200µM for 40 minutes at 37^0C. Results are expressed as the mean ± standard error of the mean (SEM) percentage of the mean control value of uptake (in pmols/100,000 cells) on each experimental day. Experiments were performed in triplicate on three separate occasions (n=9). Statistical significance (*$p<0.01$, **$p<0.001$,) was determined by one-way analysis of variance with Tukey's correction for multiple testing.

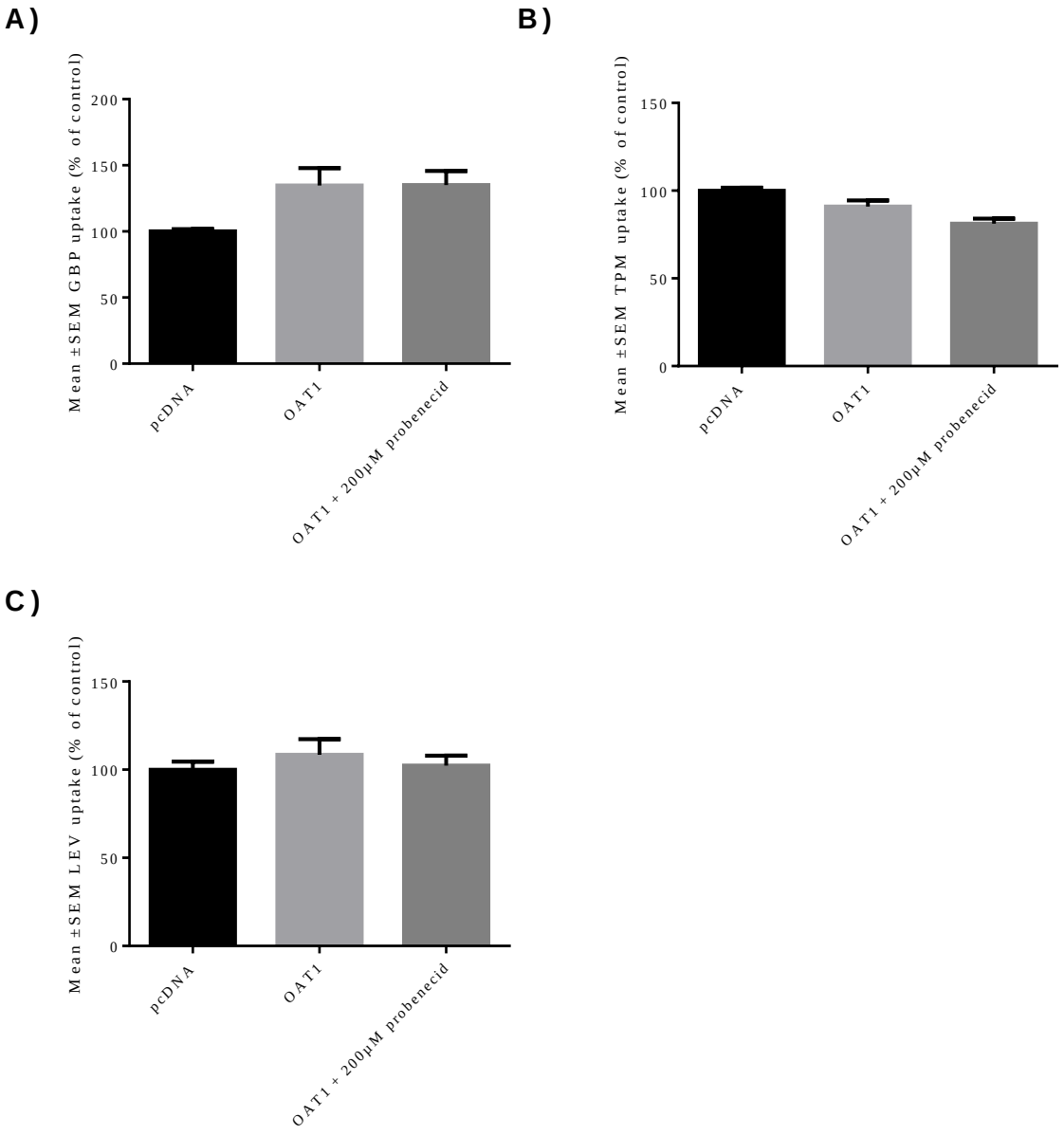

Figure 4.18: Gabapentin (GBP) **(A)**, topiramate (TPM) **(B)** and levetiracetam (LEV) uptake **(C)** into *SLC22A6*_MDCK II cells compared to control pcDNA-transfected MDCK II cells with and without the OAT1 inhibitor probenecid. Cultures were exposed to 10µM radiolabelled GBP, 10µM radiolabelled TPM or 6µM radiolabelled LEV respectively with or without probenecid at 200µM for 40 minutes at 37^0C. Results are expressed as the mean ± standard error of the mean (SEM) percentage of the mean control value of uptake (in pmols/100,000 cells) on each experimental day. Experiments were performed in triplicate on three separate occasions (n=9).

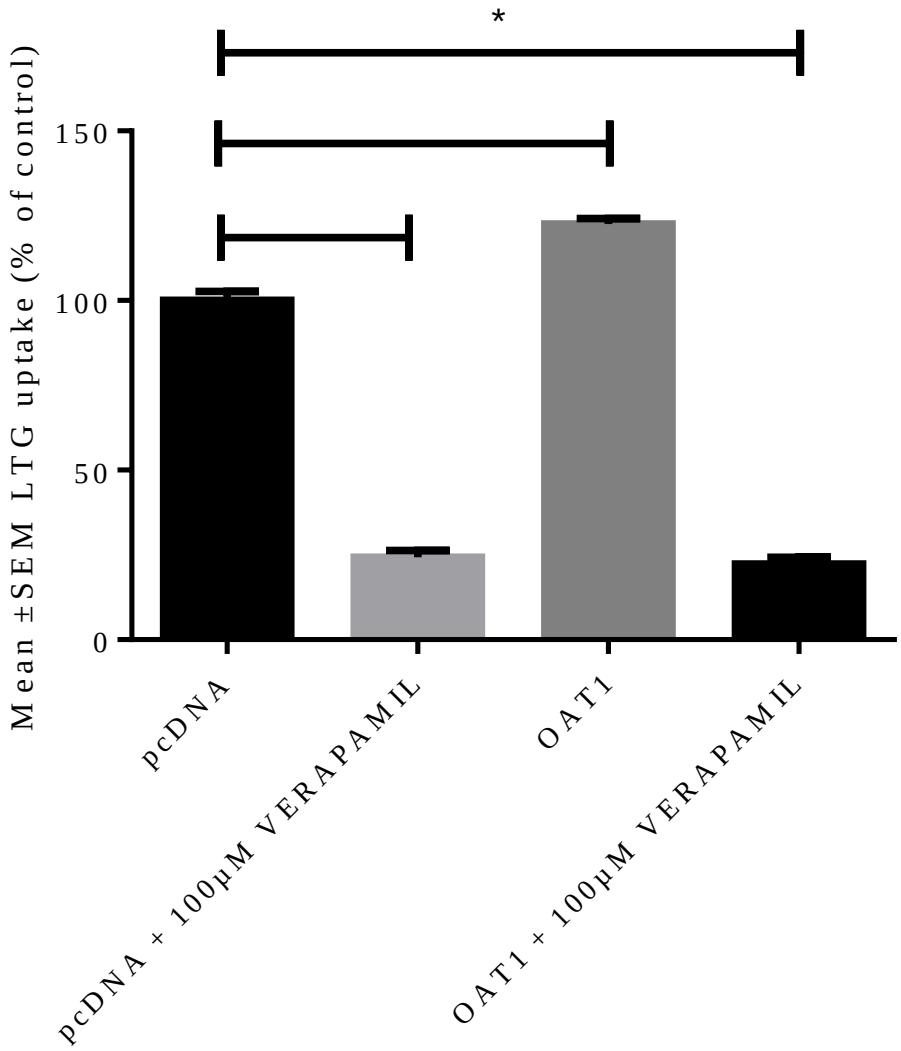

Figure 4.19: Lamotrigine (LTG) uptake into *SLC22A6*_MDCK II cells compared to control pcDNA-transfected MDCK II cells with and without the OCT inhibitor verapamil. Cultures were exposed to 10µM radiolabelled LTG with or without verapamil at 100µM for 40 minutes at 37^0C. Results are expressed as the mean ± standard error of the mean (SEM) percentage of the mean control value of LTG uptake (in pmols/100,000 cells) on each experimental day. Experiments were performed in triplicate on three separate occasions (n=9). Statistical significance (*$p<0.001$) was determined by one-way analysis of variance with Tukey's correction for multiple testing.

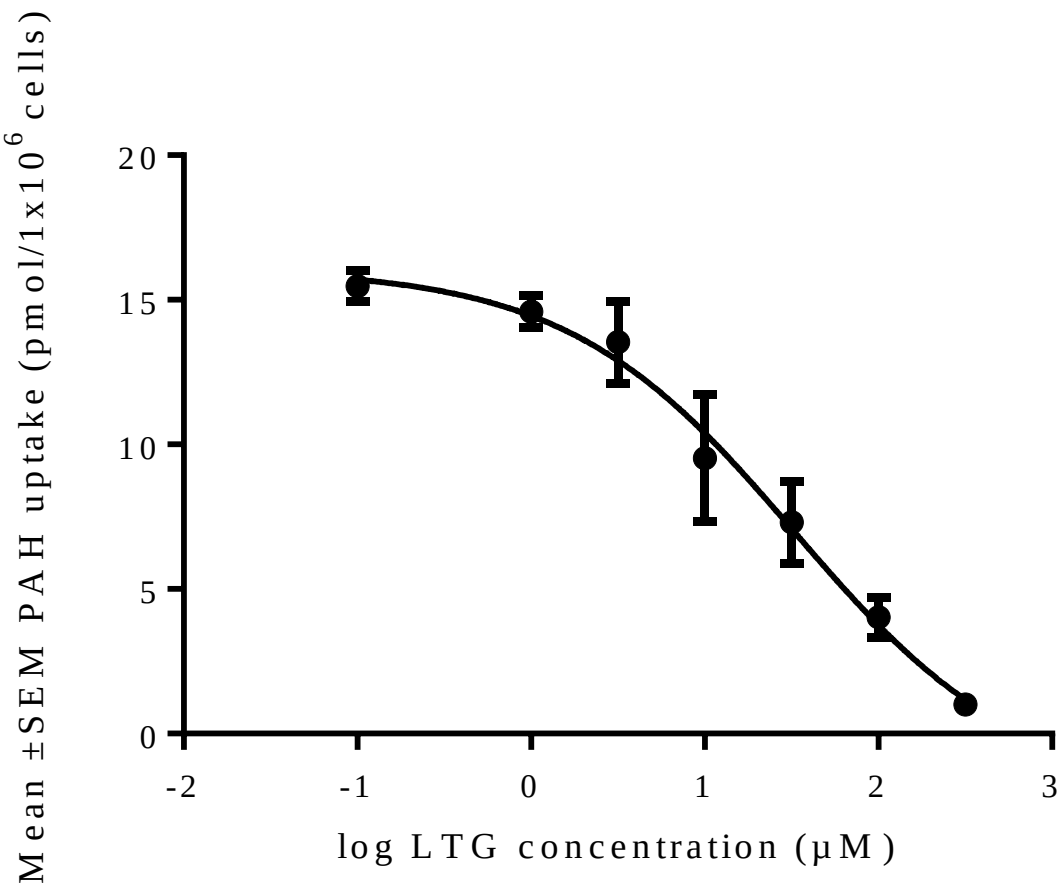

Figure 4.20: p-aminohippuric acid (PAH) uptake into *SLC22A6*_MDCK II cells in the presence of various concentrations of lamotrigine (LTG) to determine inhibitory potency. Cultures were exposed to 2µM radiolabelled PAH with and without LTG for 40 minutes at 37^0C to generate a concentration response. The concentration response included the following concentrations of LTG: 0µM vehicle only (0.1% DMSO), 1µM, 3µM, 10µM, 30µM, 100µM and 300µM. Response in mock transfected cells at the corresponding concentrations was subtracted from that in *SLC22A6*_MDCK II cells to account for passive transport and to allow determination of inhibitory effects against OAT1 mediated transport only. Results are expressed as the mean ± standard error of the mean (SEM) PAH uptake in pmol/1,000,000 cells on each experimental day. Experiments were performed in triplicate on three occasions (n=9).

4.3.7 Antiepileptic drug transport in a stably transfected *SLC22A8* MDCK II cell line

AEDs were incubated with control (mock pcDNA transfected) and *SLC22A8*_MDCK II cells with and without the OAT3 inhibitor probenecid (200µM) for 40 minutes at 37^0C. LTG uptake was higher in *SLC22A8*_MDCK II cells (121±5.1% of control) compared to control (100±2.2%; p<0.01). This effect was reversed in the presence of probenecid, with LTG uptake into *SLC22A8*_MDCK II cells returning to 103±9.5% of control (p<0.05; *figure 4.21*; table 4.3). TPM uptake was also higher in *SLC22A8*_MDCK II cells (151±3.1% of control) than in the corresponding controls (100±1.7%; $p \leq 0.001$) but this observation was not influenced by the presence of probenecid, with TPM uptake remaining at 145±2.3% of control (*figure 4.22*; table 4.3). VPA uptake was lower in *SLC22A8*_MDCK II cells (62.7 ±7.2% of control) than in the corresponding control cells (100±3.4%; p<0.05), an effect that was not influenced by the presence of probenecid, with VPA uptake remaining at 54.9±6.9% of control *(figure 4.21*; table 4.3).

Antiepileptic drug	Mean ± SEM uptake (% of control)		
	control pcDNA	OAT3	OAT3 + 200µM probenecid
Phenytoin	100 ±2.2	98.5 ±8.5	87.2 ±7.8
Carbamazepine	100 ±2.1	95.4 ±6.8	101 ±12
Sodium valproate	100 ±3.4	62.7 ±7.2*	54.9 ±6.9
Lamotrigine	100 ±1.5	121 ±5.1**	103 ±5.6*
Gabapentin	100 ±1.7	95.4 ±6.8	101 ±12
Topiramate	100 ±1.7	151 ±3.4***	145±2.3
Levetiracetam	100 ±4.6	125 ±7.0	121 ±2.5

Table 4.3: Antiepileptic drug uptake into *SLC22A8* MDCK II cells (OAT3) compared to control pcDNA-transfected MDCK II cells with and without the OAT3 inhibitor probenecid. Cultures were exposed to 25µM radiolabelled phenytoin, 20µM radiolabelled carbamazepine, 300µM radiolabelled sodium valproate, 10µM lamotrigine, 10µM radiolabelled gabapentin, 10µM topiramate or 6µM levetiracetam with or without probenecid at 200µM for 40 minutes at 37^0C. Results are expressed as the mean ± standard error of the mean (SEM) percentage of the mean control value of uptake (in pmols/100,000 cells) on each experimental day. Experiments were performed in triplicate on three separate occasions (n=9). Statistical significance (*p<0.05, **p<0.01, *** p<0.001) was determined by one-way analysis of variance with Tukey's correction for multiple testing.

To determine if the increases observed in VPA and TPM uptake in SLC22A8_MDCK II cells could be successfully reversed with alternative OAT inhibitors other than probenecid, TPM was co-incubated with a series of additional OAT3 inhibitors. Uptake of TPM in *SLC22A8*_MDCK II cells (151±3.1%) was reversed in the presence of benzyl penicillin (100µM) to 116±5.5% of control ($p \leq 0.01$). In contrast, incubation with indomethacin (100µM) observed an increase in TPM uptake in *SLC22A8*_MDCK II cells to 182±11% of control values ($p<0.01$). No significant change in TPM uptake was observed in the presence of diclofenac (100µM; *figure 4.23*). A small increase in VPA uptake was seen in the presence of indomethacin (85±20%) compared to uptake in *SLC22A8*_MDCK II cells without indomethacin (65.9±2.7%), but this did not reach statistical significance. Neither benzyl penicillin nor diclofenac had any significant effect on VPA uptake in *SLC22A8*_MDCK II cells (*figure 4.24*) and no significant differences in uptake were observed for other AEDs tested (*figures 4.21 and 4.22).*

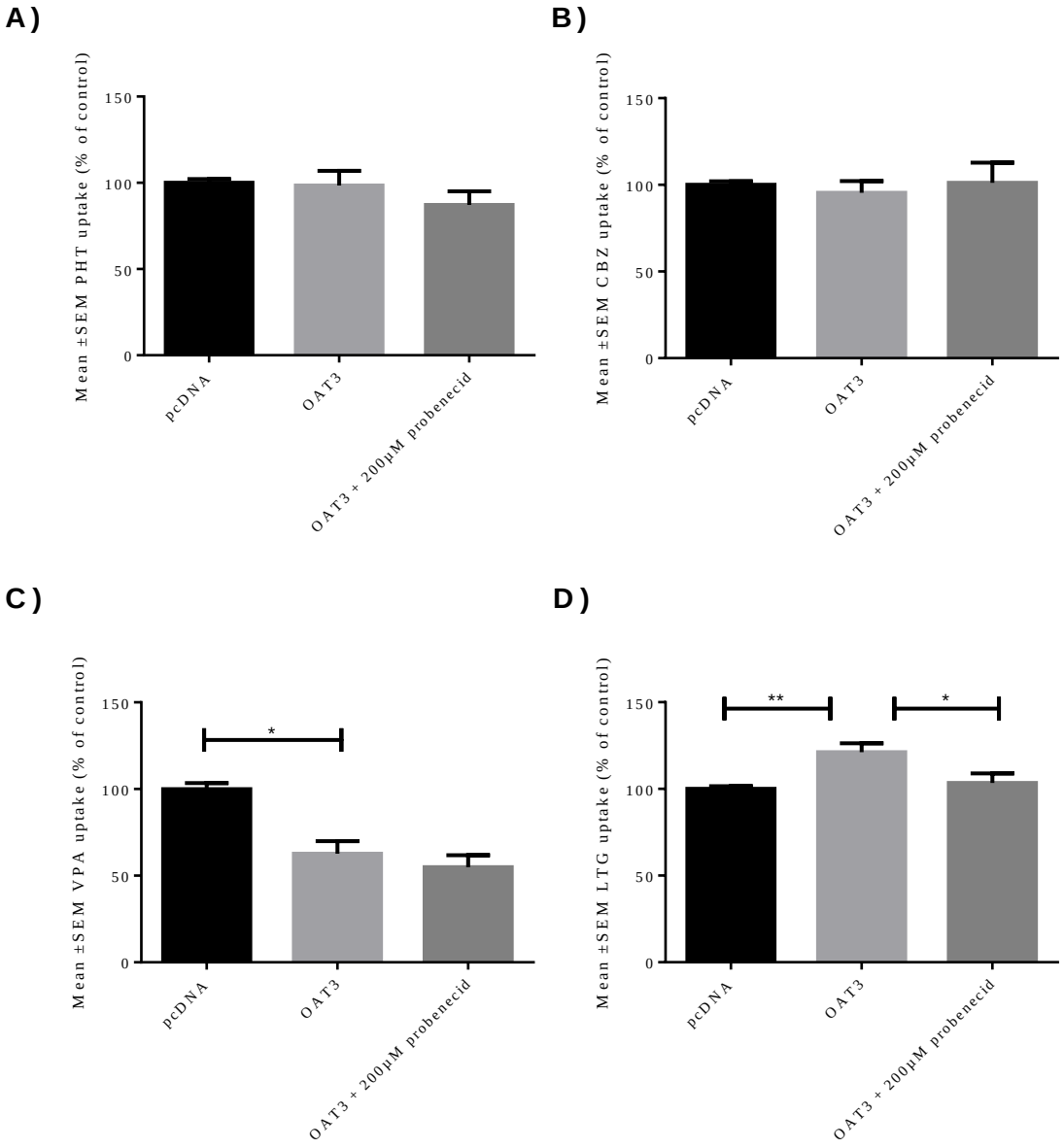

Figure 4.21: Phenytoin (PHT) **(A)**, carbamazepine (CBZ) **(B),** valproic acid (VPA) **(C)** and lamotrigine (LTG) uptake **(D)** into *SLC22A8*_MDCK II cells compared to control pcDNA-transfected MDCK II cells with and without the OAT3 inhibitor probenecid. Cultures were exposed to 25µM radiolabelled PHT, 20µM radiolabelled CBZ, 300µM radiolabelled VPA or 10µM radiolabelled LTG respectively with or without probenecid at 200µM for 40 minutes at 37^0C. Results are expressed as the mean ± standard error of the mean (SEM) percentage of the mean control value of uptake (in pmols/100,000 cells) on each experimental day. Experiments were performed in triplicate on three separate occasions (n=9). Statistical significance (*$p<0.05$, **$p<0.01$,) was determined by one-way analysis of variance with Tukey's correction for multiple testing.

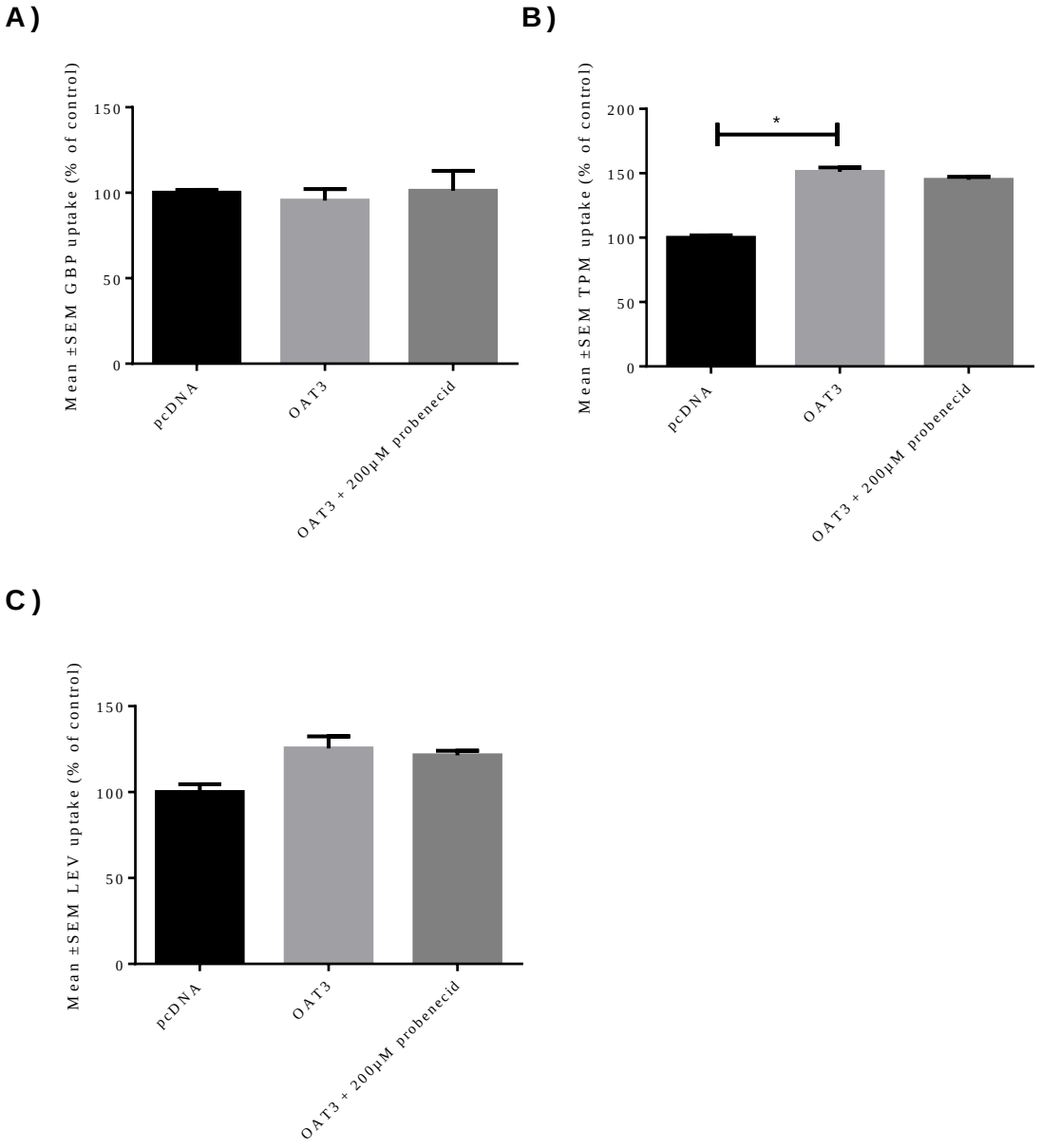

Figure 4.22: Gabapentin (GBP) **(A)**, topiramate (TPM) **(B)** and levetiracetam uptake **(C)** into *SLC22A8*_MDCK II cells compared to control pcDNA-transfected MDCK II cells with and without the OAT3 inhibitor probenecid. Cultures were exposed to 10µM radiolabelled GBP, 10µM radiolabelled TPM or 6µM radiolabelled LEV respectively with or without probenecid at 200µM for 40 minutes at 37^0C. Results are expressed as the mean ± standard error of the mean (SEM) percentage of the mean control value of uptake (in pmols/100,000 cells) on each experimental day. Experiments were performed in triplicate on three separate occasions (n=9). Statistical significance (*$p<0.001$) was determined by one-way analysis of variance with Tukey's correction for multiple testing.

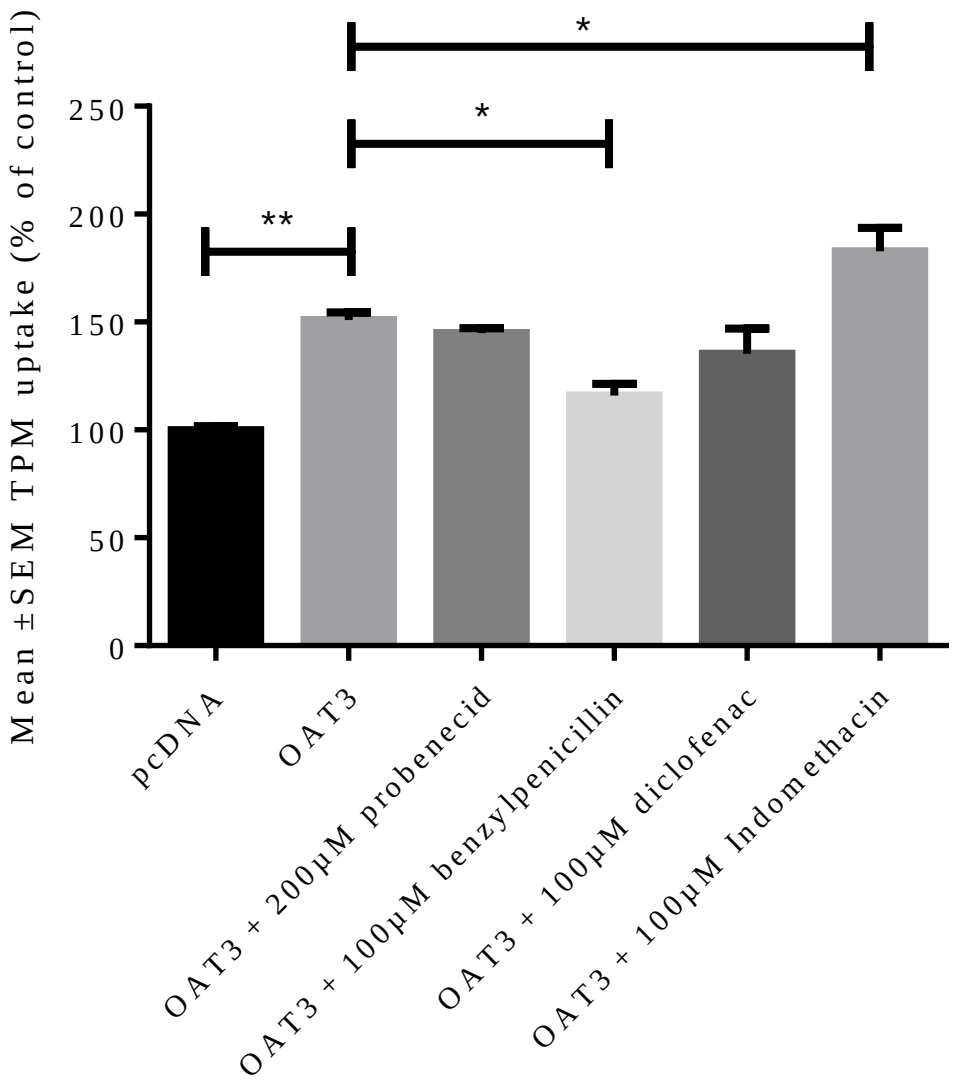

Figure 4.23: Topiramate (TPM) uptake into *SLC22A8*_MDCK II cells compared to control pcDNA-transfected MDCK II cells with and without the OAT3 inhibitors probenecid, benzyl penicillin, diclofenac and indomethacin. Cultures were exposed to 10µM radiolabelled TPM with or without probenecid at 200µM, benzyl penicillin at 100µM, diclofenac at 100µM and indomethacin at 100µM for 40 minutes at 37^0C. Results are expressed as the mean ± standard error of the mean (SEM) percentage of the mean control value of TPM uptake (in pmols/100,000 cells) on each experimental day. Experiments were performed in triplicate on three separate occasions (n=9). Statistical significance (*$p<0.01$, **$p<0.001$,) was determined by one-way analysis of variance with Tukey's correction for multiple testing.

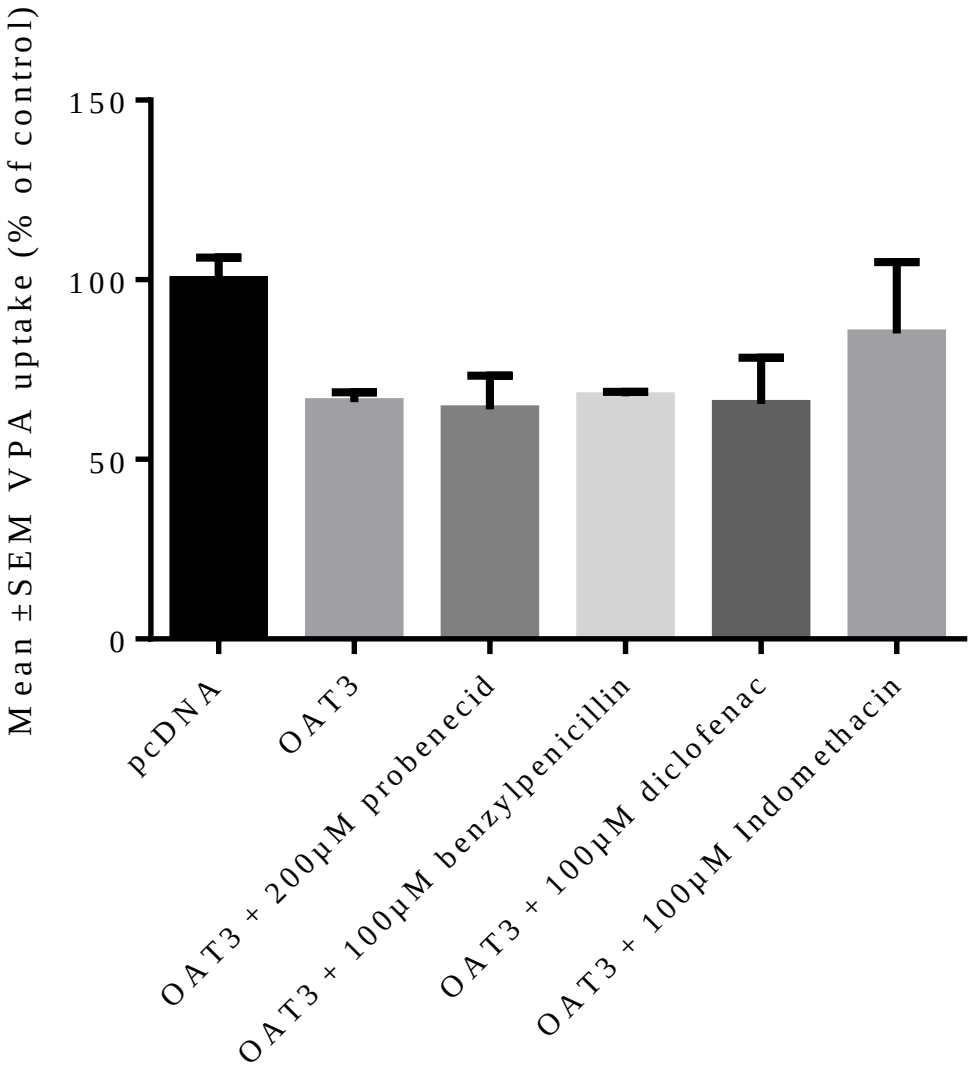

Figure 4.24: Valproic acid (VPA) uptake into *SLC22A8*_MDCK II cells compared to control pcDNA-transfected MDCK II cells with and without the OAT3 inhibitors probenecid, benzyl penicillin, diclofenac and indomethacin. Cultures were exposed to 300µM radiolabelled VPA with or without probenecid at 200µM, benzyl penicillin at 100µM, diclofenac at 100µM and indomethacin at 100µM for 40 minutes at 37^0C. Results are expressed as the mean ± standard error of the mean (SEM) percentage of the mean control value of VPA uptake (in pmols/100,000 cells) on each experimental day. Experiments were performed in triplicate on three separate occasions (n=9).

4.4 Discussion

OAT transporters are a well-researched family of SLC transporters implicated in the disposition of a number of therapeutic agents. The majority of research into OAT transporters has focused on their function at kidney proximal tubule cells, where they are known to mediate the rate limiting step in the renal clearance of a number of drugs. Recently, OAT1 and OAT3 have been suggested to be expressed at the BBB, where they could potentially impact on substrate drug penetration into the brain (Kusuhara *et al.*, 1999; Ohtsuki *et al.*, 2002; Kikuchi *et al.*, 2003; Mori *et al.*, 2003).

In this study, commercially available *SLC22A6*, *SLC22A7* and *SLC22A8* cDNA clones were purchased, sub-cloned and transfected into MDCK II cells to generate stably transfected *SLC22A6*_MDCK II, *SLC22A7*_MDCK II and *SLC22A8*_MDCK II cell lines. Unfortunately, numerous attempts to amplify the *SLC22A7* template from the I.M.A.G.E. cDNA clone were unsuccessful *(figure 4.2).* Upon further investigation and troubleshooting, the *SLC22A7* template present in the I.M.A.G.E. cDNA clone was found to be truncated. An alternative cDNA clone was offered by the suppliers; however, upon examination, this contained a single missing base pair. The impact of the deletion upon the amino acid translated was investigated to determine if the coding sequence with the missing base would produce functional OAT2 protein, however the deletion was found to be crucial in the translation of functional OAT2. With no further *SLC22A7* I.M.A.G.E. clones available, the decision was made to abandon *SLC22A7* cloning attempts and continue with *SLC22A6* and *SLC22A8* only.

SLC22A6 and *SLC22A8* genes were successfully amplified and cloned into pcDNA3.1/V5-His TOPO. Resulting plasmid DNA was transfected into MDCK II cells and clones selected and analysed at gene and protein level to confirm *SLC22A6* and *SLC22A8* expression (*figures 4.8 and 4.9).* In addition, protein function in the selected clones was analysed by uptake studies using a radiolabelled substrate (*figure 4.8 and 4.9*). The *SLC22A6*_MDCK II and *SLC22A8*_MDCK II clones with the most pronounced *SLC22A6* and *SLC22A8* expression and protein function were then selected and their transport kinetics characterised using a probe substrate to determine assay conditions for further investigation with AEDs.

*SLC22A6*_MDCK II cells exhibited a significantly enhanced ability to transport the respective probe substrate PAH in comparison to the mock transfected control cells

(*figure 4.11*). *SLC22A8*_MDCK II cells also showed an increase in the transport of the respective probe substrate E3S compared to control cells, albeit with a much less impressive elevation than that seen with *SLC22A6* (*figure 4.14*). This was at least partly explained by the lower relative gene expression in *SLC22A8*_MDCK II cells compared to *SLC22A6*_MDCK II cell clones, suggesting that *SLC22A8* transfection may not have been as efficient as that of *SLC22A6* or that MDCK II cells may not have translated the OAT3 protein as efficiently as OAT1.

Transport of VPA was significantly higher in *SLC22A6*_MDCK II and significantly lower in *SLC22A8*_MDCK II cells than in control mock transfected MDCK II cells (*figure 4.17 ad 4.21*). This finding is in agreement with previous literature suggesting that VPA is transported by an anion transporter (Adkinson *et al.*, 1996), and perhaps suggests that VPA transport is mediated by the combined action of OAT1 and OAT3. Although speculative, there is some pharmacological precedence for this conclusion. In *in vitro* studies using HEK293 cells stably transfected with *SLC22A6* and *SLC22A8* and also *in vivo* studies in rats, the transport of the fibrate compound gemcabene and also that of the angiotensin-converting enzyme inhibitor quinapril was shown to be dependent on both OAT1 and OAT3 (Yuan *et al.*, 2009). It has been suggested that OAT1 and OAT3 work in synergy at the kidney to transport anionic drugs from the blood into the kidney proximal tubule (Chennavasin *et al.*, 1979). It is possible that OAT1 and OAT3 may work in a similar manner to transport anionic drugs across the BBB. However VPA uptake was observed to decrease in *SLC22A8*_MDCK II cells, suggesting VPA is effluxed from the cell. VPA was the only AED tested in which an unexpected decrease in uptake was observed in *SLC22A8*_MDCK II cells. Although it is possible that the human OAT3 protein may be orientated in MDCK II cells to function as an efflux rather than influx transporter, this effect would certainly extend across all AEDs tested? As both LTG and TPM uptake increased in *SLC22A8*_MDCK II cells it is, although not impossible, unlikely that OAT3 could function to influx some substrates and efflux others in *SLC22A8*_MDCK II cells. OAT transporters function to transport extracellular anions in a tertiary active transport mechanism which involves the exchange of intracellular anions (Van Wert *et al*., 2010). The intracellular anion preferred by OAT1 and OAT3 is the dicarboxylate α-ketoglutarate (Rizwan *et al*., 2007; Burckhardt, 2012). However under stress such as that cells are exposed to during the transfection process, the metabolic rate of the cells may decrease and therefore the synthesis of α-ketoglutarate may decrease, forcing the transporters to utilise alternative

sources of intracellular anions. VPA also has a dicarboxylate structure. Therefore the observed decrease in VPA uptake in *SLC22A8*_MDCK II cells could alternatively be explained by intracellular VPA being utilised as the exchange anion in its own uptake and therefore actively pumped out of the cell at a higher rate than its uptake to maintain a higher extracellular anion concentration.

The decrease in VPA uptake in *SLC22A8*_MDCK II cells compared to mock-transfected controls was not reversed in the presence of OAT inhibitor probenecid, nor was it significantly attenuated by additional OAT inhibitors, including benzyl penicillin, indomethacin and diclofenac (*figure 4.24*). This suggests that at the concentrations used these OAT inhibitors do not inhibit VPA transport.

LTG transport also increased in both *SLC22A6*_MDCK II cells and *SLC22A8*_MDCK II cells when expressed as a percentage of transport in control cells. This effect was attenuated in the presence of the OAT inhibitor probenecid; although the reversal only reached statistical significance in *SLC22A8*_MDCK II cells (*figures 4.17 and 4.21*). Recently, LTG has been shown to be subject to OCT1 mediated transport (Dickens *et al.*, 2012). LTG transport in both mock transfected MDCK II cells and *SLC22A6*_MDCK II cells was significantly inhibited in the presence of the OCT inhibitor verapamil (*figure 4.19*). As MDCK II cells are derived from canine kidney it is likely that there is endogenous expression of canine cation transporters, if these canine transporters are homologous to human OCT1 it is possible that LTG is being actively transported into MDCK II cells, which would explain the indiscriminate inhibitory effect of verapamil. Furthermore, the selection process, irrespective of whether it introduced a functional gene or not, may have induced a compensatory increase in the expression of endogenous transporter proteins in *SLC22A6*_MDCK II cells therefore the 47% increase in uptake of LTG in *SLC22A6*_MDCK II cells may be attributed to increased expression of an endogenous canine OCT transporters in these cells. However, LTG was also shown to inhibit PAH uptake in the *SLC22A6*_MDCK II cells with an IC_{50} of 32.9µM (*figure 4.20*), suggesting that it acts as a weak inhibitor of OAT1 at concentrations just above the therapeutic range. Recently, it has been shown that the mouse homologues of OAT1 and OAT3 mediate the transport of a number of organic cations including verapamil (Ahn *et al.*, 2009). Assuming this is also the case for human OATs, this may offer an alternative explanation for the increase in LTG transport observed in both *SLC22A6*_MDCK II cells and *SLC22A8*_MDCK II cells.

Thus LTG transport into *SLC22A6*_MDCK II and *SLC22A8*_MDCK II cells could be attributed to combined activity of an endogenous OCT transporter and human OAT1 or OAT3 respectively. Providing the endogenous OCT transporter could be identified, this hypothesis could be tested by using siRNA to 'knock down' the canine OCT transporter in MDCK II cells (both mock transfected controls and OAT transfected) and comparing any differences in LTG uptake.

Uptake of TPM in *SLC22A8*_MDCK II cells (but not *SLC22A6*_MDCK II cells) was also significantly increased compared to uptake in the corresponding mock transfected cells (*figure 4.22*). Although this effect was not diminished in the presence of probenecid, it was attenuated in the presence of the OAT inhibitor benzyl penicillin and conversely enhanced in the presence of indomethacin (*figure 4.23*). Without more detailed understanding of the relative contributions of individual OATs to cellular transport and of the selectivity of individual inhibitory compounds, it is difficult to arrive at a plausible explanation for the effects seen with TPM. The effects observed with benzylbpenicllin may suggest inhibition of OAT3 mediated uptake of TPM which could not be achieved with probenecid, potentially due to differences in inhibitory potency of the two compounds. Conversely the effects observed with indomethacin may be due to activity of an endogenous efflux transporter. In addition to OATs indomethacin is known to inhibit efflux transporters known as multidrug resistance proteins (MRPs) (Draper *et al*., 1997). MRP transporters are known to be expressed in the human kidney where they contribute to the transport of renally cleared substrate drugs (Inui *et al*., 2000). Therefore assuming the transporter expression profile is similar in canine kidney and providing TPM is a substrate for a canine MRP transporter, the increases in TPM uptake observed in the presence of indomethacin may be attributed to inhibition of MRP mediated efflux of TPM. Although plausible, without analysing the effects of indomethacin on TPM transport in mock transfected MDCK II cells this hypothesis is speculative.

A number of experimental systems can be used to investigate functionality of transporter proteins *in vitro*, including the X.*laevis* oocyte model employed to investigate AED transport by MCT1 and OATP1A2 in chapter 2 and epithelial/endothelial cell lines transiently or stably transfected with the transporter of interest. The use of transfected epithelial cell lines overexpressing a transporter protein represents a robust method to identify and characterise the individual proteins

responsible for the transport of therapeutic agents. Stable transfection was chosen over transient transfection for this investigation as the planned studies required the long term cell culture of transfected cell lines for use in an extended series of drug transport assay. Transient transfection would have risked potential loss of expression of the protein of interest over prolonged culture and a significant impact on results (Kim *et al.*, 2010). However, it is unknown what impact the stable transfection and subsequent clone selection process had on the expression profile of the native cell line. Introducing a large sequence of foreign DNA into the host genome may have caused changes in expression of endogenous genes, including transporters. Furthermore clonal selection involves and may in part explain the differences in transport data observed with LTG in *SLC22A6*_MDCK II cells.

Observations made in this chapter suggest that OAT1 and/or OAT3 may be, at least partly responsible for the transport of several AEDs in stably transfected *SLC22A6* and *SLC22A8* MDCK II cells. Although significant increases/decreases in the uptake of these AEDs was observed, the conclusions are constrained by the inability to reliably inhibit this transport with the prototypic OAT inhibitor probenecid. Further attempts to inhibit transport with additional OAT inhibitors gave conflicting results.
It is difficult to speculate why observed changes in AED transport could not be inhibited to a similar degree as observed with the inhibition of the positive control substrates PAH and E3S (*figures 4.11 and 4.14*; table 4.2 and 4.3). One explanation is that there is interference of endogenous transporters, either constitutively expressed or induced by the pressures of the transfection and selection process. Therefore there may be a number of active processes occurring in the cells contributing to both influx and efflux of AEDs therefore producing ambiguous results in terms of inhibitor selectivity. The impact of the selection process on endogenous transporter expression could be analysed by qRT-PCR to determine any increases/decreases in transporter expression, however this would rely on identifying the canine transporters endogenously expressed in MDCK II cells. Alternatively the results obtained using stably transfected *SLC22A6*_MDCK II and *SLC22A8*_MDCK II cells which underwent clonal selection could be compared to data generated in transiently transfected *SLC22A6* and *SLC22A8* MDCK cells and the impact of the selection process determined.

Chapter 5

Changes in transporter expression at the BBB following antiepileptic drug treatment

5.1 Introduction

Over the past 15 years, knowledge of transporters has grown rapidly and a number of well-characterised transporters have now been detected at the blood-brain barrier (BBB) and have been shown to affect accumulation of therapeutic agents in the brain.

Several studies have aimed to determine the expression profile of transporters at the BBB (Dauchy *et al.*, 2009; Carl *et al.*, 2010; Uchida *et al.*, 2011; Geier *et al.*, 2013). One approach evaluated the BBB expression of a panel of transporters from the SLC and ABC families using qRT-PCR arrays in human cerebral microvascular endothelial cells (hCMEC/D3), which have been proposed as a useful *in vitro* model of the BBB Expression of 70 out of 84 transporters included were observed in this analysis, which also showed a high relative expression of several transporters known to efflux a number of therapeutic agents including: *ABCB1* (P-gp), *ABCC1* (MRP1), *ABCC4* (MRP4) and *ABCC5* (MRP5). Of the SLC transporters evaluated, significant expression of the monocarboxylic acid transporters *SLC16A1* and *SLC16A3* and the equilibrative nucleoside transporters (*SLC29* family) was observed. However very few transporters, known to be clinically relevant in drug disposition such as the transporters belonging to the *SLCO* and *SLC22* families were detected (Carl *et al.*, 2010). More recently, the expression of SLC and ABC transporters was investigated in enriched human brain microvessels (BMVs) and showed that the BBB is rich and diverse in expression of both ABC and SLC transporters. Expression of 244 out of 344 SLC transporters included and 42 out of 49 ABC transporters included was detected in BMVs, a number of which had not previously been shown to be expressed at the BBB. These included the multifunctional anion exchangers of the *SLC26* family, the thiamine transporter *SLC19A3*, the GABA neurotransmitter transporter *SLC6A13* and the multidrug and toxin extrusion (MATE2) transporter *SLC47A2* (Geier *et al.*, 2013). In addition quantitative protein expression utilising a proteomics approach investigated transporter expression in human BMVs and reported highest expression of *ABCG2* (BCRP), while expression of *ABCB1* (P-gp) was less abundant in humans than previously reported in mice (Kamiie *et al.*, 2008). Interestingly, members of the multidrug resistance-associated proteins (MRPs), organic anion transporters (OATs) and organic anion transporting polypeptides (OATPs) were below quantification limits in this analysis, with the exception of MRP4 (Uchida *et al.*, 2011).

The transporter hypothesis aims to explain resistance to AEDs as a result of changes in expression of transporters at the BBB. Research surrounding the transporter hypothesis has focused on the role of transporters in brain penetration of substrate AEDs; however the role of transporter regulation and its implications in multidrug resistance has also received attention and has produced conflicting results.

There is existing evidence which supports changes in brain transporter expression in people with epilepsy (Lauritzen *et al.*, 2011; Leroy *et al.*, 2011; Aronica *et al.*, 2012). Different mechanisms have been postulated and investigated to explain these differences in expression; however what is not clear, and which remains disputed, is whether the difference in transporter expression is intrinsic or acquired. That is to say, are the changes in BBB transporter expression due to the underlying pathology, the consequence of uncontrolled seizures, the result of chronic AED treatment or a combination of all of these factors (Aronica *et al.*, 2012)? Supporters of an intrinsic mechanism argue that increased expression of transporters such as P-gp is present before the onset of seizures and the institution of AED treatment and therefore is a result of disease pathophysiology. Malformations of cortical development (MCDs) are known to be a common cause of refractory epilepsy, with most people who have MCDs going on to develop the disease. As such, people with MCDs could be considered to be 'pre-epileptic'. The expression of P-gp was investigated in brain tissue from AED naive people and found an overexpression of P-gp in 10 out of 16 MCD samples analysed compared to 2 out of 16 controls, supporting an intrinsic difference in transporter expression in those individuals (Sisodiya *et al.*, 1999).

The arguments for an intrinsic mechanism are opposed by the ability of various AEDs to induce the expression of a number of transporters. A recent study investigating P-gp expression in the rat brain, demonstrated that changes in P-gp activity could be monitored *in vivo* by measuring the brain to plasma ratio of the P-gp substrate rhodamine 123. A decrease in the brain concentration of rhodamine 123 was observed, suggesting increased P-gp activity, following chronic (21 day) treatment with PHT, phenobarbital (PB) and CBZ. In addition, immunohistochemistry showed that P-gp was localised mainly to brain endothelial cells in both cortex and hippocampus (Wen *et al.*, 2008). Furthermore, P-gp expression has been investigated in mouse brain utilising a radiolabelled P-gp substrate, ^{11}C-desmethylloperamide. The authors' analysed

concentrations of this ligand in control mouse brain *in vivo* compared to mice pre-treated with therapeutic and supra-therapeutic doses of LEV, TPM, PHT and VPA. A decrease in cerebral ^{11}C-desmethylloperamide concentration was observed in mice pre-treated with therapeutic doses of LEV, TPM and PHT but not VPA, suggesting induction of P-gp with selected AEDs. However, at supra-therapeutic doses, there was no difference in the brain concentration of ^{11}C-desmethylloperamide between pre-treated and control mice, suggesting that induction of P-gp by AEDs is dose-dependent (Moermana *et al.*, 2011).

Investigation into changes in the brain expression of P-gp in epilepsy has received more attention to date than studies of other transporters. Nevertheless, several studies have investigated changes in the expression of influx transporters of the SLC family in both animal models of epilepsy and human epilepsy tissue. As discussed in chapter 3 MCT1 was found to be deficient on cerebral microvessels in surgically resected brain tissue from people with AED resistant temporal lobe epilepsy (Lauritzen *et al.*, 2011). Conversely, up- regulation of the BBB glucose transporters GLUT1 *(SLC2A1)* and GLUT3 (*SLC2A3*) and the monocarboxylic acid transporters MCT1 *(SLC16A1)* and MCT2 *(SLC16A2)* was observed in a lithium-pilocarpine induced rat model of temporal lobe epilepsy (Leroy *et al.*, 2011).

Investigations described in this chapter employed the hCMEC/D3 cell line and a commercially available human transporter qRT-PCR array to investigate the expression profile of a panel of human transporters in an *in vitro* model of the BBB. The effects of AED treatment on transporter expression were determined following a 48 hour exposure with seven commonly prescribed AEDs employed throughout this thesis.

5.2 Methods

5.2.1 Materials

Taqman Human Transporter Gene Array Plates, Taqman Gene Expression Master Mix, High Capacity cDNA Reverse Transcription Kit, rat tail collagen type I, chemically defined lipid concentrate and foetal bovine serum (FBS) were purchased from Life Technologies (Paisley, UK). Cell culture plasticware was purchased from Nunc Fisher Scientific (Loughborough, UK). EBM-2 medium was purchased from Lonza (Slough, UK). PHT, CBZ, VPA, LTG, GBP, TPM, LEV and all other chemicals not described were purchased from Sigma-Aldrich (Poole, Dorset, UK). The hCMEC/D3 cell line was provided courtesy of Dr Ignacio Romero (Department of Life Sciences, The Open University, Milton Keynes, UK) and Professor Pierre Couraud (Institut Cochin, Université Paris Descartes, Paris, France).

5.2.2 Cell culture

hCMEC/D3 cells were cultured in rat tail collagen type I (100ug/ml) coated T175 flasks and maintained in EBM-2 medium supplemented with 5% FBS, 1% penicillin-streptomycin, 0.5% chemically defined lipid concentrate, 10mM HEPES, 1.4µM hydrocortisone, 5µg/ml ascorbic acid and 1ng/ml basic fibroblast growth factor (referred to as complete media from here on). Cells were passaged every 2-3 days and seeded onto collagen type I coated six-well plates at a density of $3x10^6$cells/well, as required. The passage/seeding procedure was as follows; media was removed from the T175 flasks using a serological pipette and cells washed twice in 10ml of warm Hanks balanced salt solution (HBSS). Cells were then removed from the flask surface with 10ml of 0.25% trypsin-EDTA and left to incubate at 37^0C for 5 minutes. Thereafter, 20ml of complete media was added to neutralise the trypsin, and the cell suspension transferred to a 50ml Falcon tube and centrifuged at 250 x *g* for 5 minutes to pellet the cells. Pellets were re-suspended in 10ml of complete media and a cell count made (see section 3.2.4 for protocol). The cell suspension was diluted with complete media to give a density of $1.5x10^6$cells/ml and 2ml of the suspension added to each well. The remainder of the suspension was returned to three T175 flasks at a 1 in 5 dilution and allowed to grow on.

5.2.3 MTT Assays

An MTT reduction assay was used to determine if therapeutic concentrations of PHT, CBZ, VPA, LTG, GBP, TPM and LEV elicit any cytotoxicity. Each AED included in the study was assessed for 24, 48 and 72 hours in triplicate at the following concentrations: 1µM, 3µM, 10µM, 30µM and 100µM, with the exception of VPA, which was assessed at the following concentrations: 10µM, 30µM, 100µM, 300µM and 1000µM.

Firstly, hCMEC/D3 cells were passaged as described in section 5.2.2, counted (see section 3.2.4 for cell count protocol) and diluted to give a density of 0.5×10^6 cells/ml. A 50µl aliquot of the cell solution was then transferred to each well of a 96 well flat bottom plate and allowed to incubate for 30 minutes at 37^0C. Each AED solution (AED stock solutions were made up at 1000x final concentration in DMSO) and DMSO controls were then diluted in complete media at double the desired final concentrations and 50µl was added to the appropriate wells. Media plus 0.1% DMSO was added to three wells per time point to act as blanks. Plates were then incubated at 37^0C for 24, 48 and 72 hours. After 24, 48 or 72 hours incubation 20µl of 5M 3-(4,5-dimethylthiazol-2-yl)-2,5-diphenyltetrazolium bromide (MTT) solution (5mg of MTT in 1ml HBSS) was added to each well and incubated at 37^0C for 2 hours. A 200µl aliquot of lysis buffer (20g sodium dodecyl sulphate in 50:50 dimethylformamide:water) was then added to each well and incubated for a minimum of 4 hours in darkness. Fluorescence was then measured on a microplate reader at 570nm.

5.2.4 AED treatment of hCMEC/D3 cells

hCMEC/D3 cells were seeded onto 6 well plates as described previously in section 5.2.2 and incubated with AEDs at concentrations similar to those observed clinically in patient serum (PHT 25µM, CBZ 20µM, VPA 300µM, LTG 10µM, GBP 60µM, TPM 10µM and LEV 90µM) for 48 hours. Control, non AED treated cells were incubated with vehicle (DMSO; 0.1%) only.

5.2.5 RNA extraction

After 48 hours incubation, RNA from AED treated and control hCMEC/D3 cells was extracted using Trizol reagent according to the manufacturer's protocol, as described in section 4.2.11. The resulting RNA was quantified on a Nanodrop spectrophotometer (see section 2.2.3 for protocol) and diluted to a concentration of 200ng/µl with PCR grade water for subsequent reverse transcription.

5.2.6 Reverse transcription to cDNA

RNA extracted from AED treated and control hCMEC/D3 cells was reverse transcribed to its corresponding cDNA using High Capacity cDNA Reverse Transcription reagents (Life technologies) according to the manufacturer's protocol, as described in section 4.2.12.

5.2.7 qRT-PCR

qRT-PCR was performed using human transporter TaqMan Array 96-well plates and Taqman Gene Expression Mastermix according to the manufacturer's protocol. Briefly, cDNA and gene expression mastermix were added to RNase and DNase free, 1.5ml Eppendorf tubes to give a volume sufficient for 96 x 20µl reactions. Each tube was then gently vortexed to mix the solution, centrifuged briefly and kept on ice. In parallel, Taqman array plates were centrifuged briefly and the plate seal removed. A 20µl aliquot of the cDNA plus master mix solution was then added to each well of the 96 well of an array plate. 8 array plates in total were prepared for each condition (control (DMSO; 0.1%) and seven AEDs at concentrations described previously). Plates were then covered with an optical adhesive seal, briefly centrifuged and kept at 4^0C before loading into the instrument. Thermal cycling conditions were as follows: 50^0C for 2 minutes, 95^0C for 10 minutes followed by 40 PCR cycles of 95^0C for 15 seconds and 60^0C for 1 minute.

5.2.8 qRT-PCR Analysis

Ct values calculated from the amplification curve generated by Amplicon 3 software were normalised to the mean Ct of 3 housekeeping genes (*GAPDH* (glyceraldehyde 3-phosphate dehydrogenase), *HPRT1* (hypoxanthine phosphoribosyltransferase) and *GUSB* (beta-glucuronidase) and the relative abundance or expression presented according to the comparative Ct method of calculation:

$$2^{-\Delta CT} = [(C_T \text{ gene of interest} - C_T \text{ internal control})$$

$$2^{-\Delta\Delta CT} = [(C_T \text{ gene of interest} - C_T \text{ internal control}) \text{ sample A} - (C_T \text{ gene of interest} - C_T \text{ internal control}) \text{ sample B}]$$

5.2.9 Statistical analysis

MTT assay data was assessed for normality using the Shapiro-Wilk test and found to be normally distributed in all cases. A one-way analysis of variance (ANOVA) was performed on the data with Tukey's post hoc test for multiple comparisons. A value of $p \leq 0.05$ was taken to indicate statistical significance. Gene expression data from quantitative RT-PCR analysis was generated at n=1 therefore statistical analysis could not be applied. Instead any changes in expression that were observed and that represented a more than two fold difference from control were taken to be of potential importance.

5.3 Results

5.3.1 Effects of increasing AED concentration on hCMEC/D3 cell viability

To evaluate possible cytotoxic effects of the AEDs investigated, an MTT reduction assay was performed. Cytotoxicity was observed following 48 hours and 72 hours treatment with 100µM PHT, with hCMEC/D3 cell viability reduced to 73.4 ±4.1% ($p \leq 0.05$) and 70.0 ±9.8% of control values (100 ±5.5% and 100 ±7.2), respectively (*figure 5.1*). Cytotoxicity was also observed following 48 hours and 72 hours treatment with 100µM CBZ, with hCMEC/D3 cell viability reduced to 75.2 ±1.65% and 77.5 ±5.16% respectively, however only the 48 hour treatment time reached statistical significance (*figure 5.1*). No significant cytotoxicity was observed with lower concentrations of PHT or CBZ at any of the time points investigated (*figure 5.1*). Cell viability in hCMEC/D3 cells also decreased following 72 hours treatment with 100µM LTG (71.4 ±6.2%) compared to control (100 ±7.2%), however did not reach statistical significance (*figure 5.2*). No significant cytotoxicity was observed within the test concentration range for other AEDs following incubation of up to 72 hours (*figures 5.2-5.4*).

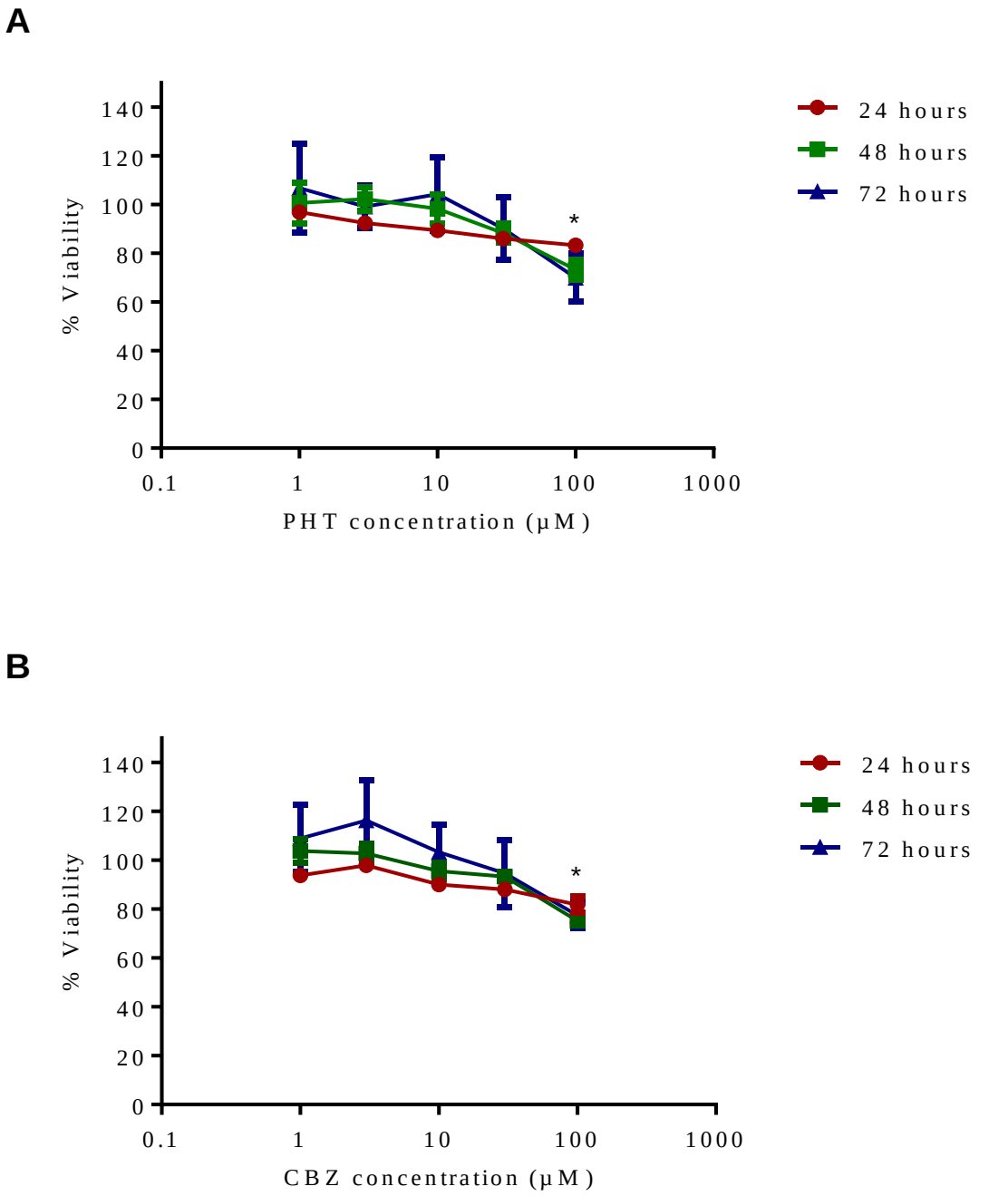

Figure 5.1: Effects of **(A)** phenytoin (PHT) and **(B)** carbamazepine (CBZ) on hCMEC/D3 cell viability. Cultures were exposed to 1µM, 3µM, 10µM, 30µM and 100µM PHT or CBZ for 24, 48 and 72 hours at 37^0C and cell viability determined by MTT reduction assay. Results are expressed as the mean percentage ± standard error of the mean (SEM) of mean control viability, as determined in hCMEC/D3 cells incubated with 0.1% DMSO only. Experiments were performed in triplicate for each time point, with statistical differences from control explored using one-way analysis of variance with Tukey's correction for multiple testing (*$p<0.05$ for 100uM PHT and CBZ at 48h incubation and 100 uM PHT at 72h incubation).

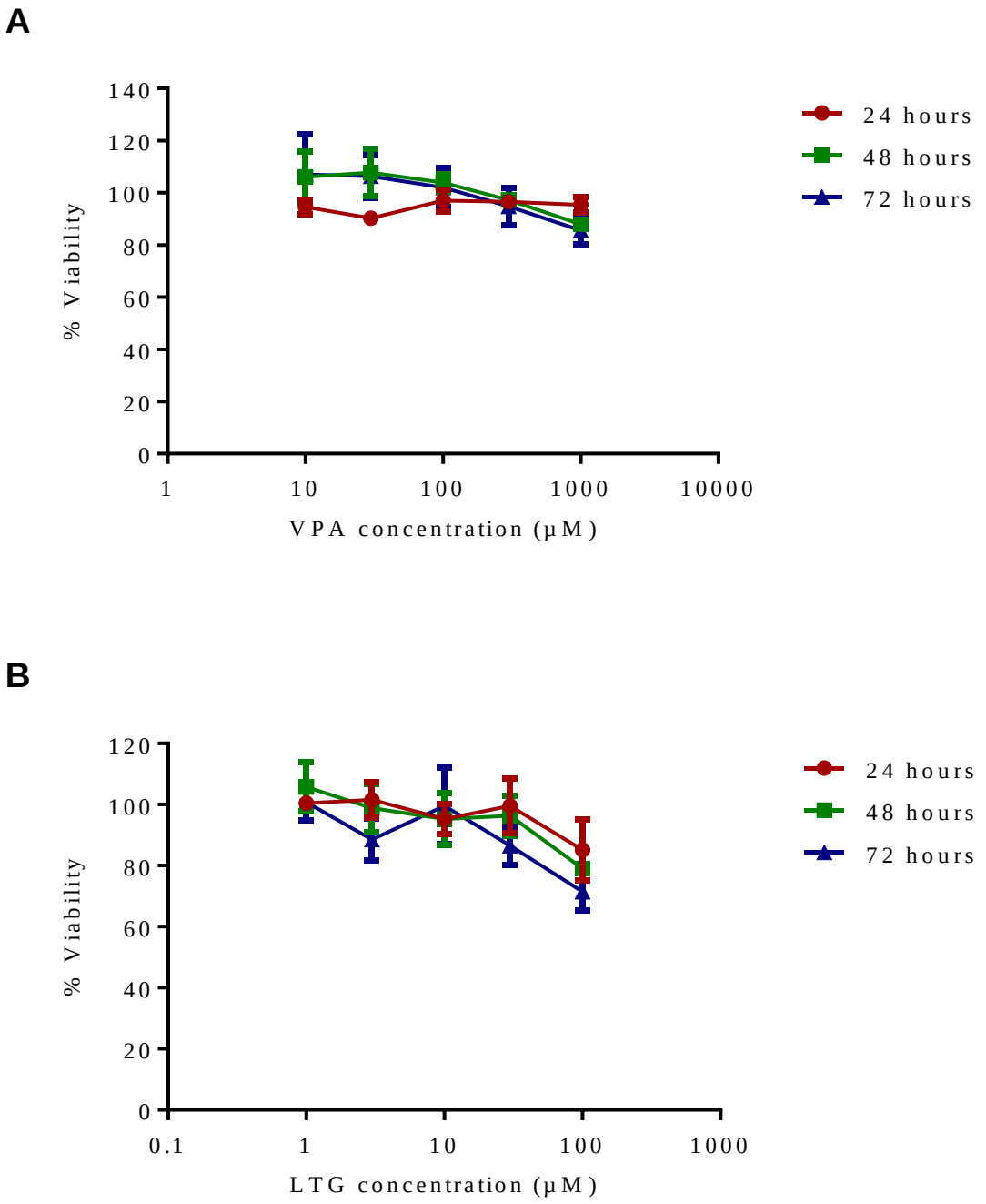

Figure 5.2: Effects of **(A)** valproate (VPA) and **(B)** lamotrigine (LTG) on hCMEC/D3 cell viability. Cultures were exposed to 10µM, 30µM, 100µM, 300µM and 1000µM VPA or 1µM, 3µM, 10µM, 30µM and 100µM LTG for 24, 48 and 72 hours at 37^0C and cell viability determined by MTT reduction assay. Results are expressed as the mean percentage ± standard error of the mean (SEM) of mean control viability, as determined in hCMEC/D3 cells incubated with 0.1% DMSO only. Experiments were performed in triplicate for each time point, with statistical differences from control explored using one-way analysis of variance with Tukey's correction for multiple testing.

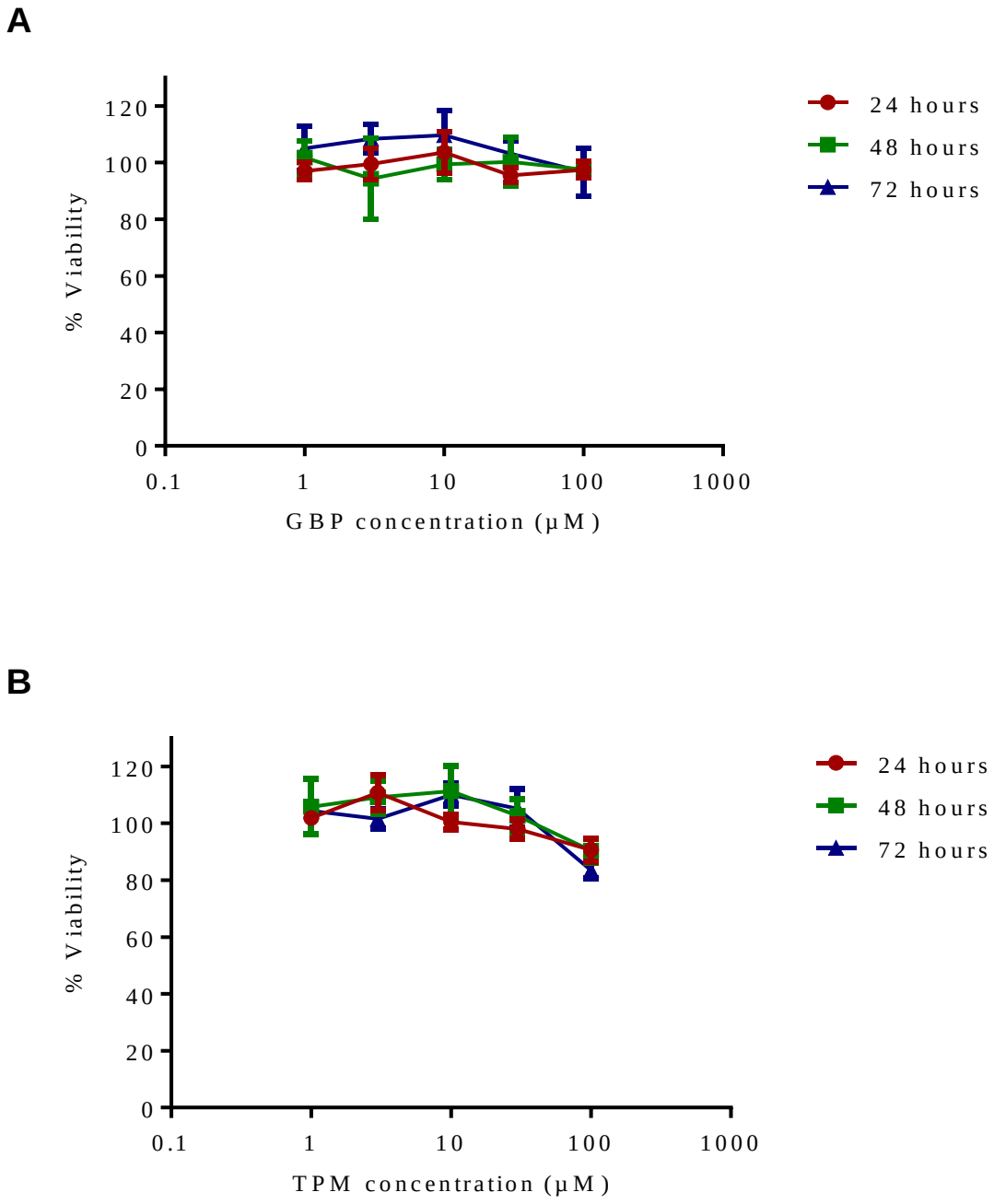

Figure 5.3: Effects of **(A)** gabapentin (GBP) and **(B)** topiramate (TPM) on hCMEC/D3 cell viability. Cultures were exposed to 1µM, 3µM, 10µM, 30µM and 100µM GBP or TPM for 24, 48 and 72 hours at 37^0C and cell viability determined by MTT reduction assay. Results are expressed as the mean percentage ± standard error of the mean (SEM) of mean control viability, as determined in hCMEC/D3 cells incubated with 0.1% DMSO only. Experiments were performed in triplicate for each time point, with statistical differences from control explored using one-way analysis of variance with Tukey's correction for multiple testing.

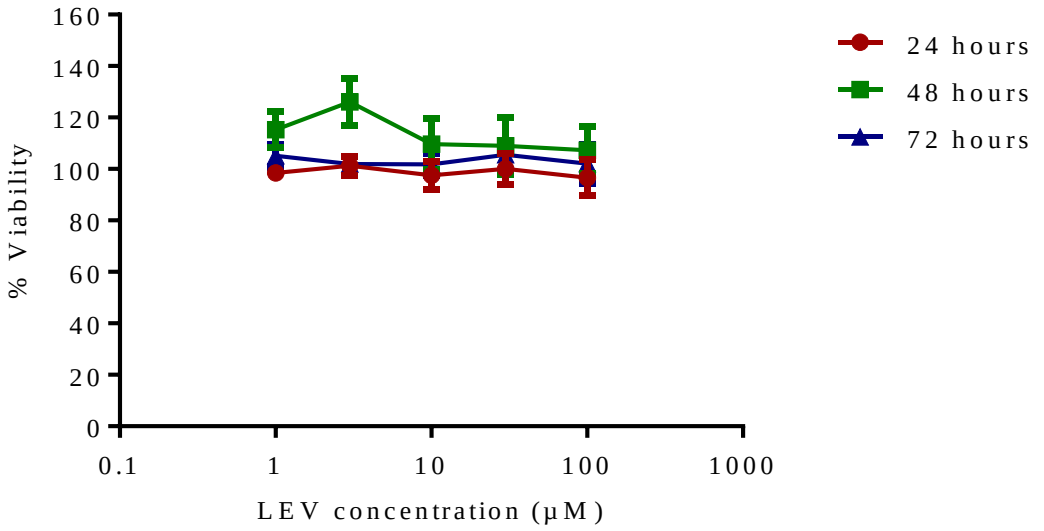

Figure 5.4: Effects of levetiracetam (LEV) on hCMEC/D3 cell viability. Cultures were exposed to 1µM, 3µM, 10µM, 30µM and 100µM LEV for 24, 48 and 72 hours at 37^0C and cell viability determined by MTT reduction assay. Results are expressed as the mean percentage ± standard error of the mean (SEM) of mean control viability, as determined in hCMEC/D3 cells incubated with 0.1% DMSO only. Experiments were performed in triplicate for each time point, with statistical differences from control explored using one-way analysis of variance with Tukey's correction for multiple testing.

5.3.2 Expression of human transporter protein genes in hCMEC/D3 cells

Of the 84 transporters included in this analysis, 57 were found to be expressed in hCMEC/D3 cells (table 5.1, 5.2 and 5.3). The transporters with the highest relative abundance (defined as higher abundance than the mean abundance of three housekeeping genes (1)) were largely nutrient transporters including: *SLC16A3* (monocarboxylate transporter 4: 1.385), *SLC2A1* (facilitative glucose transporter 1; 1.157) and *SLC7A5* (large neutral amino acid transporter; 1.753) (table 5.2). High relative expression of *ATP6* (lysosomal ATPase transporter; 7.890), *MVP* (major vault protein; 1.165) and *VDAC1* (voltage dependant anion channel 1; 1.815) was also detected (table 5.3). No expression was detected in control hCMEC/D3 cells for 27 of the test genes included (tables 5.1, 5.2 and 5.3).

Transporter gene	Description	Relative abundance
ABCA1	ATP-Binding Cassette Sub-Family A Member 1 (cholesterol efflux regulatory protein)	0.059
ABCA12	ATP-Binding Cassette Sub-Family A Member 12 (lipid transporter)	0.002
ABCA13	ATP-Binding Cassette Sub-Family A Member 13	0.001
ABCA2	ATP-Binding Cassette Sub-Family A Member 2	0.066
ABCA3	ATP-Binding Cassette Sub-Family A Member 3 (lipid transporter)	0.232
ABCA4	ATP-Binding Cassette Sub-Family A Member 4 (retinal specific: transports retinoid substrates	0.003
ABCA9	ATP-Binding Cassette Sub-Family A Member 9 (lipid transporter)	No Ct
ABCB1	ATP-Binding Cassette Sub-Family B Member 1 (multidrug resistance protein 1 (P-gp))	0.796
ABCB11	ATP-Binding Cassette Sub-Family B Member 11 (bile salt efflux (hepatic))	No Ct
ABCB4	ATP-Binding Cassette Sub-Family B Member 4 (multidrug resistance protein 3)	No Ct
ABCB5	ATP-Binding Cassette Sub-Family B Member 5 (multidrug resistance protein 5)	No Ct
ABCB6	ATP-Binding Cassette Sub-Family B Member 6 (mitochondrial transporter)	0.047
ABCC1	ATP-Binding Cassette Sub-Family C Member 1 (multidrug resistance-associated protein 1)	0.123
ABCC10	ATP-Binding Cassette Sub-Family C Member 10 (multidrug resistance-associated protein 7)	0.058
ABCC11	ATP-Binding Cassette Sub-Family C Member 11 (multidrug resistance-associated protein 8)	No Ct
ABCC12	ATP-Binding Cassette Sub-Family C Member 12 (multidrug resistance-associated protein 9)	No Ct
ABCC2	ATP-Binding Cassette Sub-Family C Member 2 (multidrug resistance-associated protein 2)	0.002
ABCC3	ATP-Binding Cassette Sub-Family C Member 3 (multidrug resistance-associated protein 3)	0.050
ABCC4	ATP-Binding Cassette Sub-Family C Member 4 (multidrug resistance-associated protein 4)	0.064
ABCC5	ATP-Binding Cassette Sub-Family C Member 5 (multidrug resistance-associated protein 5)	0.332
ABCC6	ATP-Binding Cassette Sub-Family C Member 6 (multidrug resistance-associated protein 6)	0.006
ABCD1	ATP-Binding Cassette Sub-Family D Member 1 (adrenoleukodystrophy protein)	0.022
ABCD3	ATP-Binding Cassette Sub-Family D Member 3	0.398
ABCD4	ATP-Binding Cassette Sub-Family D Member 4	0.032
ABCF1	ATP-Binding Cassette Sub-Family F Member 1 (protein translation / ribosome biogenesis)	0.199
ABCG2	ATP-Binding Cassette Sub-Family G Member 2 (breast cancer resistance protein)	0.006
ABCG8	ATP-binding cassette sub-family G member 8 (enterocyte transport of dietary cholesterol)	No Ct

Table 5.1: Abundance of a panel of ABC transporters in hCMEC/D3 cells. Cultures of hCMEC/D3 cells were treated with 0.1% DMSO and incubated for 48 hours at 37^0C. Total RNA was then extracted, reverse-transcribed into cDNA, and the cDNA used to quantify relative expression for each ABC transporter. Mean Ct values obtained from test gene amplification plots were normalised to the mean Ct of three housekeeping genes (*GAPDH*, *HPRT1* and *GUSB*) and are presented as the relative test gene abundance in hCMEC/D3 cells, according to the comparative Ct method.

Transporter gene	Description	Relative abundance
SLC10A1	Solute carrier family 10 member 1 (sodium/bile acid co-transporter)	No Ct
SLC10A2	Solute carrier family 10 member 2 (sodium/bile acid co-transporter)	No Ct
SLC15A1	Solute carrier family 15 member 1 (oligopeptide transporter)	No Ct
SLC15A2	Solute carrier family 15 member 2 (oligopeptide transporter (kidney)	0.004
SLC16A1	Solute carrier family 16 member 1 (monocarboxylic acid transporter 1)	0.401
SLC16A2	Solute carrier family 16 member 2 (monocarboxylic acid transporter 8)	0.013
SLC16A3	Solute carrier family 16 member 3 (monocarboxylic acid transporter 4)	1.385
SLC19A1	Solute carrier family 19 member 1 (folate transporter)	0.321
SLC19A2	Solute carrier family 19 member 2 (high affinity thiamine transporter)	0.064
SLC19A3	Solute carrier family 19 member 3 (high affinity thiamine transporter)	0.018
SLC22A1	Solute carrier family 22 member 1 (organic cation transporter 1)	0.002
SLC22A2	Solute carrier family 22 member 2 (organic cation transporter 2)	No Ct
SLC22A3	Solute carrier family 22 member 3 (organic cation transporter 3)	No Ct
SLC22A6	Solute carrier family 22 member 6 (organic anion transporter 1)	No Ct
SLC22A7	Solute carrier family 22 member 7 (organic anion transporter 2)	No Ct
SLC22A8	Solute carrier family 22 member 8 (organic anion transporter 3)	No Ct
SLC22A9	Solute carrier family 22 member 9 (organic anion transporter 4)	No Ct
SLC25A13	Solute carrier family 25 member 13 (aspartate/glutamate carrier)	0.173
SLC28A1	Solute carrier family 28 member 1 (concentrative nucleoside transporter 1)	No Ct
SLC28A2	Solute carrier family 28 member 2 (concentrative nucleoside transporter 2)	No Ct
SLC28A3	Solute carrier family 28 member 3 (concentrative nucleoside transporter 3)	0.002
SLC29A1	Solute carrier family 29 member 1 (equilibrative nucleoside transporter 1)	0.235
SLC29A2	Solute carrier family 29 member 2 (equilibrative nucleoside transporter 2)	0.013
SLC2A1	Solute carrier family 2 member 1 (facilitated glucose transporter 1)	1.157
SLC2A2	Solute carrier family 2 member 2 (facilitated glucose transporter 2)	No Ct
SLC2A3	Solute carrier family 2 member 3 (facilitated glucose transporter 3)	0.137
SLC31A1	Solute carrier family 31 member 1 (high affinity copper transporter)	0.420
SLC38A2	Solute carrier family 38 member 2 (system N amino acid transporter 2)	0.908
SLC38A5	Solute carrier family 38 member 5 (system N amino acid transporter 5)	0.853
SLC3A1	Solute carrier family 3 member 1 (neutral/dibasic amino acid transporter)	No Ct
SLC3A2	Solute carrier family 38 member 2 (large neutral amino acid transporter 2)	0.859
SLC5A1	Solute carrier family 5 member 1 (sodium/glucose cotransporter 1)	No Ct
SLC5A4	Solute carrier family 5 member 4 (sodium/glucose cotransporter 3)	0.008
SLC7A11	Solute carrier family 7 member 11 (anionic amino acid transporter 11)	0.117
SLC7A5	Solute carrier family 7 member 5 (L type amino acid transporter 1)	1.753
SLC7A6	Solute carrier family 7 member 6 (Y+L type amino acid transporter 2)	0.153
SLC7A7	Solute carrier family 7 member 7 (Y+L type amino acid transporter 1)	0.003
SLC7A8	Solute carrier family 7 member 8 (L type amino acid transporter 2)	0.130
SLC7A9	Solute carrier family 7 member 9 (B type amino acid transporter 1)	No Ct
SLCO1A2	Solute Carrier organic anion transporter family member 1A2	No Ct
SLCO1B1	Solute Carrier organic anion transporter family member 1B1	No Ct
SLCO1B3	Solute Carrier organic anion transporter family member 1B3	No Ct
SLCO2A1	Solute Carrier organic anion transporter family member 2A1	0.005
SLCO2B1	Solute Carrier organic anion transporter family member 2B1	No Ct
SLCO3A1	Solute Carrier organic anion transporter family member 3A1	0.013
SLCO4A1	Solute Carrier organic anion transporter family member 4A1	0.097

Table 5.2: Abundance of a panel of SLC transporters in hCMEC/D3 cells. Cultures of hCMEC/D3 cells were treated with 0.1% DMSO and incubated for 48 hours at 37^0C. Total RNA was then extracted, reverse-transcribed into cDNA, and the cDNA used to quantify relative expression for each SLC transporter. Mean Ct values obtained from test gene amplification plots were normalised to the mean Ct of three housekeeping genes (*GAPDH*, *HPRT1* and *GUSB*) and are presented as the relative test gene abundance in hCMEC/D3 cells, according to the comparative Ct method.

Transporter gene	Description / function (if known)	Relative abundance
AQP1	Aquaporin 1	0.001
AQP7	Aquaporin 7	No Ct
AQP9	Aquaporin 9	No Ct
ATP6V0C	Lysosomal ATPase, H+ transporter 16kDa, V0 Subunit (acidification of a variety of intracellular compartments)	7.890
ATP7A;LOC644732	ATPase, copper transporter alpha polypeptide (copper homeostasis)	0.064
ATP7B	ATPase, copper transporter beta polypeptide (copper homeostasis)	0.054
MVP	Major vault protein	1.165
TAP1	ATP-binding cassette sub-family B member 1 (peptide transporter involved in antigen processing 1)	0.392
TAP2	ATP-binding cassette sub-family B member 2 (peptide transporter involved in antigen processing 2)	0.145
VDAC1	Voltage-dependent anion channel 1	1.815
VDAC2	Voltage-dependent anion channel 2	0.025

Table 5.3: Abundance of miscellaneous transporters and transport-related genes in hCMEC/D3 cells. Cultures of hCMEC/D3 cells were treated with 0.1% DMSO and incubated for 48 hours at 37^0C. Total RNA was then extracted, reverse-transcribed into cDNA, and the cDNA used to quantify relative expression for each gene. Mean Ct values obtained from test gene amplification plots were normalised to the mean Ct of three housekeeping genes (*GAPDH*, *HPRT1* and *GUSB*) and are presented as the relative test gene abundance in hCMEC/D3 cells, according to the comparative Ct method.

5.3.3 Effects of AED treatment on ABC transporter expression in hCMEC/D3 cells

Of the 27 ABC transporters analysed in this study, 15 appeared to have their expression induced or suppressed following treatment of hCMEC/D3 cells with AEDs. Any change in expression following AED treatment which differed more than 2 fold from control expression (no treatment = 1) was considered important. Treatment of hCMEC/D3 cells with PHT and CBZ increased *ABCA1* expression in hCMEC/D3 cells 5 fold (4.96) and 4 fold (3.71) respectively. Conversely, the modest expression of *ABCA13* observed in control hCMEC/D3 cells was lost when cells were treated with PHT, however expression increased when cells were treated with CBZ (13.0) and VPA (3.44) (*figure 5.5;* table 5.4). Expression of *ABCC1* (5.75), *ABCC10* (3.14), *ABCC6* (3.21), *ABCD1* (3.21), *ABCD4* (2.89), *ABCF1* (5.75) and *ABCG2* (3.28) increased from between 2 to 6 fold following treatment with CBZ when compared to expression in hCMEC/D3 cells untreated (*figures 5.5, 5.7 and 5.8;* table 5.4). A decrease in expression of *ABCB1* was observed following exposure of hCMEC/D3 cells to VPA (0.522), LTG (0.203), GBP (0.181) and TPM (0.274), but no change was observed following PHT (0.650), CBZ (0.808) and LEV (0.630) treatment (*figure 5.6*; table 5.4). Expression of *ABCB6* also decreased in hCMEC/D3 cells treated with PHT (0.314), LTG (0.330), GBP (0.183) and LEV (0.427), however no significant effect was observed following treatment with CBZ (0.765), VPA (1.29) and TPM (0.808; *figure 5.6*; table 5.4). TPM treatment was also observed to decrease the expression of *ABCD3* (0.436) in hCMEC/D3 cells (*figure 5.8*; table 5.4). Expression of *ABCA4* (2.89), *ABCC2* (2.74), *ABCC4* (2.89), *ABCC6* (2.29), *ABCD3* (2.78), *ABCD4* (4.87) and *ABCG2* (3.30) increased following exposure to VPA (*figures 5.7 and 5.8;* table 5.4). As did expression of *ABCD4* following treatment with GBP (3.08), TPM (2.59) and LEV (2.72; *figure 5.8*; table 5.4). Increases in the expression of *ABCC1* and *ABCF1* were also observed in hCMEC/D3 cells following treatment with PHT (2.22) and TPM (3.23) respectively (*figures 5.7* and *5.8*; table 5.4).

Transporter gene	Untreated	PHT treated	CBZ treated	VPA treated	LTG treated	GBP treated	TPM treated	LEV treated
ABCA1	1.00	4.96	3.71	0.929	1.61	1.01	1.41	1.67
ABCA12	1.00	0.829	1.65	1.251	0.779	0.903	0.694	0.781
ABCA13	1.00	0.000	13.0	3.442	1.33	1.69	1.32	1.10
ABCA2	1.00	1.00	1.55	0.781	0.841	0.922	0.843	0.831
ABCA3	1.00	0.595	1.03	0.613	0.476	0.407	0.340	0.634
ABCA4	1.00	1.30	1.48	2.895	1.38	1.04	1.07	1.45
ABCB1	1.00	0.651	0.809	0.522	0.203	0.181	0.274	0.630
ABCB6	1.00	0.314	0.765	1.295	0.330	0.183	0.808	0.427
ABCC1	1.00	2.22	5.75	1.295	1.88	1.10	1.71	1.62
ABCC10	1.00	1.23	3.15	1.120	0.895	0.714	1.50	1.11
ABCC2	1.00	1.27	1.32	2.738	0.582	0.897	1.06	0.526
ABCC3	1.00	0.660	1.26	0.675	0.603	0.694	1.04	0.584
ABCC4	1.00	1.03	1.51	2.895	0.835	0.786	1.30	1.67
ABCC5	1.00	0.732	0.935	1.260	0.563	0.464	0.552	0.592
ABCC6	1.00	1.43	3.21	2.287	0.737	0.843	1.19	0.885
ABCD1	1.00	1.39	3.21	1.845	1.14	1.04	1.30	1.01
ABCD3	1.00	1.17	2.00	2.777	0.697	0.541	0.436	0.608
ABCD4	1.00	1.45	2.89	4.868	0.763	3.08	2.59	2.72
ABCF1	1.00	0.818	5.75	1.757	1.09	0.849	3.23	0.719
ABCG2	1.00	1.33	3.28	3.302	0.940	1.28	0.891	1.28
AQP1	1.00	0.418	2.42	2.119	0.387	0.552	0.464	0.634
ATP6V0C	1.00	0.172	0.056	0.071	0.050	0.045	0.049	0.056
ATP7A	1.00	0.344	0.464	0.792	0.274	0.274	0.245	0.245
ATP7B	1.00	0.747	0.837	1.009	0.392	0.580	0.452	0.572
MVP	1.00	0.889	1.35	0.744	0.824	0.292	0.471	0.704
TAP1	1.00	0.847	767	4.64	0.395	0.430	3.44	0.617
TAP2	1.00	1.13	16.4	1.10	16.0	1.58	0.568	2.93
VDAC1	1.00	0.473	0.474	1.92	1.49	0.254	0.382	0.487
VDAC2	1.00	1.54	1.10	2.18	0.785	0.754	0.770	1.84

Table 5.4: Effects of AED treatment on the expression of selected transporter genes in hCMEC/D3 cells. Cultures were treated with either 25µM phenytoin (PHT), 20µM carbamazepine (CBZ), 300µM valproate (VPA), 10µM lamotrigine (LTG), 60µM gabapentin (GBP), 10µM topiramate (TPM) or 90µM levetiracetam (LEV) for 48 hours at 37^0C. A further batch of cells (untreated) received vehicle (0.1% DMSO) only. Total RNA was then extracted, reverse-transcribed into cDNA, and the cDNA used to quantify relative expression for each gene. Mean Ct values obtained from test gene amplification plots were normalised to the mean Ct of three housekeeping genes (GAPDH, HPRT1 and GUSB) and are presented as the relative test gene expression compared to expression in untreated hCMEC/D3 cells (relative expression = 1), according to the comparative Ct method.

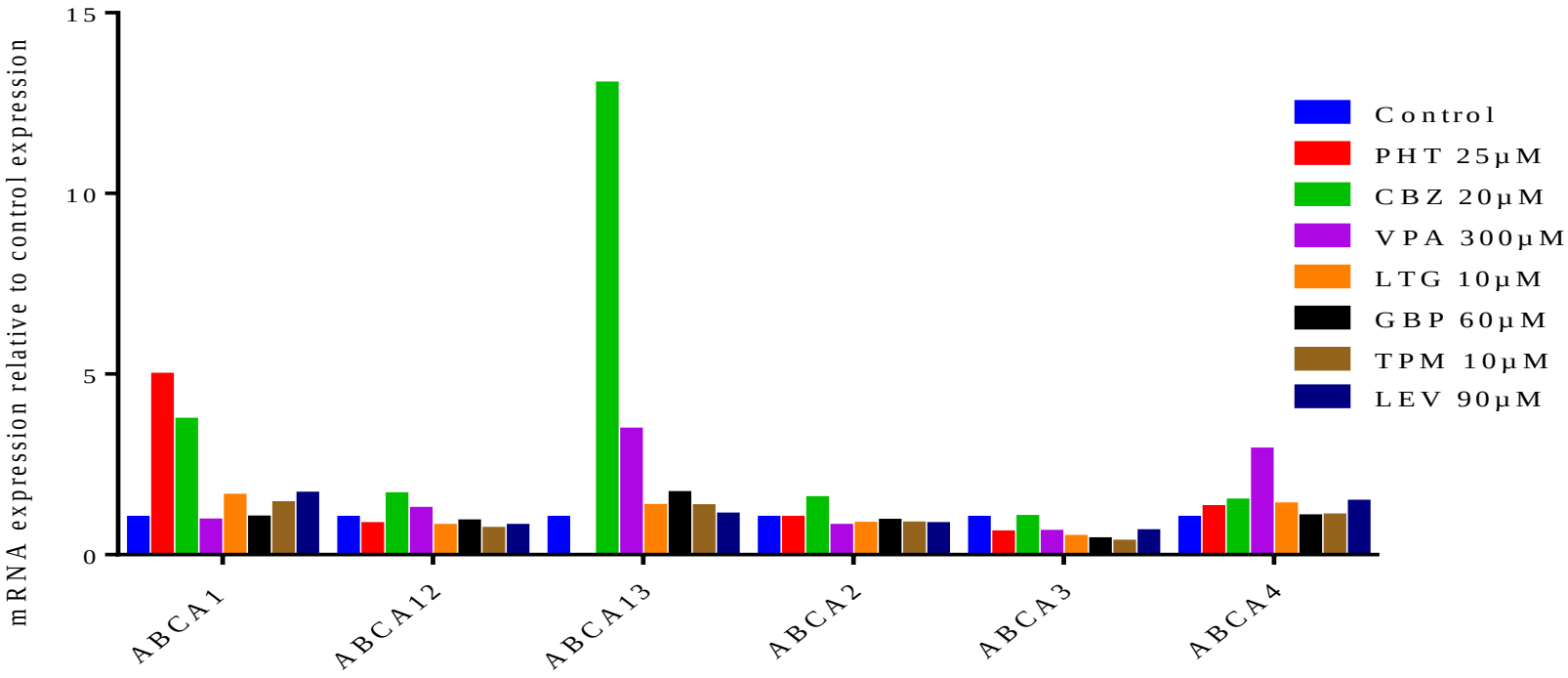

Figure 5.5: Effect of AED treatment on expression of *ABCA* transporter genes in hCMEC/D3 cells. Cultures were treated with either 25µM phenytoin (PHT), 20µM carbamazepine (CBZ), 300µM valproate (VPA), 10µM lamotrigine (LTG), 60µM gabapentin (GBP), 10µM topiramate (TPM) or 90µM levetiracetam (LEV) for 48 hours at 37^0C. A further batch of cells (control) received vehicle (0.1% DMSO) only. Total RNA was then extracted, reverse-transcribed into cDNA, and the cDNA used to quantify relative expression for each gene. Mean Ct values obtained from test gene amplification plots were normalised to the mean Ct of three housekeeping genes (*GAPDH*, *HPRT1* and *GUSB*) and are presented as the relative test gene expression compared to expression in untreated hCMEC/D3 cells (relative expression = 1), according to the comparative Ct method.

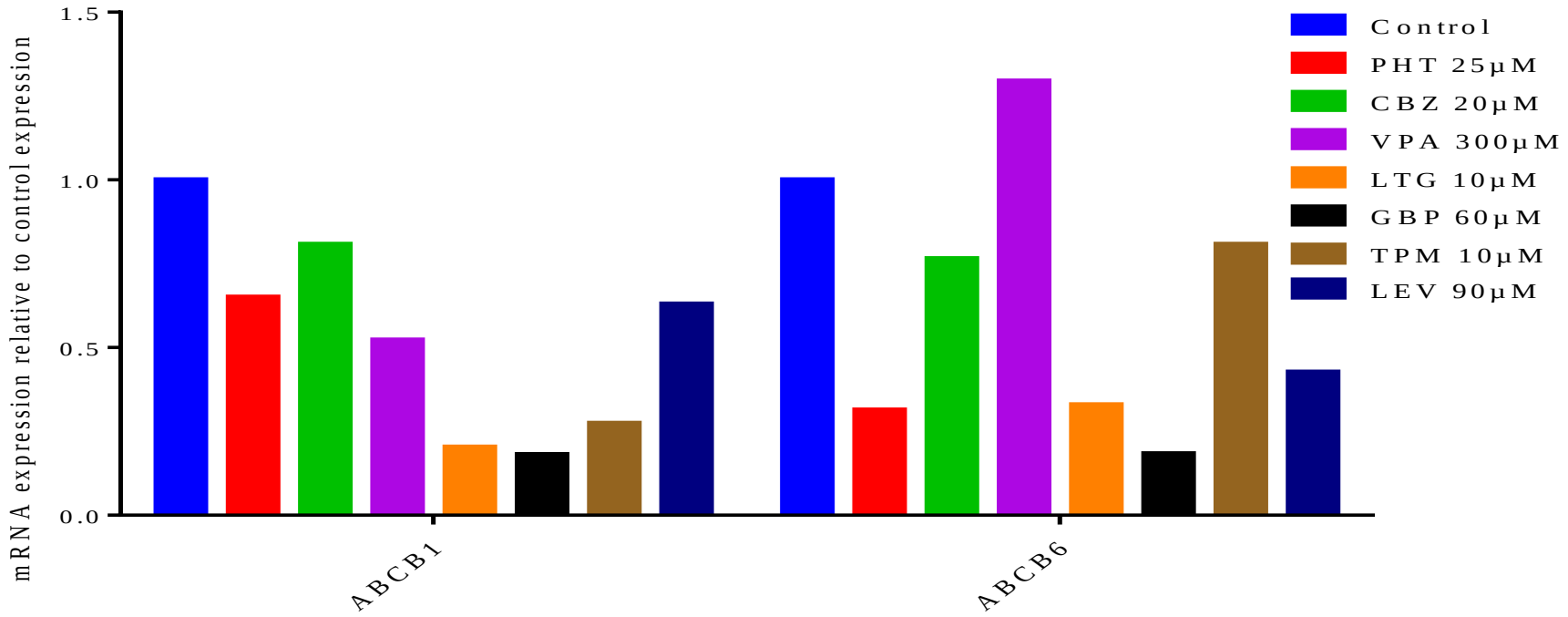

Figure 5.6: Effect of AED treatment on expression of *ABCB* transporter genes in hCMEC/D3 cells. Cultures were treated with either 25µM phenytoin (PHT), 20µM carbamazepine (CBZ), 300µM valproate (VPA), 10µM lamotrigine (LTG), 60µM gabapentin (GBP), 10µM topiramate (TPM) or 90µM levetiracetam (LEV) for 48 hours at 37^0C. A further batch of cells (control) received vehicle (0.1% DMSO) only. Total RNA was then extracted, reverse-transcribed into cDNA, and the cDNA used to quantify relative expression for each gene. Mean Ct values obtained from test gene amplification plots were normalised to the mean Ct of three housekeeping genes (*GAPDH*, *HPRT1* and *GUSB*) and are presented as the relative test gene expression compared to expression in untreated hCMEC/D3 cells (relative expression =1), according to the comparative Ct method.

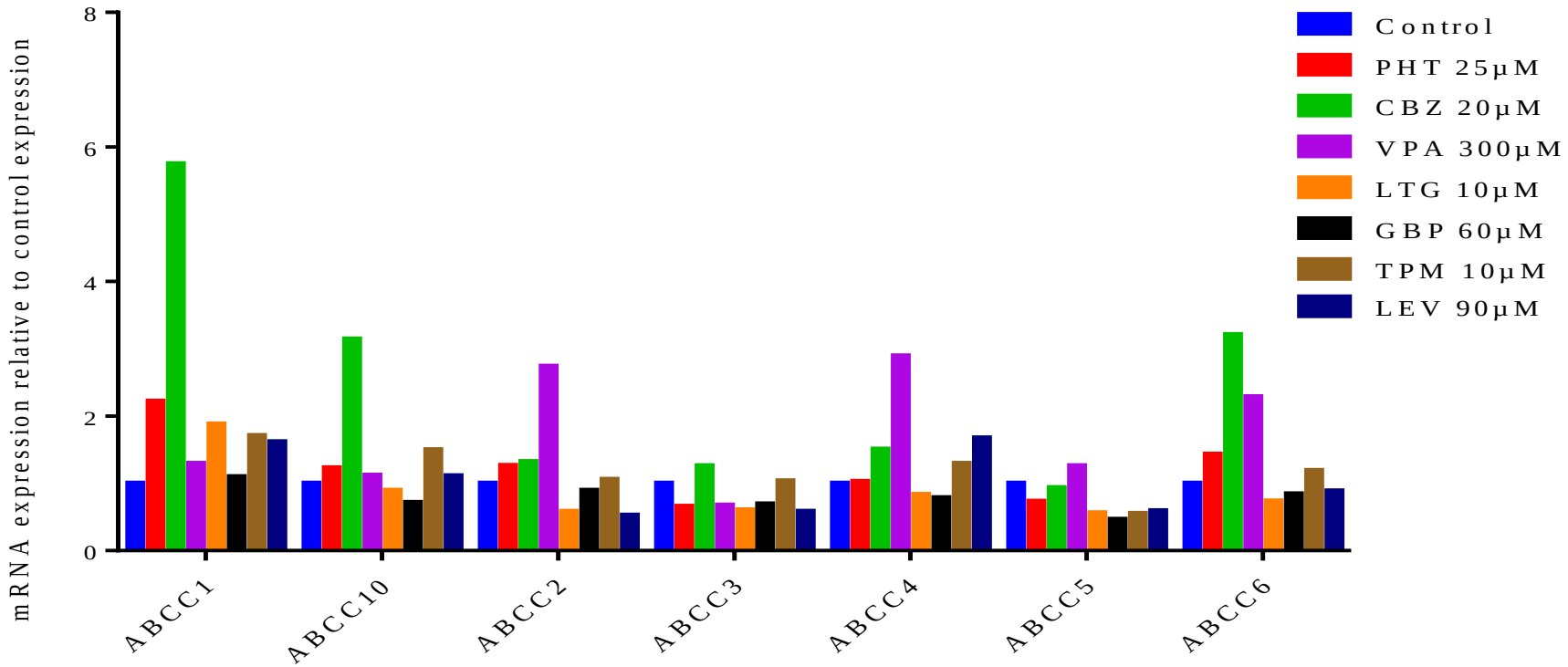

Figure 5.7: Effect of AED treatment on expression of *ABCC* transporter genes in hCMEC/D3 cells. Cultures were treated with either 25µM phenytoin (PHT), 20µM carbamazepine (CBZ), 300µM valproate (VPA), 10µM lamotrigine (LTG), 60µM gabapentin (GBP), 10µM topiramate (TPM) or 90µM levetiracetam (LEV) for 48 hours at 37^0C. A further batch of cells (control) received vehicle (0.1% DMSO) only. Total RNA was then extracted, reverse-transcribed into cDNA, and the cDNA used to quantify relative expression for each gene. Mean Ct values obtained from test gene amplification plots were normalised to the mean Ct of three housekeeping genes (*GAPDH*, *HPRT1* and *GUSB*) and are presented as the relative test gene expression compared to expression in untreated hCMEC/D3 cells (relative expression =1), according to the comparative Ct method.

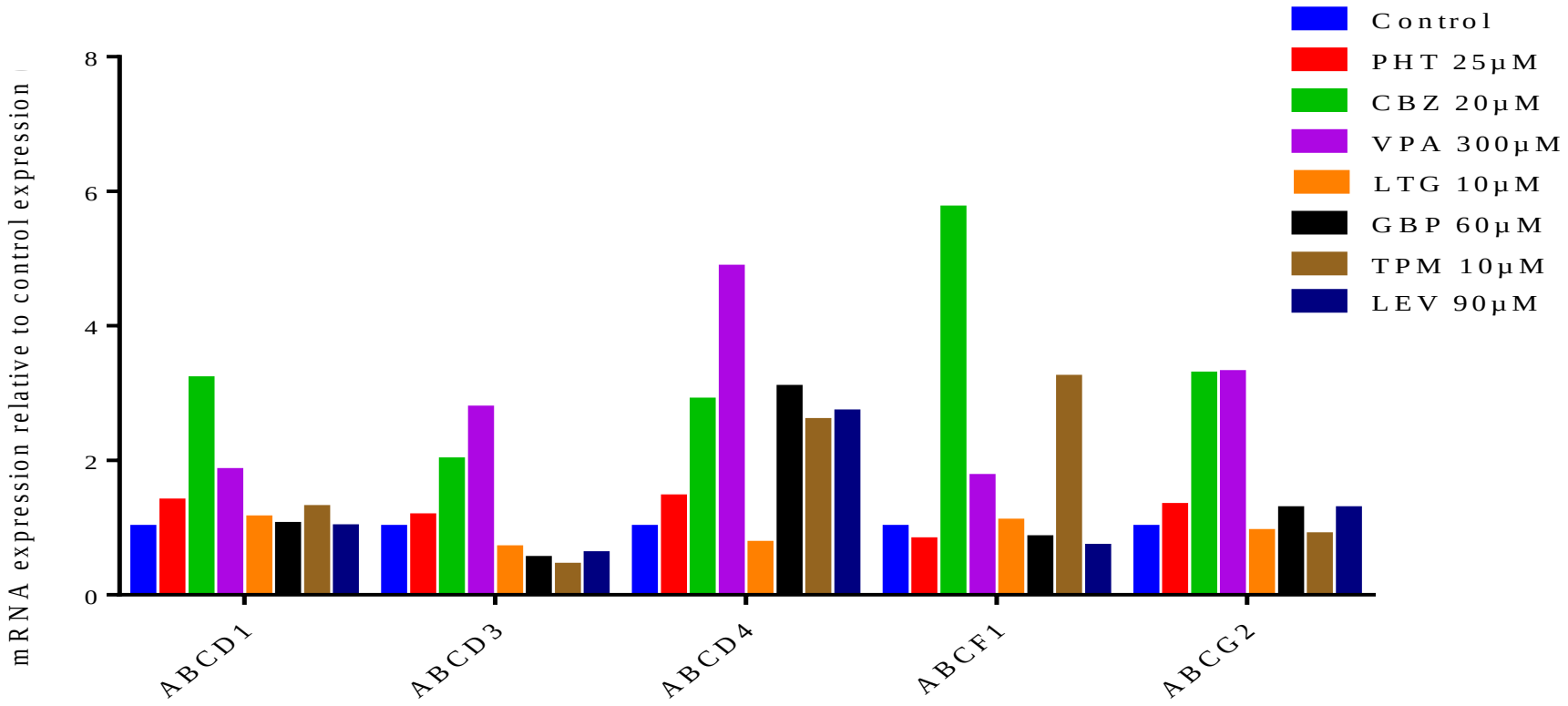

Figure 5.8: Effect of AED treatment on expression of other *ABC* transporter genes in hCMEC/D3 cells. Cultures were treated with either 25µM phenytoin (PHT), 20µM carbamazepine (CBZ), 300µM valproate (VPA), 10µM lamotrigine (LTG), 60µM gabapentin (GBP), 10µM topiramate (TPM) or 90µM levetiracetam (LEV) for 48 hours at 37^0C. A further batch of cells (control) received vehicle (0.1% DMSO) only. Total RNA was then extracted, reverse-transcribed into cDNA, and the cDNA used to quantify relative expression for each gene. Mean Ct values obtained from test gene amplification plots were normalised to the mean Ct of three housekeeping genes (*GAPDH*, *HPRT1* and *GUSB*) and are presented as the relative test gene expression compared to expression in untreated hCMEC/D3 cells (relative expression =1), according to the comparative Ct method.

5.3.4 Effects of AED treatment on SLC transporter expression in hCMEC/D3 cells

Of the 46 SLC transporters analysed in this study, 19 appeared to have their expression induced or suppressed following treatment of hCMEC/D3 cells with AEDs. Again, any change in expression following AED treatment which differed more than 2 fold from control expression (no treatment = 1) was considered important. Expression of *SLC16A2* increased following both CBZ (3.69) and VPA (7.48) treatment in hCMEC/D3 cells (*figure 5.9*; table 5.5). Conversely, expression of *SLC16A3* decreased following exposure to VPA (0.385), LTG (0.473), GBP (0.455), TPM (0.252) and LEV (0.421; *figure 5.9*; table 5.5). Expression of *SLC38A5* decreased following treatment with all AEDs tested (PHT 0.447; CBZ 0.280; LTG 0.202; GBP 0.284; TPM 0.328; LEV 0.326), with the exception of VPA with which an increase in *SLC38A5* expression was observed (2.50; *figure 5.11*; table 5.5). Expression of *SLC5A4* decreased following treatment with LTG (0.325), GBP (0.251), TPM (0.416) and LEV (0.354; *figure 5.11*; table 5.5). Expression of the genes encoding L-type amino acid transporters (LATs) was also affected by AED exposure; expression of *SLC7A5* (LAT1) was reduced by CBZ (0.345), VPA (0.335), LTG (0.351), GBP (0.484), TPM (0.328) and LEV (0.445; *figure 5.12*; table 5.5). *SLC7A8* (LAT2) expression was reduced following exposure to all AEDs tested (PHT 0.045; CBZ 0.032; VPA 0.115; LTG 0.049; GBP 0.021; TPM 0.022 and LEV 0.026; *figure 5.12*; table 5.5). Increases in expression of *SLC22A1* (4.80) and *SLC29A2* (4.27) were observed following CBZ treatment (*figure 5.10;* table 5.5), as were increases in the expression of *SLC15A2* (2.37), *SLC31A1* (2.87), *SLCO3A1* (76.8) and *SLCO4A1* (control 4.83) following VPA exposure (*figures 5.9, 5.11 and 5.13*; table 5.5). An increase in the expression of *SLC2A3* was also observed in hCMEC/D3 cells treated with TPM (4.60; *figure 5.11*; table 5.5). Changes in the expression of *SLCO2A1* and *SLCO3A1* were also observed following treatment with LEV (*SLCO2A1* 18.5; *SLCO3A1* 577) and TPM (*SLCO2A1* 3.32; *SLCO3A1* 0.393; *figure 5.13*; table 5.5).

In addition decreases in the expression of *SLC19A1* (0.466), *SLC19A3* (0.0483) were observed in hCMEC/D3 cells treated with LTG (*figure 5.9*), as were decreases in the expression of *SLC28A3* (0.439), *SLC2A1* (0.433) and *SLC7A7* (0.477) following treatment with GBP and *SLC19A1* (0.471) following TPM treatment (*figures 5.9-5.12*).

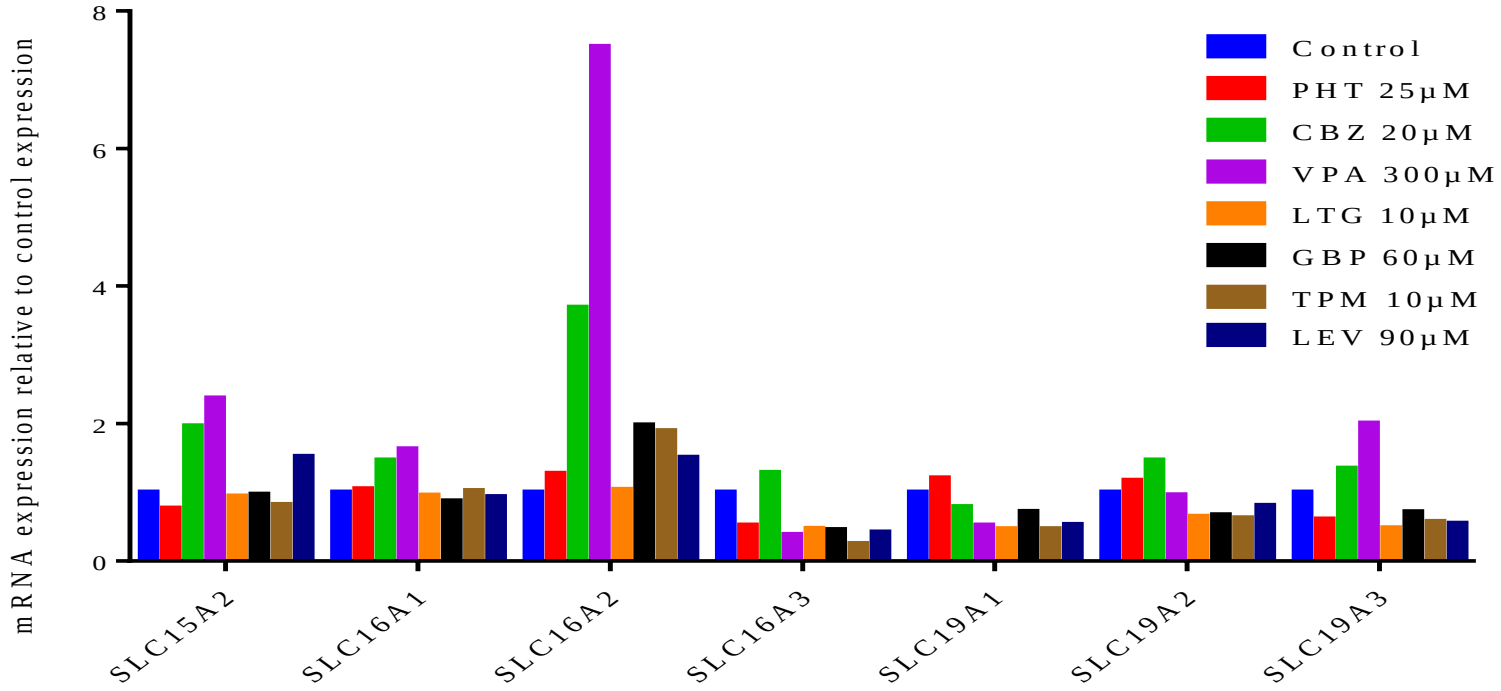

Figure 5.9: Effect of AED treatment on expression of selected *SLC15, SLC16 and SLC19* transporter genes in hCMEC/D3 cells. Cultures were treated with either 25µM phenytoin (PHT), 20µM carbamazepine (CBZ), 300µM valproate (VPA), 10µM lamotrigine (LTG), 60µM gabapentin (GBP), 10µM topiramate (TPM) or 90µM levetiracetam (LEV) for 48 hours at 37^0C. A further batch of cells (control) received vehicle (0.1% DMSO) only. Total RNA was then extracted, reverse-transcribed into cDNA, and the cDNA used to quantify relative expression for each gene. Mean Ct values obtained from test gene amplification plots were normalised to the mean Ct of three housekeeping genes (*GAPDH*, *HPRT1* and *GUSB*) and are presented as the relative test gene expression compared to expression in untreated hCMEC/D3 cells (relative expression =1), according to the comparative Ct method.

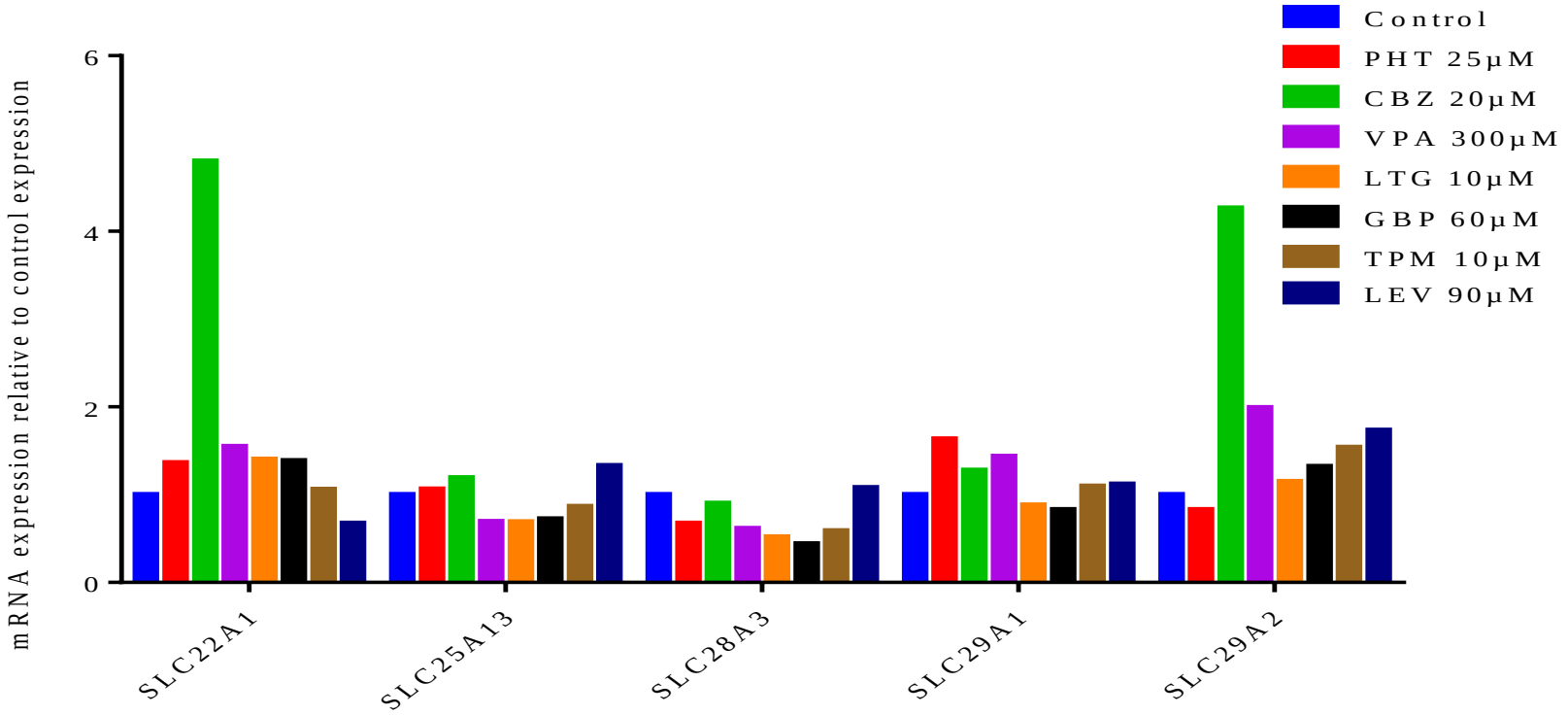

Figure 5.10: Effect of AED treatment on expression of selected *SLC22, SLC25, SLC28 and SLC29* transporter genes in hCMEC/D3 cells. Cultures were treated with either 25µM phenytoin (PHT), 20µM carbamazepine (CBZ), 300µM valproate (VPA), 10µM lamotrigine (LTG), 60µM gabapentin (GBP), 10µM topiramate (TPM) or 90µM levetiracetam (LEV) for 48 hours at 37^0C. A further batch of cells (control) received vehicle (0.1% DMSO) only. Total RNA was then extracted, reverse-transcribed into cDNA, and the cDNA used to quantify relative expression for each gene. Mean Ct values obtained from test gene amplification plots were normalised to the mean Ct of three housekeeping genes (*GAPDH*, *HPRT1* and *GUSB*) and are presented as the relative test gene expression compared to expression in untreated hCMEC/D3 cells (relative expression =1), according to the comparative Ct method.

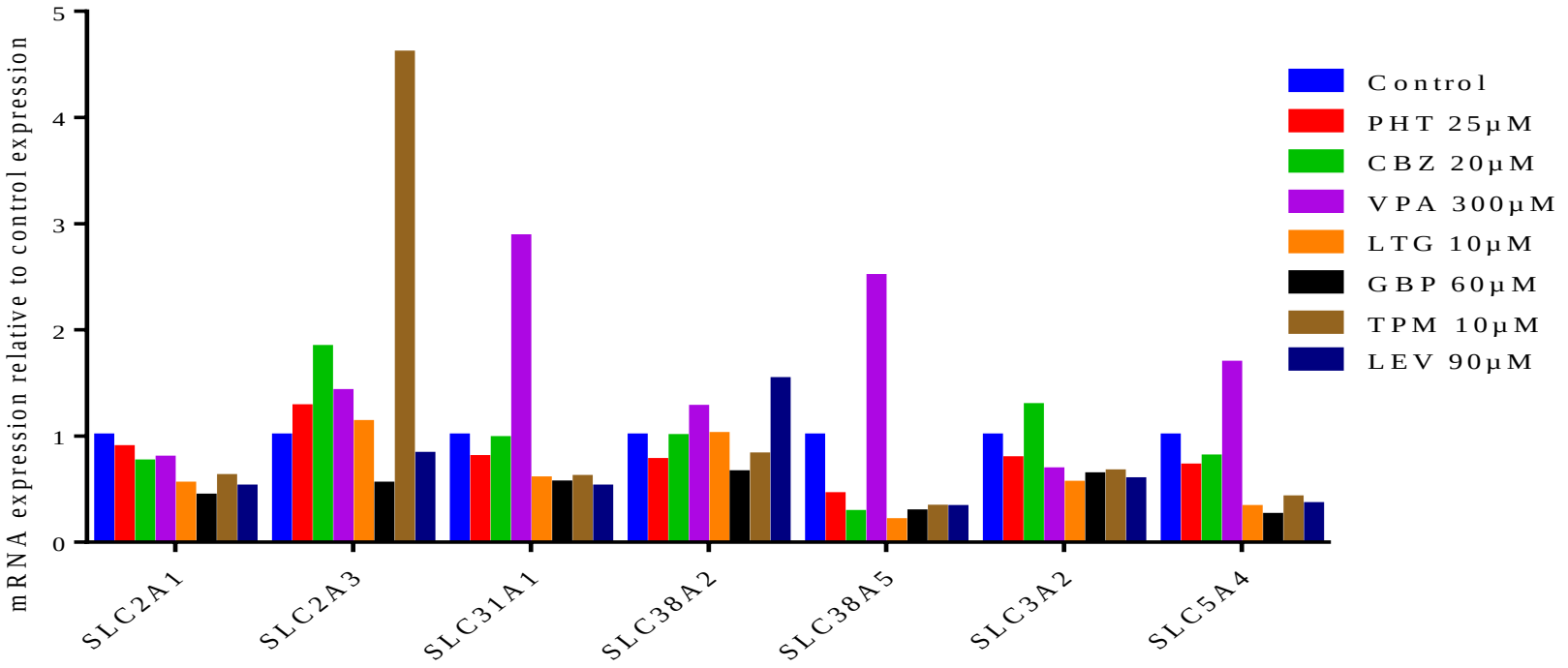

Figure 5.11: Effect of AED treatment on expression of selected *SLC2, SLC3, SLC5, SLC31 and SLC38* transporter genes in hCMEC/D3 cells. Cultures were treated with either 25µM phenytoin (PHT), 20µM carbamazepine (CBZ), 300µM valproate (VPA), 10µM lamotrigine (LTG), 60µM gabapentin (GBP), 10µM topiramate (TPM) or 90µM levetiracetam (LEV) for 48 hours at 37^0C. A further batch of cells (control) received vehicle (0.1% DMSO) only. Total RNA was then extracted, reverse-transcribed into cDNA, and the cDNA used to quantify relative expression for each gene. Mean Ct values obtained from test gene amplification plots were normalised to the mean Ct of three housekeeping genes (*GAPDH*, *HPRT1* and *GUSB*) and are presented as the relative test gene expression compared to expression in untreated hCMEC/D3 cells (relative expression =1), according to the comparative Ct method.

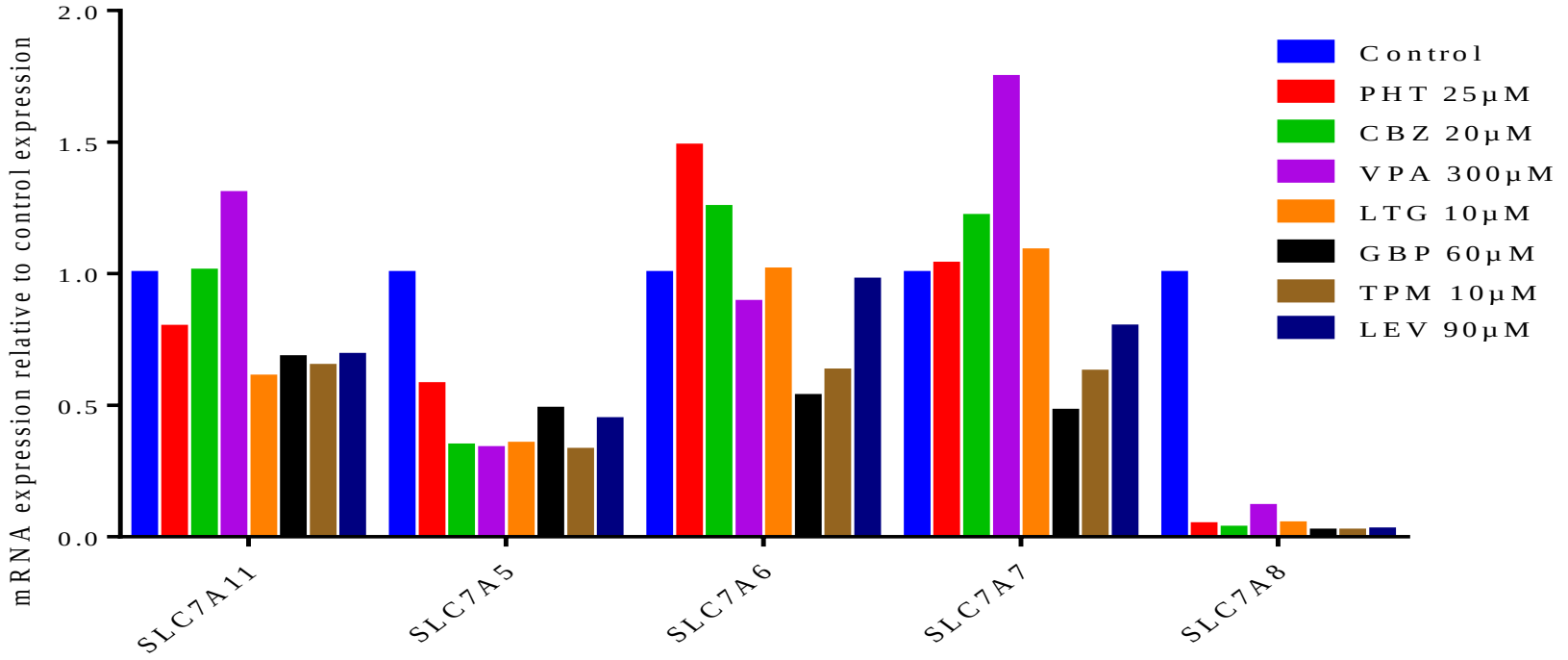

Figure 5.12: Effect of AED treatment on expression of selected *SLC7* transporter genes in hCMEC/D3 cells. Cultures were treated with either 25µM phenytoin (PHT), 20µM carbamazepine (CBZ), 300µM valproate (VPA), 10µM lamotrigine (LTG), 60µM gabapentin (GBP), 10µM topiramate (TPM) or 90µM levetiracetam (LEV) for 48 hours at 37^0C. A further batch of cells (control) received vehicle (0.1% DMSO) only. Total RNA was then extracted, reverse-transcribed into cDNA, and the cDNA used to quantify relative expression for each gene. Mean Ct values obtained from test gene amplification plots were normalised to the mean Ct of three housekeeping genes (*GAPDH*, *HPRT1* and *GUSB*) and are presented as the relative test gene expression compared to expression in untreated hCMEC/D3 cells (relative expression =1), according to the comparative Ct method.

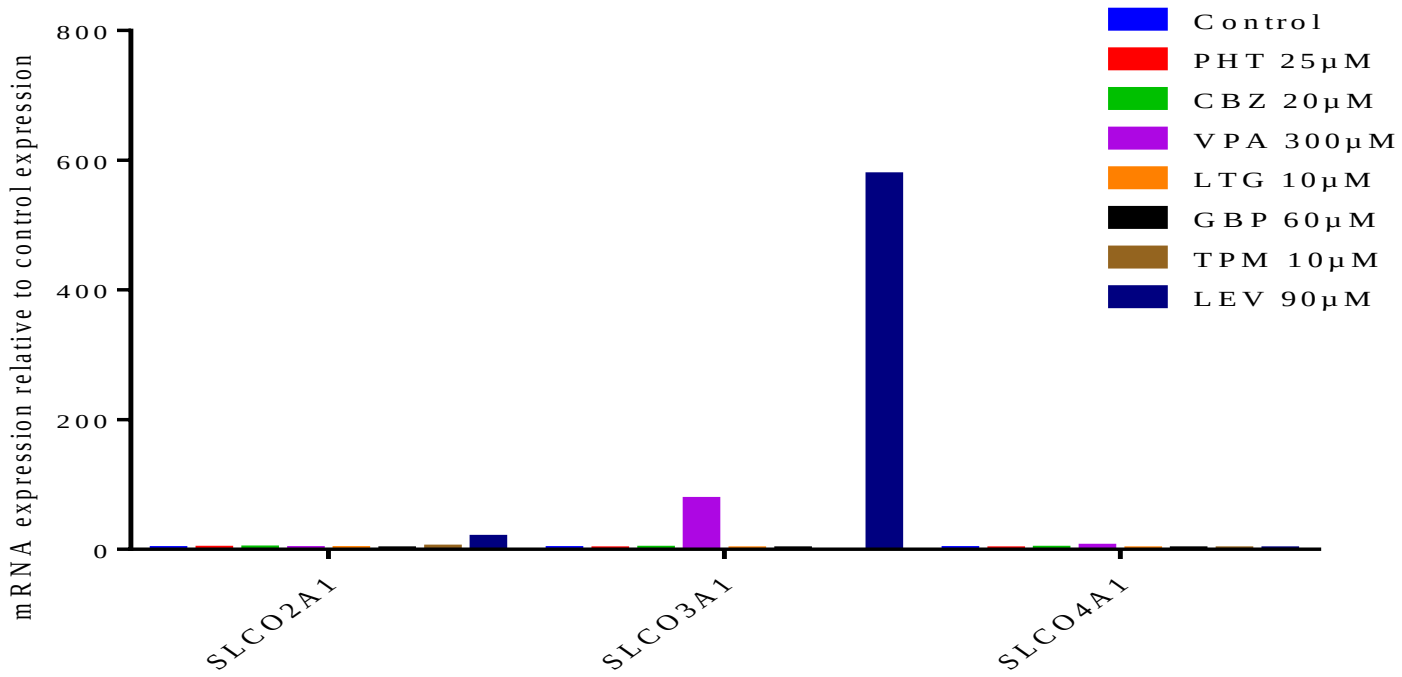

Figure 5.13: Effect of AED treatment on expression of selected *SLCO* transporter genes in hCMEC/D3 cells. Cultures were treated with either 25µM phenytoin (PHT), 20µM carbamazepine (CBZ), 300µM valproate (VPA), 10µM lamotrigine (LTG), 60µM gabapentin (GBP), 10µM topiramate (TPM) or 90µM levetiracetam (LEV) for 48 hours at 37^0C. A further batch of cells (control) received vehicle (0.1% DMSO) only. Total RNA was then extracted, reverse-transcribed into cDNA, and the cDNA used to quantify relative expression for each gene. Mean Ct values obtained from test gene amplification plots were normalised to the mean Ct of three housekeeping genes (*GAPDH*, *HPRT1* and *GUSB*) and are presented as the relative test gene expression compared to expression in untreated hCMEC/D3 cells (relative expression =1), according to the comparative Ct method.

5.3.5 Effects of AED treatment on miscellaneous transporter gene expression in hCMEC/D3 cells

A number of miscellaneous membrane transporters and genes associated with transport were analysed in this study, some of which appeared to be subject to induction or suppression by AEDs. A decrease in expression of *ATP6* was observed following treatment with all AEDs included in the study (PHT 0.172; CBZ 0.056: VPA 0.072: LTG 0.050: GBP 0.045; TPM 0.049; LEV 0.056). As was a decrease in expression of *ATP7A* after exposure to all AEDs (PHT 0.344; CBZ 0.464; LTG 0.274; GBP 0.274; TPM 0.245; LEV 0.245) other than VPA (0.792; *figure 5.14*; table 5.4) and ATP7B following exposure to LTG (0.392) and TPM (0.452; *figure 5.14*; table 5.4). Changes in the expression of *AQP1* were observed in hCMEC/D3 cells following treatment with PHT (0.417), CBZ (2.42), VPA (2.12), LTG (0.387) and TPM (0.464; *figure 5.14*; table 5.4). Expression of *TAP1* was increased following treatment with CBZ (767), VPA (4.64) and TPM (3.44) and decreased following treatment with LTG (0.395) and GBP (0.430; *figure 5.15*; table 5.4). The expression of *TAP2* also increased after exposure to CBZ (16.4), LTG (16.0) and LEV (2.93; *figure 5.15*; table 5.4). Conversely, decreases in the expression of *VDAC1* were observed following treatment with PHT (0.473), CBZ (0.474), GBP 0.254), TPM (0.382) and LEV (0.487; *figure 5.15*; table 5.4). A decrease in the expression of *MVP* was also observed in hCMEC/D3 cells treated with TPM (0.471; *figure 5.14*; table 5.4), while an increase in the expression of *VDAC2* was observed following VPA treatment (2.18) in hCMEC/D3 cells (*figure 5.15*; table 5.4).

Transporter gene	Untreated	PHT treated	CBZ treated	VPA treated	LTG treated	GBP treated	TPM treated	LEV treated
SLC16A1	1.00	1.05	1.47	1.628	0.959	0.873	1.02	0.935
SLC16A2	1.00	1.27	3.69	7.482	1.04	1.98	1.90	1.51
SLC16A3	1.00	0.521	1.29	0.385	0.473	0.455	0.252	0.421
SLC19A1	1.00	1.21	0.792	0.522	0.467	0.719	0.471	0.530
SLC19A2	1.00	1.17	1.47	0.961	0.651	0.671	0.626	0.808
SLC19A3	1.00	0.611	1.35	2.005	0.483	0.714	0.576	0.548
SLC22A1	1.00	1.37	4.80	1.551	1.40	1.39	1.06	0.675
SLC25A13	1.00	1.06	1.19	0.694	0.693	0.724	0.867	1.33
SLC28A3	1.00	0.674	0.903	0.617	0.521	0.439	0.588	1.08
SLC29A1	1.00	1.64	1.28	1.437	0.883	0.831	1.10	1.12
SLC29A2	1.00	0.829	4.27	1.991	1.15	1.32	1.54	1.73
SLC2A1	1.00	0.889	0.754	0.792	0.547	0.433	0.617	0.519
SLC2A3	1.00	1.27	1.83	1.417	1.13	0.545	4.61	0.825
SLC31A1	1.00	0.796	0.975	2.875	0.595	0.556	0.608	0.519
SLC38A2	1.00	0.768	0.995	1.269	1.01	0.652	0.820	1.53
SLC38A5	1.00	0.448	0.280	2.502	0.202	0.284	0.328	0.326
SLC3A2	1.00	0.785	1.29	0.680	0.555	0.634	0.661	0.588
SLC5A4	1.00	0.717	0.803	1.686	0.325	0.251	0.416	0.354
SLC7A11	1.00	0.796	1.01	1.304	0.607	0.680	0.648	0.689
SLC7A5	1.00	0.578	0.345	0.335	0.351	0.484	0.328	0.445
SLC7A6	1.00	1.48	1.25	0.891	1.01	0.533	0.630	0.975
SLC7A7	1.00	1.04	1.22	1.75	1.09	0.477	0.626	0.797
SLC7A8	1.00	0.045	0.032	0.115	0.049	0.021	0.022	0.026
SLCO2A1	1.00	1.52	1.79	1.089	0.920	0.643	3.32	18.5
SLCO3A1	1.00	0.877	1.45	76.8	0.590	0.617	0.393	577
SLCO4A1	1.00	0.768	1.38	4.83	0.574	0.526	0.545	0.714

Table 5.5: Effects of AED treatment on the expression of selected SLC transporter genes in hCMEC/D3 cells. Cultures were treated with either 25µM phenytoin (PHT), 20µM carbamazepine (CBZ), 300µM valproate (VPA), 10µM lamotrigine (LTG), 60µM gabapentin (GBP), 10µM topiramate (TPM) or 90µM levetiracetam (LEV) for 48 hours at 37^0C. A further batch of cells (untreated) received vehicle (0.1% DMSO) only. Total RNA was then extracted, reverse-transcribed into cDNA, and the cDNA used to quantify relative expression for each gene. Mean Ct values obtained from test gene amplification plots were normalised to the mean Ct of three housekeeping genes (GAPDH, HPRT1 and GUSB) and are presented as the relative test gene expression compared to expression in untreated hCMEC/D3 cells (relative expression = 1.00), according to the comparative Ct method.

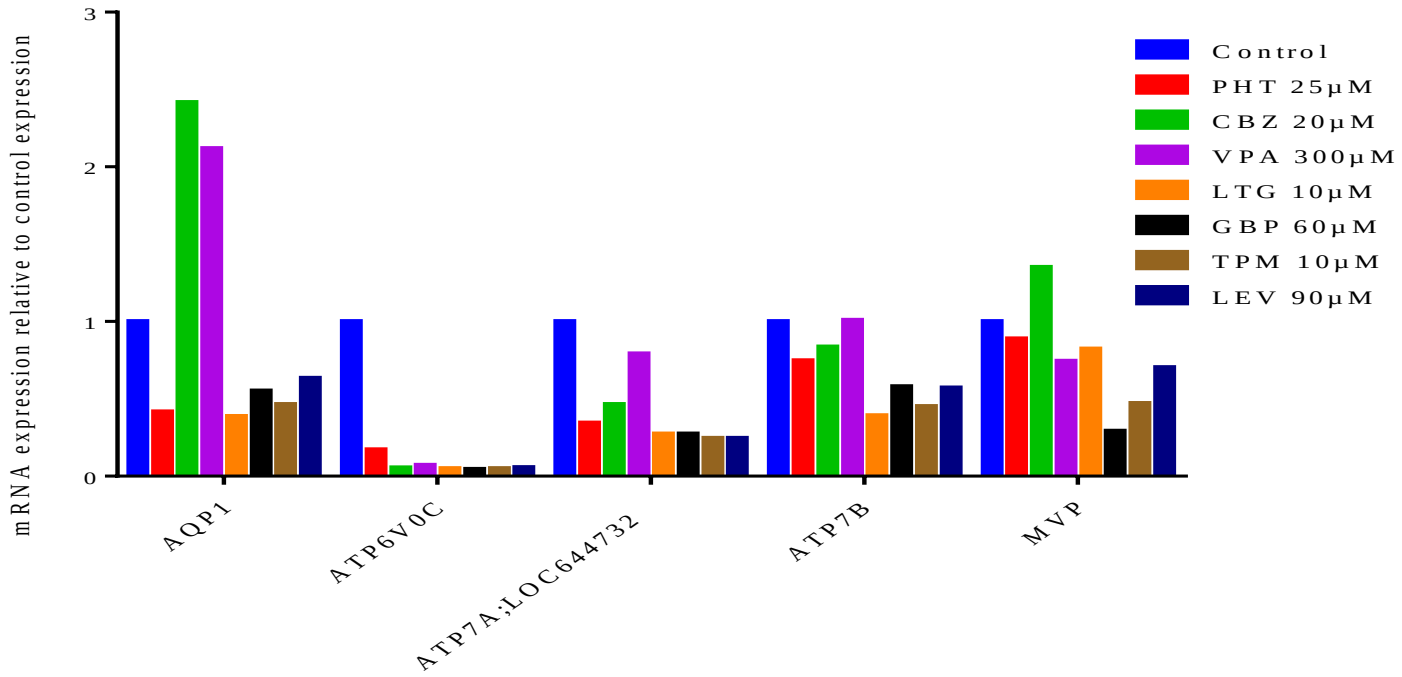

Figure 5.14: Effect of AED treatment on expression of various transporter related genes in hCMEC/D3 cells. Cultures were treated with either 25µM phenytoin (PHT), 20µM carbamazepine (CBZ), 300µM valproate (VPA), 10µM lamotrigine (LTG), 60µM gabapentin (GBP), 10µM topiramate (TPM) or 90µM levetiracetam (LEV) for 48 hours at 37^0C. A further batch of cells (control) received vehicle (0.1% DMSO) only. Total RNA was then extracted, reverse-transcribed into cDNA, and the cDNA used to quantify relative expression for each gene. Mean Ct values obtained from test gene amplification plots were normalised to the mean Ct of three housekeeping genes (*GAPDH*, *HPRT1* and *GUSB*) and are presented as the relative test gene expression compared to expression in untreated hCMEC/D3 cells (relative expression =1), according to the comparative Ct method.

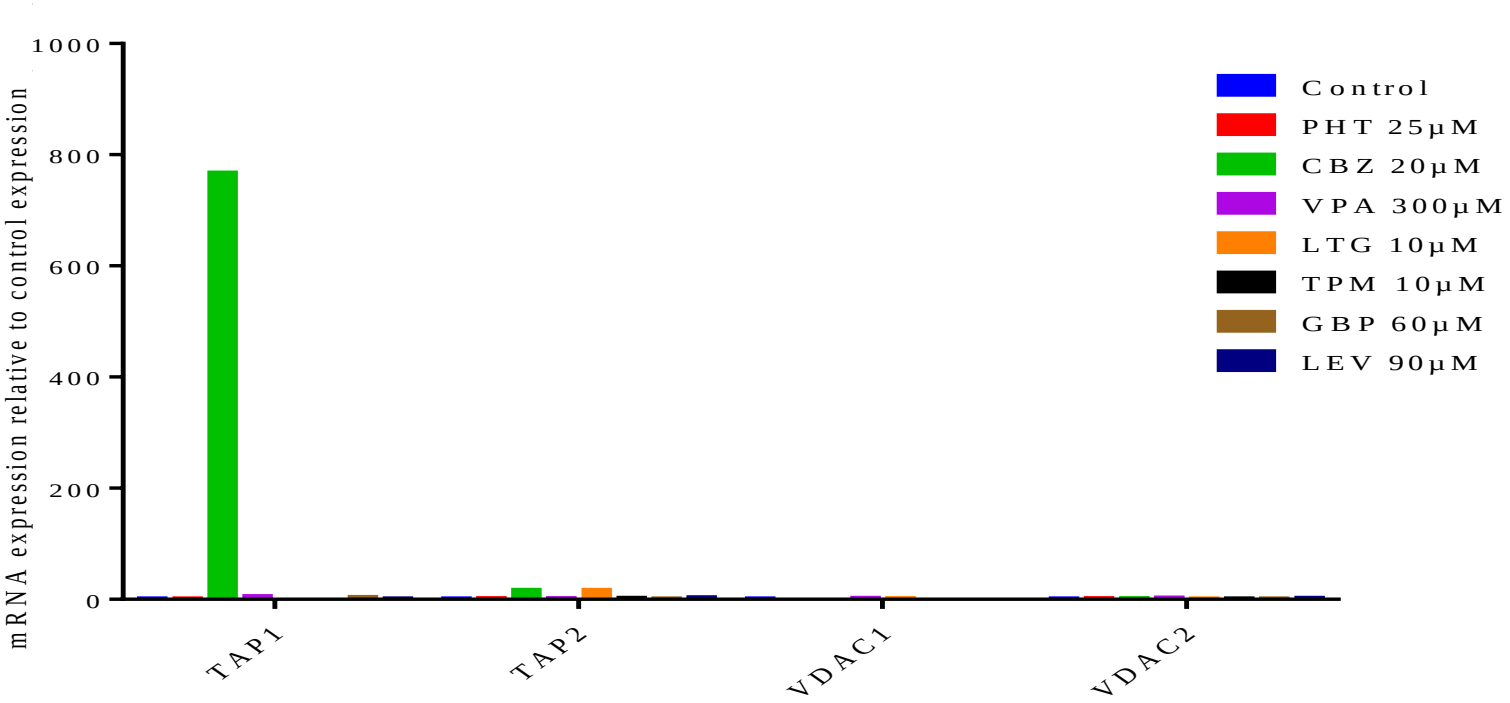

Figure 5.15: Effect of AED treatment on expression of various transporter-related genes in hCMEC/D3 cells. Cultures were treated with either 25µM phenytoin (PHT), 20µM carbamazepine (CBZ), 300µM valproate (VPA), 10µM lamotrigine (LTG), 60µM gabapentin (GBP), 10µM topiramate (TPM) or 90µM levetiracetam (LEV) for 48 hours at 37^0C. A further batch of cells (control) received vehicle (0.1% DMSO) only. Total RNA was then extracted, reverse-transcribed into cDNA, and the cDNA used to quantify relative expression for each gene. Mean Ct values obtained from test gene amplification plots were normalised to the mean Ct of three housekeeping genes (*GAPDH*, *HPRT1* and *GUSB*) and are presented as the relative test gene expression compared to expression in untreated hCMEC/D3 cells (relative expression =1), according to the comparative Ct method.

5.4 Discussion

Transporter proteins are known to be critical for BBB protection and supply of essential nutrients (Urquhart *et al.,* 2009). In addition, they are also known to play a role in the brain accumulation of substrate drugs (Giacomini *et al.,* 2010). Evidence exists that people with epilepsy have altered brain transporter expression (Tishler *et al.,* 1995; Lauritzen *et al.,* 2011; Aronica *et al.,* 2012). However, what is not clear is whether the changes in brain transporter expression observed in epilepsy are a result of the pathophysiology of the disease or a result of chronic AED treatment.

This chapter aimed to characterise expression of both ABC and SLC transporters in an *in vitro* model of the BBB and to explore changes in transporter expression following treatment with commonly prescribed AEDs at concentrations similar to those seen clinically in the serum of people with epilepsy.

Of the 84 transporter genes included in this analysis, 57 were expressed in control hCMEC/D3 cells. The expression profile of ABC transporters is summarised in table 1. Relatively high expression of *ABCB1* (which encodes P-gp) was observed in hCMEC/D3 cells, in line with a large body of evidence which suggests P-gp is the major efflux transporter expressed at the BBB (Tsuji *et al.,* 1992; Abbott *et al.,* 2010). Very low or no expression was found for all other multidrug resistance proteins (MDRs) and multidrug resistance-associated proteins (MRPs) analysed in this study. Of the SLC transporters that were investigated, those involved in nutrient transport unsurprisingly had the highest expression. In particular, the facilitative glucose transporter *SLC2A1,* the monocarboxylate transporters *SLC16A1* and *SLC16A3,* and the neutral amino acid transporters *SLC38A2* and *SLC38A5* showed the most significant expression. Generally, the transporter expression profile observed in this study was in agreement with that published previously in the hCMEC/D3 model (Carl *et al.,* 2010). However, of note, is that the sensitivity of the methods employed in this study appears to be reduced, with significantly lower relative Ct values than were previously reported. Interestingly, and in keeping with Carl and colleagues (2010), no expression of organic anion transporters (encoded by *SLC22A6, SLC22A7* and *SLC22A8*) was detected. Conversely, Geier and colleagues (2013) have observed expression of organic anion transporters in fresh human brain microvessels, suggesting a possible discrepancy between immortalised cell models and their respective primary cells.

The expression of a number of transporters was altered following exposure to AEDs; this data is summarised in figures 5.5 to 5.15, with observations of note discussed here. Expression of *ABCB1* (which encodes P-gp) decreased following treatment with VPA, LTG, GBP and TPM. It has been shown and widely accepted for many years that P-gp is overexpressed in drug resistant epilepsy (Tishler *et al.*, 1995; Zhang *et al.*, 1999; Dombrowski *et al.*, 2001; Volk *et al.*, 2005). Therefore, the observation that treatment with several AEDs decreases P-gp expression is unexpected and suggests that overexpression of P-gp in drug resistant epilepsy may be a result of disease pathology or recurrent seizure activity rather than chronic drug treatment. Interestingly, the expression of ATP synthase *(ATP6)* also decreased following treatment with all AEDs used in the study; reduced ATP synthase and ultimately reduced ATP availability to the cells may explain, at least in part, the reduced expression of P-gp.

The expression of *ABCA1*, a transporter involved in brain cholesterol homeostasis, was seen to increase following treatment with PHT and CBZ suggesting that *ABCA1* is induced by PHT and CBZ. This may be elicited through direct induction of the gene or by activation of the transcription factor responsible for regulation of *ABCA1*, the liver X receptor (LXR). Interestingly, in addition to its predominant role in cholesterol homeostasis, LXR and its ligands have been suggested to promote neurogenesis in the developing brain and to prevent neurodegeneration and protect from neuroinflammation in the adult brain (Wang, 2002; Karasinska *et al.*, 2013; Theofilopoulos *et al.*, 2013). Treatment of hCMEC/D3 cells with CBZ also appeared to induce *ABCC1* expression; strong evidence suggests that *ABCC1* and *ABCA1*, amongst other ABC transporters including *ABCB1*, are involved in a 'phase III' detoxification process by which they are critically involved in the efflux of xenobiotics and steroids (Ishikawa, 1992; Adachi *et al.*, 2007). Accumulating evidence also exists that inducers of phase I and/or phase II metabolising enzymes such as PHT and CBZ can alter the expression of transporters implicated in this postulated phase III detoxification process (Nakata *et al.*, 2006). This suggests that CBZ and possibly PHT may induce transcription factors involved in these detoxification processes and providing they are substrates for *ABCA1* and/or *ABCC1* may induce their own efflux from the brain.

Expression of *SLC16A3* (which encodes MCT4) decreased following treatment with all AEDs investigated other than CBZ, whereas expression of the closely related *SLC16A2*

was seen to increase following VPA treatment alone. Lauritzen and colleagues (2011) showed in surgically resected brain tissue from people with drug resistant temporal lobe epilepsy, that a deficiency of *SLC16A1* (monocarboxylic acid transporter 1) is present on cerebral microvessels. The observation that monocarboxylate transporters (MCTs) can be induced and/or suppressed following AED treatment suggests that AEDs are able to modulate MCT expression at the BBB and may explain, at least partly, any differential expression reported in studies of resected human tissue.

Treatment with AEDs also had significant effects on various amino acid transporters expressed at the BBB. Expression of the genes encoding L-type amino acid transporters (*SLC7A5* and *SLC7A8)* and the neutral amino acid transporter (*SLC38A5)* decreased following treatment with the majority of AEDs; VPA in contrast appeared to induce expression of *SLC38A5*. However, expression of the cationic amino acid transporter *SLC7A9* increased following treatment with all AEDs. The brain is a large consumer of amino acids; this observation suggests that in response to AEDs there is a shift in the pattern of amino acid transporter expression. *SLC38A5* is known to supply the brain with essential molecules including glycine and glutamine which underpin the major route for biosynthesis of the neurotransmitter glutamic acid (Bröer, 2014). Glycine and glutamic acid are also the predominant inhibitory neurotransmitters in the CNS and it could be postulated that induction of *SLC38A5* following VPA treatment may in part contribute to the therapeutic action of VPA, by increasing availability of inhibitory neurotransmitters in the brain.

Expression of *SLC31A1,* the gene encoding an influx transporter involved in copper regulation, increased by three fold following VPA treatment. Although there is no current evidence to link *SLC31A1* to epilepsy or to the transport of VPA, it is known to be critical for normal cell function and has received interest in the field of oncology due to its ability to transport platinum containing chemotherapy agents, such as cisplatin and its potential to modulate cell signalling pathways involved in development and progression of certain cancers (Katano *et al.,* 2002; Wee *et al.,* 2013).

Expression of genes encoding several members of the OATP family was also observed to increase following AED treatment. Moderate expression of *SLCO2B1* was observed following treatment with TPM despite *SLCO2B1* being undetectable in control

hCMEC/D3 cells and the expression of *SLCO3A1* and *SLCO4A1* was increased almost 10- and 7-fold respectively following VPA exposure. *SLCO2B1*, *SLCO3A1* and *SLCO4A1* have been implicated in the transport of drugs such as benzyl penicillin (Roth *et al.*, 2012). Interestingly, TPM and VPA form anions at physiological pH and although no transport by *SLCO1A2* was observed for either AED in the study described in chapter 2 of this thesis (table 2.1), the observation that both AEDs can induce expression of OATP transporters at the BBB may suggest that TPM and VPA are subject to transport by *SLCO2B1* and *SLC03A1* and/or *SLCO4A1*, respectively.

Another interesting observation, although not directly relevant to brain penetration of AEDs in drug resistant epilepsy, was the 300-fold increase in expression of *TAP1*, a transporter involved in transporting antigens from the cytoplasm to the endoplasmic reticulum for association with MHC class I molecules, following treatment with CBZ. CBZ is known to cause hypersensitivity reactions in 5-10% of patients and in rare cases can cause Stevens-Johnson syndrome and toxic epidermal necrolysis (Vittorio *et al.*, 1995). The observation that CBZ can dramatically induce expression of a transporter involved in antigen processing suggests this association may be implicated in the mechanism by which a hypersensitivity reaction to CBZ is initiated.

Due to the cost of the Taqman transporter gene arrays used in this study it was only possible to generate a single set of data for each AED at a single concentration. This lack of replicate data limits the study and the conclusions that can be drawn. At least one duplicate study would have been necessary to demonstrate that the observations are reproducible. Despite these limitations, data generated in this study suggests that AED treatment causes changes in the expression profile of multiple transporter genes in an *in vitro* BBB model. It is likely that these changes are elicited by a multifaceted regulatory system in response to treatment with AEDs, however further work is needed to reproduce the study employed in this chapter and furthermore elucidate if chronic AED treatment is responsible for changes in brain transporter expression observed in people with epilepsy.

Chapter 6

Determination of physicochemical properties that influence BBB permeation of AEDs

6.1 Introduction

For any neurotherapeutic agent to reach its molecular target in the brain and exert its pharmacological effects, it must first penetrate a specialised, protective barrier which lines almost all cerebral microvessels, otherwise known as the blood-brain barrier (BBB). It is assumed that small molecules can pass through this barrier by simple diffusion (both transcellular and paracellular), however it has been estimated that 100% of large molecules and more than 98% of small molecule drugs cannot cross the BBB in this manner (Pardridge, 2005). The BBB compromises a monolayer of endothelial cells, specialised in their barrier function due to the presence of elaborate junctional complexes that eliminate gaps between neighbouring cells and effectively prevent the passage of polar hydrophilic drugs, toxins and blood-borne substances from penetrating the brain via paracellular diffusion (Abbott, 2013).

The restricted paracellular transport at the BBB necessitates that to passively diffuse across the BBB; CNS active agents must use the transcellular pathway which is largely governed by a compound's lipophilicity. It has been accepted for a number of years that the octanol/water coefficients (distribution coefficient log D and partition coefficient log P) of a drug directly correlate with its ability to cross a lipid membrane via the transcellular route. However, a number of other physicochemical properties have also been shown to influence permeability across a lipid bilayer.

Lipinski's rule of 5 has been widely adopted to predict if a molecule has sufficiently favourable physicochemical properties to be well absorbed orally. Lipinski demonstrated that for a compound to be well absorbed it must have a molecular weight < 500, a log P < 5 and restricted hydrogen bonding (less than 5 hydrogen bond donors and/or less than 10 hydrogen bond acceptors) (Lipinski *et al.*, 1997). In addition to the properties outlined in Lipinski's rule of 5, complementary research has demonstrated a role of the polar surface area of a drug and its influence on passive permeation, suggesting that for a compound to be well absorbed orally it must also have a polar surface area no larger than 100 $Å^2$ and a total surface area no larger than 350 $Å^2$ (Palm *et al.*, 1997).

Recently, it has been suggested that predictors of good oral absorption (i.e. permeation across the gastrointestinal tract epithelium) do not accurately predict a molecule's

ability to cross the BBB and that physicochemical factors governing BBB permeation are more stringent (Pajouhesh *et al.*, 2005). It has been estimated that for a molecule to pass through the BBB passively it must have a molecular weight under 450, a polar surface area of below 90Å^2, no more than 5 hydrogen donors and/or 10 hydrogen acceptors, and a log D value greater than 0 but less than 3 (Waterbeemd *et al.*, 1998). Furthermore BBB permeation has been shown to be optimal when Log P values are between 1.5 and 2.7 and although a compound with up to 5 hydrogen bond donors and/or 10 hydrogen bond acceptors will penetrate the BBB, currently marketed CNS active drugs have on average only 1.5 hydrogen bond donors and 2.12 hydrogen bond acceptors (Hansch *et al.*, 1979; Leeson *et al.*, 2004)

Many CNS active agents do not meet these criteria and yet still achieve adequate brain penetration. It is known that specific transport systems are expressed at the BBB to supply essential molecules such as glucose and amino acids to the brain (Pardridge *et al.*, 1977; Pardridge, 1986). It is therefore reasonable that drugs that achieve adequate brain uptake despite unfavourable physicochemical properties may also enter the brain via a similar transport system. For example, the muscle relaxant baclofen is known to cross the BBB despite being highly hydrophilic and is thought to gain entry to the brain via the L-amino acid transporter system (van Bree *et al.*, 1988; van Bree *et al.*, 1991). In addition, the AED gabapentin displays good brain uptake despite its hydrophilic nature and has also been suggested to enter the brain by the L-amino acid transporter system (Welty *et al.*, 1993).

The work described in this chapter first aimed to determine *in silico*, the physicochemical properties known to influence BBB permeation of seven commonly prescribed AEDs, utilising the integrated chemical database SciFinder® (https://scifinder.cas.org/scifinder/login). Experimentally determined log D values for each AED, obtained from liquid scintillation counting of radiolabelled drug and LC-MS/MS analysis of unlabelled drug, were then compared with predicted log D values from SciFinder®. The collective physicochemical properties were then analysed in an attempt to determine if the AEDs included in earlier studies of this thesis possess physicochemical properties likely to favour passive entry into the brain or if they are likely to require a transporter system. Observed physicochemical data was also analysed

by multivariate linear regression to determine which, if any, properties predict AED accumulation in hCMEC/D3 cells, as reported in chapter 3.

6.2 Materials and methods

6.2.1 Materials

[^{3}H]-lamotrigine (specific activity 5Ci/mmol), [^{3}H]-levetiracetam (specific activity 5Ci/mmol), [^{3}H]-topiramate (specific activity 8Ci/mmol) and [^{3}H]-gabapentin (specific activity 110Ci/mmol) were purchased from American Radiolabeled Chemicals Inc. (St. Louis, USA). [^{3}H]-phenytoin (specific activity 1.1Ci/mmol), [^{3}H]-carbamazepine (specific activity 10Ci/mmol) and [^{3}H]-valproic acid (specific activity 55Ci/mmol) were purchased from Moravek (Brea, California, USA). Hanks balanced salt solution (HBSS) was purchased from Life Technologies (Paisley, UK). Phenytoin-d_{10}, carbamazepine-d_{10}, valproic acid-d_4, gabapentin-d_4, topiramate-d_{12} and levetiracetam-d_6 were purchased from C/D/N isotopes (Quebec, Canada), lamotrigine-$^{13}C_3$was purchased from Medical Isotopes (Pelham, New Hampshire, USA). All other reagents, unless otherwise stated, were purchased from Sigma Aldrich (Poole, UK).

6.2.2 Computational determination of physicochemical properties

In silico determination of physicochemical properties for the seven AEDs included in this study was carried out using the SciFinder® integrated chemical database (https://scifinder.cas.org/scifinder/login). Registration to access the database is available through the University of Liverpool electronic library. A search for each AED was carried out using the 'substance identifier' tool. This returned all known information including chemical name, structure, regulatory information and experimental properties for each drug. Any physicochemical information relevant to BBB permeation was then collated and compared with experimentally determined physicochemical properties.

6.2.3 Log D analysis with radiolabelled AEDs

Octanol/water distribution experiments employed a radiolabel concentration of 0.4µCi/ml supplemented with non-radiolabelled drug to give final concentrations of 50µM PHT, 40µM CBZ, 600µM VPA, 20µM LTG, 20µM TPM, 20µM GBP and 90µM LEV, all prepared in transport medium (HBSS supplemented with 25mM HEPES and 0.1% bovine serum albumin (BSA), pH7.4). A radiolabel concentration of 0.4µCi/ml (0.2 µCi/ml final concentration) afforded sufficient disintegrations per minute to give accurate readings of radioactive content without saturating the scintillation counter. A 1ml aliquot of transport buffer containing AED was added to 1ml of octanol in a 15ml Falcon tube to give final concentrations of 25µM PHT, 20µM

CBZ, 300µM VPA, 10µM LTG, 10µM TPM, 10µM GBP and 90µM LEV. Each buffer/octanol solution was vigorously shaken by hand for 15 minutes and then centrifuged at 800 *x g* for 10 minutes to separate the aqueous and organic fractions. Samples (500µl) of both aqueous and octanol fractions were added to individual scintillation vials. This was repeated 4 times for each AED to give 4 replicates for each experiment. Samples (500µl) of transport buffer alone (blanks) were also taken and added to individual scintillation vials to allow estimation of background radiation. A 4ml volume of scintillation fluid was then added to all scintillation vials and each vial was mixed by inverting several times before the radioactive content was determined using a scintillation counter (1500 Tri Carb LS Counter; Packard). Results in dpm were corrected for background counts, and a mean of 4 replicate octanol and aqueous samples calculated for each AED. The dpm in the octanol phase was then divided by the dpm in the aqueous phase and log transformed to give a partition coefficient (log D) value for each AED at pH 7.4. The mean log D value for each AED was finally calculated from 3 independent experiments, each comprising 4 replicates.

6.2.4 Log D analysis using LC-MS/MS

AEDs were prepared in transport medium (HBSS supplemented with 25mM HEPES and 0.1% BSA, pH7.4). A 1ml aliquot of transport buffer containing AED was added to 1ml of octanol in a 15ml Falcon tube, giving final concentrations of 25µM PHT, 20µM CBZ, 300µM VPA, 10µM LTG, 10µM TPM, 10µM GBP and 90µM LEV. Each buffer/octanol solution was vigorously shaken by hand for 15 minutes and then centrifuged at 800 *x g* for 10 minutes to separate the aqueous and organic fractions. Samples (500µl) of both aqueous and octanol fractions were added to individual Eppendorf tubes. This was repeated 4 times for each AED to give 4 replicate experiments. Samples were dried down overnight using a vacuum evaporator and reconstituted in 100% LC-MS grade methanol. Samples were then stored at -20^{0}C overnight and transported to the Buxton Laboratories at the Walton Centre NHS foundation Trust the following morning for LC-MS/MS analysis. Samples were analysed on the Waters liquid chromatography tandem mass spectrometry (LC-MS/MS) system according to local standard operating procedures for analysis of samples for AED content, under the direction of Katherine Birch (clinical biochemist).

As PHT, CBZ, VPA and LTG are amongst the most widely used AEDs, an assay had previously been optimised at the Buxton laboratories in which samples for PHT, CBZ, VPA , LTG, carbamazepine epoxide and phenobarbital could all be analysed simultaneously in the same run. Only single assays were available for GBP, TPM and LEV, therefore samples for these AEDs were analysed in separate LC-MS/MS runs. Firstly, previously prepared standards of known concentration and quality controls (QCs) for each AED were allowed to thaw at room temperature. Standards were prepared in phosphate buffered saline with 0.1% BSA at the concentrations listed in table 6.1. For PHT, CBZ, VPA and LTG, individual standards (1, 2, 3, 4 and 5) were mixed to enable simultaneous detection. Two MassCheck Antiepileptic Drug Plasma Controls (low (16.5mg/L) and high (64.9mg/L) concentration, respectively) were used as internal QCs; controls were provided as lyophilised human plasma samples and were reconstituted in water according to the manufacturer's protocol (Chromsystems, Gräfelfing, Germany). Deuterated forms of each AED were used as internal assay standards to compensate for variation in extraction and ionisation on the LC-MS/MS system. The combined internal standard for PHT, CBZ, VPA and LTG consisted of 4mg/L phenytoin-d_{10}, 1.2mg/L carbamazepine-d_{10}, 5 mg/L carbamazepine epoxide-d_{10}, 8 mg/L valproic acid-d_4, 550 µg/L lamotrigine-$^{13}C_3$ and 5mg/L phenobarbital-d_5 in LC-MS grade methanol. Individual internal standards were prepared in methanol for GBP (1mg/L gabapentin-d_4), TPM (10mg/L topiramate-d_{12}) and LEV (10mg/L levetiracetam-d_6). A 20µl aliquot of each sample/standard/QC was transferred to a 96-well deep well plate and 80µl of the appropriate internal standard added to each well. The plate was then heat-sealed, vortexed for 5 minutes, and centrifuged at 3000 *x g* for 5 minutes. The seal was then removed and 80µl of LC-MS grade water added to each well. The plate was again heat-sealed, vortexed for 5 minutes, and centrifuged at 3000 *x g* for 5 minutes. Plates were then placed in the autosampler of the LC-MS/MS instrument. After ensuring that sufficient volume of mobile phase solvents and wash were present, the LC-MS run was then initiated. The mobile phases were first primed, before switching the MS into operate mode and turning both API and collision gases on. The mobile phase gradient was run to prepare the column, and the samples were then injected onto the LC column. Resulting chromatograms were analysed to ensure the correct peak was integrated and AED concentrations were calculated from a calibration curve generated by Masslynx software (Waters, UK). Concentrations calculated for each sample were used to determine the log D value for each AED as described in

section 6.2.3. Data was expressed as mean ± standard error of the mean (SEM) log D, calculated for each AED from three separate experiments each comprising 4 replicates.

	Blank	**Standard 1**	**Standard 2**	**Standard 3**	**Standard 4**	**Standard 5**
Phenytoin	0 mg/L	3.1 mg/L	6.3 mg/L	12.5 mg/L	25 mg/L	50 mg/L
Carbamazepine	0 mg/L	1.9 mg/L	3.8 mg/L	7.5 mg/L	15 mg/L	30 mg/L
Valproic acid	0 mg/L	12.5 mg/L	25 mg/L	50 mg/L	100 mg/L	200 mg/L
Lamotrigine	0 mg/L	1.6 mg/L	3.1 mg/L	6.3 mg/L	12.5 mg/L	25 mg/L
Gabapentin	0mg/L	5mg/L	15mg/L	40mg/L	50mg/L	
Topiramate	0mg/L	5mg/L	15mg/L	25mg/L	40mg/L	50mg/L
Levetiracetam	0mg/L	10mg/L	20mg/L	40mg/L	80mg/L	

Table 6.1: Final concentrations of phenytoin, carbamazepine, valproic acid, lamotrigine, gabapentin, topiramate and levetiracetam employed as calibration standards in LC-MS/MS analysis.

6.2.5 Multivariate linear regression

Raw data (table 6.2) generated from cellular uptake experiments with radiolabelled PHT, CBZ, VPA, LTG, GBP, TPM and LEV, as described in chapter 3 (see section 3.2.5 for methodology), was used to generate a multivariate linear regression model. Cellular uptake data for all drugs and all physicochemical properties determined in the work described in this chapter, both computationally and experimentally, were analysed using the SPSS statistical package, with cellular accumulation employed as the dependent variable. All other variables were selected as independent variables and a stepwise regression model was used.

Radiolabelled AED	Concentration (μM)	Cellular accumulation (pmol/100000 cells))
[^{3}H]-phenytoin	20μM	138 ±11.2
[^{3}H]-carbamazepine	25μM	17.5 ± 1.00
[^{3}H]-valproic acid	300μM	47.0± 4.93
[^{3}H]-lamotrigine	10μM	55.3 ± 2.71
[^{3}H]-gabapentin	10μM	865± 30.8
[^{3}H]-topiramate	10μM	21.2± 3.86
[^{3}H]-levetiracetam	6μM	9.07± 1.12

Table 6.2: Cellular uptake of antiepileptic drugs (AEDs) in a human cerebral microvascular endothelial cell line (hCMEC/D3). Cultures were exposed to radiolabelled AEDs (25μM phenytoin, 20μM carbamazepine, 300μM valproic acid, 10μM lamotrigine, 10μM gabapentin, 10μM topiramate, 6μM levetiracetam) for one hour at 37^{0}C. Results are expressed as the mean ± standard error of the mean (SEM) disintegrations per minute (DPM) for 5 independent experiments, where n=3 per experiment. Further details are reported in Chapter 3.

6.3 Results

6.3.1 Determination of physicochemical properties using computational methods

The molecular weight of all AEDs included in this study was found to be below the suggested limit of 450 for adequate BBB permeation (table 6.3). In addition, none of the AEDs were found to have 5 or more hydrogen bond donors and/or 10 hydrogen bond acceptors (table 6.3). However, both LTG and TPM had polar surface areas above the suggested 90Å^2 limit for adequate BBB permeation (90.7Å^2 and 124Å^2, respectively) (table 6.3). The predicted log D value for all AEDs was also within the suggested limits (0 to 3) for adequate BBB penetration, with the exception of GBP (-1.42) and LEV (-0.88) (table 6.4). Furthermore, the log P values predicted for PHT (1.42), LTG (1.24), GBP (1.08) and LEV (-0.88) were outside of the suggested limits for adequate BBB permeation (1.5 to 2.7) (table 6.3).

Drug	Molecular weight	Polar surface area (A^{o2})	H bond donors	H bond acceptors	Log P (250C)
Phenytoin	252	58.2	2	4	1.42
Carbamazepine	236	46.3	2	3	1.90
Valproic acid	144	37.3	1	2	2.58
Lamotrigine	256	90.7	4	5	1.24
Gabapentin	171	63.3	3	3	1.08
Topiramate	339	124	2	9	2.16
Levetiracetam	170	63.4	2	4	-0.88

Table 6.3: Molecular weight, polar surface area, hydrogen bonding and partition coefficients (log P) of seven commonly prescribed antiepileptic drugs determined using the integrated chemical database SciFinder® (https://scifinder.cas.org/scifinder/login).

	log D values at varying pH									
AED	**pH 1**	**pH 2**	**pH 3**	**pH 4**	**pH 5**	**pH 6**	**pH 7**	**pH 8**	**pH 9**	**pH 10**
Phenytoin	1.42	1.42	1.42	1.42	1.42	1.42	1.41	1.29	0.78	-0.01
Carbamazepine	1.88	1.89	1.89	1.89	1.89	1.89	1.89	1.89	1.89	1.89
Valproic acid	2.58	2.58	2.57	2.52	2.18	1.37	0.40	-0.50	-1.09	-1.16
Lamotrigine	-1.25	-1.20	-0.90	-0.13	0.71	1.15	1.23	1.24	1.24	1.24
Gabapentin	-2.02	-2.02	-1.99	-1.85	-1.55	-1.43	-1.42	-1.42	-1.44	-1.59
Topiramate	2.16	2.16	2.16	2.16	2.16	2.16	2.15	2.13	1.96	1.34
Levetiracetam	-0.89	-0.88	-0.88	-0.88	-0.88	-0.88	-0.88	-0.88	-0.88	-0.88

Table 6.4: Distribution coefficients (log D) of seven commonly prescribed antiepileptic drugs at pH 1-10, determined using the integrated chemical database SciFinder® (https://scifinder.cas.org/scifinder/login).

6.3.2 Comparison of log D values obtained experimentally and *in silico* at pH 7.4

The log D values for VPA and LEV determined by liquid scintillation counting (0.22 ± 0.01 and -0.68 ± 0.01, respectively) were similar to the predicted log D values generated *in silico* (0.04 and -0.88, respectively). However, the log D values for VPA and LEV determined using LC-MS/MS (1.25 ± 0.01 and -0.09 ± 0.02) were significantly different from those obtained by liquid scintillation counting. Conversely, the log D for LTG determined by LC-MS/MS (1.05 ± 0.11) was similar to that predicted computationally (1.23), but higher than that determined by liquid scintillation counting (-0.03 ± 0.02). Interestingly, for GBP and TPM conflicting values were obtained; log D for GBP by liquid scintillation counting was -0.64 ± 0.04, by LC-MS/MS was 0.28 ± 0.03, and predicted computationally was -1.42, log D for TPM by liquid scintillation counting was -1.08 ± 0.01, by LC-MS/MS was -0.56±0.04, and predicted computationally was 2.14. Log D values for PHT and CBZ were comparable for all three methods employed (PHT - liquid scintillation counting 1.75 ± 0.20, LC-MS/MS 1.36 ± 0.03, computationally 1.36; CBZ - liquid scintillation counting 1.17 ± 0.03, LC-MS/MS 1.46 ± 0.03, computationally 1.89). All log D data is reported in table 6.5 for comparative purposes.

AED	Computationally determined log D	Experimentally determined log D	
		Liquid scintillation counting	LC-MS/MS
Phenytoin	1.36	1.36 ± 0.03	1.75 ± 0.20
Carbamazepine	1.89	1.17 ± 0.03	1.46 ± 0.03
Valproic acid	0.04	0.22 ± 0.01	1.25 ± 0.01
Lamotrigine	1.23	-0.03 ± 0.02	1.05 ± 0.11
Gabapentin	-1.42	-0.64 ± 0.04	0.28 ± 0.03
Topiramate	2.14	-1.08 ± 0.01	-0.56 ± 0.04
Levetiracetam	-0.88	-0.68 ± 0.01	-0.09 ± 0.02

Table 6.5: A comparison of log D values for seven commonly prescribed antiepileptic drugs (AEDs) at pH7.4, determined *in silico* and experimentally. Predicted log D values from *in silico* analysis were obtained using the integrated chemical database SciFinder® (https://scifinder.cas.org/scifinder/login). Experimentally determined log D values were obtained using radiolabelled compounds (measured by liquid scintillation counting) and unlabelled compounds (measured by liquid chromatography tandem mass spectrometry (LC-MS/MS)) following partition into 50:50 (v/v) octanol: aqueous buffer solution. AED concentrations in experimental studies were as follows; phenytoin (PHT, 25µM), carbamazepine (CBZ, 20µM), valproic acid (VPA, 300µM), lamotrigine (LTG, 10µM), gabapentin (GBP, 10µM), topiramate (TPM, 10µM) and levetiracetam (LEV, 90µM). Results are expressed as mean ± standard error of the mean (SEM) log D from three independent experiments, each comprising 4 replicates.

6.3.3 Multivariate linear regression analysis

Multivariate linear regression analysis failed to identify any association between the various physicochemical parameters observed in this study (log D, log P, molecular weight, hydrogen bonding and polar surface area) and the extent of cellular uptake of the respective AED in hCMEC/D3 cells (table 6.6).

Predictor	Significance
Molecular weight*	0.234
Hydrogen bond donors*	0.232
Hydrogen bond acceptors*	0.281
Log D computational*	0.155
Log D liquid scintillation counting	0.318
Log D LC-MS/MS	0.314
Polar surface area*	0.407
Log P*	0.430

Table 6.6: Descriptive statistics output from multivariate linear regression analysis. None of the physicochemical properties included in the regression model was found to be associated with the extent of cellular accumulation of AEDs in hCMEC/D3 cells. Predictors marked with an asterisk (*) were determined *in silico* using the integrated chemical database SciFinder® (https://scifinder.cas.org/scifinder/login).

6.4 Discussion

It has been accepted for a number of years that the octanol/water coefficients (log D and log P) of a drug directly correlate with its ability to cross a lipid membrane via the transcellular route. However, a number of other physicochemical properties have been shown to additionally influence permeability across a lipid membrane. Lipinski's rule of 5 has been widely adopted to predict if a molecule or drug has sufficiently favourable physicochemical properties to be well absorbed orally (Lipinski *et al.*, 1997). However, recently it has been suggested that predictors of good oral absorption do not accurately predict a molecule's ability to cross the BBB and that physicochemical factors governing BBB permeation are more stringent (Pajouhesh *et al.*, 2005).

In this chapter, the physicochemical properties known to influence BBB penetration were investigated for seven commonly prescribed AEDs using the integrated chemical database SciFinder®. The distribution coefficient (log D) for each AED was also determined using two experimental approaches; liquid scintillation counting and LC-MS/MS respectively, in an attempt to compare values determined experimentally to those that had been predicted. All of the resulting physicochemical parameters, irrespective of whether they had been determined *in silico* or experimentally, were then employed in a regression model to determine if any could reliably predict the cellular uptake of AEDs in hCMEC/D3 cells.

When comparing log D values obtained by the two experimental methods employed, conflicting values were obtained for a number of AEDs. The log D value for VPA obtained by liquid scintillation counting matched that predicted by SciFinder, but was lower than that determined by LC-MS/MS. At physiological pH, VPA is almost completely ionised to its corresponding sodium salt. It is therefore possible that the greater log D value observed with LC-MS/MS may have been due to a larger percentage of the ionised, more lipophilic form being present in the sample. Similarly, the log D value determined by liquid scintillation counting for LTG and GBP, both of which are also highly ionised at physiological pH, was significantly lower than that determined by LC-MS/MS. The distribution coefficient (log D) takes into account both un-ionised and ionised forms of the test molecule therefore must be calculated at a known pH (Smith *et al.*, 2012). Inconsistencies in experimental determination of log D values for highly ionised AEDs may therefore be due to variable sensitivity in the analysis of ionised

forms in experimental samples, therefore overall concentrations of LTG and GBP in the samples. Furthermore GBP is known to have limited stability in solution, therefore over time the radiolabelled compound may have degraded and may have affected measurement of log D by liquid scintillation counting when compared to LC-MS/MS which utilised freshly prepared solutions.

Experimentally determined log D values were consistent with predicted log D values for PHT and CBZ, neither of which is highly ionised at physiological pH. In addition, PHT and CBZ were the only AEDs in this study that were found to possess optimal physicochemical properties for passive brain uptake, which was reflected in their marked accumulations in hCMEC/D3 cells.

Interestingly, for TPM, the log D values determined by both experimental methods were in agreement but were significantly lower than that predicted by *in silico* analysis (i.e. TPM is predicted to be much more lipophilic than it appears). In addition, TPM was also found to have several physicochemical properties which might restrict its brain uptake, including a large polar surface area and high number of hydrogen bond acceptors. Passive BBB permeation is typically restricted to those molecules that possess a molecular weight no greater than 400, a polar surface area no larger than $90A^2$, no more than 10 hydrogen bond acceptors and/or 5 hydrogen bond donors, and a log D between 0 and 3 (Waterbeemd *et al.*, 1998; Pajouhesh *et al.*, 2005). Despite not meeting these criteria, TPM still displays substantial uptake in hCMEC/D3 cells. TPM contains a sulphonamide group in its structure similar to the antipsychotic drugs sulpiride and amisulpride, which also achieve adequate brain uptake despite a polar surface area over the limit suggested for passive diffusion across the BBB. Sulpiride transport has been demonstrated to be subject to inhibition by a number of PEPT1 (peptide transporter 1), OCTN1 (organic cation/carnitine transporter 1) and OCTN2 (organic cation/carnitine transporter 2) substrates and/or inhibitors in a caco-2 cell line. In addition sulpiride has also been demonstrated to be transported by OCT1 and OCT2 in both hCMEC/D3 cells and HEK293 cells overexpressing OCT1 and OCT2 (Pereira *et al.*, 2014). Furthermore amisulpride was observed to be transported by OCT1, OCT2, OCT3, OCTN1 and OCTN2 in HEK293 cells overexpressing each transporter respectfully (Pereira *et al.*, 2014). Therefore it is plausible that one or more of these transporters may transport sulpiride across the intestinal epithelium (Watanabe *et al.*,

2002). PEPT1 and OCT1 are expressed in hCMEC/D3 cells (Carl *et al.*, 2010) and OCTN2 has been suggested to be expressed at the BBB *in vivo* (Kusuhara *et al.*, 2005), therefore the substantial TPM uptake observed in hCMEC/D3 cells may be due to carrier mediated uptake of TPM by one or more of these transporters. In addition in mdr1 knockout mice, brain concentrations of TPM were greater than that observed in wild-type mice, strongly suggesting TPM is a substrate for efflux transport by P-gp (Sills *et al.*, 2002).

Like TPM, LTG and GBP showed physicochemical properties that might be suggestive of limited passive brain uptake. The polar surface area of LTG was found to be over the suggested limit for adequate BBB penetration and the log D values for GBP, derived from both *in silico* and experimental studies were less than or close to 0, and thereby below the suggested limit for passive diffusion across the BBB. Interestingly, these AEDs have previously been suggested to be subject to carrier-mediated uptake by OCT1 and LAT1 respectively (Welty *et al.*, 1993; Dickens *et al.*, 2012).

Linear regression analysis failed to find an association between the various physicochemical properties of these seven AEDs and the extent of their accumulation in hCMEC/D3 cells. This would suggest that, in the *in vitro* environment at least, cellular uptake of AEDs is essentially independent of their physicochemical properties and may therefore be mediated by active (i.e. transporter-dependent) processes.

In conclusion, the experiments described in this chapter suggest firstly, that log D values determined for highly ionised molecules are subject to experimental variation and that *in silico* predictions may not be accurate in these cases. Secondly, despite displaying marked cellular uptake in a human BBB model, several AEDs, including LTG, GBP and TPM, possess one or more unfavourable physicochemical properties that may limit their ability to passively enter the brain. Finally, multivariate linear regression analysis failed to find an association between physicochemical properties and AED uptake in hCMEC/D3 cells. These observations suggest that several AEDs namely LTG, GBP and TPM are unlikely to have accumulated in hCMEC/D3 cells by passive diffusion and that a carrier mediated transport system is likely to play a role in the uptake of these AEDs into hCMEC/D3 cells and conceivably the BBB *in vivo*.

Providing uptake of AEDs into hCMEC/D3 cells correlates with uptake in cerebral endothelial cells *in vivo.*

Chapter 7

General Discussion

Despite the availability of a growing number of AEDs, up to 30% of people with epilepsy are not adequately controlled with AED therapy and are classified as pharmacoresistant. The majority of observed drug resistance occurs relatively soon after diagnosis in early treatment and any further attempt to control seizures with drug treatment is usually futile. This suggests that the mechanism by which individuals become resistant is de novo, does not develop over time, and is not associated with prolonged therapy (Kwan et al., 2000). The causative biological mechanism of drug resistance in epilepsy is poorly understood but is likely to be multifactorial; an important observation of drug resistant epilepsy is that resistance is to multiple AEDs with different mechanisms of action, suggesting a general pharmacokinetic mechanism of pharmacoresistance.

The transporter hypothesis accounts for this observation and postulates that over-expression of drug efflux transporters on cerebral microvascular endothelial cells which contribute to the integrity of the BBB may reduce AED accumulation in the brain, preventing therapeutically active concentrations of AEDs from reaching their targets. However, this hypothesis relies on the fundamental assumption that multiple AEDs are substrates for one or more transporter systems at the BBB. Research supporting this hypothesis has up to now focused almost exclusively on the investigation of AED transport by P-gp. Such investigation has reported conflicting findings (see table 1.1) with in vitro studies returning largely negative data while in vivo investigations have returned largely positive or inconclusive data (Owen et al., 2001; Potschka et al., 2001; Potschka et al., 2002; Sills et al., 2002; Crowe et al., 2006; Dickens et al., 2013)(Feldmann *et al.*, 2013). Other efflux transporters have received some attention but similarly have returned ambiguous findings (Potschka et al., 2001; Cerveny et al., 2006). Although research to date surrounding the transporter hypothesis of drug resistant epilepsy is yet to yield conclusive evidence in its support, much can be learned concerning the significance of the investigative system used to assess transporter systems and the danger of relying on a single experimental model to characterise a complex pharmacological relationship.

In addition to the expression of efflux transporters such as P-gp, the BBB is known to possess a rich and diverse expression of influx transporters belonging to the SLC superfamily. Despite over a decade of research surrounding the drug transporter

hypothesis, the role SLC transporters might play in this theory remains largely unaddressed. Hence the major focus of this thesis was to investigate and identify transporter systems of interest that are expressed at the BBB and determine which, if any AEDs are substrates for such transporter systems. Seven of the most commonly prescribed AEDs (PHT, CBZ, VPA, LTG, GBP, TPM and LEV) were investigated in this thesis and of these, VPA and GBP showed the greatest evidence for SLC-mediated transport, while other compounds were largely unremarkable in this respect.

The findings of this thesis are summarised as follows (*figure 7.1*); in chapter 2 OATP1A2 was shown not to transport any of the AEDs tested in *SLCO1A2* transfected *X. laevis* oocytes. Furthermore GBP was shown to be transported by MCT1 in *SLC16A1* transfected *X. laevis* oocytes, however transport could not be reliably inhibited with the MCT1 inhibitor employed. In chapter 3 several AEDs tested namely PHT, LTG, TPM and GBP, were sensitive to MCT transport inhibitors. Overlapping substrate specificity of the inhibitors employed prevented clear conclusions being made in terms of crediting the observed effects as inhibition of MCT transporters specifically. However data generated strongly suggested GBP is transported by MCT1 and or MCT4 in hCMEC/D3 cells. In chapter 4 VPA, LTG and TPM transport increased in *SLC22A6*_MDCK II cells however these increases could not be attenuated by inclusion of the OAT1 inhibitor probenecid. LTG and TPM transport increased in *SLC22A8*_MDCK II cells, while VPA transport decreased. LTG transport could be significantly inhibited with the inclusion of the OAT3 inhibitor probenecid, however the changes in transport observed for VPA and TPM could not be attenuated by inclusion of probeneicd. Further attempts to inhibit the changes in AED transport observed in both *SLC22A6*_MDCK II and *SLC22A8*_MDCK II cells were unsuccessful. In chapter 5 all of the AEDs tested were observed to supress and/or inhibit the expression of a number of transporter genes in hCMEC/D3 cells including P-gp, MRP transporters, MCT transporters, organic anion transporting polypeptides and amino acid transporters. Finally in chapter 6 analysis of the physicochemical properties of the AEDs included in this thesis revealed that a number of AEDs, namely LTG, TPM and GBP possess unfavourable characteristics to enter the brain passively and so it is plausible they enter via active uptake by transporters.

SLC transporters are known to be expressed at the BBB where they play a critical role in brain delivery of nutrients, which are otherwise restricted from entering the brain (Pardridge et al., 1977; Pardridge, 1986). It is therefore plausible that AEDs may utilize influx transport systems expressed at the BBB and that changes in expression of these transporters may impact on AED brain penetration and therefore prevent therapeutic concentrations of AEDs reaching brain targets.

Endothelial cells constituting the BBB are unique in the fact that they possess specialised tight junctions which almost completely restrict paracellular transport (Pardridge, 2005; Abbott, 2013). It is therefore a challenge to experimentally model the human BBB in vivo. Surrogate BBB models such as Caco-2 and MDCK-MDR1 cells may provide a simple and inexpensive alternative for high throughput screening in industry; however these models do not accurately reflect the morphology of the BBB and lack expression of tight junction proteins expressed on cerebral endothelial cells (Hellinger et al., 2012). To address this, a number of immortalised human in vitro models of the BBB have been established and characterised, including the hCMEC/D3 cell line (Poller et al., 2008; Mkrtchyan et al., 2009; Eigenmann et al., 2013; Weksler et al., 2013). The main advantage of the hCMEC/D3 cell line as a BBB model is that it maintains a stable phenotype which mimics the in vivo BBB phenotype and is easy to culture. The hCMEC/D3 cell line is also well adapted to studying transport at the BBB. The expression of an array of human transporters in hCMEC/D3 cells was investigated in chapter 5 and found a similar expression profile to that previously reported (Carl et al., 2010), although a generally lower level of expression was observed for almost all transporters in my study in comparison to expression levels previously reported. This may be due to differences in passage of cells used in the analysis and sensitivity of

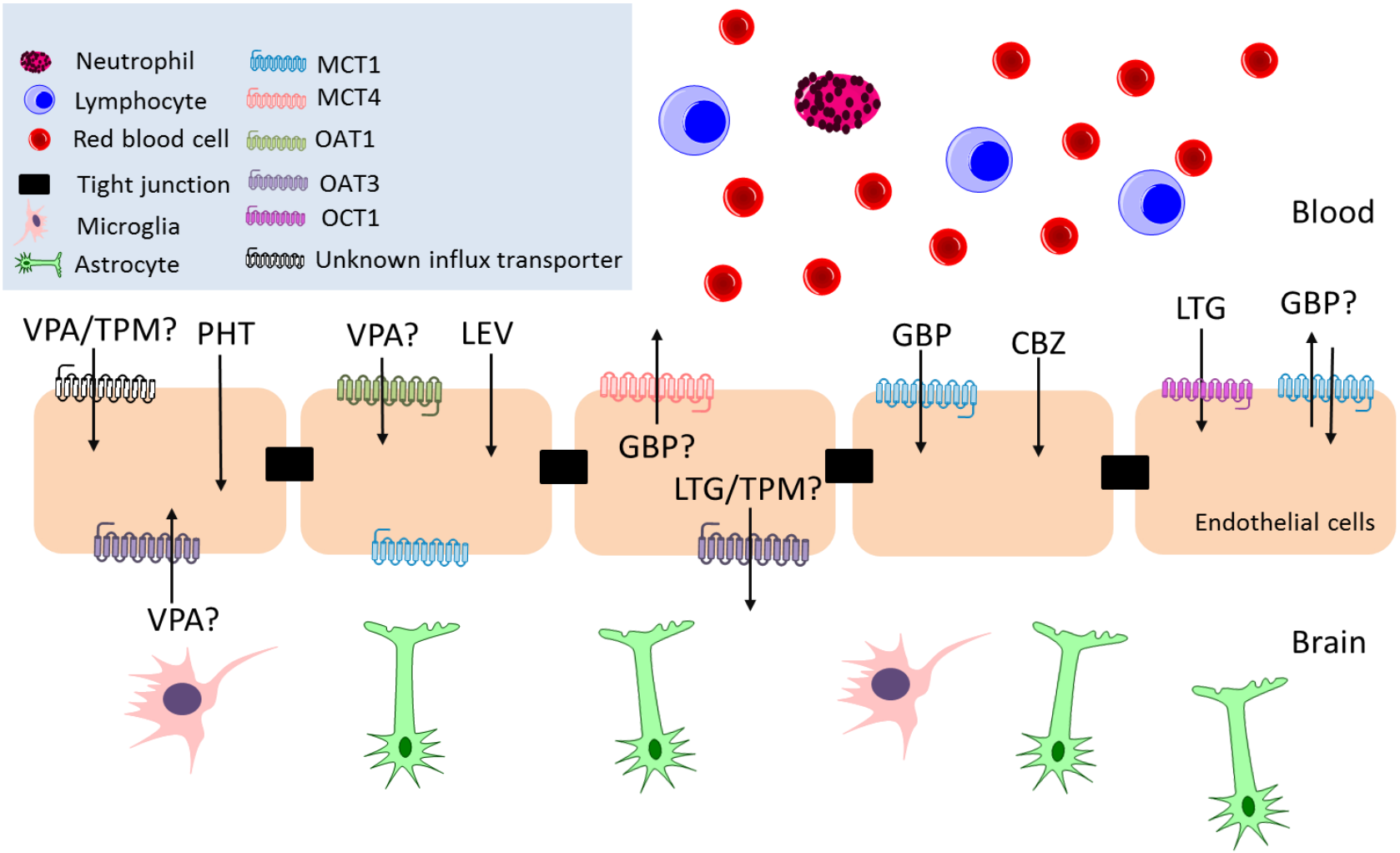

Figure 7.1: Antiepileptic drug transport at the blood-brain barrier by the solute carrier family. A summary of the findings generated in this thesis and current knowledge from literature.

analytical methods employed, however it must be considered that the lack of replicate date generated in chapter 5 limits the study and the conclusions that can be drawn. Although data from this chapter gives thought-provoking insight into future investigation, any conclusions are speculative and findings would need to be reproduced to prove any observations of interest. Of all SLC transporters, highest expression in hCMEC/D3cells was seen with nutrient transporter systems (chapter 5 and (Carl et al., 2010), which is not surprising given the high metabolic demands of the brain.

Research into the role of SLC transporters in the transport of AEDs is limited but MCT transporters have received specific attention and MCT1 in particular. MCT1 was shown to be severely deficient on the endothelium of microvessels at the epileptogenic focus from tissue surgically resected in the treatment of individuals with drug resistant TLE (Lauritzen et al., 2011). A similar deficiency was also observed on the endothelium of microvessels in three novel rat models of the TLE. These authors also observed a corresponding increase in astrocyte MCT1 expression (Lauritzen et al., 2012). It is difficult to speculate why MCT1 might be deficient on the endothelium of microvessels in drug resistant TLE but one can reasonably suggest that a deficiency of MCT1 may contribute to drug resistance (Fischer et al., 2008). Monocarboxylates such as lactate, pyruvate and ketones are critical for normal brain function and rely on the MCT transport system to gain entry into the brain (Halestrap et al., 1999). Although glucose is the brain's main energy source, ketone bodies are important in energy storage in times of glycolytic restriction and may have direct anticonvulsant effects by enhancing GABAergic neurotransmission (Masino et al., 2012). Furthermore, MCT1 has been implicated in the transport of VPA at the BBB (Utoguchi et al., 2000; Fischer et al., 2008); therefore suggesting that VPA resistance in patients with TLE may be attributed to a loss of MCT1 in the epileptogenic focus. Despite VPA being more than 99% ionised at physiological pH and reasonably hydrophilic, it is known to readily penetrate the BBB (Löscher, 2002). It is therefore reasonable that VPA may enter the brain via a carrier mediated process.

In chapter 2, I investigated transport of VPA in MCT1 transfected *X. laevis* oocytes, however no increase in VPA uptake was observed when compared to control. Previous work suggesting VPA may be subject to MCT-mediated transport utilised cell models

which have inherent expression of other transport proteins (Utoguchi et al., 2000; Fischer et al., 2008) and it is therefore possible that another MCT is responsible for changes in VPA transport observed in these studies. However, further investigation exposing hCMEC/D3 cells to VPA with and without a panel of MCT transport inhibitors (chapter 3) added additional weight to the conviction that VPA is not subject to transport by an MCT.

This study is the first to investigate VPA transport by MCT1 in both a physiologically relevant in vitro model and an in vitro model in which MCT1 is exclusively overexpressed. While the discrepancies in findings in studies that have investigated MCT transport of VPA are perplexing, it is important to note that many of those proposing transport of VPA by an MCT system were achieved using rodent cell models. We have learnt from the P-gp story the misconceptions of extrapolating between species and that transport of a drug by a rodent transporter does not necessarily mean the human orthologue will also transport the same drug. All investigations to date carried out in human cell models has involved application of VPA, with and without MCT transport inhibitors, to cell lines such as Caco-2 cells (Fischer et al., 2008), BeWo cells (Utoguchi et al., 2000) and hCMEC/D3 cells (chapter 3), which express endogenous levels of MCT transporters but also inherently express other transporters. The major limitation of such an investigational approach to the study of drug transport is that available inhibitors have overlapping specificities and lack selectivity. Chemical transport inhibitors are notoriously promiscuous and typically inhibit transporters from several families, albeit with varying potency. Therefore, although this kind of investigation can shed light on possible transporter systems involved in the penetration of a drug across biological membranes, it cannot categorically determine which transporter system is involved.

Almost 15 years before the investigation of VPA transport by an MCT transporter system, VPA uptake was investigated in an in situ rat brain perfusion model, which showed that uptake could be inhibited in the presence of anion transport substrates/inhibitors (Adkinson et al., 1996). The same investigators had previously investigated VPA transport in isolated rat brain endothelial cells and observed similar results (Naora et al., 1995). They went on to suggest that the observed inhibition may be due to uptake of VPA by rodent OAT3. A number of prototypic monocarboxylate

inhibitors used in the investigation of VPA transport by the MCT system are also known to inhibit anion transport (Halestrap et al., 2004). It is therefore possible to speculate that inhibition of VPA uptake observed in these studies may be due to inhibition of an anion transporter system.

A number of OATs are thought to be expressed at the BBB and have been investigated in the pursuit of a transporter system for VPA (Sekine et al., 1997; Cihlar et al., 1999; Kusuhara et al., 1999; Ohtsuki et al., 2002; Eraly et al., 2003; Kikuchi et al., 2003; Mori et al., 2003; Bleasby et al., 2006; Terbach et al., 2011; Roth et al., 2012). OAT1 and OAT3 are known to be involved in the disposition of a number of drugs and are thought to be expressed at the BBB in vivo (Sekine et al., 1997; Cihlar et al., 1999; Ohtsuki et al., 2002; Eraly et al., 2003; Kikuchi et al., 2003; Mori et al., 2003; Bleasby et al., 2006). As previously described (Carl et al., 2010) and replicated in chapter 5, the OATs of the SLC22 family are not expressed in hCMEC/D3 cells. In an attempt to specifically determine if VPA transport is mediated by OAT1 and/or OAT3, stably transfected MDCK II cells overexpressing the OAT1 and OAT3 genes were generated (chapter 4). Curiously, VPA uptake increased in MDCK II cells transfected with OAT1 but decreased in MDCK II cells transfected with OAT3, suggesting a bidirectional transport of VPA that is mediated by the OAT transport system. OAT1 and OAT3 functionality in the kidney has received the most research interest to date, owing to the role of these transporters in the renal elimination of anions. There is evidence to suggest that OAT1 and OAT3 function in synergy in the kidney (Chennavasin et al., 1979), therefore it is plausible that this is also the case at the BBB. Additionally, the gene encoding OAT1 (i.e.SLC22A6), is found paired with the gene encoding OAT3 (i.e. SLC22A8) on chromosome 11q12.3, and such pairing may further indicate a potential partnership in both tissue distribution and transport function (Eraly et al., 2003). In addition to showing here that VPA may be transported by OAT1 and OAT3, another transporter family has been implicated in the transport of VPA. Cellular uptake of VPA was investigated in the *Dictyostelium discoideum* model and proposed to be carrier mediated and dependent on pH and a proton gradient (Terbach et al, 2011). VPA was also seen to compete with bicarbonate for uptake suggesting that a bicarbonate transporter may be involved. Furthermore, the authors went on to identify a gene in Dictyostelium which is homologous to mammalian bicarbonate transporters of the SLC4 family and which they speculated to be SLC4A11 on the basis of sequence

identity (Terbach et al., 2011). The ability of VPA to accumulate adequately in the brain despite its variable pharmacokinetics and moderately low log D (chapter 6) has prompted research groups to investigate and identify the carrier system involved; however despite much research, the mechanism by which VPA enters the brain still eludes us. It is likely that transport at the BBB is to some extent mediated by the anion transporters OAT1 and OAT3 and possibly members of the SLC4 family. However, the relationship is likely to be more complex than can be explained by interaction with a single transporter. VPA is known to show variable organ concentrations in vivo, which suggests that the mechanism by which VPA is transported across a particular membrane is organ-specific and that several transport systems may be implicated depending on the site of transport.

It has been known for some time that GBP uptake into the brain is likely to involve the L-type amino acid transporter LAT-1 (Welty et al., 1993). GBP is highly lipophilic at physiological pH but possesses several structural properties which limit its ability to passively permeate cellular membranes (chapter 6). Uptake via the LAT-1 transporter is therefore believed to account for GBP reaching adequate concentrations in brain following a therapeutic dose. Despite this and perhaps because of a lack of expression of LAT-1 in the gut (Prasad et al., 1999), GBP shows variable and dose dependent bioavailability thought to be the result of saturation of a low capacity transporter system (Gidal et al., 1998). To combat this, XP13512, a novel gabapentin pro-drug was recently developed; it was designed to be absorbed through the gut by high capacity nutrient transporters, later confirmed to be MCT1 and the sodium dependent multivitamin transporter (SMAT) (Cundy et al., 2004). This drug has yet to reach the clinic and it is arguable whether it ever will, not least because investigation of AED transport in MCT1 transfected *X. laevis* oocytes (chapter 2) and hCMEC/D3 cells (chapter 3) would suggest that GBP is also subject to MCT1 mediated transport, potentially dispelling any benefit of XP13512.

In addition to the substantial research efforts aimed at investigating P-gp transport of AEDs, research has also attempted to understand the role of transporter regulation, and that of P-gp in particular, and its implications in multidrug resistance in epilepsy.

There is existing evidence which supports changes in brain transporter expression in epilepsy (Sisodiya et al., 1999; Sisodiya et al., 2002; Aronica et al., 2003; Wen et al., 2008; Ambroziak et al., 2010; Moermana et al., 2011). However what is not clear and which remains disputed, is whether the difference in transporter expression is intrinsic or acquired. That is to say, are the changes in BBB transporter expression due to the underlying pathology, the consequence of uncontrolled seizures, the result of chronic AED treatment, or a combination of all of these factors (Aronica et al., 2012)? Supporters of an intrinsic mechanism argue that increased expression of transporters such as P-gp is present before the onset of seizures and the initiation of AED treatment and is therefore a result of disease pathophysiology. The arguments for an intrinsic mechanism are opposed by the ability of various AEDs to induce the expression of a number of transporters (Wen et al., 2008; Leroy et al., 2011; Moermana et al., 2011).

P-gp has been shown to be induced in several in vitro investigations. Firstly, chronic treatment with PHT, PB and CBZ was shown to decrease levels of the P-gp substrate rhodamine 123 in rat brain suggesting induced function and/or expression of P-gp following treatment with the respective AEDs (Wen et al., 2008). Treatment with AEDs, in this case PHT, TPM and LEV, has also been shown to decrease brain concentrations of the P-gp substrate desmethyl-loperamide in the mouse, again suggesting induced expression of P-gp (Moermana et al., 2011). Interestingly, in the latter of these investigations, induction of P-gp was seen to be concentration dependent, whereby therapeutic concentrations of PHT, TPM and LEV were reported to induce P-gp, while supra-therapeutic concentrations did not. In contrast, my investigation in hCMEC/D3 cells showed a decrease in expression of P-gp following treatment with VPA, LTG, GBP and TPM for 48 hours. In vitro studies, including findings from chapter 5, have largely reported that treatment with AEDs does not alter expression of P-gp (Aronica et al., 2012). However, there are several discrepancies between in vitro and in vivo findings (Wen et al., 2008; Moermana et al., 2011) that could account for the conflicting findings reported. In vivo investigations have typically involved treated animals with AEDs for much longer time periods than those employed in in vitro studies, which could reasonably explain differences in the extent of induction observed. However, it is unlikely that this can fully explain why induction is observed in vivo but not in vitro. In addition to the capacity to induce the expression of P-gp, it has been shown that some drugs can also activate P-gp; i.e. induce the transport of a substrate

without induction at the gene level (Sterz et al., 2009). As the majority of in vivo investigations have drawn conclusions from the observation that P-gp substrate concentrations are decreased in the brain following AED treatment, it is possible that the decreased substrate concentration observed in these studies is the result of activation of P-gp by AEDs rather than induction of its expression.

Several studies have investigated changes in the expression of influx transporters of the SLC family in both animal models of epilepsy and human epilepsy tissue. As discussed previously, MCT1 has been shown to be deficient on the endothelium of microvessels at the epileptogenic focus in tissue resected in the treatment of drug resistant TLE (Lauritzen et al., 2011). The same authors reported a similar deficiency in MCT1 on the endothelium of microvessels in 3 novel rat models of TLE. Recently, and in contrast to the reduced expression of MCT1 observed by Lauritzen and colleagues (2011), MCT1 has been shown to be upregulated in the lithium-pilocarpine model of TLE (Leroy et al., 2011). Conflicting findings observed in these studies may be the result of differing methodologies, with one report investigating whole brain expression and the other studying microvessel expression only. Interestingly, in addition to microvessel expression analysis, Lauritzen and colleagues (2012) also analysed astrocyte expression of MCT1 in rat models of TLE and reported an increase (Lauritzen et al., 2012). Thus, the increase in overall expression of MCT1 observed by Leroy and colleagues (2011) may represent the cumulative change in expression of MCT1 in TLE, assuming that changes in astrocytic expression outweigh those observed at brain microvessels. Furthermore, as described in chapter 5, MCT1 expression in hCMEC/D3 cells was induced following treatment with CBZ and VPA, while VPA also increased MCT2 expression (chapter 5). These findings are intriguing and imply that changes in brain expression of MCT transport systems in people with epilepsy may be due to a combination of underlying disease pathology, uncontrolled seizures and chronic AED treatment.

The ability of a drug to passively cross the BBB or to require carrier mediated brain uptake has been shown to be largely dependent on the octanol/water coefficient, i.e. its lipophilicity in addition to a number of physiochemical properties (Waterbeemd et al., 1998; Pajouhesh et al., 2005). The properties of AEDs that are known to influence their BBB permeability were investigated in chapter 6. A number of AEDs, including LTG,

GBP and TPM, possessed unfavourable properties and are thus unlikely to passively cross the BBB. Despite this, LTG, GBP and TPM reach adequate brain concentrations and may therefore exploit a carrier mediated uptake system. Indeed, LTG has been shown to be transported OCT1 (Dickens et al., 2012), in addition to weak transport by OAT1 and OAT3 (chapter 4). GBP is known to be transported by LAT-1 (Welty et al., 1993; Dickens et al., 2012) and MCT1 (chapters 2 and 3), while TPM has been shown to be transported by P-gp (Sills et al., 2002) and is suggested to utilize PEPT1, OCTN1 or OCTN2 or a combination of all three systems at the level of absorption from the gut (Watanabe et al., 2002).

A number of AEDs achieve adequate brain accumulation despite unfavourable physiochemical properties and may thus be substrates for SLC transporters. It is increasingly unlikely that changes in expression of transporters at the BBB prevent AEDs from reaching their intended targets in the brain and thereby causing drug resistance. The scientific plausibility of the drug transporter hypothesis relies on the fundamental premise that multiple AEDs are substrates for one or more transporter systems at the BBB. Despite almost two decades of research, it still remains largely unclear whether AEDs are transported by P-gp, far less any other ABC or SLC transporter. Individual differences in transporter expression at the BBB may be responsible for variability in brain concentrations of AEDs that rely on carrier mediated systems but this is unlikely to be clinically significant.

Future work investigating the transporter hypothesis is unlikely to be of value, however the potential implication of transporter science in AED design to improve pharmacokinetics of current and future AEDs merits further attention.

To overcome candidate drug attrition due to poor oral bioavailability the pharmaceutical industry have employed strategies to develop prodrugs which have been structurally designed to be recognised by high capacity uptake transporters expressed at the gastrointestinal epithelium (Majumdar *et al*., 2004). Once across the gastrointestinal barrier the prodrugs are transformed chemically or enzymatically to the active drug. There has been some success using this strategy, for example in the design of prodrugs which are recognised by peptide (Balimane *et al*., 1998) or monocarboxylic acid transporters (Cundy *et al*., 2004) expressed at the gastrointestinal tract. More recently

exploitation of transporters for tissue-specific delivery of drugs has emerged as a promising strategy for overcoming efficacy and toxicity issues (Zhou *et al*., 2015). For example activators of glucokinase represent promising targets in the treatment of type 2 diabetes (Leighton *et al*., 2005). However their use is limited by concerns that systemic distribution will result in over activation of glucokinase expressed in the pancreas, eliciting risk of hypoglycaemia and increased stress on β-cells (Bebernitz *et al*., 2009). To overcome this, hepato-selective glucokinase activators have been designed to be recognised by the liver OATP transporters OATP1B1, OATP1B3 and OATP2B1, which are not expressed in pancreas, therefore enhancing liver uptake and minimising pancreatic exposure (Pfefferkorn *et al.*, 2012).

To date transporter targeted delivery across the BBB has not been actively pursued, potentially due to the lack of detailed characterisation of BBB transporters when compared to organs such as the intestine, kidney and liver. However it is plausible that a similar strategy could be employed in the future to target delivery of CNS acting drugs such as AEDs to the brain. Therefore improving brain accumulation and limiting exposure to other tissues, albeit providing the targeted transporter is not ubiquitously expressed.

Recently an orphan transporter of the major facilitator family with unknown function; *MFSD2A*, has been shown to be specifically and constitutively expressed at the BBB (Ben-Zvi *et al*., 2014; Nguyen *et al*., 2014). Interestingly *MFSD2A* has been demonstrated to maintain two functions at the BBB. To provide the major transport route of the essential omega-3 fatty acid docosahexaenoic into the brain (Nguyen *et al*., 2014) and to regulate transcytosis in cerebral endothelial cells (Ben-Zvi *et al*., 2014). The later of the two functions has been demonstrated to be critical in the maintenance of the BBB. Knock-out mice lacking the *MFSD2A* gene develop a 'leaky' BBB, permeable to large molecules, attributed to increased transcytosis opposed to tight-junction disruption (Ben-Zvi *et al*., 2014). In addition to its constitutive expression at the functional BBB, *MFSD2A* has been demonstrated to be expressed at various stages in mouse embryogenesis suggesting *MFSD2A* plays a role in the formation of the BBB (Ben-Zvi *et al*., 2014).

The identification of *MFSD2A* at the BBB represents an exciting opportunity for both BBB restoration and targeted CNS delivery. This is the first transporter selectively expressed at the BBB and therefore could be exploited to specifically target delivery of new antiepileptic drugs (or indeed existing AEDs) to the brain. Although extensive further work would be necessary to fully understand the physiological role of this membrane transporter and characterise the essential structural features for substrate binding, AEDs could be developed to be recognised by *MFSD2A* and actively transported across the BBB, therefore selectively enhancing exposure to the brain. Alternatively *MFSD2A* could be pharmacologically suppressed to enhance transcytosis-mediated drug delivery to the brain, although this strategy is likely to be met with adverse effects.

Transporter science may not have provided us with an adequate explanation for why some individuals with epilepsy experience pharmacoresistant seizures but it is nonetheless important to understand the role of carrier mediated systems in the disposition of AEDs and the potential of transporter-targeted delivery as a strategy to improve future AED development.

8. Bibliography

Abbott JN (2013). Blood-brain barrier structure and function and the challenges for CNS drug delivery. *Journal of Inherited Metabolism Disease* **36**(3)**:** 437-449.

Abbott NJ, Patabendige AAK, Dolman DEM, Yusof SR, Begley DJ (2010). Structure and function of the blood-brain barrier. *Neurobiology of Disease* **37**(1)**:** 13-25.

Abbott NJ, Romero IA (1996). Transporting theraputics across the blood-brain barrier. In: *Molecular Medicine Today*, pp 106-113: Elsevier Science LTD.

Adachi T, Nakagawa H, Chung I, Hagiya Y, Kazuyuki Hoshijima1, Noguchi N, *et al.* (2007). Nrf2-dependent and -independent induction of ABC transporters ABCC1, ABCC2, and ABCG2 in HepG2 cells under oxidative stress. *Journal of experimental Theraputics and Oncology* **6:** 335-348.

Adkinson KDK, Shen DD (1996). Uptake of Valproic Acid into Rat Brain Is Mediated by a Medium-Chain Fatty Acid Transporter. *Pharmacology and Experimental Theraputics* **276:** 1189-1200.

Ahn S-Y, Eraly SA, Tsigelny I, Nigam SK (2009). Interaction of Organic Cations with Organic Anion Transporters. *Journal of Biological Chemistry* **284**(45)**:** 31422-31430.

Anari MR, Burton RW, Gopaul S (2000). Metabolic profiling of valproic acid by cDNA-expressed human cytochrome P450 enzymes using negative-ion chemical ionisation gas chromatography-mass spectrometry. *Journal of Chromatography B: Biomedical Sciences and Applications* **742:** 217-227.

Ander JB-S, Pfeiffer SE, Fuller SD, Simons K (1984). Development of cell surface polarity in the epithelial Madin-Darby canine kidney (MDCK) cell line. *The EMBO Journal* **3**(11)**:** 2687-2694.

Anhut H, Ashman P, Feuerstein TJ, Sauermann W, Saunders M, Schmidt B (1994). Gabapentin (Neurontin) as add on therapy in patients with partial seizures: a double-blind, placebo-controlled study. *Epilepsia* **35:** 795-801.

Anonymous (1988). Sodium valproate. *Lancet* **2**(8622)**:** 1229-1231.

Anonymous (2003). The History and Stigma of Epilepsy. *Epilepsia* **44**(6)**:** 12-14.

Anzai N, Kanai Y, Endou H (2006). Organic anion transporter family: Current knowledge. *Journal of Pharmacological Sciences* **100**(5)**:** 411-426.

Aronica E, Gorter JA, Jansen GH, van Veelen CWM, van Rijen PC, Leenstra S, *et al.* (2003). Expression and cellular distribution of multidrug transporter proteins in two major causes of medically intractable epilepsy: focal cortical dysplasia and glioneuronal tumors. *Neuroscience* **118:** 417-429.

Aronica E, Sisodiya SM, Gorter JA (2012). Cerebral expression of drug transporters in epilepsy. *Advanced Drug Delivery Reviews* **64:** 919-929.

Aslamkhan AG, Han Y-H, Yang X-P, Zalups RK, Pritchard JB (2003). Human Renal Organic Anion Transporter 1-Dependent Uptake and Toxicity of Mercuric-Thiol Conjugates in Madin-Darby Canine Kidney Cells. *Molecular Pharmacology* **63**(2)**:** 590–596.

Badagnani I, Castro RA, Taylor TR, Brett CM, Huang CC, Stryke D, *et al.* (2006). Interaction of methotrexate with organic-anion transporting polypeptide 1A2 and its genetic variants. *Journal of Pharmacology and Experimental Therapeutics* **318**(2)**:** 521-529.

Balimane PV, Tamai I, Guo A, Nakanishi T, Kitada H, *et al*. (1998). Direct evidence for Peptide Transporter (PepT1)-mediated Uptake of a Nonpeptide Prodrug, Valacyclovir. *Biochemical and Biophysical Research Communications* **250**: 246-251.

Bankstahl J, Loescher W (2008). Resistance to antiepileptic drugs and expression of P-glycoprotein in two rat models of status epilepticus. *Epilepsy Research* **82:** 70-85.

Bebernitz GR, Beaulieu V, Dale BA, Deacon R, Duttaroy A, *et al*. (2009). Investigation of Functionally Liver Selective Glucokinase Activators for the Treatment of Type 2 Diabetes. *Journal of Medicinal Chemistry* **52** (19)**:** 6142–6152.

Benarroch EE (2012). Blood-brain barrier: Recent developments and clinical correlations. *Neurology* **78:** 1268-1276.

Ben-Zvi A, Lacoste B, Kur E, Andreone BJ, Mayshar Y (2014). *MFSD2A* is critical for the formation and function of the blood-brain barrier. *Nature* **509:** 507-511.

Bialer M, White HS (2010). Proposed mechanisms of action of currently available AEDs at excitatory and inhibitory synapses. *Nature Reviews Drug Discovery* **9:** 68-82.

Bleasby K, Castle JC, Roberts CJ, Cheng C, Bailey WJ, Sina JF, *et al.* (2006). Expression profiles of 50 xenobiotic transporter genes in humans and pre-clinical species: A resource for investigations into drug disposition. *Xenobiotica* **36**(10-11)**:** 963–988.

Blom S (1962). Trigeminal neuralgia: its treatment with a new anticonvulsant drug (G-32883). *Lancet* **1:** 829-840.

Booth L, Thompson G (2010). Epilepsy statistics, Statistics SaG (ed): House of Commons Library.

Borst P, Evers R, Kool M, Wijnholds J (2000). A Family of Drug Transporters: the Multidrug Resistance-Associated Proteins. *Journal of the National Cancer Institute* **92**(16)**:** 1295-1302.

Bourgeois BFD (2000). Pharmacokinetics and Pharmacodynamics of Topiramate. *Journal of Child Neurology* **15**(supplement 1)**:** 27-30.

Brandt C, Bethmann K, Gastens AM, Löscher W (2006). The multidrug transporter hypothesis of drug resistance in epilepsy: Proof-of-principle in a rat model of temporal lobe epilepsy. *Neurobiology of Disease* **24**(1)**:** 202-211.

Braun D, Kim TD, Coutre PL, Köhrle J, Hershman JM, Schweizer U (2011). Tyrosine kinase inhibitors noncompetitively inhibit MCT8 mediated Iodothyronine transport *The Journal of Clinical Endocrinology and Metabolism* **97**(1-6).

Brodie MJ (1992). Drug interactions in epilepsy. *Epilepsia* **33**(Supplement 1)**:** 13-22.

Brodie MJ (2010). Antiepileptic drug therapy the story so far. *Seizure* **19:** 650-655.

Brodie MJ, Dichter MA (1996a). Antiepileptic Drugs. *New England Journal of Medicine* **334**(7).

Brodie MJ, Dichter MA (1996b). New Antiepileptic drugs. *New England Journal of Medicine* **334**(24)**:** 1583-1590.

Bröer S (2014). The SLC38 family of sodium–amino acid co-transporters. *European Journal of Physiology* **466**(1)**:** 155-172

Burckhardt G (2012). Drug transport by Organic Anion Transporters (OATs). *Pharmacology and Therapeutics* **136:** 106-130.

Burckhardt G, Burckhardt BC (2011). In Vitro and In Vivo Evidence of the Importance of Organic Anion Transporters (OATs) in Drug Therapy. In: Fromm MF, Kim RB (eds). *Handbook of Experimental Pharmacology*, edn, Vol. 201. Berlin: Springer-Verlag. p^pp 29-104.

Byrne S, Kearns J, Carolan R, McMenamin J, Klepper J, Webb D (2011). Refractory absence epilepsy associated with GLUT-1 deficiency syndrome. *Epilepsia* **52**(5)**:** 1021-1024.

Cardoso FL, Brites D, Brito MA (2010). Looking at the blood-brain barrier: Molecular anatomy and possible investigation approaches. *Brain Research Reviews* **64:** 328-363.

Carl SM, Lindley DJ, Couraud PO, Weksler BB, Romero I, Mowery SA, *et al.* (2010). ABC and SLC transporter expression and pot substrate chracterization across the human hCMEC/D3 blood-brain barrier cell line. *Molecular Pharmaceutics* **7**(4)**:** 1057–1068.

Cerveny L, Pavek P, Malakova J, Staud F, Fendric Z (2006). Lack of Interactions between Breast Cancer Resistance Protein (BCRP/ABCG2) and Selected Antiepileptic Agents. *Epilepsia* **47**(3)**:** 461-468.

Cha SH, Sekine T, Fukushima J-I, Kanai Y, Kobayashi Y, Goya T, *et al.* (2001). Identification and Characterization of Human Organic Anion Transporter 3 Expressing Predominantly in the Kidney. *Molecular Pharmacology* **59:** 1277–1286.

Cha SH, Sekine T, Kusuhara H, Yu E, Kim JY, Kim DK, *et al.* (2000). Molecular cloning and characterization of multispecific organic anion transporter 4 expressed in the placenta. *Journal of Biological Chemistry* **275**(6)**:** 4507-4512.

Chen C, Mireles RJ, Campbell SD, Lin J, Mills JB, Xu JJ et al (2005). Differential interaction of 3-hydroxy-3-methylglutaryl-coA reductase inhibitors with ABCB1, ABCC2, and OATP1B1. *The American Society for Pharmacology and Experimental Therapeutics* **33**(4)**:** 537-546.

Chennavasin P, Seiwell R, Brater DC, Liang WMM (1979). Pharmacodynamic analysis of the furosemide-probenecid interaction in man. *Kidney International* **16:** 187-195.

Choi MK, Song IS (2008). Organic cation transporters and their pharmacokinetic and pharmacodynamic consequences. *Drug Metabolism and Pharmacokinetics* **23**(4)**:** 243-253.

Chu X-Y, Bleasby K, Yabut J, Cai X, Chan GH, Hafey MJ, *et al.* (2007). Transport of the Dipeptidyl Peptidase-4 Inhibitor Sitagliptin by Human Organic Anion Transporter 3, Organic Anion Transporting Polypeptide 4C1, and Multidrug Resistance P-glycoprotein. *Pharmacology and Experimental Theraputics* **321**(2)**:** 673–683.

Ciarimboli G (2008). Organic cation transporters. *Xenobiotica* **38**(7-8)**:** 936-971.

Cihlar T, Lin DC, Pritchard JB, Fuller MD, Mendel DB, Sweet DH (1999). The Antiviral Nucleotide Analogs Cidofovir and Adefovir Are Novel Substrates for Human and Rat Renal Organic Anion Transporter 1. *Molecular Pharmacology* **56:** 570-580.

Cohen AF, Land GS, Breimer DD (1987). Lamotrigine, a new anticonvulsant: pharmacokinetics in normal humans. *Clinical Pharmacology and Therapeutics* **42:** 535-541.

Conseil G, Baudichon-Cortay H, Dayan G, Jault JM, Barron D, Di Pietro A (1998). Flavonoids: a class of modulators with bifunctional interactions at vicinal ATP and steroid binding sites on mouse P-glycoprotein. *PNAS* **95:** 9831-9836.

Corpe CP, Eck P, Wang J, Al-Hasani H, Levine M (2013). Intestinal Dehydroascorbic Acid (DHA) Transport Mediated by the Facilitative Sugar Transporters, GLUT2 and GLUT8. *The Journal of Biological Chemistry* **288**(13)**:** 9092–9101.

Cropp CD, Komori T, Shima JE, Urban TJ, Sook WY, More SS, *et al.* (2008). Organic anion transporter 2 (SLC22A7) is a facilitative transporter of cGMP. *Molecular Pharmacology* **73**(4)**:** 1151-1158.

Cross JH, Riney CJ (2009). Topiramate. In: *The Treatment of Epilepsy*, Shorvon S, Perucca E, Engel J (eds), 3 edn, pp 673-683: Blackwell Publishing LTD.

Crowe A, Teoh Y-K (2006). Limited P-glycoprotein mediated efflux for anti-epileptic drugs. *Journal of Drug Targetting* **14**(5)**:** 291-300.

Cundy KC, Branch R, Chernov-Rogan T, Dias T, Estrada T, Hold K, *et al.* (2004). XP13512, A Novel Gabapentin Prodrug: I. Design, Synthesis, Enzymatic Conversion to Gabapentin, and Transport by Intestinal Solute Transporters. *The Journal of Pharmacology and Experimental Theraputics* **311**(1)**:** 315-323.

Dallas S, Miller DS, Bendayan R (2006). Multidrug resistance-associated proteins: Expression and function in the central nervous system. *Pharmacological Reviews* **58**(2)**:** 140-161.

Dauchy S, Miller F, Couraud P-O, Weaver RJ, Weksler B, Romero I-A, *et al.* (2009). Expression and transcriptional regulation of ABC transporters and cytochromes P450 in hCMEC/D3 human cerebral microvascular endothelial cells. *Biochemical Pharmacology* **77:** 897-909.

de Lange ECM (2004). Potential role of ABC transporters as a detoxification system at the blood-CSF barrier. *Advanced Drug Delivery Reviews* **56:** 1793-1809.

Dickens D, Owen A, Alfirevica A, Giannoudis A, Davies A, Weksler B, *et al.* (2012). Lamotrigine is a substrate for OCT1 in brain endothelial cells. *Biochemical Pharmacology* **83**(6)**:** 805-814.

Dickens D, Yusof SR, Abbott NJ, Weksler B, Romero IA, Couraud P-O, *et al.* (2013). A Multi-System Approach Assessing the Interaction of Anticonvulsants with P-gp. *PLOS One* **8**(5)**:** 1-10.

Dimmer K-S, Friedrich B, Lang F, Deitmer JW, Bröer S (2000). The low-affinity monocarboxylate transporter MCT4 is adapted to the export of lactate in highly glycolytic cells. *Biochemical Journal* **350:** 219-227.

Dombrowski SM, Desai SY, Marroni M, Cucullo L, Goodrich K, Bingaman W, *et al.* (2001). Overexpression of multiple drug resistance genes in endothelial cells from patients with refractory epilepsy. *Epilepsia* **42:** 1501-1506.

Draper MP, Martell RL, Levy SB (1997). Indomethacin-mediated reversal of multidrug resistance and drug efflux in human and murine cell lines overexpressing MRP, but not P-glycoprotein. *British Joural of Cancer* **75(**6): 810–815.

Dreifuss FE, Bancaud J, Henriksen O (1981). Proposal for revised clinical and electroencephalographic classification of epileptic seizures. *Epilepsia* **22**(4)**:** 489-501.

Dresser MJ, Leabman MK, Giacomini KM (2000). Transporters Involved in the Elimination of Drugs in the Kidney: Organic Anion Transporters and Organic Cation Transporters. *Journal of Pharmaceutical Sciences* **90**(4)**:** 397-421.

Eadie MJ (2009). Phenytoin. In: Shorvon S, Perucca E, Engel J (eds). *The Treatment of Epilepsy*, edn: Blackwell Publishing LTD. p^pp 605-618.

Eechoute K, Franke RM, Loos WJ, Scherkenbach LA, Boere I, Verweij J, *et al.* (2011a). Environmental and genetic factors affecting transport of imatinib by OATP1A2. *Clinical Pharmacology and Therapeutics* **89**(6)**:** 816-820.

Eechoute K, Sparreboom A, Burger H, Franke RM, Schiavon G, Verweij J, *et al.* (2011b). Drug transporters and imatinib treatment: Implications for clinical practice. *Clinical Cancer Research* **17**(3)**:** 406-415.

Eigenmann DE, Xue G, Kim KS, Moses AV, Hamburger M, Oufir M (2013). Comparative study of 4 immortalized human brain capillary endothelial cell lines, HCMEC/D3, HBMEC, TY10 and BB19, and optimization of culture conditions, for an *in vitro* blood-brain barrier model for drug permeability studies. *Fluids and Barriers of the CNS* **10**(33).

Ekberg H, Qi Z, Pahlman C, Veress B, Bundick RV, Craggs RI, *et al.* (2007). The Specific Monocarboxylate Transporter-1 (MCT-1) Inhibitor, AR-C117977, Induces Donor-Specific Suppression, Reducing Acute and Chronic Allograft Rejection in the Rat. *Transplantation* **84**(9)**:** 1191-1199.

Elger CE, Schmidt D (2008). Modern management of epilepsy: A practical approach. *Epilepsy & Behaviour* **12**(4): 501-539

Elmorsi YM, El-Haggar SM, Ibrahim OM, Mabrouk MM (2013). Effect of ketoprofen and indomethacin on methotrexate pharmacokinetics in mice plasma and tumor tissues. *European Journal Of Drug Metabolism And Pharmacokinetics* **38:** 27–32.

Enerson BE, Drewes LR (2003). Molecular Features, Regulation, and Function of Monocarboxylate Transporters: Implications for Drug Delivery. *Journal of Pharmaceutical Sciences* **92**(8)**:** 1531-1544.

Enomoto A, Takeda M, Shimoda M, Narikawa S, Kobayashi Y, Kobayashi Y, *et al.* (2002). Interaction of Human Organic Anion Transporters 2 and 4 with Organic Anion Transport Inhibitors. *Pharmacology and Experimental Theraputics* **301:** 797–802.

Eraly SA, Hamilton BA, Nigam SK (2003). Organic anion and cation transporters occur in pairs of similar and similarly expressed genes. *Biochemical and Biophysical Research Communications* **300:** 333–342.

Estudante M, Morais JG, Soveral G, Benet LZ (2013). Intestinal drug transporters: An overview. *Advanced Drug Delivery Reviews* **65:** 1340-1356.

Feldmann M, Asselin M-C, Liu J, Wang S, McMahon A, Anton-Rodriguez J, *et al.* (2013). P-glycoprotein expression and function in patients with temporal lobe epilepsy: a case-control study. *Lancet Neurology* **12:** 777-785.

Fischer W, Praetor K, Metzner L, Neubert RHH, Brandsch M (2008). Transport of valproate at intestinal epithelial (Caco-2) and brain endothelial (RBE4) cells: Mechanism and substrate specificity. *European Journal of Pharmaceutics and Biopharmaceutics* **70**(2)**:** 486-492.

Fisher RS, van Emde Boas W, Blume W, Elger C, Genton P, Lee P, *et al.* (2005). Epileptic Seizures and Epilepsy: Definitions Proposed by the International League Against Epilepsy (ILAE) and the International Bureau for Epilepsy (IBE). *Epilepsia* **46**(4)**:** 470–472.

Forman SA, Verkman AS, Dix JA, Solomon AK (1982). Interaction of phloretin with the anion transport protein of the red blood cell membrane. *Biochimica et Biophysica Acta (BBA) - Biomembranes* **689**(3): 531-538.

Fotiadisa D, Kanaib Y, Palacínc M (2013). The SLC3 and SLC7 families of amino acid transporters. *Molecular Aspects of Medicine* **34**(2-3)**:** 139-158.

Franke D, Diletti E, Hoffmann C (1995). Relative bioavailability of different valproic acid formulations. *International Journal of Clinical Pharmacology and Therapeutics* **33:** 653-657.

French JA, Tonner F (2009). Levetiracetam. In: *The Treatment of Epilepsy*, Shorvon S, Perucca E, Engel J (eds), 3 edn: Blackwell Publishing LTD.

Friesema ECH, Ganguly S, Abdalla A, Manning Fox JE, Halestrap AP, Visser TJ (2003). Identification of monocarboxylate transporter 8 as a specific thyroid hormone transporter. *Journal of Biological Chemistry* **278**(41)**:** 40128-40135.

Fujiwara K, Adachi H, Nishio T, Unno M, Tokui T, Okabe M, *et al.* (2001). Identification of thyroid hormone transporters in humans: Different molecules are involved in a tissue-specific manner. *Endocrinology* **142**(5)**:** 2005-2012.

Gallegos TF, Martovetsky G, Kouznetsova V, Bush KT, Nigam SK (2012). Organic Anion and Cation SLC22 ‘‘Drug’’ Transporter (Oat1, Oat3, and Oct1) Regulation during Development and Maturation of the Kidney Proximal Tubule. *PLOS One* **7**(7)**:** 1-13.

Garcia CK, Goldstein JL, Pathak RK, Anderson RGW, Brown MS (1994). Molecular characterization of a membrane transporter for lactate, pyruvate, and other monocarboxylates: Further study of the effect implications for the Cori cycle. *Cell* **76:** 865-873.

Geier EG, Chen EC, Webb A, Papp AC, Yee SW, Sadee W, *et al.* (2013). Profiling Solute Carrier Transporters in the Human Blood-Brain Barrier. *Clinical Pharmacology and Therapeutics* **94**(6)**:** 636-639.

Genton P, Vleymen BV (2000). Piracetam and levetiracetam: close structural similarities but different pharmacological and clinical profiles. *Epileptic Disorders* **2:** 99-105.

Gerhart DZ, Enerson BE, O Y Zhdankina, Leino RL, Drewes LR (1997). Expression of monocarboxylate transporter MCT1 by brain endothelium and glia in adult and suckling rats. *american Journal of Physiology - Endocrinology and Metabolism* **273**(1)**:** 207-213.

Giacomini KM, Huang SM, Tweedie DJ, Benet LZ, Brouwer KLR, Chu X, *et al.* (2010). Membrane transporters in drug development. *Nature Reviews Drug Discovery* **9**(3)**:** 215-236.

UK Gabapentin Study Group (1990). Gabapentin in partial epilepsy. *Lancet* **335:** 1114-1117.

Guile SD, Bantick JR, Cheshire DR, Cooper ME, Davis AM, Donald DK, *et al.* (2006). Potent blockers of the monocarboxylate transporter MCT1: Novel immunomodulatory compounds. *Bioorganic & Medicinal Chemistry Letters* **16:** 2260–2265.

Hagenbuch B, Gui C (2008). Xenobiotic transporters of the human organic anion transporting polypeptides (OATP) family. *Xenobiotica* **38**(7-8)**:** 778-801.

Hagenbuch B, Meier PJ (2003). The superfamily of organic anion transporting polypeptides. *Biochimica et Biophysica Acta - Biomembranes* **1609**(1)**:** 1-18.

Hagenbuch B, Meier PJ (2004). Organic anion transporting polypeptides of the OATP/SLC21 family: Phylogenetic classification as OATP/SLCO super-family, new nomenclature and molecular/functional properties. *Pflugers Archiv European Journal of Physiology* **447**(5)**:** 653-665.

Hagos Y, Bahn A, Vormfelde SV, Brockmöller J, Burckhardt G (2007). Torasemide Transport by Organic Anion Transporters Contributes to Hyperuricemia. *Journal of the American Society of Nephrology* **18:** 3101–3109.

Hagos Y, Wolff NA (2010). Assessment of the Role of Renal Organic Anion Transporters in Drug-Induced Nephrotoxicity. *Toxins* **2:** 2055-2082.

Halestrap AP (2013). The SLC16 gene family - Structure, role and regulation in health and disease. *Molecular Aspects of Medicine* **34:** 337-349.

Halestrap AP, Meredith D (2004). The SLC16 gene family -from monocarboxylate trasnporters (MCTs) to aromatic amino acid transporters and beyond. *European Journal of Physiology* **447:** 619-628.

Halestrap AP, Poole RC, Cranmer SL (1990). Mechanisms and regulation of lactate, pyruvate and ketone body transport across the plasma membrane of mammalian cells and their metabolic consequences. *Biochemical Society Transactions* **18**(6)**:** 1132-1135.

Halestrap AP, Price NT (1999). The proton-linked monocarboxylate transporter (MCT) family: structure, function and regulation. *Biochemical Journal* **343:** 281-299.

Hansch C, Leo A (1979). *Substituent constant for correlation analysis in chemistry and biology*. edn. Wiley: New York.

Hartkoorn RC, Kwan WS, Shallcross V, Chaikan A, Liptrott N, Egan D, *et al.* (2010). HIV protease inhibitors are substrates for OATP1A2, OATP1B1 and OATP1B3 and lopinavir plasma concentrations are influenced by SLCO1B1 polymorphisms. *Pharmacogenetics and Genomics* **20**(2)**:** 112-120.

Hauptmann A (1912). Luminal bei Epilepsie. *Munch Med Wochenschr* **59:** 1907-1909.

He L, Vasiliou K, Nebert DW (2009). Analysis and update of the human solute carrier (SLC) gene superfamily. *Human genomics* **3**(2)**:** 195-206.

Hertz L, Dienel GA (2004). Lactate Transport and Transporters: General Principles and Functional Roles in Brain Cells. *Journal of Neuroscience Research* **79:** 11-18.

Heuer H, Visser TJ (2009). Minireview: Pathophysiological Importance of Thyroid Hormone Transporters. *Endocrinology* **150**(3)**:** 1078-1083.

Hirano M, Maeda K, Shitara Y, Sugiyama Y (2004). Contribution of OATP2 (OATP1B1) and OATP8 (OATP1B3) to the hepatic uptake of pitavastatin in humans. *The Journal of Pharmacology and Experimental Therapeutics* **311:** 139-146.

Hirano M, Maeda K, Shitara Y, Sugiyama Y (2006). Drug-drug interaction between pitavastatin and various drugs via oatp1b1. *Drug Metabolism and Disposition* **34:** 1229-1236.

Ho RH, Tirona RG, Leake BF, Glaeser H, Lee W, Lemke CJ *et al*. (2006). Drug and bile acid transporters in rosuvastatin hepatic uptake: function, expression, and pharmacogenetics. *Gastroenterology* **130:** 1793-1806.

Hu S, Franke RM, Filipski KK, Hu C, Orwick SJ, Bruijn EAd, *et al.* (2008). Interaction of Imatinib with Human Organic Ion Carriers. *Clinical Cancer Research* **14:** 3141-3148.

Huber RD, Gao B, Pfändler MAS, Zhang-Fu W, Leuthold S, Hagenbuch B, *et al.* (2007). Characterization of two splice variants of human organic anion transporting polypeptide 3A1 isolated from human brain. *American Journal of Physiology - Cell Physiology* **292**(2)**:** 795-806.

Inui K, Masuda S, Saito H (2000). Cellular and molecular aspects of drug transport in the kidney. *Kidney Internationa*l **58:** 944–958.

Ishikawa T (1992). The ATP-dependent glutathione S-conjugate export pump. *Trends in Biochemical Sciences* **17:** 463-468.

Joost H-G, Thorens B (2001). The extended GLUT-family of sugar/polyol transport facilitators: nomenclature, sequence characteristics, and potential function of its novel members. *Molecular Membrane Biology* **18:** 247-256.

Juhász V, Beéry E, Nagy Z, Bui A, Molnár É, Zolnerciks JK, *et al.* (2013). Chlorothiazide is a Substrate for the Human Uptake Transporters OAT1 and OAT3. *Journal of Pharmaceutical Sciences* **102**(5)**:** 1683-1687.

Juliano R, Ling V (1976). A surface glycoprotein modulating drug permeability in chinese hamster ovary cell mutants. *Biochimica et Biophysica Acta (BBA)* **455:** 152-162.

Kalliokoski A, Niemi M (2009). Impact of OATP transporters on pharmacokinetics. *British Journal of Pharmacology* **158**(3)**:** 693-705.

Kamiie J, Ohtsuki S, Iwase R, Ohmine K, Katsukura Y, Yanai K, *et al.* (2008). Quantitative atlas of membrane transporter proteins: development and application of a highly sensitive simultaneous LC/MS/MS method combined with novel in-silico peptide selection criteria. *Pharmaceutical Research* **25**(6)**:** 1469-1483.

Kanner AM, Frey M (2000). Adding valproate to lamotrigine: a study of their pharmacokinetic interaction. *Neurology* **55:** 588-591.

Karasinska JM, Haan Wd, Franciosi S, Ruddle P, Fan J, Kruit JK, *et al.* (2013). ABCA1 influences neuroinflammation and neuronal death. *Neurobiology of Disease* **54:** 445–455.

Katano K, Kondo A, Safaei R, A Holzer, Samimi G, Mishima M, *et al.* (2002). Acquisition of resistance to cisplatin is accompanied by changes in the cellular pharmacology of copper. *Cancer Research* **62**(22)**:** 6559–6565.

Kikuchi R, Kusuhara H, Sugiyama D, Sugiyama Y (2003). Contribution of Organic Anion Transporter 3 (SLC22A8) to the Elimination of p-Aminohippuric acid and Benzylpenicillin across the Blood Brain Barrier. *The Journal of Pharmacology and Experimental Theraputics* **306:** 51-58.

Kim TK, Eberwine JH (2010). Mammalian cell transfection: the present and the future. *Analytical and Bioanalytical Chemistry* **397:** 3173–3178.

Kirk P, Wilson MC, Heddle C, Brown MH, Barclay AN, Halestrap AP (2000). CD147 is tightly associated with lactate transporters MCT1 and MCT4 and facilitates their cell surface expression. *EMBO Journal* **19**(15)**:** 3896-3904.

Klaassen CD, Aleksunes LM (2010). Xenobiotic, bile acid, and cholesterol transporters: Function and regulation. *Pharmacological Reviews* **62**(1)**:** 1-96.

Kobayashi M, Otsuka Y, Itagaki S, Hirano T, Iseki K (2006). Inhibitory effects of statins on human monocarboxylate transporter 4 *International Journal of Pharmaceutics* **317:** 19-25.

Kobayashi Y, Ohshiro N, Sakai R, Ohbayashi M, Kohyama N, Yamamoto T (2005). Transport mechanism and substrate specificity of human organic anion transporter 2 (hOat2 [SLC22A7]). *Journal of Pharmacy and Pharmacology* **57:** 573–578.

Kobow K, El-Osta A, Blümcke I (2013). The methylation hypothesis of pharmacoresistance in epilepsy *Epilepsia* **54**(Supplement 2)**:** 41-47.

Koepsell H, Lips K, Volk C (2007). Polyspecific Organic Cation Transporters: Structure, Function, Physiological Roles, and Biopharmaceutical Implications. *Pharmaceutical Research* **24**(7)**:** 1227-1251.

Komatsu T, Hiasa M, Miyaji T, Kanamoto T, Matsumoto T, Otsuka M (2011). Characterization of the human MATE2 proton-coupled polyspecific organic cation exporter. *International Journal of Biochemistry and Cell Biology* **43:** 913-918.

König J, Müller F, Fromm MF (2013). Transporters and Drug-Drug Interactios: Important Determinants of Drug Disposition and Effects. *Pharmacological Reviews* **65:** 944-966.

Kooijmans SAA, Senyschyn D, Mezhiselvam MM, Morizzi J, Charman SA, Weksler B, *et al.* (2012). The Involvement of a Na+- and Cl−-Dependent Transporter in the Brain Uptake of Amantadine and Rimantadine. *Molecular Pharmaceutics* **9:** 883-893.

Kopplow K, Letschert K, Konig J, Walter B, Keppler D (2005). Human hepatobiliary transport of organic anions analysed by quadruple-transfected cells. *Molecular Pharmacology* **68:** 1031-1038.

Kullak-Ublick GA, Ismair MG, Stieger B, Landmann L, Huber R, Pizzagalli F, *et al.* (2001). Organic anion-transporting polypeptide B (OATP-B) and its functional comparison with three other OATPs of human liver. *Gastroenterology* **120**(2)**:** 525-533.

Kuo CC (1998). A common anticonvulsant binding site for phenytoin, carbamazepine, and lamotrigine in neuronal Na+ channels. *Molecular Pharmacology* **54:** 712-721.

Kusuhara H, Sekine T, Utsunomiya-Tate N, Tsuda M, Kojima R, Cha SH, *et al.* (1999). Transporter from Rat Brain a New Multispecific Organic Anion Molecular Cloning and Characterization of a New Multispecific Organic Anion Transporter from Rat Brain. *The Journal of Biological Chemistry* **274:** 13675-13680.

Kusuhara H, Sugiyama Y (2005). Active efflux across the blood-brain barrier: Role of the solute carrier family. *NeuroRx* **2**(1)**:** 73-85.

Kutt H, Winters W, Kokenge R, McDowell F (1964). Diphenylhydantoin metabolism, blood levels, and toxicity. *Archives of Neurology* **11:** 642-648.

Kwan P, Arzimanoglou A, Berg AT, Brodie MJ, Hauser WA, Mathern G, *et al.* (2010). Definition of drug resistant epilepsy: Consensus proposal by the ad hoc Task Force of the ILAE Commission on Therapeutic Strategies. *Epilepsia* **51**(6)**:** 1069-1077.

Kwan P, Brodie MJ (2000). Early identification of refractory epilepsy. *New England Journal of Medicine* **342:** 314-319.

Kwan P, Brodie MJ (2004). Phenobarbital for the treatment of epilepsy in the 21st cetury: a critical review. *Epilepsia* **45**(9)**:** 1141-1149.

Lal R, Sukbuntherng J, Luo W, Virna VV, Blumenthal R, Ho J, *et al.* (2010). Clinical pharmacokinetic drug interaction studies of gabapentin enacarbil, a novel transported prodrug of gabapentin, with naproxen and cimetidine. *British Journal of Clinical Pharmacology* **69**(5)**:** 498-507.

Lamb RJ, Leach MJ, Miller AA, Hardenberg PJ (1985). Anticonvulsant profile in mice of lamotrigine, a novel anticonvulsant. *British Journal of Pharmacology* **85**.

Lauritzen F, de Lanerolle NC, Lee TSW, Spencer DD, Kim JH, Bergersen LH, *et al.* (2011). Monocarboxylate transporter 1 is deficient on microvessels in the human epileptogenic hippocampus. *Neurobiology of Disease* **41**(2)**:** 577-584.

Lauritzen F, Perez EL, Melillo ER, Roh JM, Zaveri HP, Lee TSW, *et al.* (2012). Altered expression of brain monocarboxylate transporter 1 in models of temporal lobe epilepsy. *Neurobiology of Disease* **45**(1)**:** 165-176.

Leach MJ, Marden CM, Miller AA (1986). Pharmacological studies on lamotrigine, a novel potential antiepileptic drug: II. Neurochemical studies on the mechanism of action. *Epilepsia* **27:** 490-497.

Lee SY, Williamson B, Caballero OL, Chen YT, Scanlan MJ, Ritter G, *et al.* (2004). Identification of the gonad-specific anion transporter SLCO6A1 as a cancer/testis (CT) antigen expressed in human lung cancer. *Cancer Immunity* **4**.

Leen WG, Klepper J, Verbeek MM, Leferink M, Hofste T, Engelen BGv, *et al.* (2010). Glucose transporter-1 deficiency syndrome: the expanding clinical and genetic spectrum of a treatable disorder. *Brain* **133:** 655–670.

Leeson PD, Davis AM (2004). Time-related differences in the physical property profiles of oral drugs. *Journal of Medicinal Chemistry* **47**(25)**:** 6338-6348.

Leighton B, Atkinson A, Coghla MP (2005). Small molecule glucokinase activators as novel anti-diabetic agents. *Biochemical Society Transactions* **33** (2)**:** 371-374.

Leroy C, Pierre K, Simpson IA, Pellerin L, Vannucci SJ, Nehlig A (2011). Temporal changes in mRNA expression of the brain nutrient transporters in the lithium-pilocarpine model of epilepsy in the immature and adult rat. *Neurobiology of Disease* **43:** 588–597.

Leslie EM, Mao Q, Oleschuk CJ, Deeley RG, Cole SP (2001). Modulation of multidrug resistance protein 1 (MRP1/ABCC1) transport and atpase activities by interaction with dietary flavonoids. *Molecular Pharmacology* **59:** 1171-1180.

Lipinski CA, Lombardo F, Dominy BW, Feeney PJ (1997). Experimental and computational approaches to estimate solubility and permeability in drug discovery and development settings. *Advanced Drug Delivery Reviews* **23:** 3-25.

Liu J, Thom M, Catarino C (2012). Neuropathology of the blood-brain barrier and pharmaco-resistance in human epilepsy. *Brain* **135:** 3115-3133.

Löscher W (2002). Basic pharmacology of valproate. A review after 35 years of clinical use for the treatment of epilepsy. *CNS Drugs* **16:** 669-694.

Loscher W, Frey H-H (1984). Kinetics of Penetration of Common Antiepileptic Drugs into Cerebrospinal Fluid. *Epilepsia* **25**(3)**:** 346-352.

Löscher W, Potschka H (2005a). Blood-Brain Barrier Active Efflux Transporters: ATP-Binding Cassette Gene Family. *NeuroRX* **2**(1)**:** 86-98.

Löscher W, Potschka H (2005b). Drug resistance in brain diseases and the role of drug efflux transporters *Nature Reviews Neuroscience* **6:** 591-602.

Luna-Toetos C, Fedrowitz M, Löscher W (2008). Several major antiepileptic drugs are substrates for human p-glycoprotein *Neuropharmacology* **55**(8)**:** 1364-1375.

Macdonald RL (1999). Cellular actions of antiepileptic drugs. In: Eadie MJ, Vajda F (eds). *Antiepileptic Drugs: Pharmacology and Therapeutics*, edn. Berlin: Springer. p^pp 123-150.

Maeda T, Takahashi K, Ohtsu N, Oguma T, Ohnishi T, Atsumi R, *et al.* (2007). Identification of influx transporter for the quinolone antibacterial agent levofloxacin. *Molecular Pharmaceutics* **4**(1)**:** 85-94.

Maiche AG (1986). Acute renal failure due to concomitant action of methotrexate and indomethacin. *The Lancet* **327**(8494).

Majumdar S, Duvvuri S, Mitra AK (2004). Membrane transporter/receptor-targeted prodrug design: strategies for human and vetinary drug development. *Advanced Drug Delivery Reviews* **56:** 1437-1452.

Manning Fox JE, Meredith D, Halestrap AP (2000). Characterisation of human monocarboxylate transporter 4 substantiates its role in lactic acid efflux from skeletal muscle. *Journal of Physiology* **529**(2)**:** 285-293.

Manoharan C, Wilson MC, Sessions RB, Halestrap AP (2006). The role of charged residues in the transmembrane helices of monocarboxylate transporter 1 and its ancillary protein basigin in determining plasma membrane expression and catalytic activity. *Molecular Membrane Biology* **23**(6)**:** 486-498.

Margineanu DG, Klitgaard H (2009). Mechanisms of drug resistance in epilepsy: Relevance for antiepileptic drug discovery. *Expert Opinion on Drug Discovery* **4**(1)**:** 23-32.

Markovich D (2008). Expression cloning and radiotracer uptakes in Xenopus laevis oocytes. *Nature Protocols* **3**(12)**:** 1975-1980.

Martin H-J, Kornmann F, Fuhrmann GF (2003). The inhibitory effects of flavonoids and antiestrogens on the Glut1 glucose transporter in human erythrocytes. *Chemico-Biological Interactions* **146:** 225–235.

Maryanoff BE, Nortey S, Gardocki JF, Shank RP, Dodgson SP (1987). Anticonvulsant O-Alkyl Sulfamates. 2,3:4,5-Bis-O-(l-methylethy1idene)-6-D-fructopyranose Sulfamate and Related Compounds. *Journal of Medicinal Chemistry* **30**(5)**:** 880-887.

Masino SA, Rho JM (2012). Mechanisms of Ketogenic Diet Action. In: *Jasper's Basic Mechanisms of the Epilepsies*, Noebels JL, Avoli M, Rogawski MA (eds), 4th edn. Bethesda (MD): National Center for Biotechnology Information (US)

Matsuo F, Riaz A (2009). Lamotrigine. In: Shorvon S, Perucca E, Engel J (eds). *The Treatment of Epilepsy*, edn: Blackwell Publishing LTD. p^pp 535-558.

Merritt HH, Putnam TJ (1938a). A new series of anticonvulsant drugs tested by experiments in animals. *Archives of Neurology and Psychiatry* **39:** 1003-1015.

Merritt HH, Putnam TJ (1938b). Sodium diphenyl hydantoinate in the treatment of convulsive disorders. *The Journal of the American Medical Association* **111:** 1068-1073.

Meunier H, Carraz G, Meunier Y, Eymard P, Almarro M (1963). Pharmacodynamic properties of dipropylactic acid 1. Anticonvulsive action. *Therapie* **18:** 435-438.

Middleton E, Kandaswami C, Theoharides TC (2000). The Effects of Plant Flavonoids on Mammalian Cells: Implications for Inflammation, Heart Disease, and Cancer. *Pharmalogical Reviews* **52:** 673-751.

Mikkaichi T, Suzuki T, Onogawa T, Tanemoto M, Mizutamari H, Okada M, *et al.* (2004). Isolation and characterization of a digoxin transporter and its rat homologue expressed in the kidney. *Proceedings of the National Academy of Sciences of the United States of America* **101**(10)**:** 3569-3574.

Moermana L, Wyffelsa L, Slaets D, Raedt R, Boonb P, Vos FD (2011). Antiepileptic drugs modulate P-glycoproteins in the brain: A mice study with 11C-desmethylloperamide. *Epilepsy Research* **94:** 18-25.

Mori S, Takanaga H, Ohtsuki S, Deguchi T, Kang Y-S, Hosoya K-I, *et al.* (2003). Rat Organic Anion Transporter 3 (rOAT3) Is Responsible for Brain to Blood Efflux of Homovanillic Acid at the Abluminal Membrane of Brain Capillary Endothelial Cells. *Journal of Cerebral Blood Flow and Metabolism* **23:** 432-440.

Morris ME, Felmlee MA (2008). Overview of the Proton-coupled MCT (SLC16A) Family of Transporters: Characterization, Function and Role in the Transport of the Drug of Abuse γ-Hydroxybutyric Acid. *The AAPS Journal* **10**(2)**:** 311-321.

Morselli PL (1995). *Carbamazepine: absorption, distribution and excretion*. 4th edn. New York: Raven Press.

Mullen SA, Marini C, Suls A, Mei D, Giustina ED (2011). Glucose Transporter 1 Deficiency as a Treatable Cause of Myoclonic Astatic Epilepsy. *Archives of Neurology* **68**(9)**:** 1152-1154.

Müller F, König J, Hoier E, Kathrin Mandery K, Fromm MF (2013). Role of organic cation transporter OCT2 and multidrug and toxin extrusion proteins MATE1 and MATE2-K for transport and drug interactions of the antiviral lamivudine. *Biochemical Pharmacology* **86:** 808-815.

Murray CM, Hutchinson R, Bantick JR, Belfield GP, Benjamin AD, Brazma D, *et al.* (2005). Monocarboxylate transporter MCT1 is a target for immunosuppression. *Nature Chemical Biology* **1**(7)**:** 371-376.

Nakata K, Tanaka Y, Nakano T, Adachi T, Tanaka H, Kaminuma T, *et al.* (2006). Nuclear receptor-mediated transcriptional regulation in Phase I, II, and III xenobiotic metabolizing systems. *Drug Metabolism and Pharmacokinetics* **21:** 437-457.

Naora K, Shen DD (1995). Mechanism of valproic acid uptake by isolated rat brain microvessels. *Epilepsy Research* **22:** 97-106.

Neuhoff S, Ungell A-L, Zamora I, Artursson P (2005). pH-Dependent passive and active transport of acidic drugs across Caco-2 cell monolayers. *European Journal of Pharmaceutical Sciences* **25:** 211-220.

Neurvonen PJ (1979). Bioavailability of phenytoin: clinical pharmacokinetic and therapeutic implications. *Clinical Pharmacokinetics* **4:** 91-103.

Nguyen LN, Ma D, Shui G, Wong P, Cazenave-Gassiot A, *et al*. (2014). *MFSD2A* is a transporter for the essential omega-3 fatty acid docosahexaenoic acid. *Nature* **509:** 503-506.

Ohtsuki S, Asaba H, Takanaga H, Deguchi T, Hosoya K-i, Otagiri M, *et al.* (2002). Role of blood–brain barrier organic anion transporter 3 (OAT3) in the efflux of indoxyl sulfate, a uremic toxin: its involvement in neurotransmitter metabolite clearance from the brain. *Journal of Neurochemistry* **83:** 57-66.

Ovens MJ, Davis AJ, Wilson MC, Murray CM, Halestrap AP (2010a). AR-C155858 is a potent inhibitor of monocarboxylate transporters MCT1 and MCT2 that binds to an intracellular site involving transmembrane helices 7-10. *Biochemical Journal* **425:** 523-530.

Ovens MJ, Manoharan C, Wilson MC, Murray CM, Halestrap AP (2010b). The inhibition of monocarboxylate transporter 2 (MCT2) by AR-C155858 is modulated by the associated ancillary protein *Biochemical Journal* **431:** 217-225.

Owen A, Pirmohamed M, Tettey JN, Morgan P, Chadwick D, Park BK (2001). Carbamazepine is not a substrate for P-glycoprotein. *British Journal of Clinical Pharmacology* **51:** 345-349.

Pajouhesh H, Lenz GR (2005). Medicial Chemical Properties of Successful Central Nervous System Drugs. *The Journal of the American Society for Experimental NeuroTherapeutics* **2:** 541-553.

Palm K, Stenberg P, Luthman K, Arturson P (1997). Polar molecular surface properties predict the intestinal absorption of drugs in humas. *Pharmaceutical Research* **14:** 568-571.

Pardridge WM (1986). Blood-Brain Barrier Transport of Nutrients. *Nutrition reviews* **44**(Supplement)**:** 15-25.

Pardridge WM (2005). The Blood-Brain Barrier: Bottleneck in Brain Drug Development. *The Journal of the American Society for Experimental NeuroTherapeutics* **2:** 3-14.

Pardridge WM, Oldendorf WH (1977). Transport of metabolic substrates through the blood brain barrier. *Journal of Neurochemistry* **28**(1)**:** 5-12.

Patsalos PN (2005). Properties of Antielieptic Drugs in the Treatment of Idiopathic Generalised Epilepsies *Epilepsia* **46:** 140-148.

Pedley TA (2009). Major advances in epilepsy in the last century: A personal perspective. *Epilepsia* **50**(3)**:** 358-363.

Pellerin L, Halestrap AP, Pierre K (2005). Cellular and subcellular distribution of monocarboxylate transporters in cultured brain cells and in the adult brain. *Journal of Neuroscience Research* **79**(1-2)**:** 55-64.

Pereira JNDS, Tadjerpisheh S, Abed MA, Saadatmand AR, Weksler B, Romero IA, *et al.* (2014). The Poorly Membrane Permeable Antipsychotic Drugs Amisulpride and Sulpiride Are Substrates of the Organic Cation Transporters from the SLC22 Family. *The AAPS Journal*.

Pefferkorn JA, Guzman-Perez A, Litchfield J, Aiello R, Treadway JL (2012). Discovery of (S)-6-(3-cyclopentyl-2-(4-(trifluoromethyl)-1H-imidazol-1-yl)propanamido)nicotinic acid as a hepatoselective glucokinase activator clinical candidate for treating type 2 diabetes mellitus. *Journal of Medicinal Chemistry* **55** (3)**:** 1318-1333.

Pierre K, Pellerin L (2005). Monocarboxylate transporters in the central nervous system: Distribution, regulation and function. *Journal of Neurochemistry* **94**(1)**:** 1-14.

Poller; B, Heike Gutmann, Krähenbühl S, Weksler B, IgnacioRomero, Couraud P-O, *et al.* (2008). The human brain endothelial cell line hCMEC/D3 as a human blood-brain barrier model for drug transport studies. *Journal of Neurochemistry* **107**(5)**:** 1358-1368.

Poole RC, Halestrap AP (1997). Interaction of the erythrocyte lactate transporter (monocarboxylate transporter 1) with an integral 70-kDa membrane glycoprotein of the immunoglobulin superfamily. *Journal of Biological Chemistry* **272**(23)**:** 14624-14628.

Potschka H, Fedrowitz M, Loscher W (2002). P-Glycoprotein-mediated efflux of phenobarbital, lamotrigine, and felbamate at the blood-brain barrier: evidence from microdialysis experiments in rats. *Neuroscience Letters* **327:** 173-176.

Potschka H, Fedrowitz M, Löscher W (2001). P-glycoprotein and multidrug resistance-associated protein are involved in the regulation of extracellular levels of the major antiepileptic drug carbamazepine in the brain. *Neuropharmacology and Neurotoxicology* **12**(16)**:** 3557-3560.

Price NT, Jackson VN, Halestrap AP (1998). Cloning and sequencing of four new mammalian monocarboxylate transporter (MCT) homologues confirms the existence of a transporter family with an ancient past. *Biochemical Journal* **329:** 321-328.

Qian X, Cheng Y-H, Mruk DD, Cheng CY (2013). Breast cancer resistance protein (Bcrp) and the testis—an unexpected turn of events. *Asian Journal of Andology* **15:** 455-460.

Race JE, Grassl SM, Williams WJ, Holtzman EJ (1999). Molecular Cloning and Characterization of Two Novel Human Renal Organic Anion Transporters (hOAT1 and hOAT3). *Biochemical and Biophysical Research Communications* **255:** 508 –514.

Redzic Z (2011). Molecular biology of the blood-brain and the blood-cerebrospinal fluid barriers: Similarities and differences. *Fluids and Barriers of the CNS* **8**(1).

Reid G, Wolff NA, Dautzenberg FM, Burckhardt G (1998). Cloning of a Human Renal p-Aminohippurate Transporter, hROAT1. *Kidney Blood Pressure Research* **21:** 233–237.

Remy S, Gabriel S, Urban BW, Dietrich D, Lehmann TN, Elger CE, *et al.* (2003). A Novel Mechanism Underlying Drug Resistance in Chronic Epilepsy. *Annals of Neurology* **53:** 469-479.

Riedmaier AE, Nies AT, Schaeffeler E, Schwab M (2012). Organic Anion Transporters and Their Implications in Pharmacotherapy. *Pharmacological Reviews* **64:** 421-449.

Rizwan AN, Burckhardt G (2007). Organic Anion Transporters of the SLC22 Family: Biopharmaceutical, Physiological, and Pathological Roles. *Pharmaceutical Research* **24**(3)**:** 450-470.

Roberts LM, Woodford K, Zhou M, Black DS, Haggerty JE, Tate EH, *et al.* (2008). Expression of the Thyroid Hormone Transporters Monocarboxylate Transporter-8 (SLC16A2) and Organic Ion Transporter-14 (SLCO1C1) at the Blood-Brain Barrier. *Endocrinology* **149**(12)**:** 6251-6261.

Rogawski MA (2013). The intrinsic severity hypothesis of pharmacoresistance to antiepileptic drugs. *Epilepsia* **54**(Supplement 2)**:** 33-40.

Rogawski MA, Porter RJ (1990). Antiepileptic drugs: Pharmacological mechanisms and clinical efficacy with consideration of promising developmental stage compounds. *Pharmacological Reviews* **42**(3)**:** 223-286.

Roth M, Obaidat A, Hagenbuch B (2012). OATPs, OATs and OCTs: the organic anion and cation transporters of the SLCO and SLC22A gene superfamilies. *British Journal of Pharmacology* **165:** 1260-1287.

Samrén EB, M vDC, Koch S, Hiilesmaa VK, Klepel H, Bardy AH, *et al.* (1997). Maternal Use of Antiepileptic Drugs and the Risk of Major Congenital Malformations: A Joint European Prospective Study of Human Teratogenesis Associated with Maternal Epilepsy. *Epilepsia* **38**(9)**:** 981-990.

Sato M, Iwanaga T, Mamada H, Ogihara T, Yabuuchi H, Maeda T, *et al.* (2008). Involvement of Uric Acid Transporters in Alteration of Serum Uric Acid Level by Angiotensin II Receptor Blockers. *Pharmaceutical Research* **25**(3)**:** 639-646.

Schindler W, Häfliger F (1954). Über Derivate des Iminodibenzyls *Helvetica Chimica Acta* **37:** 472-483.

Sekine T, Cha SH, Endou H (2000). The multispecific organic anion transporter (OAT) family. *Pflugers Archiv European Journal of Physiology* **440**(3)**:** 337-350.

Sekine T, Watanabe N, Hosoyamada M, Kanai Y, Endou H (1997). Expression Cloning and Characterization of a Novel Multispecific Organic Anion Transporter. *The Journal of Biological Chemistry* **272:** 18526-18529.

Shawahna R, Uchida Y, Declèves X, Ohtsuki S, Yousif S, Dauchy S et al (2011). Transcriptomic and Quantitative Proteomic Analysis of Transporters and Drug Metabolising Enzymes in Freshly Isolated Human Brain Microvessels. *Molecular Pharmaceutics* **8:** 1332-1341.

Shin HJ, Lee CH, Park S-J, Shin J-G, Song I-S (2010). Establishment and Characterization of Mardin-Darby Canine Kidney Cells Stably Expressing Human Organic Anion Transporters. *Archives of Pharmacal Research* **33**(5)**:** 709-716.

Shirasaka Y, Shichiri M, Mori T, Nakanishi T, Tamai I (2012). Major Active Components in Grapefruit, Orange, and Apple Juices Responsible for OATP2B1-Mediated Drug Interactions. *Journal of Pharmaceutical Sciences* **102**(1)**:** 280-288.

Shorvon SD (2009a). Drug treatment of epilepsy in the century of the ILAE: The first 50 years, 1909-1958. *Epilepsia* **50**(Supplement 3)**:** 69-92.

Shorvon SD (2009b). Drug treatment of epilepsy in the century of the ILAE: The second 50 years, 1959-2009. *Epilepsia* **50**(supplement 3)**:** 93-130.

Sillanpää M, Haataja L, Tomson T, Johannessen SI (2009). Carbamazepine. In: Shorvon S, Perucca E, Engel J (eds). *The Treatment of Epilepsy*, 3rd edn: Blackwell Publishing LTD. p^pp 459-474.

Sills GJ (2006). The mechanisms of action of gabapentin and pregabalin. *Current Opinion in Pharmacology* **6:** 108-113.

Sills GJ, Kwan P, Butler E, C.M. dLE, Berg D-Jvd, Brodie MJ (2002). P-glycoprotein-mediated efflux of antiepileptic drugs: preliminary studies in mdr1a knockout mice *Epilepsy & Behaviour* **3:** 427-432.

Simonson GD, Vincent AC, Roberg KJ, Huang Y, Iwanij V (1994). Molecular cloning and characterization of a novel liver-specific transport protein. *Journal of Cell Science* **107,:** 1065-1072.

Sisodiya SM, Heffernan J, Squier MV (1999). Over-expression of Pglycoprotein in malformations of cortical development. *NeuroReport* **10:** 3437-3441.

Sisodiya SM, Lin WR, Harding BN, Squier MV, Thom M (2002). Drug resistance in epilepsy: expression of drug resistance proteins in common causes of refractory epilepsy. *Brain* **125:** 22-31.

Smith DA, Allerton C, Kalgutkar AS, Waterbeemd Hvd, Walker DK (2012). Physicochemistry. In. *Pharmacokinetics and Metabolism in Drug Design*, Third edn: Wiley-VCH Verlag GmbH & Co. KGaA. p^pp 1-17.

Somerville ER, Michell AW (2009). Gabapentin. In: *The Treatment of Epilepsy*, Shorvon S, Perucca E, Engel J (eds), 3 edn, pp 519-526: Blackwell Publishing LTD.

Splinter MY (2005). Pharmacokinetic Properties of New Antiepileptic Drugs. *Journal of Pharmacy Practice* **18**(6)**:** 444-460.

Stanley LA, Horsburgh BC, Ross J, Scheer N, Wolf CR (2009). Drug transporters: Gatekeepers controlling access of xenobiotics to the cellular interior. *Drug Metabolism Reviews* **41**(1)**:** 27-65.

Staud F, Cerveny L, Ahmadimoghaddam D, Ceckova M (2013). Multidrug and toxin extrusion proteins (MATE/SLC47); role in pharmacokinetics. *The International Journal of Biochemistry & Cell Biology* **45:** 2007-2011.

Stephen LJ, Kelly K, Parker P, Brodie MJ (2011). Levetiracetam monotherapy—Outcomes from an epilepsy clinic. *Seizure* **20:** 554-557.

Stieger B, Gao B (2015). Drug Transporters in the Central Nervous System. *Clinical Pharmacokinetics* **54:** 225-242.

Sun W, Wu RR, van Poelje PD, Erion MD (2001). Isolation of a Family of Organic Anion Transporters from Human Liver and Kidney. *Biochemical and Biophysical Research Communications* **283:** 417– 422

Szakács G, Váradi A, Özvegy-Laczka C, Sarkadi B (2008). The role of ABC transporters in drug absorption, distribution, metabolism, excretion and toxicity (ADME–Tox). *Drug Discovery Today* **13**(9-10)**:** 379-393.

Tai LM, Reddy PS, Lopez-Ramirez MA, Davies HA, Male ADK, Loughlin AJ, *et al.* (2009). Polarized P-glycoprotein expression by the immortalised human brain endothelial cell line, hCMEC/D3, restricts apical-to-basolateral permeability to rhodamine 123. *Brain Research* **1292:** 14-24.

Tamai I, Nezu JI, Uchino H, Sai Y, Oku A, Shimane M, *et al.* (2000). Molecular identification and characterization of novel members of the human organic anion transporter (OATP) family. *Biochemical and Biophysical Research Communications* **273**(1)**:** 251-260.

Temkin O (1945). *The falling Sickness*. edn. Baltimore: The John Hopkins University Press.

Terbach N, Shah R, Kelemen R, Klein PS, Gordienko D, Brown NA, *et al.* (2011). Identifying an uptake mechanism for the antiepileptic and bipolar disorder treatment valproic acid using the simple biomedical model *Dictyostelium*. *Cell Science* **124:** 2267-2276.

Theofilopoulos S, Wang Y, Kitambi SS, Sacchetti P, Sousa KM, Bodin K, *et al.* (2013). Brain endogenous liver X receptor ligands selectively promote midbrain neurogenesis. *Nature Chemical Biology* **9:** 126-134.

Thomas J, Wang L, Clark RE, Pirmohamed M (2004). Active transport of imatinib into and out of cells: implications for drug resistance. *blood* **104:** 3739-3745.

Thyss A, Kubar J, Milano G, Namer M, Schneider M (1986). Clinical and pharmacokinetic evidence of a life-threatening interaction between methotrexate and ketoprofen. *The Lancet* **327**(8475)**:** 256–258.

Tirona RG, Leake BF, Merino G, Kim RB (2001). Polymorphisms in OATP-C: Identification of multiple allelic variants associated with altered transport activity among European- and African-Americans. *Journal of Biological Chemistry* **276**(38)**:** 35669-35675.

Tishler DM, Weinburg KI, Hinton DR, Barbaro N, Annett GM, Raffel C (1995). MDR1 gene expression in brain of patients with medically intractable epilepsy. *Epilepsia* **36**(1)**:** 1-6.

Tomson T, Bertilsson L, Andersson DH, Schlaifer D, Arlet P, Ollier S, *et al.* (1989). Carbamazepine update. *Lancet* **2**(8669)**:** 980-981.

Toyoda Y, Hagiya Y, Adachi T, Hoshijima K, Kuo MT, Ishikawa T (2008). MRP class of human ATP binding cassette (ABC) transporters: historical background and new research directions. *Xenobiotica* **38**(7-8)**:** 833-862.

Tsuji A, Terasaki T, Takabatake Y, Tenda Y, Tamaia I, Yamashima T, *et al.* (1992). P-glycoprotein as the drug efflux pump in primary cultured bovine brain capillary endothelial cells. *Life Sciences* **51:** 1427-1437.

Uchida Y, Ohtsuki S, Katsukura Y, Ikeda C, Suzuki T, Kamiie J, *et al.* (2011). Quantitative targeted absolute proteomics of human blood-brain barrier transporters and receptors. *Journal of Neurochemistry* **117:** 333–345.

Uldry M, Thorens B (2004). The SLC2 family of facilitated hexose and polyol transporters. *European Journal of Physiology* **447:** 480-489.

Urquhart BL, Kim RB (2009). Blood-brain barrier transporters and response to CNS-active drugs. *European Journal of Clinical Pharmacology* **65**(11)**:** 1063-1070.

Utoguchi N, Audus KL (2000). Carrier-mediated transport of valproic acid in BeWo cells, a human trophoblast cell line. *International Journal of Pharmaceutics* **195**(1-2)**:** 115-124.

van Bree JB, Audus KL, Borchardt RT (1988). Carrier-mediated transport of baclofen across monolayers of bovine brain endothelial cells in primary culture. *Pharmaceutical Research* **5**(6)**:** 1369-1371.

van Bree JB, Heijligers-Feijen CD, Boer AGd, Danhof M, Breimer DD (1991). Stereoselective transport of baclofen across the blood-brain barrier in rats as determined by the unit impulse response methodology. *Pharmaceutical Research* **8**(2)**:** 259-262.

van der Bliek AM, Kooiman PM, Schneider C, P PB (1988). Sequence of mdr3 cDNA encoding a human P-glycoprotein. *Gene* **71:** 401-411.

van Vliet EA, van Schaik R, Edelbroek PM, Voskuyl RA, Redeker S, Aronica E, *et al.* (2007). Region-Specific Overexpression of P-glycoprotein at the Blood-Brain Barrier Affects Brain Uptake of Phenytoin in Epileptic Rats. *Pharmacology and Experimental Theraputics* **22:** 141-147.

VanWert AL, Gionfriddo MR, Sweet DH (2010). Organic anion transporters: Discovery, pharmacology, regulation and roles in pathophysiology. *Biopharmaceutics and Drug Disposition* **31**(1)**:** 1-71.

Verrey F, Closs E, Wagner CA, Palacin M, Endou H, Kanai Y (2003). CATs and HATs: the SLC7 family of amino acid transporters. *Pflgers Archiv European Journal of Physiology* **447**(5)**:** 532-542.

Vittorio CC, Muglia JJ (1995). Anticonvulsant hypersensitivity syndrome. *Archives of internal medicine* **155**(21)**:** 2285-2290.

Volk C (2014). OCTs, OATs, and OCTNs: structure and function of the polyspecific organic ion transporters of the SLC22 family. *WIREs Membrane Transport and Signalling* **3:** 1-13.

Volk HA, Löscher W (2005). Multidrug resistance in epilepsy: rats with drug-resistant seizures exhibit enhanced brain expression of P-glycoprotein compared with rats with drug-responsive seizures. *Brain* **128:** 1358-1368.

Wagner CA, Friedrich B, Setiawan I, Lang F, Broer S (2000). The Use of Xenopus laevis Oocytes for the Functional Characterization of Heterologously Expressed Membrane Proteins. *Cellular Physiology and Biochemistry* **10:** 1-12.

Waldbaum S, Liang L-P, Patel M (2010). Persistent impairment of mitochondrial and tissue redox status during lithium-pilocarpine-induced epileptogenesis. *Journal of Neurochemistry* **115:** 1172–1182.

Wang L (2002). Liver X receptors in the central nervous system: from lipid homeostasis to neuronal degeneration. *Proceedings of the National Academy of Sciences of the United States of America* **99:** 13878–13883.

Wang Q, Darling IM, Morris ME (2006). Transport of gamma-hydroxybutyrate in rat kidney membrane vesicles: Role of monocarboxylic acid transporters. *Journal of Experimental Pharmacology and Theraputics* **318**(2)**:** 751-761.

Watanabe K, Sawano T, Endo T, Sakata M, Sato J (2002). Studies on Intestinal Absorption of Sulpiride (2): Transepithelial Transport of Sulpiride Across the Human Intestinal Cell Line Caco-2. *Biological and Pharmaceutical Bulletin* **25**(10)**:** 1345-1350.

Waterbeemd HVD, Camenisch G, Folkers G, Chretien JR, Raevsky OA (1998). Estimation of Blood-Brain Barrier Crossing of Drugs Using Molecular Size and Shape, and H-bonding Descriptors. *Journal of Drug Targetting* **6**(2)**:** 151-165.

Wee NKY, Weinstein DC, Fraser ST, Assinder SJ (2013). The mammalian copper transporters CTR1 and CTR2 and their roles in development and disease. *The International Journal of Biochemistry & Cell Biology* **45**(5)**:** 960-963.

Weksler B, Romero IA, Couraud P-O (2013). The hCMEC/D3 cell line as a model of the human blood brain barrier. *Fluids and Barriers of the CNS* **10**(16).

Welty DF, Schielke GP, Vartanian MG, Taylor CP (1993). Gabapentin anticonvulsant action in rats: disequilibrium with peak drug concentrations in plasma and brain microdialysate. *Epilepsy Research* **16:** 175-181.

Wen T, Liu Y-C, Yang H-W, Liu H-Y, Liu X-D, Wang G-J, *et al.* (2008). Effect of 21-day exposure of phenobarbital, carbamazepine and phenytoin on P-glycoprotein expression and activity in the rat brain. *Journal of the Neurological Sciences* **28:** 99-106.

Westholm DE, Stenehjem DD, Rumbley JN, Drewes LR, Anderson GW (2009). Competitive inhibition of organic anion transporting polypeptide 1c1-mediated thyroxine transport by the fenamate class of nonsteroidal antiinflammatory drugs. *Endocrinology* **150**(2)**:** 1025-1032.

WHO (2012). Epilepsy fact sheet: World Health Organisation.

Widemann BC, Adamson PC (2006). Understanding and Managing Methotrexate Nephrotoxicity. *The Oncologist* **11:** 694-703.

Wilson MC, Jackson VN, Heddle C, Price NT, Pilegaard H, Juel C, *et al.* (1998). Lactic acid efflux from white skeletal muscle is catalyzed by the monocarboxylate transporter isoform MCT3. *Journal of Biological Chemistry* **273:** 15920-15926.

Wilson MC, Meredith D, Fox JEM, Manoharan C, Davies AJ, Halestrap AP (2005). Basigin (CD147) Is the Target for Organomercurial Inhibition of Monocarboxylate Transporter Isoforms 1 and 4. *280* **29:** 27213–27221.

Wilson MC, Meredith D, Halestrap AP (2002). Fluorescence resonance energy transfer studies on the interaction between the lactate transporter MCT1 and CD147 provide information on the topology and stoichiometry of the complex in Situ. *Journal of Biological Chemistry* **277**(5)**:** 3666-3672.

Wu X, Kekuda R, Huang W, Fei YJ, Leibach FH, Chen J, *et al.* (1998). Identity of the organic cation transporter OCT3 as the extraneuronal monoamine transporter (uptake2) and evidence for the expression of the transporter in the brain. *Journal of Biological Chemistry* **273**(49)**:** 32776-32786.

Xia CQ, Milton MN, Gan LS (2007). Evaluation of drug-transporter interactions using in vitro and in vivo models. *Current Drug Metabolism* **8**(4)**:** 341-363.

Xue X, Gong L-K, Maeda K, Luan Y, Qi X-M, Sugiyama Y, *et al.* (2011). Critical Role of Organic Anion Transporters 1 and 3 in Kidney Accumulation and Toxicity of Aristolochic Acid I. *Molecular Pharmaceutics* **8:** 2183–2192.

Yamada A, Maeda K, Kamiyama E, Sugiyama D, Kondo T, Shiroyanagi Y, *et al.* (2007). Multiple Human Isoforms of Drug Transporters Contribute to the Hepatic and Renal Transport of Olmesartan, a Selective Antagonist of the Angiotensin II AT1-Receptor. *Drug Metabolism and Disposition* **35**(12)**:** 2166-2176.

Yuan H, Feng B, Yu Y, Chupka J, Zheng JY, Heath TG, *et al.* (2009). Renal Organic Anion Transporter-Mediated Drug-Drug Interaction between Gemcabene and Quinapril. *The Journal of Pharmacology and Experimental Theraputics* **330**(1)**:** 191-197.

Yuen AWC, Sander JW (2011). Impaired mitochodrial energy production: The basis of pharmacoresistance in epilepsy. *Medical Hypotheses* **77:** 536-540.

Zhang X, He X, Baker J, Tama F, Chang G, Wright SH, *et al* (2012). Twelve transmembrane helices form the functional core of mammalian MATE1 (multidrug and toxin extruder 1) protein. *Journal of Biological Chemistry* **287:** 27971-27982.

Zhang EY, Knipp GT, Ekins S, Swaan PW (2002). Structural biology and function of solute transporters: Implications for identifying and designing substrates. *Drug Metabolism Reviews* **34**(4)**:** 709-750.

Zhang S, Morris ME (2003). Effects of flavonoids biochanin A, morin, phloretin and silymarin on P-glycoprotein-mediated transport. *The Journal of Pharmacology and Experimental Theraputics* **304:** 1258-1267.

Zhang L, Ong WY, Lee T (1999). Induction of P-glycoprotein expression in astrocytes following intracerebroventricular kainate injections. *Experimental Brain Research* **126:** 509-516.

Zhang S, Yang X, Morris ME (2004). Flavonoids are inhibitors of Breast Cancer Resistance Protein (ABCG2)-mediated transport. *Molecular Pharmacology* **65:** 1208-1216.

Zhou J, Xu J, Huang Z, Wang M (2015). Transporter-mediated tissue targeting of therapeutic molecules in drug discovery. *Bioorganic & Medicinal Chemistry Letters* **25:** 993-997.